UHRF1 inhibitors targeting the epigenetic patterns in cancer cells

Liliyana Zaayter

▶ **To cite this version:**

Liliyana Zaayter. UHRF1 inhibitors targeting the epigenetic patterns in cancer cells. Cancer. Université de Strasbourg, 2018. English. NNT : 2018STRAJ017 . tel-03270781

HAL Id: tel-03270781
https://theses.hal.science/tel-03270781

Submitted on 25 Jun 2021

HAL is a multi-disciplinary open access archive for the deposit and dissemination of scientific research documents, whether they are published or not. The documents may come from teaching and research institutions in France or abroad, or from public or private research centers.

L'archive ouverte pluridisciplinaire **HAL**, est destinée au dépôt et à la diffusion de documents scientifiques de niveau recherche, publiés ou non, émanant des établissements d'enseignement et de recherche français ou étrangers, des laboratoires publics ou privés.

UNIVERSITÉ DE STRASBOURG

ÉCOLE DOCTORALE DES SCIENCES DE LA VIE ET DE DA SANTE

Laboratoire de Bioimagerie et Pathologies – CNRS UMR 7021

THÈSE présentée par :

Liliyana ZAAYTER

Soutenue le : **27 Mars 2018**

Pour obtenir le grade de : **Docteur de l'université de Strasbourg**

Discipline/ Spécialité : Pharmacologie

Recherche d'inhibiteurs d'UHRF1: Effets sur les aspects épigénétiques dans les cellules cancéreuses

THÈSE dirigée par :

M. MOUSLI Marc	CR Inserm, HDR, Université de Strasbourg

RAPPORTEURS :

M. DANTE Robert	Directeur de recherches, Université de Lyon
M. TSCHIRHART Eric	Professeur, Université de Luxembourg

AUTRES MEMBRES DU JURY :

Mme DANTZER Françoise	Directeur de recherches, IREBS

Contents

Acknowledgements

This thesis manuscript does not only contain the results of my PhD, it carries the memories of three years spent in Strasbourg with people that will always stay in my mind. PhD is far more than an individual work; it is the contribution of many supportive and kind people who deserve all my gratitude.

Firstly, I would like to express my sincere appreciation to my supervisor Dr. Marc Mousli for giving me the opportunity to join the lab and to discover such an interesting field "epigenetics". I appreciate your encouragement, understanding and all your support not only in science but in all different ways. I would like to extend my gratitude to my co-supervisor Dr. Christian Bronner for his guidance, kindness, great help and for always being available to share his knowledge, perspectives and insights.

My sincere gratefulness goes to Pr. Yves Mély who has been generous with his time, knowledge and discussions. There was never any time which was inconvenient to knock on your door and to ask for help.

I would like to thank my jury members Dr. Robert Dante, Dr. Françoise Dantzer and Pr.Eric Tschirhart for accepting to evaluate my work.

Thanks for our collaborator Dr. Mattia Mori from Italy for his invaluable contributions, his motivation and big support. Thanks for Dr. Christian Muller from Strasbourg for sharing his expertise and for creating a friendly atmosphere during our collaboration.

I would like to thank Dr. Christian Boudier for his help in ITC experiments and for his patience and kindness, Dr. Ludovic Richert for helping with the imaging platform, Dr. Hugues de Rocquigny for his advices. Many thanks for all the permanent stuff of the Laboratory of Biophotonics and Pharmacology for their scientific discussions and availability to help anytime, Dr. Nicolas Humbert, Dr. Andrey Klymchenko, Dr. Mayeul Collot, Dr. Pascal Didier, Dr.Manuel Boutant, Dr. Julien Godet, Dr. Eleonore Réal, Dr. Frédéric Przybilla, Dr. Youri Arntz and others..

Moreover, I'm thankful to Dr. Guy Duportail for his care and interesting conversations and also to Marlyse Wernert and Ingrid Barthel for their help.

To my following labmates, thank you for the enjoyable moments that we spent together, for all the discussions, help, motivation and positive energy: Rajhans, Lesia, Redouane, Doriane, Marianna, Sacha, Nina, Kuong, Manu, Sarwat, Nedal, Yosuke, Salah, Hassan, Oleksi, Bogdan, Krishna, Katya… and many others.

Special thanks to my small "UHRF1 team". Waseem Ashraf and Tanveer Ahmad who have been amazing persons in so many ways during this period. I will be always grateful to you for everything. You made this journey much easier, and much brighter with your continuous support and care.

I will never forget that this phase would have been much more difficult without my dearest friends in France and in Lebanon who were there for me through the good and the bad with their unlimited support. Thank you! Also my "strasbourgeois" friends for their fabulous company and for filling my stay here with unforgettable memories.

Lastly, all this would have been impossible without my source of pure love, mum and dad and my beloved three brothers, who supported me in all my pursuits and made me who I am today.

Thank you very much!

Liliana

List of Abbreviations

AHAQ	2-amino-3-hydroxyanthraquinone
AdoMet	S-Adenosylhomocysteine (SAH)
AML	Acute Myeloid Leukemia
DNA	Deoxyribonucleic Acid
DMEM	Dulbecco's modified Eagle's medium
Bcl2	B Cell Lymphoma
BRCA1	Breast Cancer 1
Caspase	Cystein Aspartate Protease
Cdk	Cyclin kinase dependent
CpG	Cytosine-Phosphate Guanine
DMAP1	DNA Methyltransferase-Associated Protein
DNMT1	DNA Methyltransferase 1
ECREM	Epigenetic Code Replication Machinery
eGFP	Enhanced Green Fluorescent Protein
E2F1	E2F Transcription Factor 1
EZH2	Enhancer of zeste homolog 2
FANCD2	Fanconi Anemia Complementation Group D2
FRET	Fluorescence Resonance Energy Transfer
HAT	Histone Acetyltransferase
HDAC1	Histone Deacetylase 1
HDMs	Histone Demethylases
HMT	Histone Methyltransferase
hMLH1	Human mutant L homologue 1
ICBP90	Inverted CCAAT box Binding Protein of 90 kDa
ICL	Interstrand Crosslinks
Kd	Dissociation Constant
MBD	Methyl-CpG-Binding Domain
miRNA	microRNA
MYST	MOZ, Ybf2/Sas3, Sas2 and Tip60

MTX	Mitoxantrone
NCoR	Nuclear Receptor Co-Repressor
PARP	Poly-ADPribose Polymerase
PCNA	Proliferation Cell Nuclear Antigen
PHD	Plant Homeo Domain
PI5P	Phosphatidylinostiol
PMT	Post Translational Modification
RING	Really Interesting New Gene
SRA	Set and Ring Associated
Tet	Ten Eleven Translocation
thG	Thienoguanosine
Tip60	Tat Interactive Protein 60 kDa
TSGs	Tumor Suppressor Genes
TTD	Cryptic Tandem Tudor Domain
UBL	Ubiquitin-Like Domain
UHRF1	Ubiquitin-like PHD Ring Finger 1
5-mC	5-methylcytosine
5-Aza	5-Azacytidine

PART 1
Bibliographical overview

Chapter 1: Epigenetics
The bridge between genotype and phenotype

Why each cell type of the body holds the same genome but yet behaves differently and has different fates? What is the reason that each stem cell differentiates phenotypically into different types of cells and tissues, whether to a neuron, skin cell, or a liver cell? **(Fig 1)**. The answers to these questions come under the umbrella of "epigenetics", a science that elucidates the distinct mechanisms involved in such behavior.

Figure 1. One genome, different fates. *Identical DNA from the same fertilized egg that has developed after division to many cell types with distinct functions and identities.*

1- Epigenetics

In 1942, the term of Epigenetics was coined by C.H. Waddington explaining how the genetic material can interact with its environment and can shape the final phenotype. With all the progress in knowledge of mechanisms of gene expression, the definition has evolved as "the study of changes in gene function that are mitotically and/or meiotically heritable and that do not involve a change in DNA sequence" [1]. The variety of tissues that are functionally and morphologically different is basically controlled by the gene state which can be regulated through epigenetic mechanisms. These mechanisms are driven essentially by chemical modifications on the level of

DNA, RNA or proteins, and that involves DNA methylation, histone tails modifications (methylation and/or acetylation), chromatin remodeling factors with nucleosome positioning and non-coding RNAs. The epigenetic modifications are an important control mechanism that modulate gene function and expression, and play an important role in perturbing the functionality of transcription factors towards DNA. In recent years, advances have increased in understanding the role of these mechanisms in various fundamental processes as well as in development of many pathological states as cancer [2].

2- Genome Organization

Each human cell contains approximately 2 meters of DNA if stretched end-to-end, its length is much greater than the nucleus that encloses it and that averagely measures about 6µm in diameter. In order to organize the genetic material, DNA is amazingly packaged and compacted to form the chromatin. Chromatin architecture consists of a DNA/protein complex. 146 base pairs of DNA are wrapped around an octamer of four core histone proteins, two H3–H4 and two H2A–H2B in a 1.7 left handed super helical turn to form the nucleosome which is the basic element of chromatin **(Fig 2)** [3].

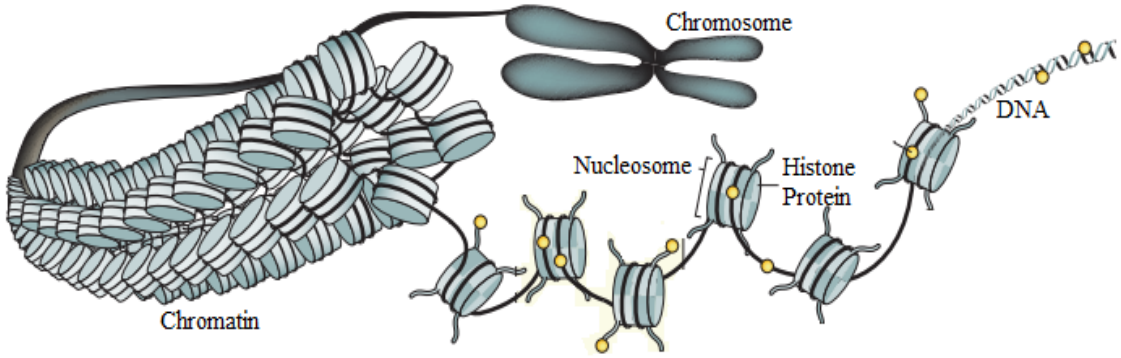

Figure 2. Organization of genetic material. *DNA coils around an octamer of histones to form the nucleosome. Repetitive units of nucleosomes form the chromatin that is further condensed to constitute the chromosome.*

3- Chromatin dynamics

Chromatin remodeling constitutes the essential basis of the regulation of gene expression. Based on its conformation that can be transcriptionally active or inactive, chromatin is divided in two types: heterochromatin and euchromatin [4].

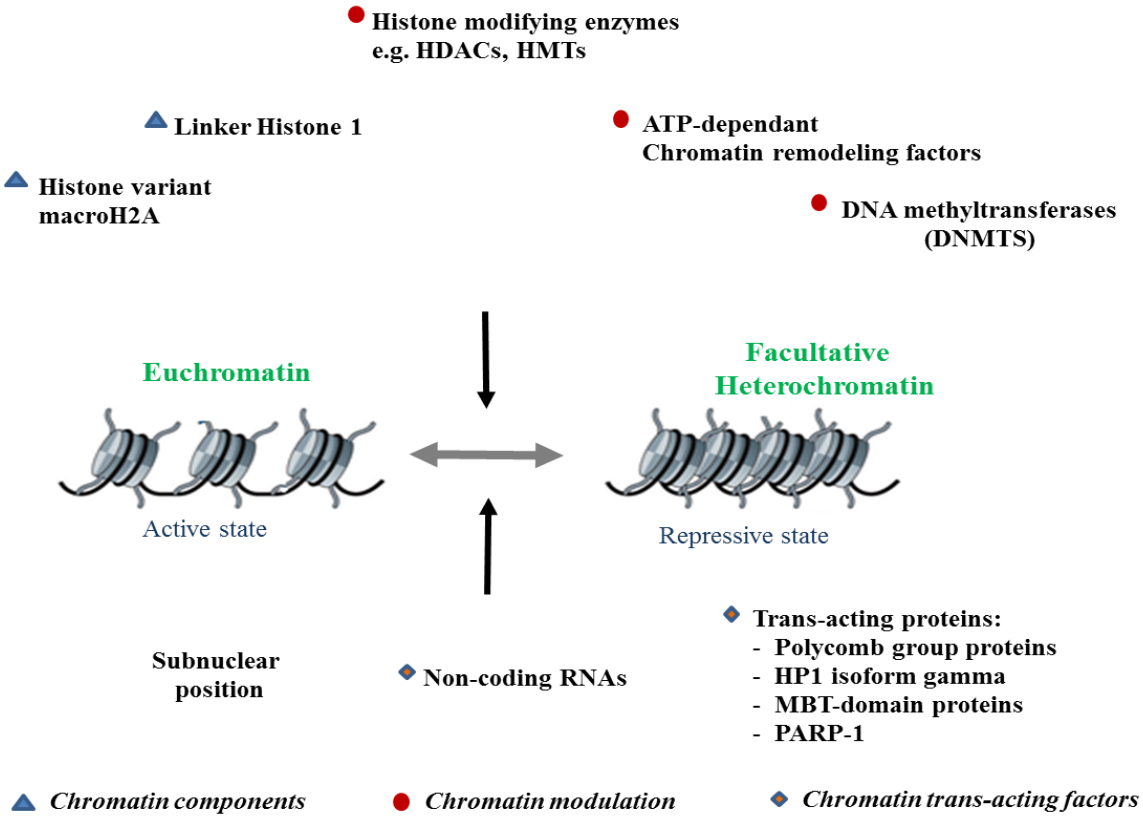

Figure 3. Machinery that influences the chromatin state. *Euchromatin can be transcriptionally silenced by various factors: exchange/incorporation of chromatin components including the linker histone 1 H1 and H2A; covalent modifications of histones and DNA for example through histone deacetylase 1 (HDACs), histone methyltransferases (HMTs) or DNA methyltransferases (DNMTs); alteration in the nucleosome positioning by ATP-dependent chromatin remodelers; involvement of RNAs; relocalization of a genomic locus within the nucleus and activation of chromatin trans-acting factors. Adopted from ref [5].*

Euchromatin presents areas of less condensed form of DNA, which is often under active transcription. In opposite, heterochromatin presents areas of highly packed DNA in condensed state, which is unreachable for transcription factors. Notably, heterochromatin can be distinguished by having two sorts: constitutive and facultative. Constitutive heterochromatin is considered to be the irreversible compact form of a chromatin that can be associated with gene-poor and late replicating

DNA sequences [4],whereas the facultative heterochromatin has the potential to undergo changes through the development stages to acquire more open conformation allowing transcription within temporal (specific cell-cycle stages), spatial and heritable (monoallelic gene expression) contexts [5]. This chromatin remodeling is orchestrated by a combination of processes among which epigenetic regulations and alterations are playing a critical role in defining the structure and dynamics of chromatin (**Fig 3**). Thereby, it controls the gene activation or repression by creating a barrier for the transcriptional machinery to access the genetic information.

4- Epigenetic modifications

4.1- DNA methylation

In mammals, DNA methylation occurs at the 5^{th} position of the cytosine residues within CpG dinucleotides catalyzed by a family of DNA methyltransferases. DNA methylation is a key epigenetic mechanism involved in several essential cellular processes [6] such as regulation of gene expression [7], control of cellular development and differentiation [8, 9], X chromosome inactivation [10], and parental imprinting [11]. It is also associated with the development of immune system [12] and cellular reprogramming as well as in brain function and behavior [13]. DNA methylation helps to maintain the genome integrity through silencing endogenous retroviruses and transposons [14]. Abnormal DNA methylation pattern is linked with a number of diseases [6], including diseases of immune system and neurological disorders [15, 16], in addition to the genesis of human cancers [17] and aging [18].

4.2- Non-coding RNAs

Small, non-coding RNA sequences are almost 16 to 22 nucleotide long RNA molecules, that have been shown to efficaciously induce posttranscriptional silencing of target genes [19]. Most miRNAs are capable to do this by sequence-specific base pairing with 3’ UTR (untranslated regions) of target mRNA, resulting in their degradation or suppression of translation [20]. miRNAs play a role in several cellular processes as cellular differentiation, apoptosis, and cell proliferation [19]. Several studies show that miRNAs are linked to epigenetics, they appear to control epigenetic regulatory network which contributes in silencing gene expression, by methylation and modification of the structure of chromatin. miRNAs target enzymes such as DNMT3A and DNMT3B, responsible for DNA methylation [21], as well as enzymes responsible for histone methylation like Enhancer of

zeste homolog 2 (EZH2), a catalytic subunit of the polycomb repressive complex 2 (PRC2) [22]. Also, it has been shown that miRNAs regulate the expression pattern of HDAC4 isoenzyme [23] and the HDAC1 [24]. Taken together, miRNAs exhibit a remarkable role in controlling gene expression patterns.

4.3- Histone modifications

Histone proteins, consist of the globular core regions and an unstructured N- terminal tails [19]. The tails are highly flexible and rich in lysine and arginine residues that can be largely targeted by numerous posttranslational covalent modifications (PTM) known as histone marks [25] which include methylation, acetylation, ubiquitylation, sumoylation and phosphorylation on specific residues (**Fig 4**) [26]. Following these modifications, several DNA processes can be affected such as transcription, repair, replication and recombination [26]. Histone modifications work either by organizing the accessibility of chromatin into active regions (euchromatin) or inactive regions (heterochromatin) or by recruiting or blocking non-histone effector proteins [19].

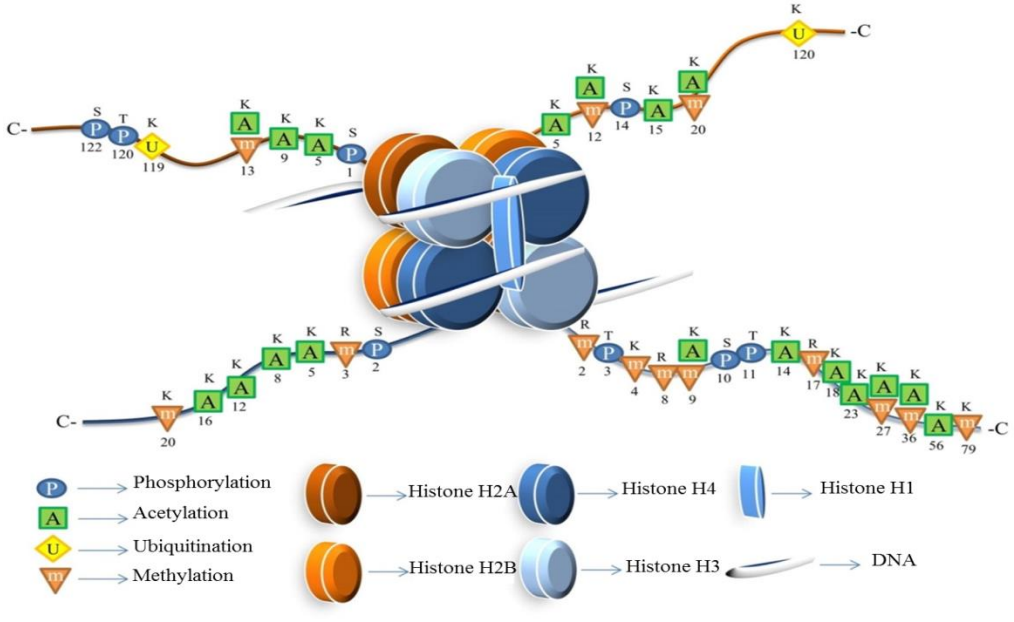

Figure 4. Histone modifications. *Nucleosome constitutes the elementary unit of chromatin. DNA is wrapped around an octamer of four cores of histones proteins H2A, H2B, H3 and H4. H1 is a linker histone associated with 10-80 bp of DNA to separate nucleosomes and to keep the wrapped DNA in place. Several modifications on different residues on histone tails can modulate the structure and function of nucleosomes. This figure shows possible modifications on Serine, Threonine, Lysine and Arginine (S, T, K and R). Adopted from ref [27].*

Behind this diversity in modifications stands a protein machinery that constitutes of protein writers, erasers or readers (**Fig 5**). These are enzymes that add, remove or recognize the histone marks. Each category of these enzymes can be divided into specific classes. Writers as histone acetyltransferases (HATs) *i.e* p300, TIP60 and histone methyltransferases (HMTs) *i.e* SET1, SUV39, erasers as histone deacetylases (HDACs) and histone demethylases (HDMs) *i.e* LSD1, JARID and readers such as PHD, chromodomain and bromodomain proteins [28].

The outcome of the histone modification can be either a transcriptional activation or repression, depending on the modified residue or the degree of modification. For example, the trimethylation of lysine 4 on histone H3 (H3K4me3) is an active mark and acts as transcriptional enhancer [29] whereas trimethylation of lysine 9 or 27 of histone 3 H3 at gene promoter, is a repressive signal associated with transcriptional repression of the gene [25]. These two modifications are considered to be the two main silencing mechanisms in mammalian cells [19]. On the other hand, acetylation of histones that is catalyzed by acethyltransferases (HATs), is a phenomenon that can regulate the gene expression patterns [30]. Acetylation leads to removal of positive charges, and reduces the interaction between the negatively charged DNA and the histones. As a consequence, the chromatin will be in less condensed structure allowing the access to the promotor regions for transcription [31]. In reverse, histone deacetylases (HDACs) mediate deacetylation, which leaves the chromatin in more condensed state and inaccessible to transcription factors.

In addition, these enzymes interplay and coordinate between histone modifications and DNA methylation at different levels to regulate various processes as chromatin status, gene activity and cellular identity. HMTs such G9a, SUV39H1 and PRMT5 can lead to gene silencing by recruiting DNMTs to specific genomic targets [32-34]. Also, HMTs and histone demethylases (HDMs) can affect the DNA methylation status by controlling the stability of DNMTs [19, 35, 36].

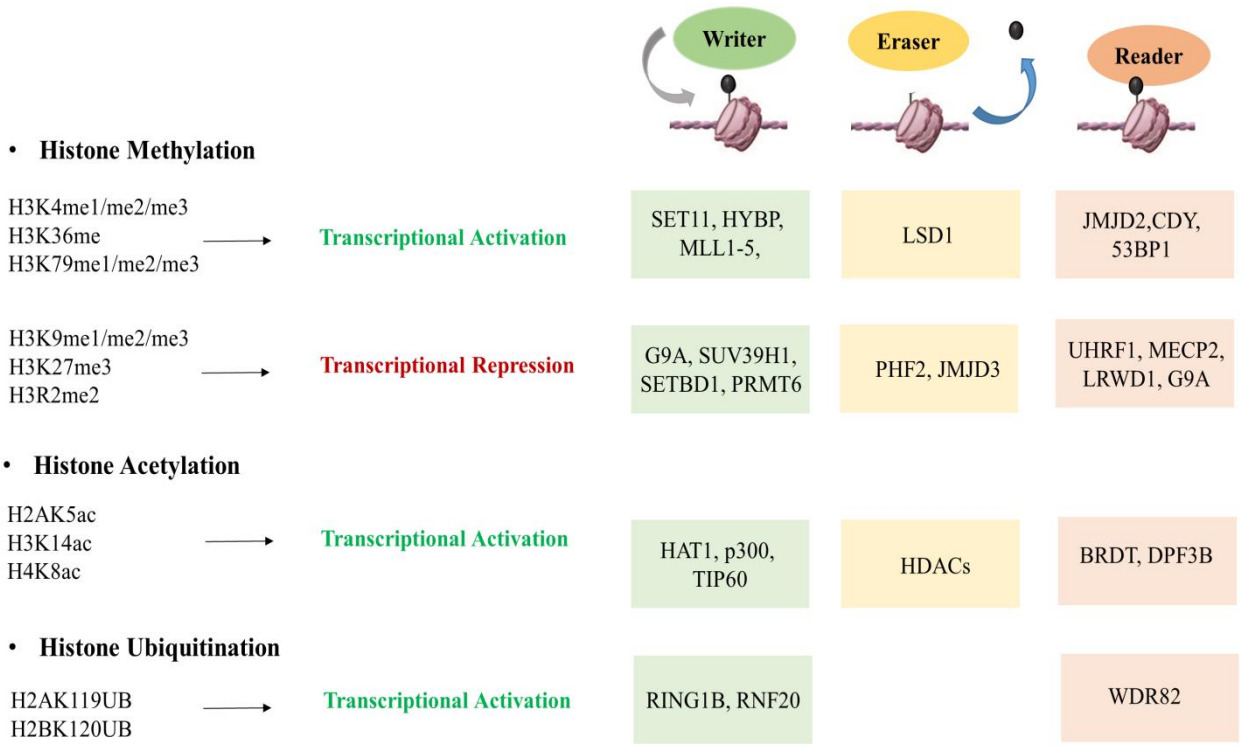

Figure 5. Epigenetic modifications on histone tails. *This illustration shows examples of enzymes (writers, erasers and readers) involved in few of the PTMs of histones (methylation, acetylation and ubiquitination). These modifications can induce or repress the transcription in chromatin. Adopted from ref [28, 37].*

Chapter 2: DNA methylation
The mark and its mediators

DNA methylation is the most studied and the best mechanistically understood epigenetic modification in mammalian cells. As a major epigenetic event, DNA methylation dynamics occupy a key role in establishing the development of mammalian genome. The field of molecular epigenetics, uncovered several questions linked to DNA methylation like how methylation patterns are initially set and how they are maintained through the lifecycle of an organism? How environmental cues can affect methylation during development? Yet, this field still faces challenges in order to fully answer these questions. Two different processes occur to set up DNA methylation patterns, *de novo* methylation, responsible for establishment of methylation state mediated by DNMT3A and DNMT3B and maintenance methylation, responsible for copying it after DNA replication to the daughter strands and mediated by DNMT1. As mentioned above, concomitantly to histone modifications, DNA methylation constitutes a pivotal process that shapes numerous fundamental cellular mechanisms such as gene regulation, chromatin architecture, development and carcinogenesis [19].

1- Localization of methylation sites

Human genome is constituted of CpG dinucleotides with approximately 60-80% of them having a methylated state. These CpGs can be distributed heterogeneously into different types of regions.
They can be located in “CpG islands”, a region characterized with high density of GpG sites (~500 bps with a ratio of CG observed / CG expected >0.65) or they can be located in regions of large repetitive sequences as centromeric repeats, retrotransposon elements [6, 7, 38].
CpG sites are usually positioned at the 5′ end of genes and constitute approximately 70% of gene promoters [39]. Generally, these sites are unmethylated in the majority of the promoters such as in tumor suppressor genes or housekeeping genes [40]. However, distribution of rich CpG sites in proximity to these promoter areas and to sites of transcription initiation makes DNA methylation a main process that shapes gene regulation and thus contribute in progression of pathological states such as cancerogenesis whenever they are abnormally methylated.
In fact, abnormal promoter methylation drives to a repression of gene activity [6] that could be promoted through two modes:

1. The first one involves recognition of methylation of CpG islands, offering binding sites for methyl-binding domain proteins (MBPs), which are capable to recruit histone deacetylases (HDACs) and other remodeling complexes that can modify the chromatin into a repressive transcriptional state [6, 41].
2. The second mode is opposite to the first one, methyl groups hinder the recognition of binding sites by transcription factors leading to transcriptional repression of the gene [42, 43].

2- Chemistry of DNA methylation

DNA methylation is a covalent modification, carried out by a catalytic activity on the 5th carbon of cytosine residue converting it to methyl cytosine. After replication, the addition of methyl group is mediated by a group of specific enzymes called DNA methyltransferases (DNMTs). DNMTs use a cofactor *S*-adenosyl-L-methionine (AdoMet or SAM) as a donor of the methyl group. After the transfer of the methyl group to the DNA bases, SAM is converted into S-adenosyl homocysteine (SAH) [6] (**Fig 6**).

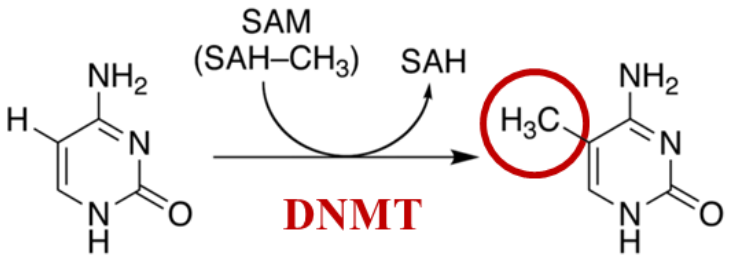

Figure 6. DNA methylation at the 5th position of the cytosine residue catalyzed by DNMTs.

3- Enzymes responsible for DNA methylation

DNMTs are the enzymes responsible for catalyzing the methylation of DNA. Mammalian DNMTs are composed of 5 members: DNMT1, DNMT2, DNMT3A, DNMT3B, and DNMT3L. Among these, only DNMT1, DNMT3A and DNMT3B are capable to methylate DNA. They are categorized into two families: DNMT1 and DNMT3s. Despite that these families are functionally different, they generally have a similar structure. They are multi-domain proteins, possessing two functional parts [44]:

(i) N-terminal regulatory part which is completely different between the DNMT1 and DNMT3s (**Fig 7**) and having many domains involved in various roles. They direct the nuclear localization of the enzymes, contribute in the allosteric regulation of the enzyme's specificity and activity and intermediate their interaction with different proteins, chromatin and regulatory nucleic acids as non-coding RNAs [45].

(ii) C-terminal part which it is formed of six highly conserved motifs , is also involved in different functions [46]. Motifs I and X are responsible for binding of the flipped cytosine, a phenomenon that is found to be common to all DNA methyltransferases, and that was recently observed in crystallography of DNMT with the DNA substrate [47]. These motifs are also responsible for AdoMet binding. Motifs IV, VI, and VIII function lies mainly in catalysis while the non-conserved region located between motifs VIII and IX, also known as Target Recognition Domain (TRD), is involved in DNA recognition [45, 48].

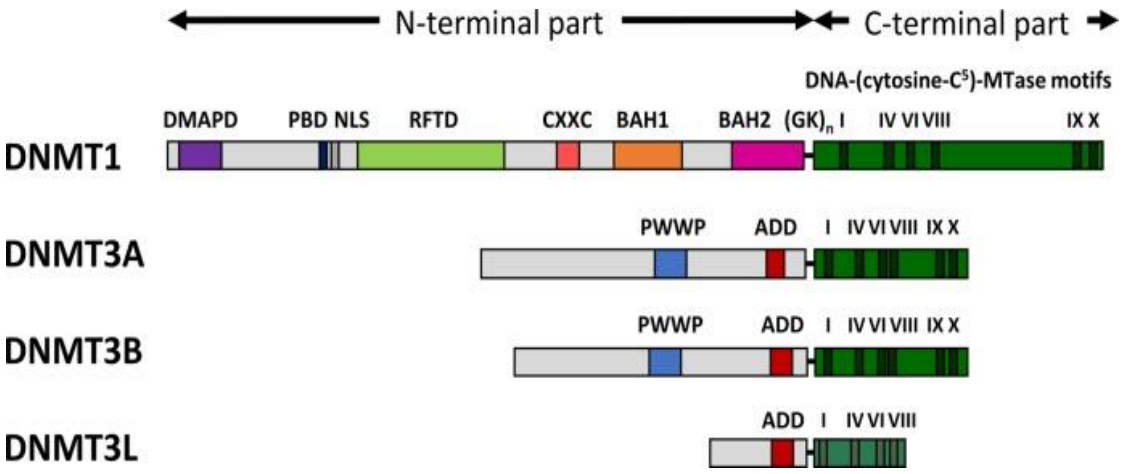

Figure 7. Architecture of mammalian DNMT1, DNMT3A, DNMT3B and DNMT3L enzymes. *The human DNMT1, DNMT3A, DNMT3B are multi domain proteins. Corresponding abbreviations of domains: DMAPD for DNA methyltransferase associated protein 1 interacting domain, PBD – PCNA binding domain, NLS for Nuclear localization signal, RFTD for Replication foci targeting domain, CXXC for CXXC domain, BAH1 and BAH2 for bromo-adjacent homology domains 1 and 2, GK_n for glycine lysine repeats, PWWP for PWWP domain, ADD for ATRX-DNMT3-DNMT3L domain. Adopted from ref [45].*

4- DNA methylation maintenance

After founding cell type identity, it must be tightly protected through the lifecycle of an organism. Thus, once DNA methylation patterns are established, they should be faithfully copied and maintained during replication. DNMT1, the first mammalian DNA methyltransferase that was characterized, is a main performer during this process [49]. For this, it is recognized as a maintenance methyltransferase, a feature that correlates with its preference to bind to hemimethylated DNA [50] as well as with its localization at the replication fork during S phase. Various genetic studies has been made on DNMT1 among which the first targeted mutation of the enzyme in ES cells of mice, resulted in a global loss of methylation, embryonic lethality before mid-gestation and developmental delay [51].

5- DNMT1

5.1- DNMT1 Functional domains

DNMT1 is a large enzyme, containing 1620 amino acids in mouse and 1616 amino acids in humans with multifunctional domains [45]. As already mentioned, N-terminal part is connected to C-terminal part by a flexible linker composed of lysine-glycine repeats (KG) [52]. N-terminal domain starts with the DMAP1 domain, which interacts with DNA methyltransferase-associated protein (DMAP1). DMAP1 is known to induce transcriptional repression and to affect the stability of DNMT1 in cells [53]. Following it, the proliferating cell nuclear antigen domain (PCNA) is involved in guiding DNMT1 to the replication foci during S phase which supports DNA methylation in cells [54, 55]. RFTD domain is responsible for targeting DNMT1 to replication foci and centromeric chromatin [49, 56]. It is also the domain that interacts with UHRF1 protein [57, 58]. This domain is followed by CXXC domain, which is composed of eight conserved cysteine residues and two zinc ions, and is capable to bind to unmethylated DNA [45, 59]. Finally, the BAH1 and BAH2 domains are involved in DNMT1 folding.

5.2- DNMT1 expression

DNMT1 expression fluctuates in a tissue-specific manner; it is highly expressed in proliferating cells while in non-dividing cells, it can be found only at low levels [60]. Throughout the cell cycle, DNMT1 mRNA expression shows a variation with a peak at the S phase [61]. For its transcriptional

regulation, it is induced by Ras-AP-1 signaling pathway [62] and by a regulatory circuit involving (pRb)-E2F1 pathway [63].

5.3- Regulation and function of DNMT1

- ***Selectivity of the target***

DNMT1 was characterized as an extremely processive enzyme due to its capacity to introduce methyl tags to long stretches of hemimethylated DNA without being dissociated from the substrate while sliding along it [45, 64]. This feature makes the enzyme ideal for the copy machinery at the replication fork.

Besides its processivity, DNMT1 is known for its sensitivity since it is able to bind preferentially to hemimethylated DNA as compared to non methylated one [47, 50, 59]. Depending on the DNA sequence, length and assay conditions, this preference is estimated to be averagely about 30-40 fold [44]. Song et al. study has revealed the crystallographic structure of murine DNMT1 in complex with hemimethylated DNA, explaining the intrinsic specificity of DNMT1 toward hemi-mCpG DNA substrates. DNMT1 recognizes the 5-mC of the parental strand by positioning the methyl group inside a hydrophobic pocket within the TRD domain formed by Cys1501, Leu1502, Trp1512, Leu1515 and Met1535. The formation of DNA-DNMT1 complex is set by two TRD loops and a catalytic loop. That is followed by the positioning of the loops at the level of major and minor grooves of DNA. The cytosine to methylate is flipped outside the DNA duplex and is situated perfectly in its catalytic pocket, in proximity to SAM [45, 47] (**Fig 8**).

At the same time, the accuracy in DNMT1 performance toward hemimethylated nucleotides is considered to be a multistep process that is generated by the contribution of other factors. Many structural studies have revealed that the reorganization of DNMT1 domains was strongly involved in its allosteric regulation, making the enzyme catalytically active. An autoinhibitory function exerted by CXXC domain proved to serve as a filter for the enzyme to ensure finally the methylation only at hemimethylated CpG dinucleotides. After binding to non methylated DNA, CXXC places the CXXC–BAH1 linker between the DNA substrate and the active site of the enzyme. As a consequence, once the active site of DNMT1 is occluded, that will stop the enzyme to go for an aberrant *de novo* methylation [65].

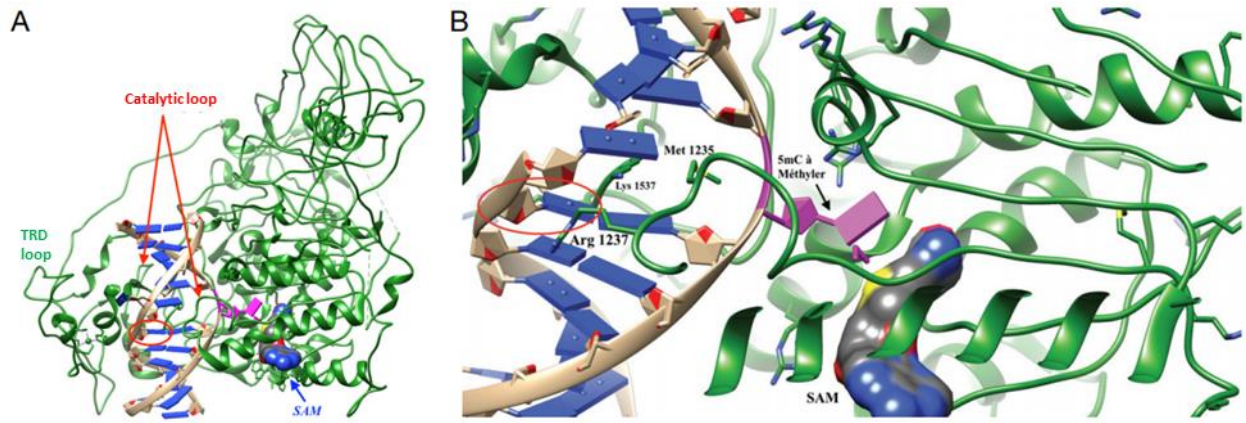

Figure 8. (A) Chrystallographic structure of murine DNMT1 in complex with hemimethylated DNA. *Green for DNMT1, Blue for bases, Beige for phosphate bridges, magenta cytosine to methylate, red circle 5mC corresponding for parent strand* ***(B)*** *Zoom on the site of stabilization of opened DNA duplex. Adopted from ref [66].*

Additional insights on the mechanisms of the enzyme show that RFT domain of DNMT1 is also contributing in structural changes and is playing an autoinhibitory role. Whenever the DNA-binding pocket at the catalytic site of DNMT1 is occupied by the RFTs, DNA loses its access to the catalytic center resulting in enzyme inhibition [67]. Recent findings have shown that UHRF1 could remove the RFTS from the catalytic domain and stimulate back the enzyme's activity by helping it to adopt more active conformation [57] .

- ***Interaction with partners***

During division, DNMT1 localizes at the replication foci during S phase and directly interacts via PBD domain (PCNA binding domain), with PCNA [54], known as processivity factor of the replication machinery. PCNA forms a ring around the DNA helix and helps DNMT1 to be loaded on the newly synthesized DNA. Nevertheless, the interaction of DNMT1 with PCNA is transient and partially dispensable for this process, since deletion of parts of PBD domain resulted in a 2-folded reduction in amount of methylation activity in vivo [55, 68].

Findings have also shown that an additional pathway is involved in targeting DNMT1, which is guided by UHRF1. UHRF1, through its SRA or PHD domain recruits the enzyme to the specific sites of the genome to methylate the daughter strand of the DNA during cell division. This pathway will be reviewed further in UHRF1 section.

Moreover, DNMT1 does not work in an isolated manner; in fact, its role is performed impeccably due to its interactions with numerous partners in the epigenetic network (**Fig 9**). The N-terminal part serves as a platform for binding of various proteins implicated in chromatin condensation and gene regulation such as HDAC1, HDAC2, DNMT3a, DNMT3b, Suv39H1, G9a EZH2, MeCP2, USP7 [6].

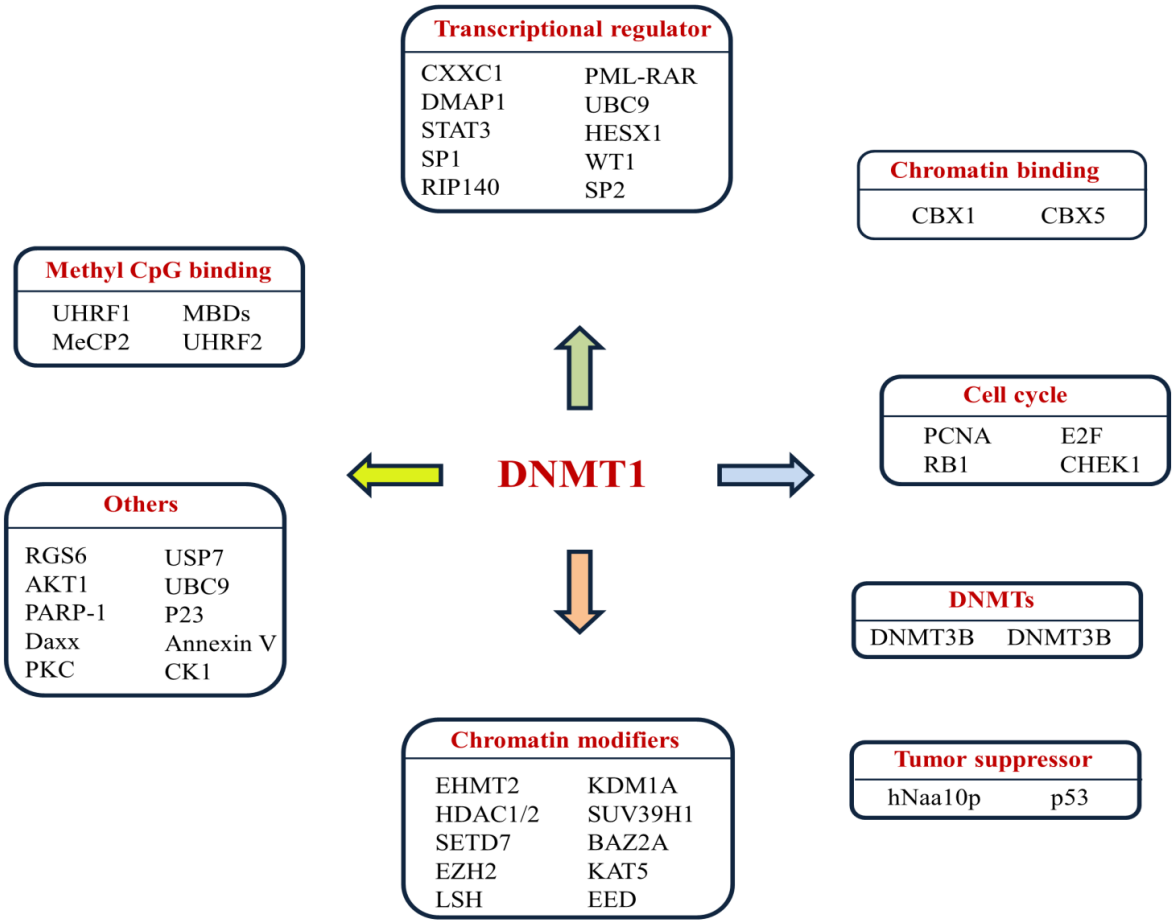

Figure 9. DNMT1 interacting partners. *DNMT1 is a part of an epigenetic network in which a variety of proteins interact with DNMT1 such as chromatin modifiers, chromatin binding proteins, tumor suppressors, cell cycle regulators, transcriptional regulators, DNA methyltransferases and DNA binding proteins.*

5.4- DNMT2

Comparably to other members of DNA methyltransferses family, little is known about the characteristics of DNMT2. Although DNMT2 shows a close structural similarity with DNMT1, biochemical and genetic studies reveal that the enzyme has a weak capacity to methylate DNA *in vivo* [69] since mutated DNMT2 gene in mouse ES cells did not affect the global methylation levels

on DNA [70]. Rather than this, Goll et al. showed that DNMT2 possesses a methylation activity toward RNAt by adding the methyl group to Asp38 of tRNA.

6- *De novo* methylation

DNA methylation directs cells to their future lineage, controls differentiation and prevents reversion into an undifferentiated state. The waves of DNA methylation patterns take place during early stages of development (**Fig 10**). Fertilization is followed by an intensive reprogramming through a genome-wide demethylation, which allows setting totipotency in the early embryo. Imprinted genes and few transposons escape the demethylation. After implantation, methylation patterns are re-established by the activity of DNMT3 enzymes, considered as the key players in *de novo* methylation. Further, a second process of *de novo* methylation occurs during germline development that plays an important role in the establishment of genomic imprinting during gametogenesis [6]. These dynamics of demethylation and remethylation during development create different methylation patterns allowing repression of specific tissue genes and thus establishing a landmark feature of the genome.

6.1- DNMT3 family

DNMT3A, DNMT3B and DNMT3L are the three members of the DNMT3 family**.** DNMT3A and DNMT3B, *de novo* methyltransferases, are the main actors in establishment of DNA methylation during early development and in germlines. Although DNMT1, serves as a guardian of DNA methylation patterns during replication, few findings suggested that DNMT3 enzymes could also be involved in this process, particularly in repetitive sequences or in densely methylated regions [71-73]. In contrast to DNMT1, these two DNMT3s do not display any preference to hemimethylated DNA over non methylated DNA [74]. DNMT3L do not contain essential motifs for the cofactor and DNA binding and it is catalytically inactive.

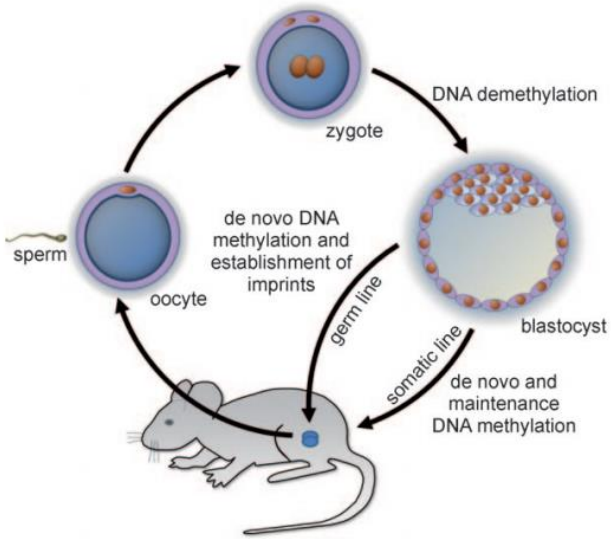

Figure 10. Dynamics of DNA methylation during early development. *Adopted from ref [6].*

7- DNA demethylation

The observations in methylation dynamics throughout the phase of embryogenesis and development, and specifically the demethylation process led the researchers to suggest the existence of DNA methylases and other few mechanisms able to potentially erase the DNA methylation [75]. Recent research has associated the removal of methyl group, to a group of proteins named ten-eleven-translocation proteins (TETs), a name that is attributed to the recurrent chromosomal translocation t (10;11) (q22; q23). DNA demethylation can be accomplished either by an active way or passive way. DNA demethylation as a passive process is a result of a failure of DNMT1 to maintain the methylation during several DNA replication cycles. Whereas, active DNA demethylation occurs when the methyl group is removed by TET family which is composed of 3 members TET1, TET2 and TET3. TET proteins catalyze the oxidation of 5 methylcytosine to 5-hydroxymethylcytosine (5hmC), that is subsequently converted into 5-formylcytosine (5-fC) and 5-carboxylsytosine (5caC) (**Fig 11**). This step can be reverted by entry to a DNA repair pathway by base excision of modified nucleotides. TET proteins are able to modify the epigenetic state of DNA, and are involved in many biological processes including epigenetic regulation of gene transcription.

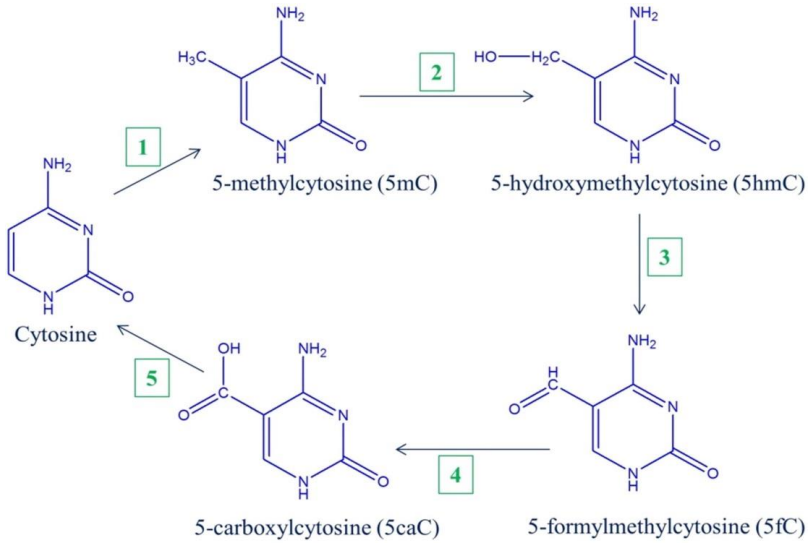

Figure 11. Active demethylation pathway mediated through TET proteins. *After methylation of cytosine residue (1), 5methylcytosine is converted into 5hmC (2) or higher oxidized species 5fC and 5caC (3, 4) by the activity of TET enzymes. Following oxidation, 5caC is converted to an unmodified cytosine (5) through a DNA repair-mediated excision pathway of the modified base. Adopted from ref [27].*

8- Methyl Binding Proteins

The methyl-CpG binding proteins (MBPs) are identified as proteins able to bind methylated DNA. Each family of these proteins adopts a certain mechanism or pathway to direct gene expression by repressing transcription [76]. So far, there are three classes of MBPs, which include the methyl-CpG binding domain protein family (MBD), Kaiso and Kaiso-like proteins and SET and Ring finger Associated (SRA) protein family.

The MBD class is considered to be the largest along all the MBP families. In 1992, the MeCP2 protein was discovered as the first member of the family. Later, another homologs were discovered among which MBD1, MBD2 and MBD4 interact with methylated DNA and contrarily, MBD3, MBD5 and MBD6 do not have any affinity to methylated DNA [77]. These proteins excluding MBD4, MBD5 and MBD6 are linked to transcriptional silencing by forming complexes with histone deacetylase (HDAC) [78]. Another MBD proteins that has been found to contribute in collaborative silencing process through chromatin remodeling complexes and modifications such as BAZ2A and BAZ2B ; SETDB1 and SETDB2 [79].

Kaiso family contains three members capable to recognize methylated CpGs and distinguish it from the unmethylated ones through their zinc finger motif. These members are Kaiso, ZBTB4 and

ZBTB38 [77]. These proteins are able to bind methylated DNA. Kaiso was shown to repress transcription by interacting with nuclear receptor co-repressor (NCoR) complex that contains histone deacetylase, linking with that methylation of DNA sequences to a highly condensed chromatin state [79].

The SRA family contains UHRF1, the founder member and UHRF2 [80] that are known to bind to methylated DNA via their SRA domain. UHRF1 has a preferential binding to hemimethylated CpGs compared to non-methylated ones. This protein directly interacts with DNMT1 and targets it to newly synthesized DNA during replication. The function of this family will be discussed further in the next chapter.

Chapter 3: UHRF1
The faithful partner of DNMT1

The high fidelity by which DNMT1 performs its function in the transmission of methylation marks questions if it is only based on its preference to hemimethylated DNA. In fact, this preference is not sufficient to guarantee the fidelity; which is actually linked also to the interaction of DNMT1 with another protein UHRF1. UHRF1 is a pivotal epigenetic reader that recognizes DNA methylation and guides DNMT1 to the sites that need to be methylated. Additionally, UHRF1 reads the histone code and recruits the enzymes responsible to catalyze the histone marks. In this chapter, we will review the key properties of UHRF1, its different functions and its partnership with DNMT1.

1- UHRF family

The UHRF1 family is composed of three human proteins hUHRF1 ((ICBP90), hUHRF2 (NIRF for "Np95/ICBP90 Ring Finger") and hUHRF3 (ICBP55)) and three mouse proteins (mUHRF1 (NP95), mUHRF2 (Np97) and mUHRF3 (NP55)). The most two studied members are hUHRF1 and mUHRF1 [80].

UHRF1, originally called ICBP90 (inverted CCAAT box binding protein of 90 kDa), was identified in 2000 by the one-hybrid system, as a transcription factor that binds to the inverted CCAAT box of the topoisomerase 2α promoter and participates in regulating its expression [81]. UHRF1, is a 793-amino-acid-long protein with a calculated 90 kDa molecular weight and is encoded by the *UHRF1* gene, which is found to be localized on chromosomal 19p13.3 region [82, 83].

Similarities in amino acid sequences vary between UHRF1 members. hUHRF1 shows 74% similarity with mUHRF1, while it is about 53% between hUHRF1 and hUHRF2. The difference of the two proteins in sequence is also accompanied with a difference in functions on many levels [80, 84]. UHRF2 protein is mapped to chromosome 9p24.1 and it is found to be overexpressed during cell differentiation [85]. On the level of cell cycle progress, hUHRF1 and hUHRF2 have opposite effects, hUHRF2 overexpression induce the cell cycle arrest at G1 phase which is executed through the mechanism regulating Cdk2 activity [86]. Contrary to UHRF1, UHRF2 appears to act as a tumor suppressor gene considering that its upregulation leads to growth arrest [87].

On the level of DNA methylation maintenance, UHRF2 did not show any preferential binding to hemimethylated DNA unless it is bound via its TTD domain to H3K9me3 histone-tail peptides [85]. Structural analysis of UHRF2-SRA in complex with DNA shows that it binds preferentially to 5-hydroxymethylcytosine (5hmc) [88]. Additionally, UHRF2 is not able to recruit the DNMT1 to the replication fork during the S phase of the cycle [89]. hUHRF3 and mUHRF3 lack UBL domain which suggests that they could be involved in different roles, but that still need to be studied further [80].

2- UHRF1 structure

UHRF1 is characterized as a multifunctional and a multistructural protein having five domains (**Fig 12**): a UBL domain for (N-terminal ubiquitin-like domain), a TTD domain for (Tandem Tudor domain), a PHD domain for (Plant Homeo domain), a SRA domain for (Set and Ring Associated domain) and a RING domain for (Really Interesting New Gene domain) [80].

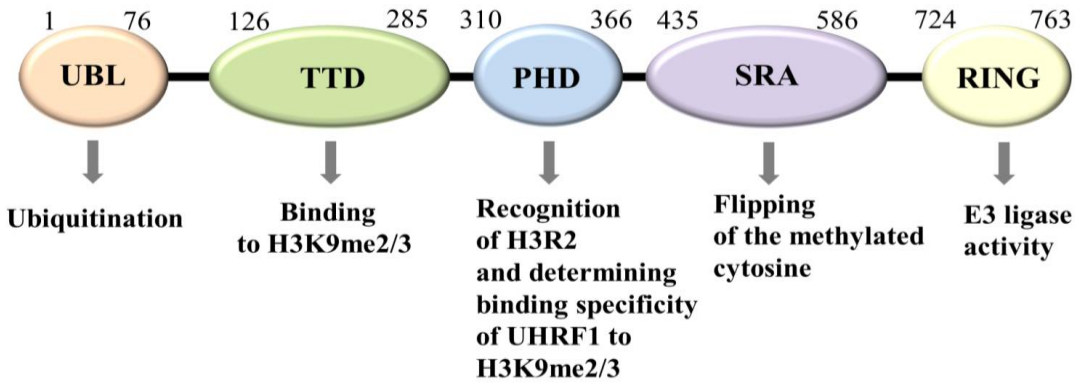

Figure 12. UHRF1 architecture. *The five structural domains of UHRF1 : UBL domain "N-terminal ubiquitin-like domain", TTD domain "Tandem Tudor domain", PHD domain "Plant Homeo domain", SRA domain "Set and Ring Associated domain" and RING domain "Really Interesting New Gene domain".*

- ***UBL domain (N-terminal ubiquitin-like domain)***

UBL domain **(**NIRF_N domain) is located at the N-terminus of UHRF1 and presents an alpha/beta ubiquitin fold. Three of surface lysines, *i.e.*, K26, K33 and K52 of this domain are structurally identical to those of ubiquitin (K29 and K48) [80]; Although the exact role of this domain is not yet fully understood, the 35% homology with ubiquitin, suggests that it could interact with proteasome

and that due to this domain, UHRF1 could also play a role during cell cycle progression, in protein degradation or gene transcription.

- ***TTD domain (Tandem Tudor domain)***

This domain plays a role in reading the histone code. TTD domain contains two subdomains TTD_N and TTD_C**.** TTD domain allows the binding and reading of di-and tri-methylated lysine residues (H3K9me2/3) by UHRF1 via formation of an aromatic cage built by residues F152, Y188 and Y191 of TTD_N [90]. A peptide-binding groove formed between the two subdomains provides a specific binding to H3K9me3 by creating a particular contact to the residues upstream and downstream of the methylated lysine [91].

- ***PHD domain (Plant Homeo domain)***

PHD domain is a Zn-finger domain. It recognizes the N-terminus of the H3-tail only when unmodified. UHRF1 binds in a specific manner via its PHD domain to histones through recognizing the unmodified arginine (R2) and lysine (K4) present on H3 [92]. Although PHD shows preference for unmethylated H3K4, the crystallography shows that it can accommodate H3K4me3 without compromising the complex formation PHD/H3 [93].

- ***Ring domain (Really Interesting New Gene domain)***

RING domain is located at the C-terminus of UHRF1, and presents the only enzymatic activity of this protein, the E3 ubiquitin ligase activity. It is composed of 2 zinc-fingers and a unique α-helix bundle structure. It has been reported that RING domain is responsible for the auto-ubiquitination of UHRF1 as well as the ubiquitination of different epigenetic substrates , a necessary step to regulate their activity and stability [94, 95].

- ***SRA domain (Set and Ring Associated domain)***

In vertebrates, SRA domain is present only in UHRF1 family. SRA domain is known to play a pivotal role in the inheritance of methylation patterns by coordinating various events mainly the recognition of hemimethylated DNA [96-98], the recruitment of DNA methyltransferase 1 (DNMT1) [99] and the interaction with different proteins involved in epigenetic regulation such HDAC1 [100] and histone methyltransferase G9a [101]. During its interaction with DNA, SRA uses the base flipping mechanism [96-98], which is widely used by nucleotide modifying enzymes such as DNA repair enzymes, RNA modification enzymes and DNA MTases [96, 102]. However,

SRA is reported to be the first DNA binding domain using the base flipping process without an enzymatic activity [96].

Recognition of hemimethylated DNA is a main property of SRA domain and it has been determined by three dimensional studies that revealed the structure of SRA in complex with DNA and proposed a model of this recognition [96-98]. After binding to hemimethylated DNA, SRA domain forms a crescent moon-like structure having two loops responsible for the CpG recognition and base flipping. This step was explained by representing SRA as a hand grasping the DNA duplex, where one loop refers to a thumb (444-449 residues) and the other as NKR finger (483-496 residues) (**Fig 13**). After the loss of Watson-Crick hydrogen bonds between the methylcytosine and its paired guanosine, the flipped out methylcytosine fits into the binding pocket of SRA situated in the palm by pi-stacking interactions by the two aromatic residues (Y478,Y466) [96].

To ensure selective binding and specificity for methylated cytosine over the non-methylated one, methylcytosine-binding pocket of the protein has many selective features:

1. It is conferred by a hemisphere of approximately 2 A˚ radius, which exactly fits the methyl group. This methyl-group-binding site is deep within the methylcytosine pocket and with an opposite scenario, when a non-methylated cytosine is being the ligand, the pocket would be occupied by solvent and thus unfavorably hydrated [98].
2. N489 residue, a part of NKR finger, also facilitates the discrimination between the methylated and ummethylated form. NKR makes contacts with the symmetric non methylated cytosine of the DNA duplex and due to sterical clash the presence of a methyl group will prevent it from flipping and therefore impairs the SRA binding guaranteeing the selectivity of the process [98].

In addition to 5-methylcytosine, DNA sequences can undergo another epigenetic modification, which is 5-hydroxymethylcytosine (5hmC), the product of oxidation of 5mC by the TET family [103, 104]. 5hmC sites play an important role in the demethylation process of the DNA. The SRA domain of UHRF1 has been shown to recognize 5hmC and induce its flipping with a similar affinity to 5mc [105]. The relevance of this latter remains elusive but it might bring new insights in DNA methylation maintenance, once resolved.

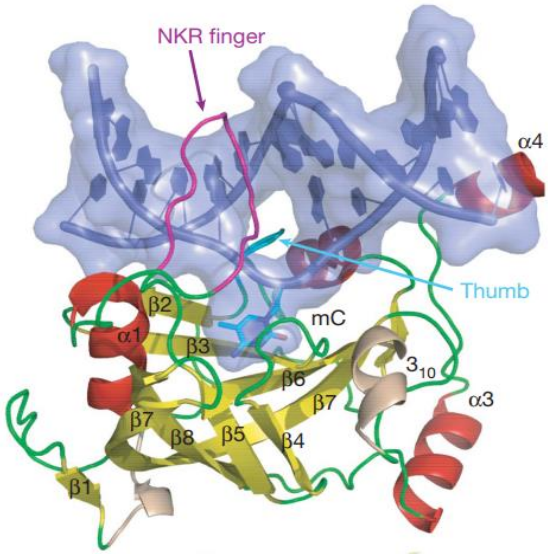

Figure 13. Structure of the domain SRA of UHRF1 in complex with hemimethylated DNA. *The SRA domain is shown with flexible loops, b-strands and a-helices are represented in green, yellow and red, respectively. The DNA duplex is shown with backbone atoms and bases in blue color. 'mC' corresponds to the flipped, methylated deoxycytidine (C6). The resulting hole in the DNA is partially filled by the NKR finger (magenta) and the thumb (a1–b2 loop). Adapted from ref [98].*

3- Roles of UHRF1

3.1- UHRF1 as regulator of DNA and histone methylation

In 2007, Bostick et al. discovered another pathway to promote efficient DNA methylation maintenance in mammals in which UHRF1, the faithful partner of DNMT1, is required for DNMT1 targeting. UHRF1 colocalizes with PCNA and DNMT1 at the replication fork during mid-to-late S phase with a preferential binding to hemi methylated DNA following by a flipping of the methylated cytosine [96, 97, 106, 107]. Then, UHRF1 directly interacts with DNMT1, via SRA domain, and recruits the enzyme to the specific sites of the genome to methylate the daughter strand of the DNA during cell division (**Fig 14**). Many findings support the importance of UHRF1 in DNA methylation maintenance. Experimental observations show that after UHRF1 knockout in ES cells, DNMT1 lost its association to chromatin [106, 107]. Moreover, UHRF1-deficient embryos showed a wide loss in global methylation with a subsequent death after gastrulation [107].

Later, it was found that not only SRA is responsible for the targeting of DNMT1, but also two other domains of UHRF1, the tandem tudor domain (TTD) and the plant homeodomain (PHD). These two domains coordinate the recognition of histone marks, and play an essential role in guidance of DNMT1 to DNA and subsequent maintenance of DNA methylation.

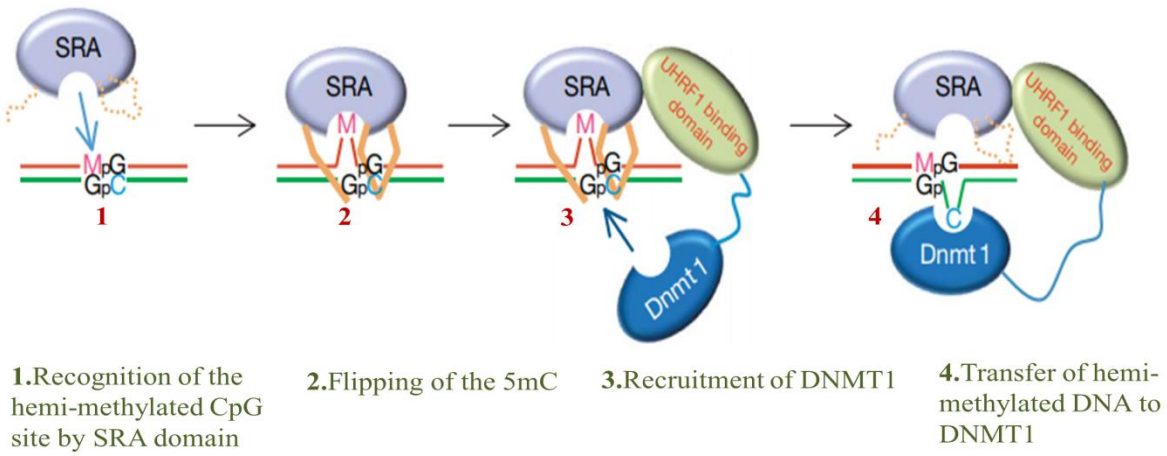

Figure 14. Schematic model for maintenance of DNA methylation patterns between UHRF1 and DNMT1. *Adopted from ref [97].*

TTD domain binds histone 3 tails methylated at lysine 9 (H3K9me3), and unmethylated lysine 4, which helps UHRF1 to localize to heterochromatin and maintain DNA methylation [108, 109]. Mutated TTD domain remarkably abolished these two functions, by preventing the binding of UHRF1 to H3K9me3 [108, 109]. While PHD domain is known to bind to H3 tails unmodified at arginine 2 (H3R2) [110, 111], a disruption at the level of this binding lead to abolish DNA methylation by DNMT1 in cells [95]. Currently, it has been also demonstrated during the differentiation of ES cells, that regulation of levels of UHRF1 and H3K9me2, controls the methylation on a global scale by affecting the recruitment of DNMT1 to the replication fork [112].

UHRF1 is recognized to act as a prerequisite targeting factor of DNMT1, beside the described mechanism, UHRF1 is also capable to stimulate the catalytic activity of DNMT1 by the removal of RFTS plug from the catalytic pocket of the enzyme and prevents the auto-inhibition driven by it [57, 58]. Moreover, recent studies showed a cooperative interplay between DNMT1 and UHRF1 chromatin interactions. The ubiquitination of H3 at K18 and K23 through UHRF1's RING domain during S phase possesses a stimulating effect on DNMT1 function since the enzyme shows a preference to ubiquitinated H3 [94, 95]. Mutants of UHRF1 presenting a catalytically inactive RING domain were not able to recruit DNMT1 to DNA replication sites [94]. Finally, UHRF1 also regulates DNMT1's stability due to its involvement in the ubiquitination of DNMT1. All this validates that UHRF1 regulates the behavior of DNMT1 in terms of recruitment, stability and activity.

3.1.1- UHRF1 spatial control dynamics

Given that UHRF1 contains several domains responsible for chromatin modifications and recognition, the question remains whether these domains synchronize with each other or act independently? Recent studies have shown that UHRF1 undergoes some changes in its conformation that are mostly established by its linker region situated between the TTD and PHD domain and spacer region situated in the C terminal part between SRA and RING domain (**Fig 15A**).

As we stated in previous parts, TTD and PHD domains provide the necessary readout of the chromatin signature within the histone H3 tail that is essential for the UHRF1-directed epigenetic inheritance of DNA methylation. At this level, the hemi-methylated DNA plays a key role in the recognition of the histone tail, by controlling both TTD and PHD domains and leading UHRF1 to acquire different conformational changes important for its activity [113].

In the absence of hemi-methylated DNA (**Fig 15B**), the closed form of UHRF1 inhibits the reading of the histone marks and the recruitment of DNMT1. This happens when the spacer between SRA and RING domain binds to TTD resulting in an inhibition of interaction of the TTD-PHD linker; consequently, recognition of H3K9me3 will be inhibited. Additionally, SRA domain will bind to PHD, which will hinder the recognition of unmodified R2 at the N terminal of H3 [113].

On the other side, the opened form of UHRF1 induced by the presence of hemimethylated DNA (**Fig 15C**), is the conformation at which UHRF1 can perfectly bind to histone tail for ubiquitylation and subsequent DNA methylation [113]. In its open form, the spacer is no longer associated to TTD facilitating the binding to DNA, and the linker binds to TTD authorizing TTD-PHD to interact with H3K9me3.

Taken together, these observations underlie the major role of the spacer region of UHRF1 and its involvement in regulating UHRF1 states by three steps:

1- Inhibition of interaction between closed-form UHRF1 and H3K9me3.
2- Mediation of interaction between SRA domain and RFTs part of DNMT1.
3- Recognition of hemimethylated DNA by SRA and facilitating heterochromatin localization of UHRF1.

Other than hemi-methylated DNA, various factors can also actively participate in UHRF1 different states such as allosteric ligands, PMTs and binding partners. For instance Gelato et al. suggested that Phosphatidylinostiol (PI5P) can bind to spacer region of UHRF1 and allosterically activate the protein by liberating the spacer from the peptide binding groove of the TTD domain, which allows UHRF1 to associate better to heterochromatin [114]. Synergically, another mechanism mediated by USP7 can also shift UHRF1 from the closed form to the opened one by the disruption of the intramolecular TTD-Spacer interaction promoting chromatin binding [115].

Taken that these modulations in UHRF1 forms affect widely the regulatory processes of the protein and consequently chromatin status, any aberrancy at the stated level can be seriously reflected by abnormal outcomes such as oncogenesis.

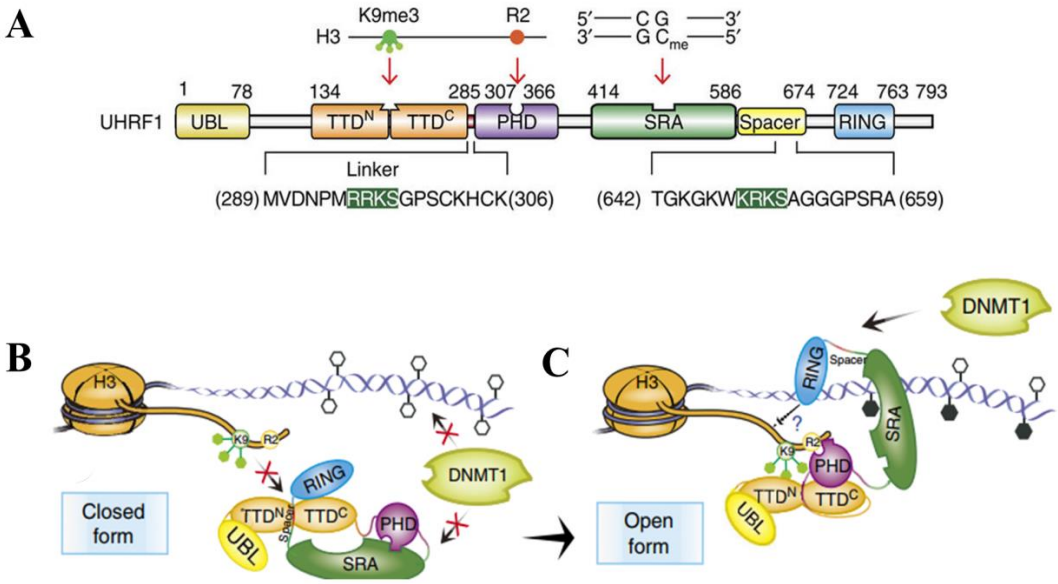

Figure 15. Illustration of the model for recognition of histone tails facilitated by hemimethylated DNA. A) *UHRF1 functional domains showing in addition the Spacer and the Linker. The highlighted residues in green bind to TTD domain.* ***B)*** *The two conformational states of UHRF1 mediated by hemimethylated DNA as described previously. Adapted from ref [113].*

3.2- UHRF1 as stability coordinator

The really interesting new gene (RING) domain of UHRF1 is linked to E3 ubiquitin ligase activity that is involved in many regulatory processes. This includes its auto-regulation since UHRF1 has an auto-ubiquitinylation function [116-118]. Besides, findings have shown that UHRF1 is a key player in a macromolecular complex with other actors Tip60, HDAC1 and USP7 that control DNMT1

levels and stability. Tip60, a histone acetyltransferase, acetylates DNMT1 and triggers UHRF1 to ubiquitinylate DNMT1. Hence, this process leads to DNMT1 degradation through a proteosomal dependent pathway [119, 120]. On the opposite side, USP7 (Ubiquitin Specific Protease) acts as a protector, it interacts with DNMT1 and UHRF1, allowing the de-ubiquitinylation of both proteins and save them from degradation by the proteasome [99, 118-121]. Accordingly, the ubiquitin status of DNMT1 and UHRF1affects the stability of both proteins, which is directed by USP7 and UHRF1. HDACs also played a protective role toward DNMT1 by deacetylation (**Fig 16**).

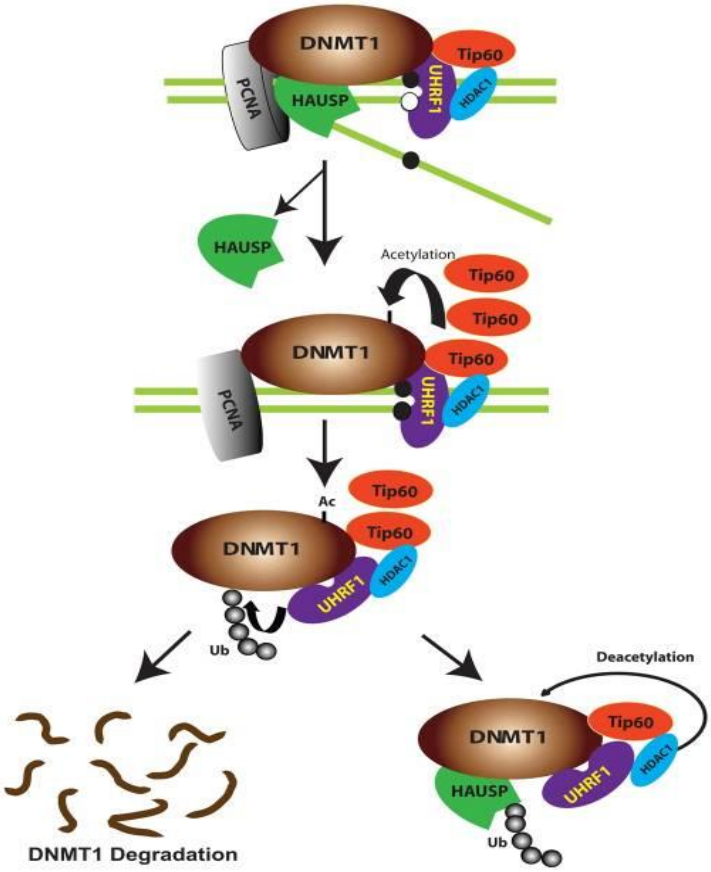

Figure 16. Regulation of DNMT1 stability. *DNMT1 interacts with HAUSP, Tip60, UHRF1, HDAC1, and PCNA. Throughout the cell cycle, actors of this complex exert their role as either destroyer either protectors of DNMT1. When DNA methylation is completed during S phase, DNMT1 degradation results from dissociation of HAUSP. Furthermore, acetylation levels of DNMT1 increase due to an increased level of Tip60 which triggers a UHRF1-driven ubiquitination of DNMT1. These events lead to degradation of DNMT1 by the proteasomal pathway. Conversly, HAUSP and HDAC1, protectors of DNMT1, induce de-ubiquitination and deacetylation respectively, thus preventing DNMT1 from degradation. Adopted from ref [122].*

Recently, Zhang et al. showed that USP7 also maintains the stability of UHRF1 by another way than its deubiquitination. UHRF1 mutants with the disrupted ability to bind to USP7 lost their capacity to autoubiquitination and to bind chromatin in HeLa cells [115].

In the model shown in (**Fig 16**), Du et al. proposed that the processes controlling DNMT1 regulation are cell cycle dependent. The actors of the macromolecular complex associate with PCNA and localize at the replication fork. As S phase ends and G2 phase starts, after the completion of methylation, DNMT1 is no longer protected. A chain of events promotes DNMT1 degradation; first, USP7 is dissociated from DNMT1. Second, increased levels of Tip60, triggers an increased acetylation of DNMT1. These events consequently induce UHRF1 to ubiquitinate DNMT1 [120].

On the other hand, UHRF1 regulation through USP7 is also cell-cycle dependent. During M phase, a phosphorylation event occurs on the serine 652 (S652) of UHRF1 at the interacting region with USP7. This event driven through CDK1-cyclin B regulates UHRF1 by affecting its stability. As a result, UHRF1 is dissociated from USP7 and subsequently undergoes proteosomal degradation [121].

3.3- UHRF1 and DNA repair

After exposure to different environmental agents or chemotherapeutic agents, cellular DNA can undergo lesions caused by chemical modification leading to mutations or/and cell death. Many of these lesions, can produce covalent adducts with DNA bases on both strands of DNA, forming interstrand cross-links, that blocks replication, and are considered to be one of the most toxic DNA damages [123] . In order to survive, many DNA repair mechanisms exist to fix this event. UHRF1 acts as a common actor in the multiple DNA damage response pathways and helps to maintain genomic stability [124]. The hindrance of DNA replication after exposure to camptothecin was fixed after interaction of RING finger of UHRF1 with the DNA repair enzyme Eme1 [125]. UHRF1 was associated with DNA interstrand crosslinks (ICLs) in vivo and *in vitro,* which highlights its feature for being a sensor of ICLs. SRA domain recognizes and recruits UHRF1 to ICL, which facilitates the recruitment of the key Fanconi anemia group D2 protein (FANCD2) to initiate the DNA repair [126]. Also, it has been suggested that UHRF1 interacts with nucleases, and this might be important for its function in the ICL lesions repair process [127].

4- UHRF1 cellular expression

UHRF family member's expression varies widely upon different tissues and species. UHRF1 levels seem to be related to cell proliferation. Actually, UHRF1 mRNA was found to be most abundant in proliferating tissues and/or in non-differentiated ones such as bone marrow, thymus and fetal tissues. In contrast, extremely differentiated tissues such as central nervous system and peripheral leukocytes, have no UHRF1 mRNA at detectable levels [80, 81].

It is evident that UHRF1 is co-localized in nucleus. The expression patterns of UHRF1 in normal cells, is cell-cycle dependent, and it is having two peaks, the first one is at late G1 phase and another during G2/M phase. Conversely, in cancer cells, UHRF1 expression does not fluctuate during the cell cycle, and remains constantly overexpressed through the phases [128, 129]. This overexpression was correlated with development and progression of multiple tumors as hepatocellular carcinoma [122], breast cancer [117], gastric cancer [130], colorectal cancer [131], gallbladder cancer [132], bladder cancer [133], prostate cancer [134], non-small cell lung cancer [135], and laryngeal squamous cell carcinoma [136].

5- Regulation of UHRF1 and cell cycle

UHRF1 regulation is known to be achieved through different signaling pathways. Triggering these pathways is often associated with a decrease in UHRF1 levels with subsequent outcomes on cell growth and apoptosis.

In Jurkat T cells, ERK1/2 signaling pathway was responsible to control cell proliferation through downregulation of UHRF1 expression. The involvement of this pathway was assumed after blocking ERK1/2 that resulted in reduced levels of UHRF1 [137]. Another pathway that controls UHRF1 regulation is the p53/p21Cip1/WAF1 checkpoint signal activated upon DNA damage. After treating with Adriamycin, UHRF1 levels were decreased in $p53^{+/+}$ HCT116 cells and not in $p53^{-/-}$ cells indicating the contribution of this checkpoint besides the p21 Cip1/WAF1 expression, in UHRF1 downregulation and consequently in cell cycle arrest at G1/S phase.

p73 pathway was also shown to interfere in the regulation of UHRF1. Treatment of p53-deficient acute lymphoblastic leukemia (ALL) Jurkat cells with thymoquinone, regulated the levels of UHRF1 after the activation of p73 dependent pathway leading the cells to undergo a cell cycle arrest at G0/G1 phase and to enter in apoptosis [138]. Both pathways p53 and p73, could decrease UHRF1 levels by either transcriptional repression or protein degradation.

The gene promoter activity of UHRF1 was blocked upon the activation of T cell receptor (TCR) pathway leading to UHRF1 downregulation. Through chromatin remodeling processes, this event downregulates the gene expression involved in G1/S transition, hinders the cells to enter S phase and therefore stimulates them to apoptosis [139].
Although many studies highlight the role of UHRF1 in apoptosis and correlate its expression levels with cell cycle arrest, the molecular mechanisms governing these processes need to be elucidated.

Cell cycle progression is regulated by the activation of Cdk-cyclin complexes. As cells progress from G1 into S phase of the cell cycle, the retinoblastoma tumor suppressor protein, RB, is regulated by phosphorylation, through cyclin-dependent kinases. In case of Prb hyperphosphorylation, it will be disrupted from E2F-1, an essential transcription factor involved in G1/S phase transition. UHRF1 gene promoter is having transcription factors binding sites that allow it to be itself regulated by other transcription factors. For instance, UHRF1's promoter contains three E2F binding sites which explains why its transcriptionally regulated by E2F-1 and its role in cell cycle transition seems to be controlled by this family of transcription factors [100, 129, 140].
UHRF1 regulation is tightly associated to its phosphorylation PKA (protein kinase A) has been also involved in UHRF1 phosphorylation through cAMP pathway. This pathway enhances binding of UHRF1 to ICB2 promoter of the TopoII alpha gene, which will be activated and thus will promote G1/S phase transition [141].

UHRF1 expression is found to be also regulated by microRNAs especially in cancer cells. UHRF1 overexpression is associated with decreased levels of few miRNAs that act as TSGs, thus high levels of UHRF1 during tumors could be attributed to aberrant expression of miRNA [142, 143]. For example, in gastric cancer the high levels of miR-146a/b lead to UHRF1 repression with activation of TSGs such as RUNX3 through hypomethylation of their promoter [130]. In highly metastatic lung cancer, miR-193a-3p reduced the levels of UHRF1 and consequently controlled metastasis [144].

6- UHRF1 partners:

As discussed previously, UHRF1 is involved in different roles and it collaborates with many epigenetic partners in order to regulate DNA methylation and histone modifications status. Among

these partners we can list histone methyltransferases, histone demethylases, histone acethyltransferases, deacetylases and many others that has been represented in (**Table 1**).

6.1- Tip60:

One of the main interacting partners of UHRF1 is Tip60. These two proteins have been found to belong to the same macromolecular complex [145], interacting together and thus regulating the activity and the stability of other proteins.

Tat Interacting Protein 60kDa, known as Tip60, is a well-categorized histone acetyltransferase from the MYST family that can also be referred as lysine acethyltransferase 5 (KAT5) [146]. It is a multi-structural protein presenting at its N terminal part a conserved chromodomain, which is able to read active or repressive methylated lysines. While at its C terminal part, it has the MYST domain which has an enzymatic function mainly driven by the HAT subdomain, responsible for the acetyl transferase activity [147]. Tip60, through its acetylating activity, plays an important role in various functions as transcription regulation, chromatin remodeling, DNA damage activation and cell cycle regulation [148-150]. Tip60 is also involved in p53-mediated apoptosis and cell cycle arrest where it has been shown that it interacts directly with UHRF1 via SRA-RING domain and negatively regulates the downstream signaling of p53 thus promoting oncogenesis [151]. Dai et al. showed that decreased levels of UHRF1 induces the p53 activation mediated by Tip60, leading to activation also of PUMA and p21 which triggers cell cycle arrest and apoptosis.

Interacting Partner	Function
DNMT1	Facilitates and maintains DNA methylation
G9a	Catalyzes di-/tri-methylation of H3 at lysine 9 which represses the transcription of its target genes
DNMT3a and DNMT3b	De novo methylation
HDAC1	Deacetylates histones and represses gene expression due to heterochromatin formation
TIP60	Regulates acetylation of H2A on lysine 5 and H4 on lysines 5,8,12,
SUV39H1	Histone methyltransferase responsible for maintaining transcriptional repressive state of genes by inducing tri-methylation of H3K9
EZH2	Histone methyltransferase responsible for maintaining transcriptional repressive state of genes by inducing tri-methylation of H3K27 Vital for faithful propagation of DNA methylation patterns by maintaining 5mC levels
JMJD6	Demethylates the methylated lysyl residue of H2A/H2B and H3/H4 via 5-hydroxylation
β-TrCP1	F-box protein which plays an important role in regulating ubiquitinylation of UHRF1 by targeting UHRF1 toward the SCF (SKP1–CUL1–F-box protein) E3 ligase complex
PARP-1	Helps in stabilizing the interaction of UHRF1 with DNMT1 and controls transcriptional silencing by maintaining H4K20me3 (repressive mark) at the pericentric heterochromatin
MBD4	involved large-scale reorganization of heterochromatin

Table 1. Interacting partners of UHRF1. *Adopted from ref [142].*

Chapter 4: Cancer epigenetics
From mechanism to therapy

1- Global burden of cancer

Cancer is a major public health problem; it is one of the leading causes of morbidity and mortality worldwide. Globally, nearly 1 in 6 deaths is due to cancer with an estimated number of 8.8 million deaths in 2015. The incidence is expected to rise for about 70% over the next two decades and in some parts of the world, it is probable to become the number one killer. High incidences are associated to unhealthy life styles which include limited physical activity, smoking and poor dietary habits [152].Estimations indicate that by 2030 the number of new cases will reach 23.6 million each year.

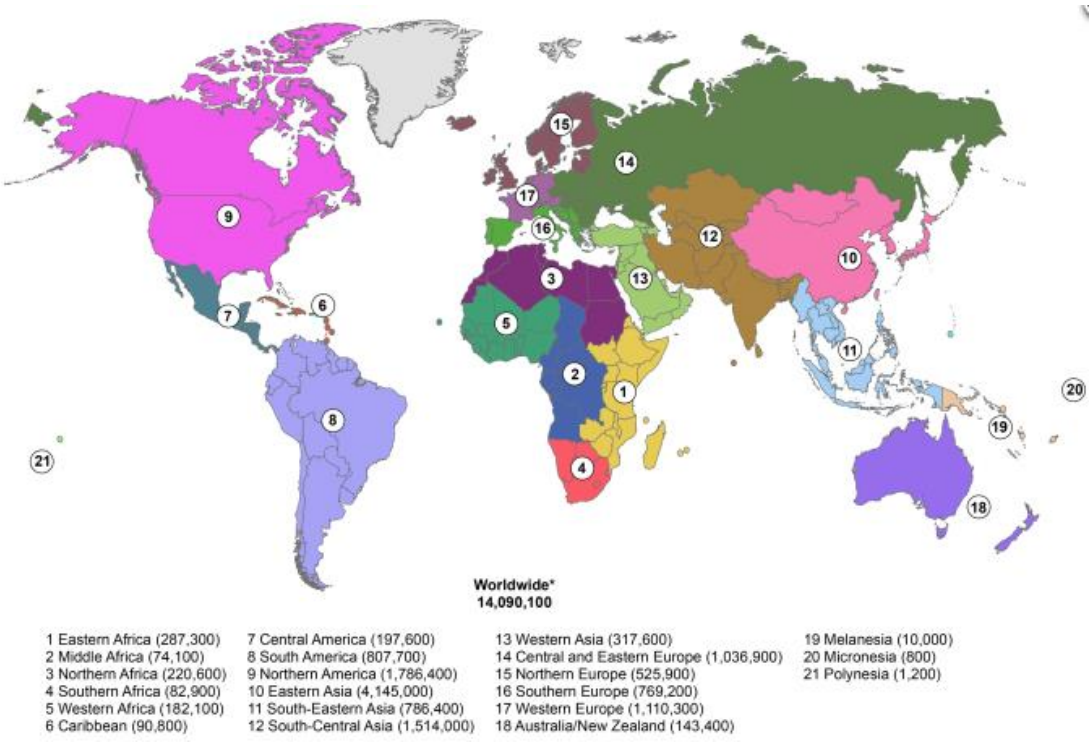

Figure 17. Estimated number of new cancer cases by world area. Source: GLOBOCAN 2012

Cancer is a group of diseases, characterized by an uncontrolled and anarchic cell growth with a potential to invade progressively the surrounding tissues and destroying them. It is known to be triggered by a complex interaction of genetic and environmental factors. Following a mutation, normal cellular functions are disrupted causing a dysregulation of the signaling pathways that

governs the control of cell growth, DNA repair and apoptosis [153].There is around 200 types of tumors that can affect all the tissues of the body [154].

2- Cancer epigenetics

Human cancers can take hundreds of different forms depending on the site, cell of origin and spectrum of genomic alterations that promote tumorogenesis. However, the different discoveries related to epigenetic markers, tend to prove that apart from classical genetic pathways, mutations on the level of epigenetic landscape (**Fig 18**) play an important role in tumor initiation and progression [153]. The reprogramming of epigenetic processes such as DNA methylation, chromatin remodeling and non-coding RNA by various factors can lead to malignant cellular transformation by abnormal activation of oncogenes, repression of tumor suppressor genes and dysregulation of non-coding RNAs [155, 156]. Tumor cells not only can be activated by epimutations but also consistently use epigenetic processes to ensure their escape from chemotherapy [157]. Therefore, it is evident that recent efforts in drug discovery have been implemented on pharmacological targeting of aberrant states of epigenome, as a way to reverse the cancer-specific epigenetic abnormalities. In this chapter, we will introduce the epigenetic drivers of cancer and the existing epigenetic therapies.

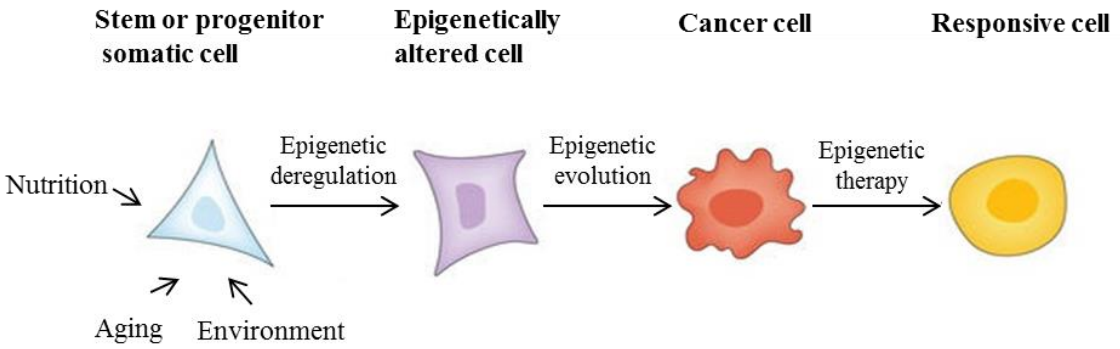

Figure 18. Somatic inheritance of acquired features in cancer. *Normal cells can undergo epigenetic alterations induced by many factors in addition to the inherited epimutations through the germline. Epigenetic therapy can restore the epigenetic abnormalities and increase the sensitivity of available treatments. Adopted from ref [157].*

3- Epigenetic dysregulations in cancer

In normal state, the complete epigenetic machinery coordinates together to reach the active chromatin conformation and the proper levels of accessibility in order to normally express the gene. However, during oncogenesis an epigenetic switch occurs, the regulatory mechanisms of the

epigenetic complex are altered resulting in an abnormal state and dysregulation of gene expression. Besides the contribution of each of the described abnormalities, cancer can also be associated to an interplay between aberrant DNA methylation, histone modifications and non-coding RNA.

3.1- Dysregulation of miRNAs in cancer

New evidences from studies show that dysregulations in expression profiles of miRNAs achieved through epigenetic alterations are related to tumorogenesis. Upon their target genes, miRNAs can act as either tumor promotors or suppressors. Many oncogenic miRNAs are often upregulated in cancer, for example, in human glioblastoma, mi-R21 that targets PTEN, is found to be upregulated. In contrary to oncogenic mi-RNA, tumor suppressor miRNAs are often repressed in cancer, for example in lung cancer, *let*-7 that targets the oncogene RAS is downregulated [19]. Some miRNAs also regulate the expression of epigenetic effectors (DNMTs) that are identified to be dysregulated in cancers [158].

3.2- Changes in histone modifications in cancer

The organization of histone PMTs can undergo several changes and many studies allied that with cancer due to the subsequent aberrations in gene expression.

On the level of the acetylation of histones, global alterations were related to tumor progression, for example, hypoacetylation mediated by HDACs, especially on H4-lysine 20 trimethylation (H4K20me3) and lysine H4-lysine 16 (H4K16ac) was responsible for the repressive state of the gene [159]. Besides that, it is known that levels of HDACs are frequently found upregulated in many types of tumors [160, 161], which made them an essential target for epigenetic-based therapy. In the same context, HATs that maintain histone acetylation levels can also be dysregulated in cancer.

Additionally, cancer cells exhibit aberrancies on the level of histone methylation. Alterations on methylation levels in H3K9 and H3K27 contribute in gene repression and are widely associated with cancer formation [162]. Moreover, dysregulation of HMTs was also responsible for silencing of tumor suppressor genes. For example, G9a, which is the H3K9 HMT was found to be overexpressed in hepatocellular carcinomas and could possibly promote malignancies via modulation of chromatin state [163, 164]. Moreover, increased levels of EZH2, the H3K27 HMT, has been found in prostate and breast cancer [165]. In addition to HMTs, lysine specific demethylases can also be involved in cancerogenesis such as LSD1. LSD1 can have two functions,

it acts either as a corepressor either as a co-activator, a feature which makes targeting HDMs a challenging but promising strategy in cancer treatment [19].

3.3- Aberrant DNA methylation

DNA methylation is the first altered epigenetic mark that has been identified and that is tightly associated to cancer initiation and development. In cancer cells, the two major and opposing altered methylation patterns are global DNA hypomethylation and hypermethylation of CpG islands on specific genes.

Multiple lines of evidence have revealed that global loss of methylcytosine (e.g., at repetitive elements, introns and retrotransposons) [166] plays a key role in different stages of cancer formation and metastasis in distinct tumor types such as cervical, prostate and brain cancers [167-170]. Moreover, the most familiar phenomenon related to loss in global DNA methylation is the upregulation of proto-oncogenes and growth factors that subsequently results in diverse events ranging from genomic instability, genetic mutations, to reactivation of cancer related genes [170-172].

Hypermethylation of promoter areas in CpG islands of TSGs is considered a hallmark of cancer. In contrary to hypomethylation that leads to genomic instability and activation of proto-oncogenes, site-specific hypermethylation is linked to tumorogenesis by silencing the expression of TSGs**.** CpG island hypermethylation has been described in almost every tumor type. In 1989, Greger et al. made the first discovery of methylation in a CpG island of the Retinoblastoma (Rb), a tumor suppressor gene in a human cancer [173].

Over the past 20 years, many of candidate TSGs has been characterized and identified for being hypermethylated and silenced in cancer. Different TSGs responsible for several cellular pathways such as cell cycle ($p15^{INK4b}$, $p14^{ARF}$), DNA repair (hMLH1, MGMT), apoptosis (DAPK) and angiogenesis are hypermethylated at their promotors during oncogenesis (**Table 2**). For example, promoter hypermethylation of p16/CDKN2A gene that is responsible for cell cycle control in various tumors [174]. In addition, the p73 gene, which is related to p53 was found to be hypermethylated in many cases of lymphomas [175]. The consequence of this aberrant state is reflected through processes of transcriptional silencing and gene inactivation leading to tumor development.

Aberrant methylation patterns have been frequently associated with alterations on the level of actors of methylation machinery. For example, DNMT1 levels were overexpressed in various cancers and presented mutations [176, 177]. High levels of UHRF1 have also been associated with deactivation of many of TSGs [178].

Gene/gene product	Functions	Tumor type
Rb	Cell cycle regulation	Retinoblastoma
APC	Wnt signal transduction	Colorectal and other
P14/ARF	Cell cycle regulation	Colorectal cancer
P15/CDKN2A	Cell cycle regulation	Leukemias
P16/CDKN2A	Cell cycle regulation	Various cancers
BRCA1	DNA repair	Breast, ovarian cancer
VHL	Tumor suppressor	Renal cell cancers
hHMLH1	DNA mismatch repair	Colorectal,gastric,endo metrial cancers
ER-alpha	Estrogen receptor alpha	Breast,colorectal,other cancers

Table 2. Hypermethylated genes in various types of tumors. *Adopted from ref [174].*

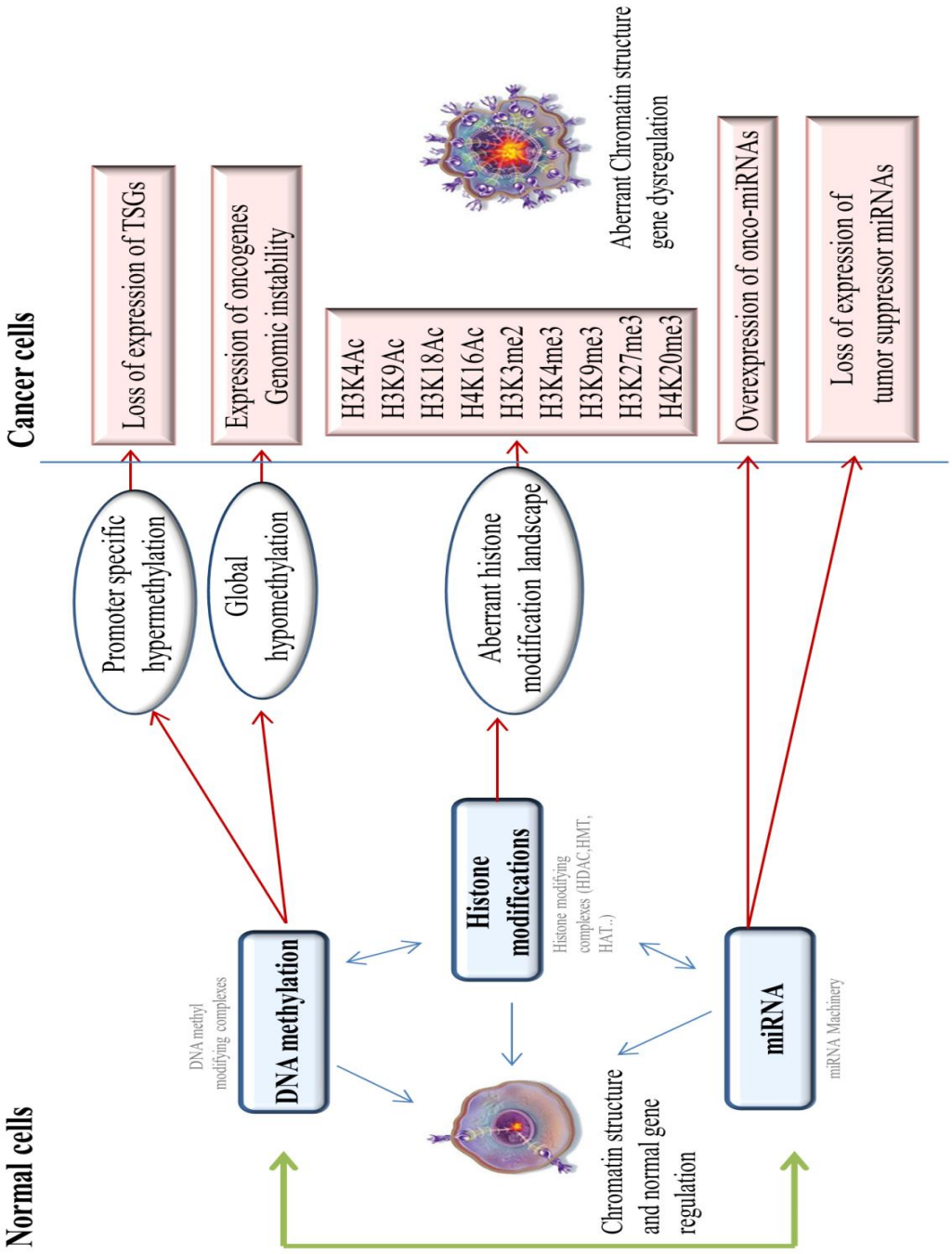

Figure 19. Alterations in epigenetic machinery during cancerogenesis. *Adopted from ref [177].*

4- Epigenetic therapy

The last few decades were crowned with successful progress in the field of epigenetics and human cancers. The understanding of cancer epigenome has provided valuable visions of the molecular mechanisms involved in cancerogenesis and possible ways of targeting them. Epigenetic modifications are known for their reversibility, a central characteristic that makes epigenetic therapy a promising strategy to restore the abnormal epigenetic landscape that occurs in cancers. Recently, many epi-drugs such as HDAC inhibitors, DNMT inhibitors, HMTi, SIRTi, HATi and various kinds of kinases have been discovered (**Fig 20**). These drugs are able to target the epigenetic machinery and re-establish the normal state of DNA methylation and histone modifications in oncogenesis.

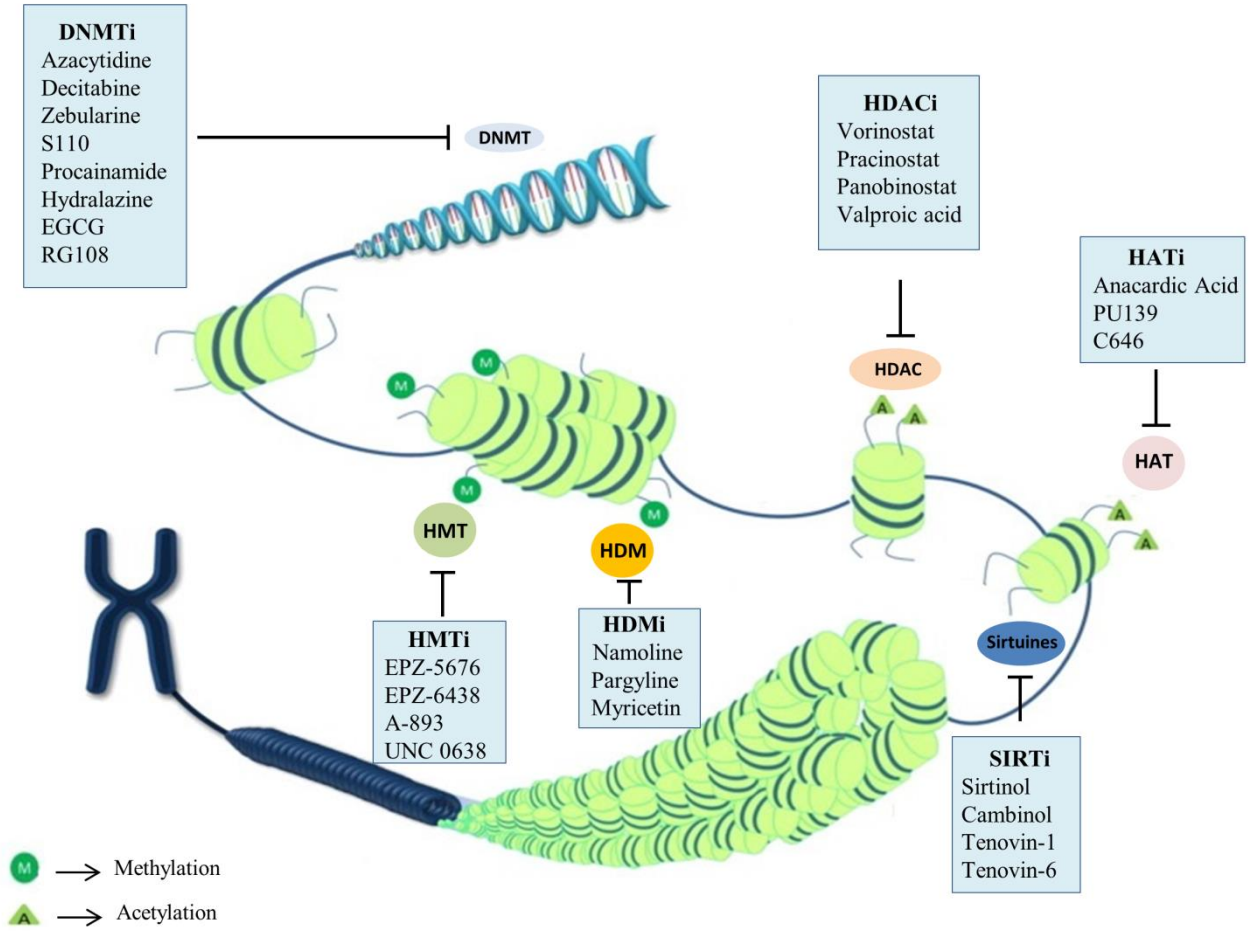

Figure 20. Classification of epigenetic drugs according to their epigenetic target*. This illustration represents the various inhibitors having the FDA approval or undergoing clinical trials. Other possible targets of epigenetic machinery are also available. Adopted from ref [27].*

5- Anti-cancer drugs targeting the UHRF1 complex

As mentioned previously, cancer epigenome can be targeted through different pathways by regulating or inhibiting a variety of epigenetic proteins and enzymes. Our study is focused on targeting UHRF1 protein, which is a part of a large regulatory complex (**Fig 21**). In this section, we will present the existing anti-cancer drugs that target partners of the complex and highlight the potential of UHRF1 as new therapeutic target.

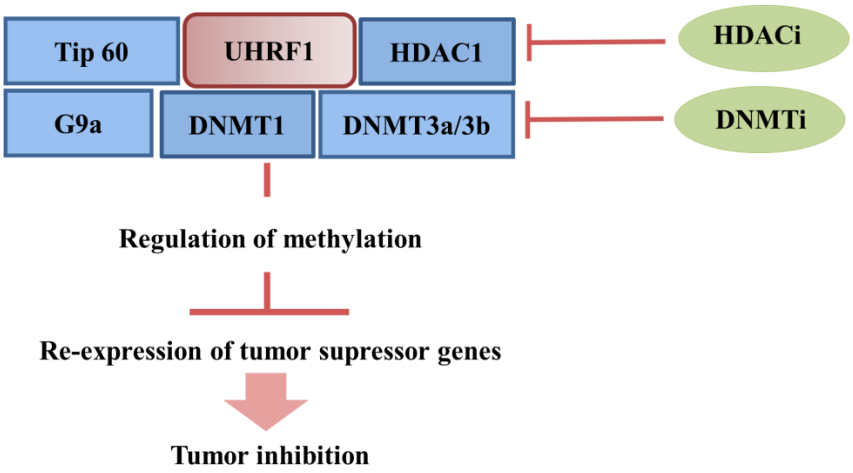

Figure 21. Representative scheme of members of UHRF1 complex. *This complex contains different histone modulators such as Tip60, G9a and HDAC1 and DNA methyltransferases. The complex acts as a suppressor for the expression of TSGs inducing tumor growth. Adopted from ref [179].*

5.1- HDAC inhibitors

One of the reported players of the UHRF1 complex is HDAC1 that could be recruited by UHRF1 to enhance heterochromatin formation and TSGs suppression through deacetylation of histones [100]. It is widely known that disturbing the balance of histone acetylation in cells can be associated with cancer development and progress of oncogenic events.

Class I	Class II	Class III	Class IV
HDAC 1,3 ,8	**IIa** : HDAC 4,5,7,9 **IIb** : HDAC 6 ,10	Sirtuines family (SIRT1-7)	HDAC 11

Table 3. The HDAC family.

The HDAC family is constituted of several members (**Table 3**) and its classification is based on cellular localization and cofactor dependence. HDACs are found to be overexpressed in different types of cancer, which explains the interest in developing HDAC inhibitors. There are four general categories of HDAC inhibitors that are hydroxamic acids, benzamides, cyclic peptides, and aliphatic fatty acids. In terms of inhibition, the benzamides present classI specificity while other categories of inhibitors has broader spectrum [180]. The plethora of anti-cancer effects exhibited by HDAC inhibitors are cell cycle arrest in G1 and G2M phases, induction of apoptosis and cell differentiation. However, they can also show an inhibitory effect on angiogenesis and metastasis, and enhance the resistance of cancer cells to chemotherapy [181]. Although being effective on cancer cells, it was reported that HDAC inhibitors are presenting side effects that could be due to non-specificity. In fact, many of them target the whole family or few members of the family instead of targeting a specific HDAC [182].

In 2006, Vorinostat (formerly called SAHA) a hydroxamic acid derivative, was the first FDA approved HDAC inhibitor for the treatment of cutaneous T cell lymphoma (CTCL). The three other FDA approved HDAC inhibitors are Romidepsin, Belinostat and Panobinostat (**Table 4**) used for treatment of different types of lymphomas and hematological malignancies [183].

HDAC inhibitor	Clinical Trial Phase
Entinostat	III
Mocetinostat	II
Panobinostat	FDA approved
Belinostat	FDA approved
Givinostat	II
Vorinostat	FDA approved
Romidepsin	FDA approved
Valproic acid	II
Butyrate	II

Table 4. HDAC inhibitors with associated clinical trial phase.

5.2- DNMT1 inhibitors

It has been stated that UHRF1 is the loyal partner of DNMT1. UHRF1 interacts with both *de novo* and maintenance DNMTs to methylate cytosine in DNA strands. DNA methylation inhibitors were among the first epigenetic drugs used as a therapeutic strategy in cancer. DNMT1 inhibitors are classified into two groups: nucleosides and non-nucleosides analogues.

5.2.1- Nucleoside analogues

- ***Azacytidine and Decitabine***

The two oldest known nucleoside analogues are Azacytidine (5-azacytidine) and Decitabine (5-aza-2'-deoxycytidine), they are both FDA approved for myelodysplastic syndromes (MDS) and chronic myelomonocytic leukemia. Commercially, they are available under the trade name of Vidaza® and Dacogen™. Although these two demethylating agents present similar therapeutic effect but they differ by their mechanism of action in tumors. For instance, Decitabine intercalates into DNA in place of cytidine during S phase while azacytidine intercalates DNA and RNA. Almost 20% of intracellular azacytidine is incorporated into DNA after its conversion to decitabine by ribonucleotide reductase (**Fig 22**) [184].

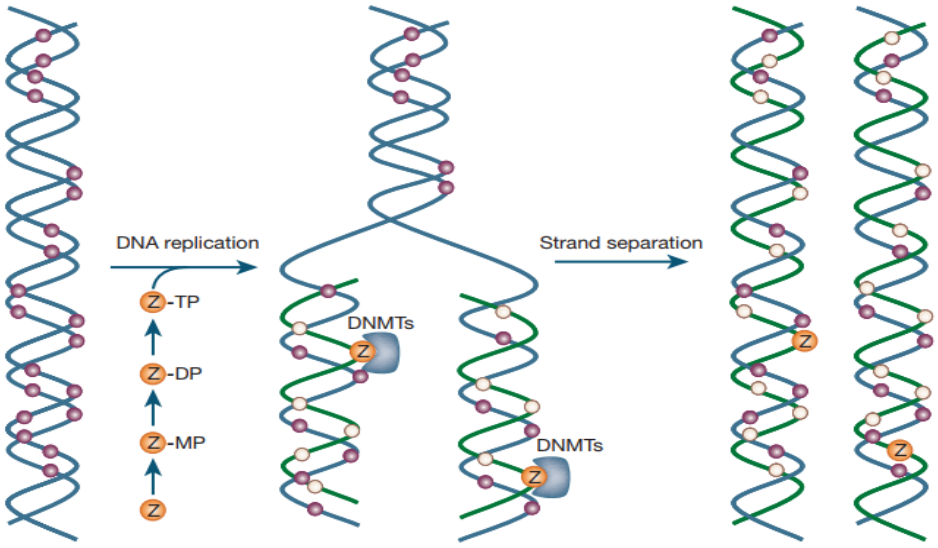

Figure 22. Mechanism of action of nucleoside analogues. *Z corresponds to 5-aza-2-deoxycytidine which is converted into the triphosphate during replication and is incorporated into DNA in place of cytosine. Once incorporated in DNA, it will trap DNMTs by covalent bonding, leading in its depletion and subsequent demethylation of DNA. Purple circles correspond to methylated CpG; yellow circles correspond to unmethylated CpG. Adapted from ref [185].*

The remaining azacytidine incorporates into RNA [186]. The intercalation into DNA will form a covalent bond with DNMT1, eventually leading to its proteosomal degradation [187]. As a consequence, DNMT1 levels are reduced, which leads to loss of DNA methylation with each cellular division through passive dilution of methylcytosines [187]. Treatment with these two molecules inhibits growth of cancer cells accompanied by re-expression of silenced TSGs [188]. However, the random incorporation of these cytidine analogues into DNA raised a concern on cytotoxic effects on normal cells and a need to improve safety profile. The toxic properties of Azacyidine and Decitabine has been addressed by developing of other nucleoside analogues as Zebularine and 5-Fluoro-2'deoxycytidine with less toxic profile.

- ***Zebularine***

Zebularine has improved anti-tumor properties compared to Decitabine and azacytidine. It has been demonstrated that treatment of HCC cell lines with zebularine induced a demethylating effect on TSGs by leading cells to cell cycle arrest and apoptosis [189]. Despite the required high concentration of the drug to attain the same demethylating effect of azacytidine and decitabine, zebularine shows less toxicity. However, the low oral bioavailability is one of his limitations [190].

- ***5-Fluoro-2'deoxycytidine***

5-Fluoro-2'deoxycytidine has the same mechanism of action as decitabine and azacytidine, it forms a covalent bond with DNMT1 and intercalates the DNA.

5.2.2- Non-Nucleoside analogues

Due to the several adverse reactions driven by cytidine analogues, many non-nucleoside inhibitors has been developed with the idea to inhibit DNMT1 by binding the catalytic site of the enzyme without incorporating the DNA [191]. Neverthless, these compounds led to only limited epigenetic variations in cells [192]. RG108 was created by *in silico* drug design, to block the active site of DNMT1. This molecule has shown anti-tumor effects but the mechanism of action needs to be studied further [183]. EGCG (-) –epigallocatechin-3-gallate derived from green tea, inhibits DNMT1 directly [193]. Few hypermethylated genes were re-activated after treatment with SGI-1027, a compound containing a decitabine moiety, and inhibiting DNMT1 without being incorporated into DNA [194]. Other compounds that were potential to induce hypomethylation have been also tested as hydralazine and procainamide [195].

6- Problems of current anti-cancer drugs targeting the epigenetic machinery

Recently, targeting the epigenetic marks and proteins has been an accredited strategy for development of anti-cancer therapies. The newly FDA approved DNMT inhibitors and HDAC inhibitors have provided an important proof of concept, which encouraged pharmaceutical industry to adopt many epigenetic drugs in their portfolios.

One of the major problems facing these drugs is lack of safety and high risk of cytotoxicity due to two main causes [179] :

- Firstly, the expression of the target protein is not restricted to cancer cells, it can be also expressed in healthy ones. For example, as in the case of cytidine analogues, DNMT1 is expressed in both type of cells, and during replication these analogues are incorporated in any genomic DNA, exposing these cells to damage.
- Secondly, the molecule does not inhibit the protein's function specifically as in case of HDAC inhibitors that target all or several HDACs.

Therefore, it is mandatory to work on new more specific molecules and new targets do reduce the damage on normal tissues.

7- Why UHRF1 is an attractive target?

The accumulated findings on the molecular and cellular mechanisms related to UHRF1 reveals widely his potential for anti-cancer therapy. So far, there is no UHRF1 inhibitor that is studied in the clinical phases. The concept of considering UHRF1 as therapeutic target can be supported and argued from distinct point of views that will be elaborated here below. First for its relation with oncogenesis and second for the beneficial effects of targeting UHRF1 compared to targeting other partners. In comparison to DNMT1 and HDAC1, UHRF1 has lower levels in all normal tissues (**Fig 23**) suggesting fewer side effects upon its inhibition in cancer.

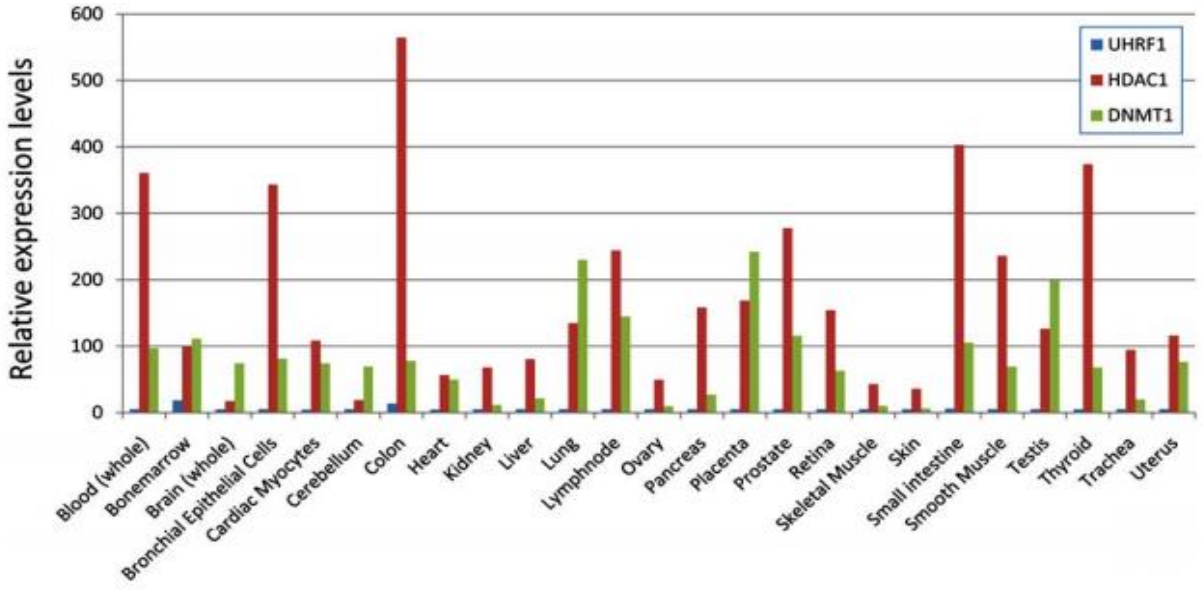

Figure 23. Comparison of relative expression levels of UHRF1, DNMT1 and HDAC1 in all normal tissues. *Adopted from ref [179].*

7.1- UHRF1 expression in cancer

The expression of UHRF1 was investigated in many tumors and consequent phenomena were examined. The common observed feature was overexpression of UHRF1 in different types of cancers along a strong correlation with tumor aggressiveness.Different studies have proved that UHRF1 functions as an oncogenic factor which increases the interest in targeting it for cancer treatment. UHRF1 regulates several biological activities such as proliferation, apoptosis, migration and cell cycle progression (**Fig 24**).

For instance, UHRF1 knockdown by (RNAi) in colorectal cancer lead to a cell cycle arrest at G0/G1 phase and induce the apoptotic pathway via activation of the $p16^{INK4A}$ [131]. Extrinsic and intrinsic apoptosis was induced through activation of different members of caspases and other mediators after silencing UHRF1 in gallbladder cancer cells. This effect was linked to re-expression of promyelocytic leukemia (PML) protein, a TSG frequently downregulated in GBC tissues. Low levels of UHRF1 in GBC also contributed in cell cycle arrest in G1/S phase via p21 pathway [132]; the migratory capacity of few cancer cell lines was reduced after depletion of UHRF1 such as in prostate, lung and gallbladder cancer [132, 135, 196]. Smaller tumors has been observed in nude mice injected with UHRF1-depleted gastric cancer cells as compared to non-depleted cells with a decrease in Ki-67 antigen, a protein associated to cellular proliferation [197].

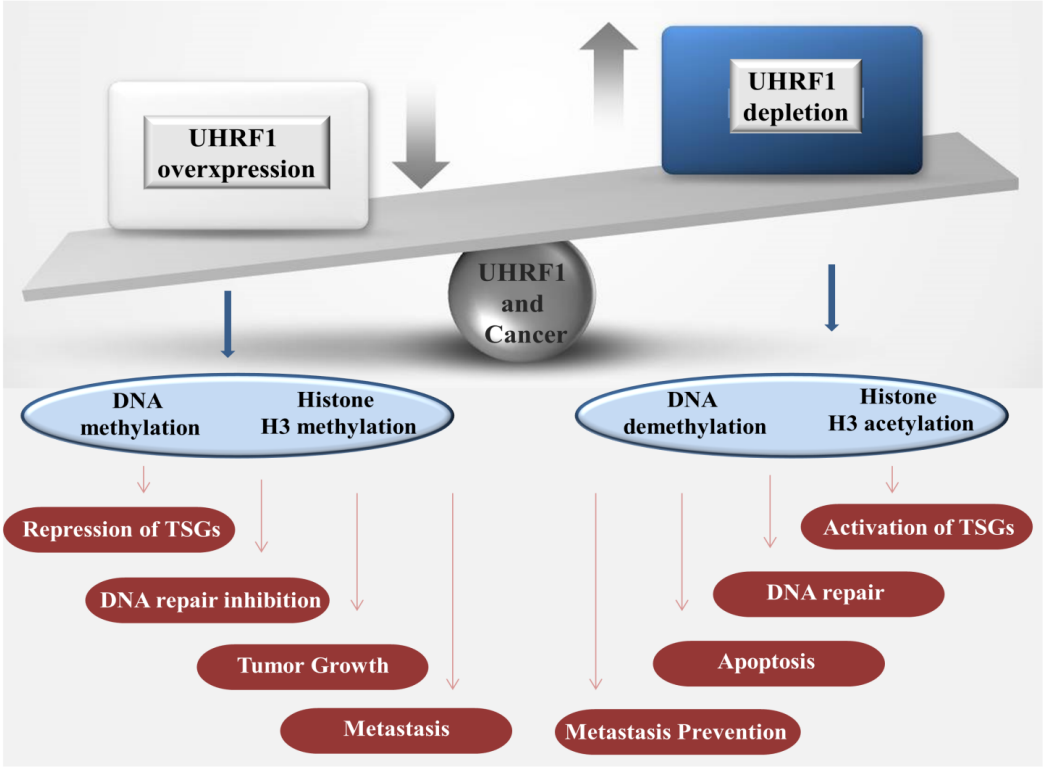

Figure 24. Effect of UHRF1 dysregulation on different biological processes. *UHRF1 is involved in various cellular processes that could lead to tumor cell survivor, proliferation and metastasis. The overexpressed UHRF1 silences TSGs, inhibits DNA repair, contributes in tumor progression and metastasis through DNA and histone H3K9 methylation. In contrast, downregulated UHRF1 by a DNA demethylation and histone H3 acetylation mechanism prevents tumor development. It activates apoptosis by re-expression of TSGs and DNA repair inhibition. Adopted from ref [198].*

7.2- Role of UHRF1 in epigenetic silencing of tumor suppressor genes in cancer

In addition to its interference in various cellular functions, UHRF1 exerts another tumor feature, which is silencing TSGs, a critical factor in cancer development and tumorigenesis. TSGs are responsible for the protection of the cell, by inducing cell cycle arrest, DNA repair and apoptosis.

It is known that UHRF1 regulates gene expression through different epigenetic mechanisms like DNA methylation [106, 107], histone deacetylation [100], histone methylation [101] and histone ubiquitination [199]. UHRF1 localizes on the methylated promoters of the tumor suppressor genes and recruits HDAC1 and DNMT1 via its SRA domain to methylate them in an aberrant manner and repress their expression [96]. For instance, through this mechanism, UHRF1 dysregulates the

expression of genes such as *PAX1 [200]*, *KiSS1 [201]*, *CDKN2A, RASSF1 [135]*, $p14^{AR}$ and $p16^{INK4A}$ [100] and thus promotes cancer.

Lately, Zhou et al. showed that the knockdown of UHRF1 re-activated 7 of the tumor suppressor genes *CDX2, CDKN2A, RUNX3, FOXO4, PPARG, BRCA1* and *PML* in gastric cancer cells through demethylation of the CpGs at the level of their promoters [197]. In the same context, UHRF1 was involved in progression of colorectal cancer by regulating the expression of peroxisome proliferator-activated receptor (PPARγ) through promoter hypermethylation after interacting with DNMT3 [202]. In breast cancer, the cooperative activity between UHRF1 and other modulators DNMT1, HDAC1, and G9a led to regulation of BRAC1 transcription after forming an inhibitory complex at its promoter, hence resulting in its hypermethylation and subsequent repression [142, 203]. All this data indicates that UHRF1 has a regulatory influence on the expression of TSGs, which ultimately leads to tumor development and progression.

8- Compounds targeting UHRF1

8.1- Chemical compounds targeting UHRF1

- ***Uracil derivative NSC232003***

This uracil derivative which was identified through an *in silico* screening is considered to be the first chemical molecule to target directly UHRF1 (**Fig 25**). NSC232003 was described to be able to fit into the binding pocket of SRA domain of UHRF1.This compound disrupted the interaction between UHRF1 and its main partner DNMT1 and induced a global hypomethyaltion that could be due to perturbation in binding between SRA and hemimethylated DNA. Further investigation should be performed in order to understand its mechanism of action and its effect on the reactivation of TSGs and on other cellular processes [204].

- ***17-AAG / HSP90 inhibitor***

Recently, based on a high throughput screening, one chemical molecule was selected and tested as an indirect inhibitor of UHRF1. 17- allylamino-17-desmethoxygeldanamycin (17-AAG) was identified as a small molecule inhibitor of HSP90 (90kDa heat-shock protein) that lead to UHRF1 degradation. The inhibition of HSP90 in HeLa cells resulted in an anti-proliferative effect through affecting UHRF1 function and stability. Upon treatment with HSP90, UHRF1 underwent ubiquitination and proteasome-dependent degradation [205].

- ***4-benzylpiperidine-1-carboximidamide (BPC)***

Lately, Houliston et al. proposed TTD-PHD module as a therapeutic target. TTD and PHD groove with the linker in between them are important parts of UHRF1, directing the conformational status of the protein. Thus, different conformational changes can lead to different chromatin-binding properties affecting the function of the protein. 4-benzylpiperidine-1-carboximidamide (BPC) allosterically disrupts the intramolecular interaction by competing the linker to bind to TTD groove. As a result, UHRF1 ability to bind H3K9me3 was reduced due to the modulation of the conformational state of the TTD-PHD domain in presence of the molecule [206]. However, the effect of this inhibitor in a cellular system needs to be investigated further.

8.1- Natural compounds targeting UHRF1signaling pathways

Several natural compounds have been capable to target the UHRF1 complex, with showing big potential as anti-cancers by reactivating TSGs, inhibiting proliferation and inducing apoptosis (**Fig 25**). These natural compounds target the signaling pathways of UHRF1 expressions but their mechanism of action need to be more understood.

- ***Luteolin***

Luteolin (30, 40, 5, 7-tetrahydroxyflavone) is one of the flavonoids that displays an important efficacy especially as an anticarcinogenic agent. Its anti-proliferative effect has been proven on cancer cells *in vitro* and *in vivo*, leading to a cell cycle arrest and apoptosis by inhibition of enzymes involved in cell activation. In colocteral cancer and in cervical cancer, Luteolin treatment lead to a downregulation of UHRF1 and its main partner DNMT1 with an concomitant upregulation of a tumor suppressor gene p16(INK4A) [207, 208].

- ***Limoniastrum guyonianum aqueous gall extract***

This extract has been used in traditional medicine to treat different diseases. It has been reported that it contains gallocatechin, epigallocatechin, and epigallocatechin-3-O-gallate which could have anti-tumoral properties. Treatment of HeLa cancer cells with the extract enhanced apoptosis and arrested the cell cycle progression in G2/M phase with a reactivation of $p16^{INK4A}$. On the level of the

epigenetic modulations, the expression of the UHRF1/DNMT1 tandem was down-regulated and associated with a decrease in the global methylation levels [208].

- ***Epigallocatechin-3-gallate (EGCG)***

Tea polyphenols have been known for their anti-cancer properties. EGCG, one of the predominant polyphenols in green tea, has been reported to up-regulate tumor suppressor genes such as $p16^{INK4A}$, retinoic acid receptor β (*RAR β*), O^6-methylguanine methyltransferase (*MGMT*) and human mutL homologue 1 (*hMLH1*) through demethylation of their promoter [193]. It has also been shown that EGCG targets DNMT1 activity and expression [193]. In Jurkat cells, EGCG succeeded to target UHRF1/DNMT1 expression through a p73-dependent mechanism. EGCG treatment lead to reactivation of $p16^{INK4A}$, which was correlated with the inability of UHRF1 to bind to the p16 gene promoter [209].

- ***Thymoquinone (TQ)***

Thymoquinone (TQ), a known anti-neoplastic drug, has demonstrated strong cytotoxic effect on different types of human cancers [210] additionally, it acts as a DNA damaging agent, by producing reactive oxygen species (ROS) producer [211-213]. The observed anti-tumoral effects of TQ are inhibition of cell growth, induction of cell death and cell cycle arrest. Treatment of lymphoblastic leukemia Jurkat cells with TQ resulted in modulation of epigenetic code modifiers; UHRF1 and two of its main partners DNMT1 and HDAC1 were intensively down-regulated. Simultaneously, TQ treatment lead to a growth inhibitory effect on cells with an induction of apoptosis through the activation of p73 gene [138].

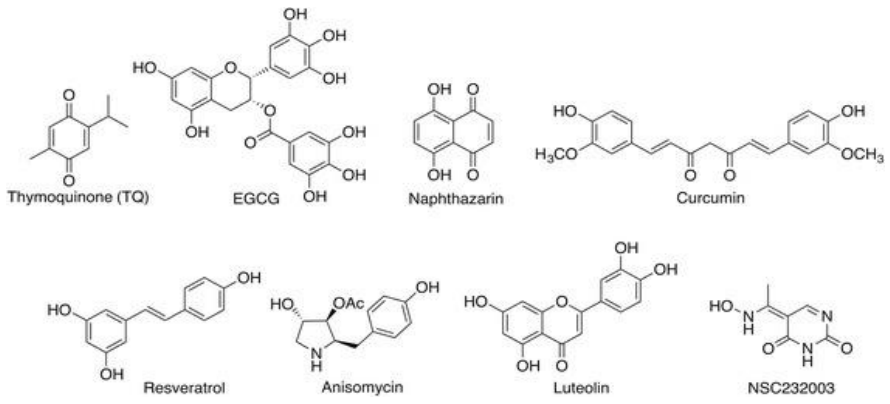

Figure 25. Chemical structures of various compounds targeting UHRF1. *Adopted from ref [214].*

- ***Red wine polyphenols (RWP)***

Concerning cancer and diets, it has been suggested by several studies that a rich diet with polyphenols is associated with lower risk of cancer. A red wine polyphenolic extract (RWP) showed some encouraging effects that could be utilized as prevention strategy. In Jurkat cells, RWP downregulated the level of UHRF1 and activated the p73-dependant and the caspase -3 pathways leading the cells to enter apoptosis [215]. Furthermore, in colorectal cancer cells, apoptosis was triggered by activation of p53 and p73 pathways [138], which are observed to act as negative upstream regulators of UHRF1 [140, 216].

- ***Bilberry extract (Antho 50)***

Anthocyanins are reputed for their protective effects in cancer with many therapeutic benefits such as angiogenesis inhibition and other anti-tumoral activities [217]. Bilberry (*Vaccinium myrtillus* L.) extract, Antho 50, one of the richest natural sources of anthocyanins, was studied in chronic lymphocytic leukemia cells. UHRF1 levels were notably downregulated, and with its strong pro-apoptotic property Antho 50 induced cell death through activation of redox-sensitive caspase 3 pathway with dysregulation of the Bad/Bcl-2 pathway [218].

- ***Naphthazarin***

Naphthazarin (DHNQ, 5,8-dihydroxy-l,4-naphthoquinone) is one of the 1,4-naphthoquinone derivatives that are known for their antitumor cytotoxic effects in cancer cells. Naphthazarin treatment of human breast cancer cells MCF-7 combined with ionized radiation therapy induced cell cycle arrest and apoptosis by activation p53-related p21 pathway. Inhibition of binding of DNMT1, UHRF1 and HDAC1 to p21 promoter after exposure to naphthazarin caused the reactivation of p21 [219].

- ***Shikonin***

Shikonin, a natural compound used in Chinese traditional medicine and extracted from Zi Cao (*purple gromwell*), is a naphtoquinone known to suppress the tumor growth. After treatment with shikonin, UHRF1 levels were downregulated in HeLa cells. Shikonin apoptotic activites were detected in HeLa cancer cells via a p73, caspase-3-dependant pathway. In addition, the compound, was able to transcriptionally activate the $p16^{INK4A}$ gene [220].

- ***Hinokitiol***

Hinokitiol (4-isopropyltropolone) is extracted from *Chymacyparis obtuse;* it is a component of essential oils, which demonstrated anti-tumor activities in several types of cancer cells by inhibiting cell proliferation and inducing apoptosis. Recently, hinokitiol was proposed as a DNA methylation inhibitor in human colon cancer cell lines. After exposing the cells to hinokitiol, UHRF1 was indirectly inhibited after DNMT1downregulation. This compound also upregulated TET1 and exhibited a demethylating effect on 10 of hypermethylated genes [221].

Chapter 5: UHRF1 a universal biomarker (Review)

Recently, efforts have been widely implemented to explore new DNA methylation signatures that can serve as biomarkers to establish a diagnostic and prognostic tool for prevention or early detection of cancer. Till date, numerous DNA methylation-based biomarkers such as syndecan 2 (*SDC2*) for colorectal cancer and short stature homeobox 2 (*SHOX2*), O^6-methylguanine DNA methyltransferase *MGMT* for lung cancer have proven to be candidates to reach the clinical phase, and some of them are even available as commercial kits [222].

As discussed in previous chapter, UHRF1, the protein responsible for maintenance of DNA methylation and histone code, is found to be strongly linked to oncogenesis. It is well documented that this expression remains high through cell cycle in multiple tumors and its level can reflect the degree of tumor invasiveness. The abnormal high levels of UHRF1 can be a result of many causes among which disruption in function of some transcription factors such as (E2F1) or dysregulation of some partners, such as USP7, and involvement of non-coding RNAs in its stability. However, UHRF1 overexpression contributes in epigenetic abnormalities related to DNA methylation and consequently deactivates TSGs and promotes tumor growth and helps the cells to escape apoptosis.

In the following part, we review the expression levels of UHRF1 in tissue samples of a variety of cancers at different stages and compare them with normal tissues; we discuss its oncogenic potential and predict its future usage as a biomarker in human malignancies. Altogether, this overview highlights the power of UHRF1 in cancer risk estimation and intervention at early stages of the disease.

www.impactjournals.com/oncotarget/ Oncotarget, 2017, Vol. 8, (No. 31), pp: 51946-51962

Review

The epigenetic integrator UHRF1: on the road to become a universal biomarker for cancer

Waseem Ashraf[1], Abdulkhaleg Ibrahim[2], Mahmoud Alhosin[3,4,5], Liliyana Zaayter[1], Khalid Ouararhni[2], Christophe Papin[2], Tanveer Ahmad[1], Ali Hamiche[2], Yves Mély[1], Christian Bronner[2,*] and Marc Mousli[1,*]

[1] Laboratory of Biophotonics and Pharmacology, Faculty of Pharmacy, University of Strasbourg, Illkirch, France

[2] Institute of Genetics and Molecular and Cellular Biology, University of Strasbourg, Illkirch-Graffenstaden, France

[3] Department of Biochemistry, Faculty of Sciences, King Abdulaziz University, Jeddah, Saudi Arabia

[4] Cancer Metabolism and Epigenetic Unit, King Abdulaziz University, Jeddah, Saudi Arabia

[5] Cancer and Mutagenesis Unit, King Fahd Centre for Medical Research, King Abdulaziz University, Jeddah, Saudi Arabia

[*] These authors are co-last authors

***Correspondence to**: Marc Mousli, **email**: marc.mousli@unistra.fr*

Keywords: cancer, biomarkers, epigenetics, UHRF1, DNA methylation

***Received**: February 03, 2017* ***Accepted**: April 02, 2017* ***Published**: April 24, 2017*

Copyright: Ashraf et al. This is an open-access article distributed under the terms of the Creative Commons Attribution License 3.0 (CC BY 3.0), which permits unrestricted use, distribution, and reproduction in any medium, provided the original author and source are credited.

ABSTRACT

Cancer is one of the deadliest diseases in the world causing record number of mortalities in both developed and undeveloped countries. Despite a lot of advances and breakthroughs in the field of oncology still, it is very hard to diagnose and treat the cancers at early stages. Here in this review we analyze the potential of Ubiquitin-like containing PHD and Ring Finger domain 1 (UHRF1) as a universal biomarker for cancers. UHRF1 is an important epigenetic regulator maintaining DNA methylation and histone code in the cell. It is highly expressed in a variety of cancers and is a well-known oncogene that can disrupt the epigenetic code and override the senescence machinery. Many studies have validated UHRF1 as a powerful diagnostic and prognostic tool to differentially diagnose cancer, predict the therapeutic response and assess the risk of tumor progression and recurrence. Highly sensitive, non-invasive and cost effective approaches are therefore needed to assess the level of UHRF1 in patients, which can be deployed in diagnostic laboratories to detect cancer and monitor disease progression.

INTRODUCTION

In cancer, the prognosis of the disease is highly dependent on the type and location of the cancer along with the stage at which it is diagnosed. The survival rate and the treatment response is better if the cancer is diagnosed early when the tumor is localized and small. Nowadays many biomolecules and epigenetic patterns are being explored as "biomarkers" to help in early diagnosis of cancers along with currently employed techniques of imaging and cytology [1]. An ideal biomarker for cancer detection must be able to differentiate between normal and tumoral cells and it should be able to predict the malignant potential and prognosis of the disease.

All cells of a multicellular mammalian organism, except germinal cells, contain the same DNA in terms of nucleotide sequence. Considering the fact that DNA is the layer of heredity and cell identity, how can cell diversity and differentiation arise from the same DNA sequence is an important question challenging the scientific community. Epigenetics is the research field that tries to answer this question by deciphering a tremendous number of cellular mechanisms of gene regulation embedded in the chromatin but not related to changes in DNA sequences. In other words, it refers to external modifications of DNA that turn *genes* "on" or "off. At the molecular level, "off" means that the genes are silenced, by means of DNA methylation and histone methylation, *e.g.,* di- and tri-methylation of lysines 9 & 27 of histone H3 (H3K9me2, H3K9me3, H3K27me2, H3K27me3) as well as chromatin structure, micro RNA and histone variants [2-5]. However, gene expression does not function as a simple "on-off" dichotomy but rather through a complex language dictated by the degree of DNA methylation and a set of epigenetic

marks appearing on the N-terminal tails of histones present in the nucleosome [3]. This complex language allows the cell to express genes as a function of precise needs during cell cycle or during lifespan and no more or less than it is required for the cell to work adequately. This complex language is profoundly modified in various diseases, including cancer [3-5].

Indeed, cancer cells exhibit profound changes in epigenetic profiles, as much on the DNA methylation side as on histone code side [6]. Cancer cells undergo global DNA hypomethylation, whereas some regions, on the contrary, undergo hypermethylation, *e.g.* promoters of tumor suppressor genes [7, 8]. On the histone code versant, several modifications have been reported in various types of cancer [9].

There are increased evidences that DNA methylation appears as an ideal biomarker for various types of cancers [10-13]. DNA methylation in mammals preferentially occurs in a CpG context, meaning that both DNA strands are methylated in an asymmetrical manner, which represents one of the layers of epigenetic information. Methylation of cytosine is slightly mutagenic, explaining the loss of CpG sites in mammalian genomes during evolution. As a consequence, CpG sites in human genome are globally found 3–4 times less often than statistically expected, except in CpG islands, which are often located in gene promoters [2, 14].

The mechanism of inheritance of the methylation patterns is relatively well documented regarding DNA but is still elusive concerning histones, although several models are under investigation for definitive validation [15]. Duplication of DNA methylation patterns in a CpG context, is subjected to prior DNA replication generating hemi-methylated DNA, *i.e.,* only one DNA strand is methylated, a state that is specifically recognized by Ubiquitin-like containing PHD and Ring Finger domain protein 1 (UHRF1) [16-20]. The sensing of hemi-methylated DNA by UHRF1, induces the recruitment of DNA methyltransferase 1 (DNMT1) which methylates the opposite unmethylated DNA strand, and consequently CpG dinucleotides are methylated on both strands. Through these properties, the tandem UHRF1/DNMT1 plays a role during cell proliferation and therefore in development and cancer [21].

THE EPIGENETIC INTEGRATOR UHRF1

Structure of UHRF1

Among the different epigenetic modulators, UHRF1, which is also known as Inverted CCAAT box Binding Protein of 90 kDa (ICBP90) or nuclear protein of 95kDa (Np95) [22-24] has gained a considerable attention during the past few years because of its high expression in most of the cancers and its ability to link important epigenetic processes such as DNA methylation and histone modifications [25].

Initially, UHRF1 was identified as a transcription factor regulating the expression of topoisomerase IIα by binding to an inverted CCAAT box located in its promoter [22]. UHRF1 was further shown to critically participate in various epigenetic processes by its different structural domains (Figure 1). Indeed, UHRF1 is composed of an N-terminal ubiquitin-like domain that is coming before the tandem tudor domain (TTD) and plant homeodomain (PHD). These domains are followed by the unique set and ring associated (SRA) domain and the really interesting new gene (RING) finger domain at the C-terminus [25]. Except for the RING domain exhibiting an E3 ligase activity towards histone H3 on lysine 23 or on lysine 18, no further enzymatic activity has been so far identified for any of the other domains. Instead, interesting binding activities were identified for each domain conferring unique capacities of readout [26-28]. One key property of UHRF1 is its ability to sense the presence of hemi-methylated DNA at the replication fork, thanks to the SRA domain [19, 20]. Concomitantly, it can also sense the di- and tri- methylated lysine 9 of histone H3 (H3K9me2/H3K9me3) in the chromatin by help of its tandem tudor domain [29-31]. Association of UHRF1 with methylated H3K9 through TTD facilitates the maintenance of DNA methylation but primarily it is the SRA domain that recruits UHRF1 to hemi-methylated DNA [32]. Indeed, we have shown that the binding of SRA domain does not induce distortion of the DNA, which is in favor of a sliding behavior along the DNA seeking for hemi-methylated CpG sites and subsequent flipping of the methylated cytosine, thus facilitating the recruitment of DNMT1 [33, 34]. It has also been shown that UHRF1, through its SRA domain, is capable of recognizing hydroxymethylcytosine [35]. The relevance of this latter remains elusive but it might bring new insights in DNA methylation maintenance, once resolved.

Beside this role, UHRF1 is considered to play a pivotal role in the epigenetic inheritance as it coordinates the action of different chromatin modifying proteins [36]. It interacts, among many others, with DNA methyltransferases (DNMTs), proliferating cell nuclear antigen (PCNA), histone deacetylase 1 (HDAC1), ubiquitin specific protease 7 (USP7), euchromatic histone-lysine N methyltransferase 2 (G9a/EHMT2) and Tat Interacting Protein 60 (Tip60) to maintain DNA methylation patterns and histone epigenetic marks in various physiological and pathological conditions [18, 19, 37-42]. Together with its partners, UHRF1 ensures the regulation, through "silencing" of a high number of tumor suppressor genes and long non-coding RNAs, including *RB1* [43], *p16* (*CDKN2A)* [44-48], *CDH13* and *SHP1* [49], *SOCS3* and *3OST2* [50], *BRCA1* [51], *CDX2, RUNX3, FOXO4, PPARG* and *PML* [52, 53], *MEG3* [54]

and *14-3-3σ* [55]. Moreover, *KISS1*, functioning as a metastasis suppressor in various cancers, also looks to be under the control of UHRF1 [56]. Altogether, these studies highlight UHRF1 as a conductor of tumor suppressor gene silencing in cancers through a DNA methylation-dependent mechanism.

UHRF1 as a tumor promoter

UHRF1 is mostly expressed in proliferating cells, while it is not found in fully differentiated tissues [22]. Levels of UHRF1 expression positively co-relate with the proliferative potential of cells. In cancer cells, UHRF1 is overexpressed and promotes the proliferation and dedifferentiation of cells [22]. In non-cancerous proliferating cells, UHRF1 expression is cell cycle regulated and peaks in late G1 and G2/M phase, while in cancerous cells, UHRF1 is continuously expressed at all stages of cell cycle [57]. UHRF1 is considered to be essential for G1/S phase transition as its depletion or down-regulation by activation of p53/p21$^{Cip1/WAF1}$ dependent DNA damage response leads to cell cycle arrest at the G1/S phase transition [58, 59]. Similarly, in another study it has been reported that depletion of UHRF1 in HCT116 cells leads to the activation of DNA damage response with subsequent cell cycle arrest at G2/M phase and induction of caspase 8-dependent apoptosis [60]. Conversely, overexpression of UHRF1 in human fibroblasts or its orthologue Np95 in terminally differentiated mouse myotubes facilitates the entry of these cells in S-phase and induces cell proliferation [43, 58].The possibility that UHRF1 behaves as an oncogene has been questioned for a while [61]. However, it is now clearly demonstrated through a recent series of studies that UHRF1 is a tumor promoter. Indeed, it was shown that overexpressed UHRF1 causes DNA hypomethylation, a hallmark of cancer cells; instead of normal maintenance of DNA methylation. Overexpressed UHRF1, through its E3 ligase activity, ubiquitinylates DNMT1 and DNMT3. Thus, by destabilizing and delocalizing them, UHRF1 induces global DNA hypomethylation [62, 63].

Several studies have also revealed that disruption of UHRF1 function results in hypersensitivity to DNA damage [64-69] supporting the idea that UHRF1 plays a critical role in the maintenance of genome stability. This is not surprising, considering that a native protein has first a physiological role before a deleterious role. The deleterious role is coming from an abnormal level of UHRF1 rather than from its function itself.

The abnormally high level of UHRF1 may result from the aberrant activity of various transcription factors regulating the expression of UHRF1 in cancers (Figure 2). E2F transcription factor 1 (E2F1) and E2F transcription factor 8 (E2F8) are upregulated in many cancers and stimulate *UHRF1* expression by directly binding to different sites in its promoter region [37, 57, 70]. Specificity protein 1 (SP1) and Forkhead Box M1 (FOXM1) also potentiate UHRF1 expression in different cancers [71, 72]. Repression of SP1 activity by T3 receptor pathway activation downregulates UHRF1, relieves p21 from UHRF1-mediated silencing and induces cell cycle arrest at G0/G1 phase in liver cancer cells [71]. Similarly, our recent study suggests that activation of highly expressed membrane integrin CD47 in astrocytoma activates NFκB-mediated signaling and UHRF1 expression, which in turn represses p16, thereby strengthening the tumor promoter role of UHRF1 [48]. High UHRF1 levels are also attributed to downregulation of its epigenetic regulator H3K9 methyltransferase (G9a) in various cancers which works along with Yin Yang transcription factor 1 (YY1) as negative upstream regulator of UHRF1 [73].

Besides increased expression of *UHRF1*, increased stability of *UHRF1 mRNA* through down-regulation of regulatory micro RNAs and increased stability of UHRF1 protein also contribute to abnormal high levels of UHRF1 in different cancers (Figure 2) [8, 74-79]. UHRF1 protein levels are controlled in normal cells by coordination of ubiquitinylating and deubiquitinylating enzymes which

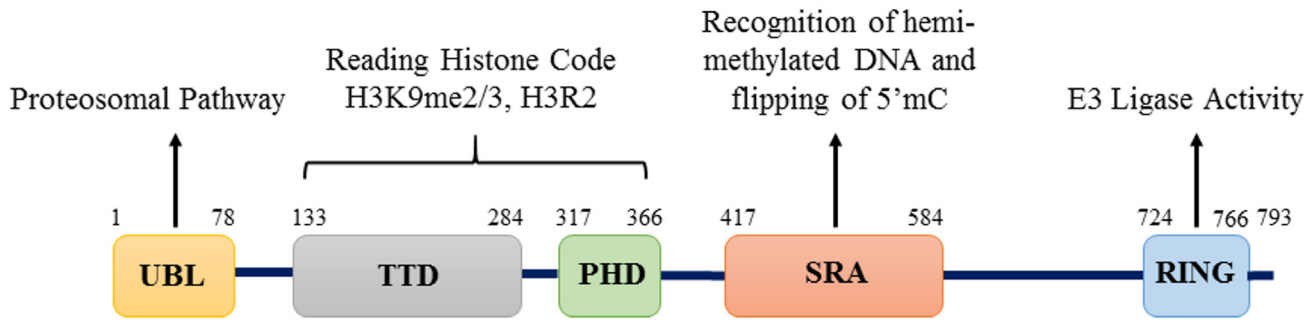

Figure 1: Structure of UHRF1 protein. Structure of UHRF1 protein showing the different domains and their functions. The protein contains 793 amino acids and five major domains: UBL (ubiquitin-like) domain, TTD (Tandem Tudor Domain), PHD (Plant Homeodomain), SRA (Set and Ring Associated) domain and RING (Really Interesting New Gene) domain.

regulate its proteosomal degradation (Figure 2). $SCF^{\beta\text{-}TrCP}$ E3 ligase or intrinsic activity of UHRF1 RING domain can induce degradation of UHRF1 by ubiquitinylation [26, 65]. Phosphorylation of serine residue at 108 by casein kinase 1δ helps $SCF^{\beta\text{-}TrCP}$ E3 ligase to recognize and ubiquitinate UHRF1 for degradation [65]. On the other hand, UHRF1 is stabilized and recruited to chromatin by its association with deubiquitinating enzyme USP7. M phase specific kinase CDK1-cyclin B which phosphorylates UHRF1 at serine 652 in the interacting region of USP7 can disrupt this association and lead to degradation of UHRF1 [40, 80]. Considering that USP7 is upregulated in many cancers, this might be one of the possible reason for high levels of UHRF1 in cancer cells [81-83]. UHRF1 is also stabilized by its interaction with long noncoding RNA UPAT (UHRF1 Protein Associated Transcript), which promotes colon tumorigenesis through inhibition of UHRF1 degradation [84]. Pharmacological inhibition of heat shock protein (HSP90) also destabilizes UHRF1 and suppress cancer cell proliferation predicting a role of HSP90 in UHRF1 turnover [85]. Altogether these events result in abnormal high level of UHRF1 in cancers which appears now to be exploitable as a biomarker.

We will now review the potential of UHRF1 to fulfil the features of a biomarker in various types of cancer.

UHRF1 EXPRESSION IN DIFFERENT CANCERS

UHRF1 in lung cancer

Lung cancer is the most common and fatal among different types of cancers with an average 5-year survival rate of around 15% [86]. According to latest data, over 1.8 million new cases of lung cancer were reported worldwide in 2012, while in the same year the death toll of lung cancer was around 1.59 million [86]. High smoking incidences and late diagnosis of cancer are major factors contributing to its high mortality rate. Various novel proteins are now being investigated, in search of a superior biomarker and

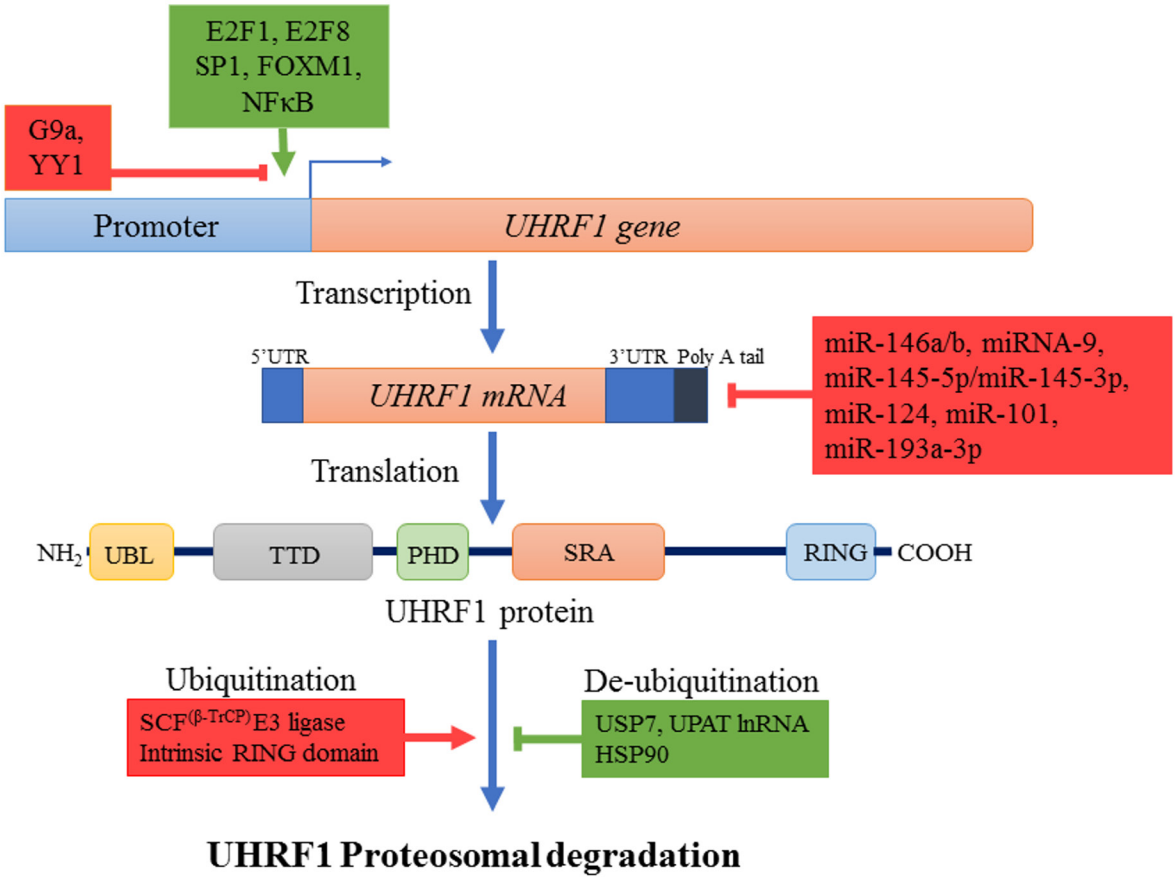

Figure 2: Regulation mechanisms of UHRF1. Different transcription factors like E2F1, E2F8, Sp1, FOXM1, NFκB (indicated in green) enhance while others such as YY1 along with lysine methyl transferase G9a (indicated in red) repress the expression of *UHRF1* at transcription level. Many small non-coding microRNAs also decrease *UHRF1* expression by destabilizing *UHRF1 mRNA* through binding to 3'UTR region. UHRF1 protein is degraded by proteosomal pathway after autoubiquitinylation or ubiquitinylation by $SCF^{\beta\text{-}TrCP}$ E3 ligase. Ubiquitinylated UHRF1 is stabilized in cells by USP7, HSP90 or UPAT lnRNA. Increased transcription factor expression, downregulation of miRNAs and increased levels of stabilizing factors (all indicated in green) result in overexpression of UHRF1.

among them UHRF1 has shown encouraging results. Immunohistochemistry (IHC) analysis of 322 lung cancer tissues from Japan and 56 samples from US, revealed an overexpression of UHRF1 in all histological types of non-small cell lung cancer (NSCLC) especially in non-adenocarcinomas [87]. Transcript analysis of samples also showed marked increase of UHRF1 mRNA in 70% of lung cancer cases. As enhanced expression significantly correlated with the advanced stages and malignancy of the cancer, authors proposed UHRF1 as a prognostic biomarker for lung cancer [87]. Similarly, a recent study in Taiwan has predicted a six-gene signature including *ABCC4*, *ADRBK2*, *KLHL23*, *PDS5A*, *UHRF1* and *ZNF551* as better prognostic marker in NSCLC for overall survival time and treatment outcome [88].

UHRF1 overexpression was also confirmed in another study including 105 NSCLC tissues (55 adenocarcinomas and 50 squamous cell carcinomas) along with DNMT1, DNMT3A and DNMT3B [89]. This overexpression resulted in silencing of tumor suppressor genes such as *RASSF1* and *p16*, via promoter hypermethylation in 32.4% and 26% of cases, respectively. Accordingly, in a cell model of lung cancer, knockdown of UHRF1 in A549 cells prevented the tumor suppressor genes *RASSF1*, *CYGB*, and *CDH13* promoters from hypermethylation [89].

UHRF1 in liver cancer

Hepatocellular carcinoma (HCC) is one of the most prevalent cancers with multiple etiological factors and is the second leading cause of cancer related deaths worldwide [86]. So far, many studies have been carried out to understand the complex nature and poor prognosis of this disease but it is still elusive. A recent study reported overexpression of UHRF1 in HCC of various etiologies and described UHRF1 as an oncogene, that drives global DNA hypomethylation by delocalizing DNMT1 [62]. In this study, expression of UHRF1 was assessed in 109 human HCC cases by qPCR and results revealed abnormally high expression of UHRF1 (averagely 2-fold higher than normal) in 95.41% (104/109) of the cases [62]. UHRF1 protein levels in samples were also in accordance with mRNA levels and were found significantly higher in 73% of tumors but were barely detectable in normal tissue

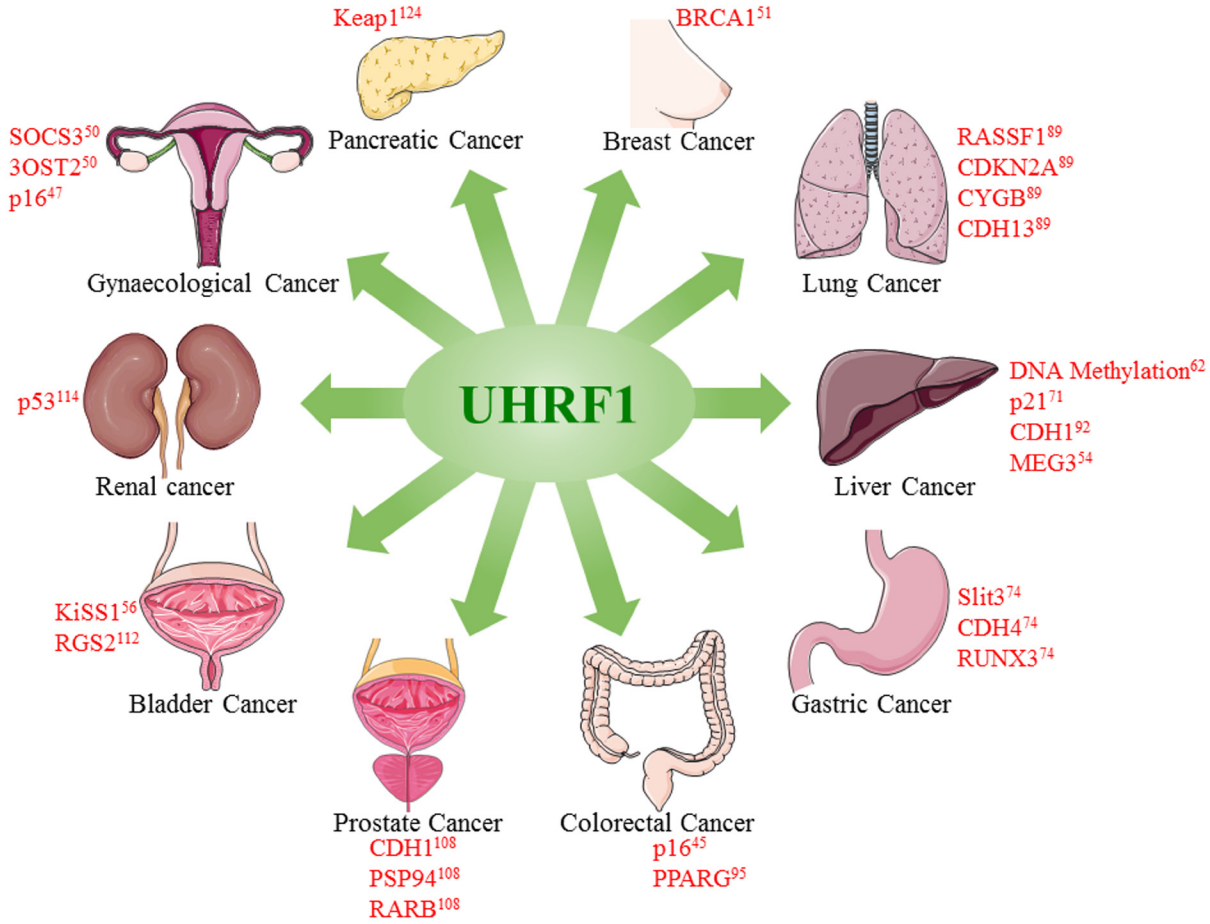

Figure 3: Overexpression of UHRF1 promotes tumorigenesis in different cancers. UHRF1 overexpression leads to epigenetic abnormalities including DNA methylation and downregulation of tumor suppressor genes or lnRNAs. Figure is made using images taken with permission from Servier Medical Arts http://servier.com/Powerpoint-image-bank.

samples [62]. Tumors with higher expression of UHRF1 also had poor prognosis with higher recurrence rate, alpha fetoprotein, microvascular invasion and lower survival rate emphasizing the diagnostic and prognostic potential of UHRF1 in HCC [62]. Similarly, high levels of UHRF1 mRNA were reported in 160 HCC patients notably during later stages II & III of cancer [71]. UHRF1 protein level were also significantly upregulated in 75.7% (52 of 70) of samples when analyzed by western blot [71]. Results were further confirmed by immunohistochemistry analysis of 136 HCC tissue samples which showed high expression of UHRF1 in tumor samples, positively correlating with tumor size, fetoprotein levels and HBV infection [71]. The diagnostic and prognostic capacities of UHRF1, as a novel biomarker in HCC, were also highlighted by a study on Chinese population including 68 HCC specimens [90]. In this study, significantly higher levels of UHRF1 were found in HCC samples by HPLC compared with the adjacent non-cancerous tissues. Of note, the levels of UHRF1 correlated with distant metastasis, tumor area and HBV [90]. Furthermore, elevated levels of UHRF1 also predicted poor prognosis as after 5 years of follow up, the survival rate in high UHRF1 expression group was 29.8% as compared with 81% in low UHRF1 expression group [90]. Another group also reported similar findings where UHRF1 mRNA expression was found significantly increased in 67% (54/80, $P < 0.05$) of HCC specimens [91]. Immunohistochemical staining of 102 pairs of HCC samples included in study also revealed significantly higher staining of UHRF1 protein in cancerous tissues (57.8% vs 32.7%) when compared to non-cancerous tissue. Like previous studies, overexpression of UHRF1 positively correlated with tumor size, staging and poor survival rate of patients [92].

On a cellular aspect, knockdown of UHRF1 inhibited the tumor growth *in vivo* and *in vitro* and induced cell cycle arrest at G2/M phase confirming the oncogenic potential of UHRF1. Targeting of UHRF1 also decreased the migration and invasion of cancer cells by hampering endothelial to mesenchymal transition (EMT) as evidenced by up regulation of (EMT opposing) E-cadherin and down regulation of (EMT favoring) β-catenin, vimentin, N-cadherin and snail in UHRF1 knockdown cells [92]. Overexpression of UHRF1 in hepatocellular carcinoma also negatively regulated the levels of tumor suppressive long non-coding RNA maternally expressed gene 3 (MEG3) via promoter hypermethylation which exerts its tumor suppressive role by induction of p53 [54, 93].

UHRF1 in gastric cancer

Gastric cancer is one of the most fatal cancers among all malignant diseases, and is accounted for approximately 723,000 world-wide deaths each year. Eastern Asian countries like China, Japan, Taiwan and Philippines have higher incidences of gastric cancer as compared with western countries [86]. In 2013, a study reported high levels of UHRF1 in gastric cancers and explored miR-146a/b mediated regulation of UHRF1 as a novel therapeutic approach in preventing metastasis and treating such cancers [74]. Immunohistochemistry staining of 106 gastric tumors revealed higher expression of UHRF1 in cancer tissues compared with adjacent normal tissues, which correlated with poor differentiation, cancer staging, increased lymph node and tissue metastasis [74]. Kaplan-Meier analysis showed that patients with higher expression of UHRF1 had poor prognosis and shorter overall survival time as compared with patients having relatively lower expression of UHRF1, suggesting abnormal high levels of UHRF1 as independent diagnostic and prognostic marker for gastric cancer [74].

At the cellular level, overexpression of UHRF1 was observed in aggressive gastric cancer cell lines (GC9811-P and MKN28M), which has been suggested to enhance the proliferating capacity of these cells [74]. Reduced levels of UHRF1, induced by miR-146a/b, reactivated tumor suppressor genes like *SLIT3*, *CDH4*, and *RUNX3* via promoter hypomethylation [74]. Consistently, with this notion, same authors further explored the prognostic value of UHRF1 expression in a study including 238 gastric cancer patients [52]. Immunohistochemistry labelling for UHRF1 was found positive in 82% of samples and significantly correlated with poor differentiation and metastasis. Indeed, patients with higher expression of UHRF1 had a very low 5-year survival rate of 19% as compared to patients with negative (38%) or low expression of UHRF1 (30%) suggesting UHRF1 as a significant predictor of gastric cancer prognosis [52].

UHRF1 in colorectal cancer

Epigenetic silencing of tumor suppressor genes via promoter hypermethylation is commonly reported besides the genetic aberrations in colorectal carcinogenesis and many mechanisms have been proposed for this deregulation. UHRF1 overexpression in colorectal cancer has been observed in several studies and is considered to be involved in promoter hypermethylation mediated repression of TSGs [7, 8, 94]. Wang *et al* first reported the overexpression of UHRF1 in colorectal cancer and suggested its use as a biomarker and a possible therapeutic target for diagnosis and treatment of colorectal cancer [45]. The authors observed a significantly increased UHRF1 expression at both transcriptomic and proteomic levels in colon cancer tissues and found positive association of this overexpression with metastasis, poor clinical staging and *p16* silencing [45]. Overexpression of UHRF1 was also observed in LoVo, DLD1, SW480 and SW620 colon cancer cell lines. Inhibition of UHRF1 in these cells led to upregulation of *p16*, decreased proliferation and migration capacity, as well as cell cycle arrest at G0/G1 and apoptosis [45]. Similarly, in colorectal cells,

overexpressed UHRF1 negatively regulated peroxisome proliferator-activated receptor gamma *(PPARG),* through epigenetic-dependent mechanisms [95]. The consequences were increased endothelial to mesenchymal transition (EMT), growth and cell viability. Furthermore, prognostic values were more significant when both UHRF1 overexpression and PPARG down-regulation were taken into account [95]. Another study in which 231 colorectal cancer tissues and 40 adenoma specimens were analyzed for UHRF1 levels reported similar results [96]. Indeed, immunohistochemistry showed high expression of UHRF1 in the nucleus of 65.8% (152/231) colorectal cancer tissues and of 87.5% (35/40) adenoma samples while little or no expression was found in normal colonic mucosa [96]. Expression of UHRF1 positively correlated with the depth of invasion and E2F-1 levels [96]. So far it is not yet clear why UHRF1 is up-regulated in cancer but some interesting leads are emerging. For instance, an inverse relationship between the levels of UHRF1 and the regulatory miRNA-9 has been reported in colorectal cells, for which high levels of UHRF1 are associated with poor survival rate of patients [75].

UHRF1 in breast cancer

Like for other cancers, many studies have reported the association of UHRF1 with breast cancer which is one of the leading causes of cancer related deaths in women world-wide, killing around 0.5 million women each year [86]. In 2003, we first reported increased expression of UHRF1 in breast cancer tissues and found a relationship between its expression and pathological grade of cancer [57]. Later UHRF1 overexpression in breast cancer patients was reported by cDNA microarray and qRT-PCR [37]. Overexpressed UHRF1 was further confirmed by the immunohistochemical staining and correlated with poor differentiation of tumors [37]. Recently, a study has investigated UHRF1 as a diagnostic and prognostic marker for breast cancer [97]. In this study, 62 tissue samples were analyzed and compared with 24 adjacent non-cancerous tissues. Higher expression of UHRF1 was observed at both mRNA and protein level in cancerous tissues which significantly correlated with stage of disease and c-erb2 status but was independent of age, menopause, estrogen and progesterone receptor levels [97].

The origin of the enhanced UHRF1 expression in breast cancer remains elusive in contrast to the down-stream events. Notably, increased expression of UHRF1 in breast cancers is believed to aggravate the pathogenesis by silencing *BRCA1* and modulating the estrogen receptor-α expression [51, 98]. UHRF1 overexpression also increased the proliferation and migration potential of breast cancer cells as exogenous expression of UHRF1 in MDA-MB-231 breast cancer cells facilitated their passage through the cell cycle by induction of cyclin D1 and prevention of apoptosis [99]. UHRF1 also confers radioresistance to breast cancer cells by promoting the expression of DNA damage repair proteins Lupus Ku autoantigen protein p70 (Ku-70) and Lupus Ku autoantigen protein p80 (Ku-80) repairing the chromosomal aberrations and also by down-regulating the expression of BAX and other pro-apoptotic proteins [100]. Similarly, it has been observed that specific inhibition of UHRF1, by mRNA targeting, decreased the oncogenic capacity in breast cancer cells and increased their sensitivity to chemotherapy [101, 102].

UHRF1 in gynecological tumors

UHRF1 expression in cervical cancer is also a good indicator for cellular proliferation and malignancy. Notably, an analysis of 99 cervical biopsies showed UHRF1 as a useful biomarker to discriminate low grade intraepithelial lesions from normal tissues with a sensitivity of 71.4% and to discriminate low grade intraepithelial lesions from high grade intraepithelial lesions with a sensitivity of 97.6% [103]. Another study on cervical squamous cell carcinoma (CSCC) also reported high expression of UHRF1 at both mRNA and protein level in 47 samples and found that silencing of UHRF1 in cervical cancer cells inhibited cell proliferation and induced apoptosis [104]. The reasons why UHRF1 is overexpressed in cervical cancer, is still not yet elucidated and again it is rather the downstream events that have been deciphered in cellular models. Indeed, polyphenolic extracts from plant sources were found to downregulate UHRF1 in the cervical cancer HeLa cell line [47]. This in turn upregulated the tumor suppressor gene *p16* and ultimately halted the progression of the cell cycle and induced apoptosis [47]. Moreover, UHRF1 overexpression in HeLa cells was shown to decrease their radio-sensitivity to γ-radiation by increasing the expression of the DNA repair proteins XRCC4, thus, enhancing the capability of these cells to repair the DNA damaged by radiation [105]. It is remarkable to notice that a paradigm is emerging concerning the decreased sensitivity of cancer cells to chemotherapy through control of the DNA repair machinery by UHRF1.

Besides cervical cancer, the diagnostic and prognostic capabilities of UHRF1 as biomarker have also been evaluated in ovarian cancer, which is the major worldwide contributor in gynecological tumors posing serious threat to the life of women. In a study including 80 samples from ovarian cancer tissues, significantly higher expression of UHRF1 was found at both transcriptomic and protein levels in tumors as compared with adjacent normal tissues. Knockdown of UHRF1 in ovarian cancer cells inhibited their proliferation and induced apoptosis, suggesting UHRF1 as a general indicator of malignancy and an attractive therapeutic target for ovarian cancers [106].

UHRF1 in prostate cancer

Prostate cancer undergoes profound epigenetic modifications via aberrant DNA methylation and histone post-translational modifications resulting in silencing of tumor suppressor genes [107]. Expression analysis by immunohistochemistry in tissue microarrays of 226 prostate tumor samples revealed significant overexpression of UHRF1 in almost half of tissue samples [108]. This overexpression correlated with poor clinical prognosis as patients with high expression of UHRF1 had reduced median survival rates (10.4 years) as compared to patients with low expression of UHRF1 (12.4 years) [108]. Recently Wan *et al* reported similar results after analyzing expression of UHRF1 in 225 prostate cancer specimens [109]. UHRF1 staining was found in 47.1% of specimens which positively correlated with the Gleason score and the pathological stage of the disease [109]. Patients with higher levels of UHRF1 were found to be at higher risk for biochemical recurrence after radical prostatectomy. Mean biochemical recurrence (BCR) free time in UHRF1-positive patients was around 23.0 months versus 38.9 months in UHRF1-negative patients while 5-year BCR-free survival rate was 12.4% in UHRF1-positive patients as compared with 51.8% in UHRF1-negative patients. These results support UHRF1 as a valuable independent prognostic factor to predict prostate cancer outcome after radical prostatectomy [109].

At the cellular level, overexpression of UHRF1 has also been reported in aggressively proliferating, androgen-independent cell lines of prostate cancer (DU145 and PC3), while low expression of UHRF1 was found in immortalized normal prostate epithelial cells (LHS) or androgen-dependent prostate adenocarcinoma cells with low metastatic potential (LNCaP and 22Rv1 cells) [108, 109]. Overexpression of UHRF1 accompanied with downregulation of tumor suppressor genes and increased expression of EZH2 (H3K27 methyltransferase) in prostate cancer cells contributed to the poor clinical prognosis and lethal progression disease. UHRF1 also recruited SUV39H1 (H3K9 methyltransferase) and DNMTs to the promoter region of many tumor suppressor genes *(CDH1, PSP94, RARB)* resulting in increased methylation of histones and DNA with subsequent silencing of TSGs [108]. Altogether these results suggest that UHRF1 may serve as a useful biomarker and therapeutic target for prostate cancer as it plays an important role in epigenetic silencing of TSGs via histone and DNA modifications

UHRF1 in bladder cancer

UHRF1 has also been described as a 'novel' diagnostic and prognostic marker for the bladder cancer, which is the second most common cancer of the urinary system [110]. Expression of UHRF1 was found significantly increased in the cancer cells and was positively correlated with histological and pathological grade, as higher expression was observed in later stages of cancer. Increased expression of UHRF1 was also associated with poor prognosis of disease as patients having higher levels of UHRF1 had poor survival rate and higher recurrence [110]. UHRF1 levels evaluated by qRT-PCR or immunohistochemistry based detection methods in surgical sections showed UHRF1 as a specific and sensitive biomarker for bladder cancer. Significantly higher levels of UHRF1 were detectable in specimens with non-invasive or superficially invasive cancers at very early stages compared to normal cells [110]. Similarly, in non-muscle-invasive bladder cancer (NMIBC) increased expression of UHRF1 was found in cancer cells, which was directly related with tumor malignancy [111]. Indeed, patients with UHRF1 overexpression had shorter survival duration (mean survival time 42.59 months) and higher incidences of recurrence (41 out of 70 cases) as compared with patients with relatively lower expression of UHRF1, who had greater survival time (mean survival time 71.36 months) and lower chances of recurrence (29 out of 70 cases) [111]. This suggests UHRF1 as an independent prognostic marker for the bladder cancers.

Other studies reported similar overexpression of UHRF1 in bladder cancers and in invasive cell lines, such as 253J, T24, KU7, along with silencing of tumor suppressor genes *e.g., KISS1* and *RGS2* [56, 112, 113]. Altogether, these studies emphasize UHRF1 as an attractive biomarker and therapeutic target for bladder cancers.

UHRF1 in renal cancer

Each year 338,000 new cases of kidney cancers, with a majority of renal cell carcinomas (RCC) are reported worldwide with a high prevalence in developed countries [86]. First evidence of UHRF1 overexpression in kidney tumors has been reported by Unoki *et al* [110]. By investigating mRNA levels, UHRF1 overexpression was found to be associated with several characteristics of kidney tumor patients, including 5-year survival rates, pathological staging and histological grade [110]. Later Ma *et al* found elevated levels of UHRF1 mRNA in 70% of RCC cases [114]. Overexpression was further confirmed by staining of UHRF1 in histological samples, which showed 74.2 % positive staining in RCC carcinoma tissues [114]. Similarly, UHRF1 overexpression, in metastatic renal cancer tissues as compared with non-metastatic tissues, correlated with downregulation of non-coding miR-146a-5p, which targets UHRF1 transcription [115]. However, another miRNA might also be involved in UHRF1 overexpression in RCC. Indeed, miRNA-101 has also been shown to regulate UHRF1 expression since its downregulation leads to UHRF1 upregulation [78]. Interestingly, in this study UHRF1 overexpression

was confirmed in sunitinib-treated RCC tissues and was associated with shorter overall survival after surgery for RCC [78].

UHRF1 in other cancers

Few studies have also predicted UHRF1 as a diagnostic and prognostic marker for various other types of cancers. Representational difference analysis (RDA) of different pathological grades of astrocytoma revealed *UHRF1* and four other genes to be differentially expressed in astrocytoma cancer tissues [116]. Results were confirmed by qPCR analysis in which 7 normal brain tissues, 9 grade I (pilocytic astrocytoma), 9 grade II (low grade astrocytoma), 11 grade III (anaplastic astrocytoma), and 22 grade IV (glioblastoma multiforme) samples were analyzed. Significant overexpression of UHRF1 was observed in cancerous tissues as compared with normal cells showing the possibility to use this differential expression of UHRF1 as a diagnostic marker for astrocytoma [116].

The diagnostic and prognostic value of UHRF1 has also been evaluated in medulloblastoma, a common malignant brain tumor. Out of 168 formalin-fixed, paraffin-embedded medulloblastoma, high levels of UHRF1 were found in 108 cases while lower expression of UHRF1 was observed in the remaining 60 samples, whilst normal cerebellum tissue samples lacked UHRF1 staining [117]. Kaplan–Meier survival analysis showed that patients with high levels of UHRF1 had poor overall survival and progression free survival rate illustrating UHRF1 as a potential independent prognostic marker for medulloblastoma [117].

UHRF1 has also been proposed as a biomarker and potential therapeutic target for gallbladder cancer, which is well known for its poor prognosis and high mortality rate [118]. Immunohistochemical results showed UHRF1-positive staining in 63.2% of cancerous tissue samples [118]. UHRF1 was overexpressed in cancerous tissues and correlated with the advanced stage and lymph node metastasis. Enhanced expression of UHRF1 was also observed at both mRNA and protein level in GBC-SD and NOZ cell lines and depletion of UHRF1 by siRNA or shRNA markedly reduced their migration potential *in vitro* and tumor forming capabilities [118]. Interestingly, knockdown of UHRF1 promoted the expression of *promyelocytic leukemia protein* (PML) and *p21* (*CDKN1A)* tumor suppressor genes, resulting in cell cycle arrest at G1 [118]. UHRF1 depletion also induced apoptosis in these cells by activating both intrinsic and extrinsic pathways for apoptosis, in accordance with previous studies suggesting that UHRF1 exhibits anti-apoptotic properties [119]. All this information suggests an oncogenic role of UHRF1 in gallbladder cancer and increased expression of UHRF1 as an independent biomarker for diagnosis and a therapeutic target of gallbladder cancers.

Correlation of UHRF1 expression with tumorigenesis has also been demonstrated in laryngeal squamous cell carcinomas (LSCC), through analysis of 60 LSCC samples [120]. UHRF1 overexpression was found in 78.3% (47/60) of cancer tissue samples, whereas remaining 13 samples had relatively lower expression of UHRF1 and in normal tissues, UHRF1 expression was barely detectable [120]. UHRF1 overexpression also correlated with the histological and pathological stages of cancer and was found in undifferentiated cells in advanced stages of cancer [120].

Similar findings were reported in esophageal squamous cell carcinoma (ESCC) where increased expression of UHRF1 was observed in 67% of human ESCC samples and overexpression positively correlated with advanced pathological and histological stages of the cancer, poor differentiation and lymph node metastasis [121]. Accordingly, overexpressed UHRF1 was also related to the radiotherapy resistance in patients with ESCC. Furthermore, results were validated by lentivirus mediated targeting of UHRF1 by shRNA in a TE-1 cell line inducing radio-sensitivity and apoptosis in ESCC derived cell line [121]. Another cohort study of 160 ESCC patients demonstrated that UHRF1 is as an attractive prognostic marker and potential target for cancer therapy as high levels of UHRF1 corresponded to poor survival rate [122].

High levels of UHRF1 have also been reported in several studies on pancreatic cancer, supporting the use of UHRF1 as a diagnostic marker for pancreatic cancer. For instance, power blot assay identified UHRF1 among differentially expressed proteins in pancreatic adenocarcinoma, which is extremely aggressive and difficult to diagnose with survival rate of less than 5% in five years [123]. Moreover, UHRF1 was selectively overexpressed in pancreatic adenocarcinoma tissues while it was not detectable in normal pancreatic tissue or chronic pancreatitis specimens [123]. UHRF1 overexpression was found at both proteomic and transcriptomic level in 80% of pancreatic ductal adenosarcoma cases and high UHRF1 levels correlated with neoplastic grade and lesion [123]. Similarly, UHRF1 overexpression was observed in 86% (114 of 132) of malignant pancreatic tumors samples [124] and 158 pancreatic cancer samples [125]. Furthermore, high UHRF1 levels positively correlated with short survival time of patients [124, 125]. All these results suggest UHRF1 as a valuable independent diagnostic marker for pancreatic cancer in clinical settings.

Similar findings were reported in thyroid cancers cells as microarray analysis showed significant upregulation of UHRF1 to identify gene expression profile that favors the progression of well differentiated tumors to aggressive, poorly differentiated or undifferentiated cancer cells [126]. UHRF1 levels were significantly higher in both differentiated and poorly differentiated cancer cells as compared with normal cells, suggesting a good

Table 1: Summary of studies describing diagnostic and prognostic potential of UHRF1 in various cancers

Cancer	Methods	Potential of UHRF1	Downregulated TSGs	Reference
Lung Cancer	qRT-PCR, IHC	UHRF1 overexpression relates to tumor stages, metastasis and poor prognosis.	*RASSF1, p16, CYGB CDH13*	[87-89]
Liver Cancer	qRT-PCR, IHC, Immunoblot assay, HPLC	UHRF1 overexpression relates to tumor size, metastasis, α-fetoprotein, relapse and short survival time.	*p21, CDH1, MEG3*	[54, 62, 71, 90-92]
Gastric Cancer	qRT-PCR, IHC	UHRF1 overexpression relates to poor differentiation, tumor stages, metastasis and low survival rate.	*SLIT3, CDH4, RUNX3, p16, FOXO4, PPARG, BRCA1, PML*	[52, 74]
Colorectal Cancer	qRT-PCR, IHC	UHRF1 overexpression relates to metastasis, tumor stage, E2F1 levels and poor survival rate.	*p16, PPARG*	[45, 75, 95, 96]
Breast Cancer	qPCR, Western Blot, IHC	UHRF1 overexpression relates to tumor stages, low survival rate and resistance to radiotherapy.	*BRCA1*	[37, 51, 97, 100]
Cervical Cancer	qRT-PCR, Western Blot, IHC	UHRF1 overexpression relates to tumor stages, poor prognosis and resistance to radiotherapy.	*p16*	[47, 103-105]
Ovarian Cancer	qRT-PCR, Western Blot	UHRF1 overexpression relates to progression of cancer.		[106]
Prostate Cancer	qRT-PCR IHC	UHRF1 overexpression relates to high Gleason score, tumor stages, recurrence and low survival rate.	*CDH1, PSP94, RARB*	[107-109]
Bladder Cancer	qRT-PCR, IHC	UHRF1 overexpression relates to tumor stages, risk of recurrence and low survival rate.	*KISS1, RGS2*	[56, 76, 77, 110-113]
Renal Cell Carcinoma	qRT-PCR, Western Blot, IHC	UHRF1 overexpression relates to tumor stages of cancer, drug (sunitinib) resistance and low survival rate	*p53*	[78, 114, 115]
Astrocytoma	RDA, qRT-PCR	UHRF1 overexpression relates to stages of cancer.		[116]
Medulloblastoma	IHC	UHRF1 overexpression relates to shorter survival and progression free time.		[117]
Gall Bladder Carcinoma	qRT-PCR, Western Blot, IHC	UHRF1 overexpression relates to tumor stages and lymph node metastasis.	*PML, p21*	[118]
Laryngeal Squamous Cell Carcinoma	qRT-PCR, IHC	UHRF1 overexpression relates to tumor stages, metastasis and low survival rate.		[120]
Esophageal Squamous Cell Carcinoma	qRT-PCR, IHC	UHRF1 overexpression relates to poor differentiation, pathological stage, low survival rate and resistance to radiotherapy.		[121, 122]
Pancreatic Carcinoma	qRT-PCR, IHC	UHRF1 overexpression relates to tumor size, metastasis, stages of cancer and low survival rate.	*RASSF1, p16, KEAP1*	[123-125]
Thyroid Cancer	qRT-PCR, IHC	UHRF1 overexpression relates to tumor stage.		[126, 127]

Abbreviations: qRT-PCR: quantitative reverse-transcriptase polymerase chain reaction; IHC: immunohistochemistry; RDA: representational difference analysis

diagnostic value for UHRF1 in thyroid cancers [126]. These results were in agreement with another study in a Chinese population showing high expression of UHRF1 in poorly differentiated anaplastic thyroid cancer cells versus papillary thyroid cancer and normal cells [127]. Targeting UHRF1 in these cells resulted in suppression of dedifferentiation and stem cell marker expression such as CD97, SOX2, OCT4 and NANOG, highlighting UHRF1 as an attractive target for thyroid cancer therapy [127].

CONCLUSIONANDFUTUREDIRECTIONS

UHRF1 overexpression is found in majority, if not all, of cancers, thus predicting UHRF1 as an independent universal diagnostic and prognostic biomarker for cancer detection, disease progression and therapeutic response monitoring (Table 1). High UHRF1 mRNA and protein levels are detected in early stages of many tumors suggesting UHRF1 as a valuable diagnostic marker for the timely detection of cancers. It is also employed to predict the prognosis of cancer as high level of UHRF1 is generally correlated to poor survival rate, resistance to therapy and recurrence of malignancy.

UHRF1 levels have been well correlated with Ki67 and PCNA which are widely used proliferation markers in cancers [52, 95, 104]. However, UHRF1 overexpression is a better diagnosis and prognostic biomarker in cancers as compared with Ki67 and PCNA since it fulfills the requirement of an independent factor. However, so far no universal biomarker is available for cancer early-onset diagnostic. Ratio of Ki67-staining vs UHRF1-staining might differentiate well between normal proliferating cells and cancer cells. Indeed, overexpression of UHRF1 is maintained throughout the cell cycle in cancer cells but not in normal cells [57]. Thus, one might expect that UHRF1-staining should be lower than Ki67 in normal tissues and as much as Ki67 or above in cancer cells. This interesting direction requires further investigations but may represent the basis for the development of a diagnostic kit.

UHRF1 overexpression has also proven to be a barrier to cure cancer because of its ability to silence tumor suppressor genes depending on the cancer type (Figure 3) or to counteract pro-apoptotic genes and to induce therapy resistance. It is therefore essential to target UHRF1 overexpression to achieve therapeutic goals in cancer patients. Many strategies can be designed to target UHRF1, including use of small molecules [128]. Therefore, following UHRF1 levels in fluids or tissues during cancer treatment could be of help in a theranostic context.

Abbreviations

UHRF1: ubiquitin-like containing PHD and Ring Finger domain protein 1; DNMT1: DNA methyltransferase 1; qRT-PCR: quantitative reverse-transcriptase polymerase chain reaction; IHC: immunohistochemistry; RDA: representational difference analysis; NSCLC: non-small cell lung cancer; HCC: hepatocellular carcinoma, NMIBC: non-muscle-invasive bladder cancer; RCC: renal cell carcinoma; ESCC: esophageal squamous cell carcinoma; LSCC: laryngeal squamous cell carcinomas.

ACKNOWLEDGMENTS

Our work on UHRF1 was supported by the Agence National de la Recherche (ANR Fluometadn), the Fondation pour la Recherche Médicale (FRM DCM20111223038), Ligue contre le Cancer and by the grant ANR-10-LABX-0030-INRT, a French State fund managed by the Agence Nationale de la Recherche under the frame program Investissements d'Avenir ANR-10-IDEX-0002-02.

CONFLICTS OF INTEREST

All authors report no conflicts of interest.

REFERENCES

1. Sandoval J, Peiro-Chova L, Pallardo FV, Garcia-Gimenez JL. Epigenetic biomarkers in laboratory diagnostics: emerging approaches and opportunities. Expert Rev Mol Diagn. 2013; 13: 457-71. doi: 10.1586/erm.13.37.
2. Jeltsch A, Jurkowska RZ. New concepts in DNA methylation. Trends Biochem Sci. 2014; 39: 310-8. doi: 10.1016/j.tibs.2014.05.002.
3. Zane L, Sharma V, Misteli T. Common features of chromatin in aging and cancer: cause or coincidence? Trends Cell Biol. 2014; 24: 686-94. doi: 10.1016/j.tcb.2014.07.001.
4. Lawrence M, Daujat S, Schneider R. Lateral thinking: how histone modifications regulate gene expression. Trends Genet. 2016; 32: 42-56. doi: 10.1016/j.tig.2015.10.007.
5. Zink LM, Hake SB. Histone variants: nuclear function and disease. Curr Opin Genet Dev. 2016; 37: 82-9. doi: 10.1016/j.gde.2015.12.002.
6. Dawson MA, Kouzarides T. Cancer epigenetics: from mechanism to therapy. Cell. 2012; 150: 12-27. doi: 10.1016/j.cell.2012.06.013.
7. Alhosin M, Sharif T, Mousli M, Etienne-Selloum N, Fuhrmann G, Schini-Kerth VB, Bronner C. Down-regulation of UHRF1, associated with re-expression of tumor suppressor genes, is a common feature of natural compounds exhibiting anti-cancer properties. J Exp Clin Cancer Res. 2011; 30: 41. doi: 10.1186/1756-9966-30-41.
8. Alhosin M, Omran Z, Zamzami MA, Al-Malki AL, Choudhry H, Mousli M, Bronner C. Signalling pathways in UHRF1-dependent regulation of tumor suppressor genes in cancer. J Exp Clin Cancer Res. 2016; 35: 174. doi: 10.1186/s13046-016-0453-5.
9. Chervona Y, Costa M. Histone modifications and cancer: biomarkers of prognosis? Am J Cancer Res. 2012; 2: 589-97.
10. Amacher DE. A 2015 survey of established or potential epigenetic biomarkers for the accurate detection of human cancers. Biomarkers. 2016; 21: 387-403. doi:

10.3109/1354750X.2016.1153724.

11. Angulo JC, Lopez JI, Ropero S. DNA Methylation and urological cancer, a step towards personalized medicine: current and future prospects. Mol Diagn Ther. 2016; 20: 531-49. doi: 10.1007/s40291-016-0231-2.
12. Lam K, Pan K, Linnekamp JF, Medema JP, Kandimalla R. DNA methylation based biomarkers in colorectal cancer: a systematic review. Biochim Biophys Acta. 2016; 1866: 106-20. doi: 10.1016/j.bbcan.2016.07.001.
13. Wu P, Cao Z, Wu S. New progress of epigenetic biomarkers in urological cancer. Dis Markers. 2016; 2016: 9864047. doi: 10.1155/2016/9864047.
14. Willbanks A, Leary M, Greenshields M, Tyminski C, Heerboth S, Lapinska K, Haskins K, Sarkar S. The evolution of epigenetics: from prokaryotes to humans and its biological consequences. Genet Epigenet. 2016; 8: 25-36. doi: 10.4137/GEG.S31863.
15. Probst AV, Dunleavy E, Almouzni G. Epigenetic inheritance during the cell cycle. Nat Rev Mol Cell Biol. 2009; 10: 192-206. doi: 10.1038/nrm2640.
16. Bostick M, Kim JK, Esteve PO, Clark A, Pradhan S, Jacobsen SE. UHRF1 plays a role in maintaining DNA methylation in mammalian cells. Science. 2007; 317: 1760-4. doi: 10.1126/science.1147939.
17. Sharif J, Muto M, Takebayashi S, Suetake I, Iwamatsu A, Endo TA, Shinga J, Mizutani-Koseki Y, Toyoda T, Okamura K, Tajima S, Mitsuya K, Okano M, Koseki H. The SRA protein Np95 mediates epigenetic inheritance by recruiting Dnmt1 to methylated DNA. Nature. 2007; 450: 908-12. doi: 10.1038/nature06397.
18. Arita K, Ariyoshi M, Tochio H, Nakamura Y, Shirakawa M. Recognition of hemi-methylated DNA by the SRA protein UHRF1 by a base-flipping mechanism. Nature. 2008; 455: 818-21. doi: 10.1038/nature07249.
19. Avvakumov GV, Walker JR, Xue S, Li Y, Duan S, Bronner C, Arrowsmith CH, Dhe-Paganon S. Structural basis for recognition of hemi-methylated DNA by the SRA domain of human UHRF1. Nature. 2008; 455: 822-5. doi: 10.1038/nature07273.
20. Hashimoto H, Horton JR, Zhang X, Bostick M, Jacobsen SE, Cheng X. The SRA domain of UHRF1 flips 5-methylcytosine out of the DNA helix. Nature. 2008; 455: 826-9. doi: 10.1038/nature07280.
21. Kent B, Magnani E, Walsh MJ, Sadler KC. UHRF1 regulation of Dnmt1 is required for pre-gastrula zebrafish development. Dev Biol. 2016; 412: 99-113. doi: 10.1016/j.ydbio.2016.01.036.
22. Hopfner R, Mousli M, Jeltsch JM, Voulgaris A, Lutz Y, Marin C, Bellocq JP, Oudet P, Bronner C. ICBP90, a novel human CCAAT binding protein, involved in the regulation of topoisomerase IIalpha expression. Cancer Res. 2000; 60: 121-8.
23. Hopfner R, Mousli M, Garnier JM, Redon R, du Manoir S, Chatton B, Ghyselinck N, Oudet P, Bronner C. Genomic structure and chromosomal mapping of the gene coding for ICBP90, a protein involved in the regulation of the topoisomerase IIalpha gene expression. Gene. 2001; 266: 15-23.
24. Hopfner R, Mousli M, Oudet P, Bronner C. Overexpression of ICBP90, a novel CCAAT-binding protein, overcomes cell contact inhibition by forcing topoisomerase II alpha expression. Anticancer Res. 2002; 22: 3165-70.
25. Bronner C, Krifa M, Mousli M. Increasing role of UHRF1 in the reading and inheritance of the epigenetic code as well as in tumorogenesis. Biochem Pharmacol. 2013; 86: 1643-9. doi: 10.1016/j.bcp.2013.10.002.
26. Jenkins Y, Markovtsov V, Lang W, Sharma P, Pearsall D, Warner J, Franci C, Huang B, Huang J, Yam GC, Vistan JP, Pali E, Vialard J, et al. Critical role of the ubiquitin ligase activity of UHRF1, a nuclear RING finger protein, in tumor cell growth. Mol Biol Cell. 2005; 16: 5621-9. doi: 10.1091/mbc.E05-03-0194.
27. Nishiyama A, Yamaguchi L, Sharif J, Johmura Y, Kawamura T, Nakanishi K, Shimamura S, Arita K, Kodama T, Ishikawa F, Koseki H, Nakanishi M. Uhrf1-dependent H3K23 ubiquitylation couples maintenance DNA methylation and replication. Nature. 2013; 502: 249-53. doi: 10.1038/nature12488.
28. Qin W, Wolf P, Liu N, Link S, Smets M, La Mastra F, Forne I, Pichler G, Horl D, Fellinger K, Spada F, Bonapace IM, Imhof A, et al. DNA methylation requires a DNMT1 ubiquitin interacting motif (UIM) and histone ubiquitination. Cell Res. 2015; 25: 911-29. doi: 10.1038/cr.2015.72.
29. Hashimoto H, Horton JR, Zhang X, Cheng X. UHRF1, a modular multi-domain protein, regulates replication-coupled crosstalk between DNA methylation and histone modifications. Epigenetics. 2009; 4: 8-14.
30. Nady N, Lemak A, Walker JR, Avvakumov GV, Kareta MS, Achour M, Xue S, Duan S, Allali-Hassani A, Zuo X, Wang YX, Bronner C, Chedin F, et al. Recognition of multivalent histone states associated with heterochromatin by UHRF1 protein. J Biol Chem. 2011; 286: 24300-11. doi: 10.1074/jbc.M111.234104.
31. Karagianni P, Amazit L, Qin J, Wong J. ICBP90, a novel methyl K9 H3 binding protein linking protein ubiquitination with heterochromatin formation. Mol Cell Biol. 2008; 28: 705-17. doi: 10.1128/MCB.01598-07.
32. Zhao Q, Zhang J, Chen R, Wang L, Li B, Cheng H, Duan X, Zhu H, Wei W, Li J, Wu Q, Han JD, Yu W, et al. Dissecting the precise role of H3K9 methylation in crosstalk with DNA maintenance methylation in mammals. Nat Commun. 2016; 7: 12464. doi: 10.1038/ncomms12464.
33. Greiner VJ, Kovalenko L, Humbert N, Richert L, Birck C, Ruff M, Zaporozhets OA, Dhe-Paganon S, Bronner C, Mely Y. Site-selective monitoring of the interaction of the SRA domain of UHRF1 with target DNA sequences labeled with 2-aminopurine. Biochemistry. 2015; 54: 6012-20. doi: 10.1021/acs.biochem.5b00419.

34. Kilin V, Gavvala K, Barthes NP, Michel BY, Shin D, Boudier C, Mauffret O, Yashchuk V, Mousli M, Ruff M, Granger F, Eiler S, Bronner C, et al. Dynamics of methylated cytosine flipping by UHRF1. J Am Chem Soc. 2017; 139: 2520-8. doi: 10.1021/jacs.7b00154.

35. Frauer C, Hoffmann T, Bultmann S, Casa V, Cardoso MC, Antes I, Leonhardt H. Recognition of 5-hydroxymethylcytosine by the Uhrf1 SRA domain. PLoS One. 2011; 6: e21306. doi: 10.1371/journal.pone.0021306.

36. Unoki M, Brunet J, Mousli M. Drug discovery targeting epigenetic codes: the great potential of UHRF1, which links DNA methylation and histone modifications, as a drug target in cancers and toxoplasmosis. Biochem Pharmacol. 2009; 78: 1279-88. doi: 10.1016/j.bcp.2009.05.035.

37. Unoki M, Nishidate T, Nakamura Y. ICBP90, an E2F-1 target, recruits HDAC1 and binds to methyl-CpG through its SRA domain. Oncogene. 2004; 23: 7601-10. doi: 10.1038/sj.onc.1208053.

38. Achour M, Fuhrmann G, Alhosin M, Ronde P, Chataigneau T, Mousli M, Schini-Kerth VB, Bronner C. UHRF1 recruits the histone acetyltransferase Tip60 and controls its expression and activity. Biochem Biophys Res Commun. 2009; 390: 523-8. doi: 10.1016/j.bbrc.2009.09.131.

39. Kim JK, Esteve PO, Jacobsen SE, Pradhan S. UHRF1 binds G9a and participates in p21 transcriptional regulation in mammalian cells. Nucleic Acids Res. 2009; 37: 493-505. doi: 10.1093/nar/gkn961.

40. Ma H, Chen H, Guo X, Wang Z, Sowa ME, Zheng L, Hu S, Zeng P, Guo R, Diao J, Lan F, Harper JW, Shi YG, et al. M phase phosphorylation of the epigenetic regulator UHRF1 regulates its physical association with the deubiquitylase USP7 and stability. Proc Natl Acad Sci U S A. 2012; 109: 4828-33. doi: 10.1073/pnas.1116349109.

41. Dai C, Shi D, Gu W. Negative regulation of the acetyltransferase TIP60-p53 interplay by UHRF1 (ubiquitin-like with PHD and RING finger domains 1). J Biol Chem. 2013; 288: 19581-92. doi: 10.1074/jbc.M113.476606.

42. Pacaud R, Brocard E, Lalier L, Hervouet E, Vallette FM, Cartron PF. The DNMT1/PCNA/UHRF1 disruption induces tumorigenesis characterized by similar genetic and epigenetic signatures. Sci Rep. 2014; 4: 4230. doi: 10.1038/srep04230.

43. Jeanblanc M, Mousli M, Hopfner R, Bathami K, Martinet N, Abbady AQ, Siffert JC, Mathieu E, Muller CD, Bronner C. The retinoblastoma gene and its product are targeted by ICBP90: a key mechanism in the G1/S transition during the cell cycle. Oncogene. 2005; 24: 7337-45. doi: 10.1038/sj.onc.1208878.

44. Achour M, Jacq X, Ronde P, Alhosin M, Charlot C, Chataigneau T, Jeanblanc M, Macaluso M, Giordano A, Hughes AD, Schini-Kerth VB, Bronner C. The interaction of the SRA domain of ICBP90 with a novel domain of DNMT1 is involved in the regulation of VEGF gene expression. Oncogene. 2008; 27: 2187-97. doi: 10.1038/sj.onc.1210855.

45. Wang F, Yang YZ, Shi CZ, Zhang P, Moyer MP, Zhang HZ, Zou Y, Qin HL. UHRF1 promotes cell growth and metastasis through repression of p16(ink(4)a) in colorectal cancer. Ann Surg Oncol. 2012; 19: 2753-62. doi: 10.1245/s10434-011-2194-1.

46. Achour M, Mousli M, Alhosin M, Ibrahim A, Peluso J, Muller CD, Schini-Kerth VB, Hamiche A, Dhe-Paganon S, Bronner C. Epigallocatechin-3-gallate up-regulates tumor suppressor gene expression via a reactive oxygen species-dependent down-regulation of UHRF1. Biochem Biophys Res Commun. 2013; 430: 208-12. doi: 10.1016/j.bbrc.2012.11.087.

47. Krifa M, Alhosin M, Muller CD, Gies JP, Chekir-Ghedira L, Ghedira K, Mely Y, Bronner C, Mousli M. Limoniastrum guyonianum aqueous gall extract induces apoptosis in human cervical cancer cells involving p16 INK4A re-expression related to UHRF1 and DNMT1 down-regulation. J Exp Clin Cancer Res. 2013; 32: 30. doi: 10.1186/1756-9966-32-30.

48. Boukhari A, Alhosin M, Bronner C, Sagini K, Truchot C, Sick E, Schini-Kerth VB, Andre P, Mely Y, Mousli M, Gies JP. CD47 activation-induced UHRF1 over-expression is associated with silencing of tumor suppressor gene p16INK4A in glioblastoma cells. Anticancer Res. 2015; 35: 149-57.

49. Sheng Y, Wang H, Liu D, Zhang C, Deng Y, Yang F, Zhang T, Zhang C. Methylation of tumor suppressor gene CDH13 and SHP1 promoters and their epigenetic regulation by the UHRF1/PRMT5 complex in endometrial carcinoma. Gynecol Oncol. 2016; 140: 145-51. doi: 10.1016/j.ygyno.2015.11.017.

50. Chen H, Zhang C, Sheng Y, Yao S, Liu Z, Zhang C, Zhang T. Frequent SOCS3 and 3OST2 promoter methylation and their epigenetic regulation in endometrial carcinoma. Am J Cancer Res. 2015; 5: 180-90.

51. Jin W, Chen L, Chen Y, Xu SG, Di GH, Yin WJ, Wu J, Shao ZM. UHRF1 is associated with epigenetic silencing of BRCA1 in sporadic breast cancer. Breast Cancer Res Treat. 2010; 123: 359-73. doi: 10.1007/s10549-009-0652-2.

52. Zhou L, Shang Y, Jin Z, Zhang W, Lv C, Zhao X, Liu Y, Li N, Liang J. UHRF1 promotes proliferation of gastric cancer via mediating tumor suppressor gene hypermethylation. Cancer Biol Ther. 2015; 16: 1241-51. doi: 10.1080/15384047.2015.1056411.

53. Guan D, Factor D, Liu Y, Wang Z, Kao HY. The epigenetic regulator UHRF1 promotes ubiquitination-mediated degradation of the tumor-suppressor protein promyelocytic leukemia protein. Oncogene. 2013; 32: 3819-28. doi: 10.1038/onc.2012.406.

54. Zhuo H, Tang J, Lin Z, Jiang R, Zhang X, Ji J, Wang P, Sun B. The aberrant expression of MEG3 regulated by UHRF1 predicts the prognosis of hepatocellular carcinoma. Mol Carcinog. 2016; 55: 209-19. doi: 10.1002/mc.22270.

55. Qin L, Dong Z, Zhang JT. Reversible epigenetic regulation of 14-3-3sigma expression in acquired gemcitabine resistance by uhrf1 and DNA methyltransferase 1. Mol Pharmacol. 2014; 86: 561-9. doi: 10.1124/mol.114.092544.

56. Zhang Y, Huang Z, Zhu Z, Zheng X, Liu J, Han Z, Ma X, Zhang Y. Upregulated UHRF1 promotes bladder cancer cell invasion by epigenetic silencing of KiSS1. PLoS One. 2014; 9: e104252. doi: 10.1371/journal.pone.0104252.

57. Mousli M, Hopfner R, Abbady AQ, Monte D, Jeanblanc M, Oudet P, Louis B, Bronner C. ICBP90 belongs to a new family of proteins with an expression that is deregulated in cancer cells. Br J Cancer. 2003; 89: 120-7. doi: 10.1038/sj.bjc.6601068.

58. Bonapace IM, Latella L, Papait R, Nicassio F, Sacco A, Muto M, Crescenzi M, Di Fiore PP. Np95 is regulated by E1A during mitotic reactivation of terminally differentiated cells and is essential for S phase entry. J Cell Biol. 2002; 157: 909-14. doi: 10.1083/jcb.200201025.

59. Arima Y, Hirota T, Bronner C, Mousli M, Fujiwara T, Niwa S, Ishikawa H, Saya H. Down-regulation of nuclear protein ICBP90 by p53/p21Cip1/WAF1-dependent DNA-damage checkpoint signals contributes to cell cycle arrest at G1/S transition. Genes Cells. 2004; 9: 131-42.

60. Tien AL, Senbanerjee S, Kulkarni A, Mudbhary R, Goudreau B, Ganesan S, Sadler KC, Ukomadu C. UHRF1 depletion causes a G2/M arrest, activation of DNA damage response and apoptosis. Biochem J. 2011; 435: 175-85. doi: 10.1042/BJ20100840.

61. Bronner C, Achour M, Arima Y, Chataigneau T, Saya H, Schini-Kerth VB. The UHRF family: oncogenes that are drugable targets for cancer therapy in the near future? Pharmacol Ther. 2007; 115: 419-34. doi: 10.1016/j.pharmthera.2007.06.003.

62. Mudbhary R, Hoshida Y, Chernyavskaya Y, Jacob V, Villanueva A, Fiel MI, Chen X, Kojima K, Thung S, Bronson RT, Lachenmayer A, Revill K, Alsinet C, et al. UHRF1 overexpression drives DNA hypomethylation and hepatocellular carcinoma. Cancer Cell. 2014; 25: 196-209. doi: 10.1016/j.ccr.2014.01.003.

63. Jia Y, Li P, Fang L, Zhu H, Xu L, Cheng H, Zhang J, Li F, Feng Y, Li Y, Li J, Wang R, Du JX, et al. Negative regulation of DNMT3A de novo DNA methylation by frequently overexpressed UHRF family proteins as a mechanism for widespread DNA hypomethylation in cancer. Cell Discov. 2016; 2: 16007. doi: 10.1038/celldisc.2016.7.

64. Muto M, Fujimori A, Nenoi M, Daino K, Matsuda Y, Kuroiwa A, Kubo E, Kanari Y, Utsuno M, Tsuji H, Ukai H, Mita K, Takahagi M, et al. Isolation and characterization of a novel human radiosusceptibility gene, NP95. Radiat Res. 2006; 166: 723-33. doi: 10.1667/RR0459.1.

65. Chen H, Ma H, Inuzuka H, Diao J, Lan F, Shi YG, Wei W, Shi Y. DNA damage regulates UHRF1 stability via the SCF(beta-TrCP) E3 ligase. Mol Cell Biol. 2013; 33: 1139-48. doi: 10.1128/MCB.01191-12.

66. Tian Y, Paramasivam M, Ghosal G, Chen D, Shen X, Huang Y, Akhter S, Legerski R, Chen J, Seidman MM, Qin J, Li L. UHRF1 contributes to DNA damage repair as a lesion recognition factor and nuclease scaffold. Cell Rep. 2015; 10: 1957-66. doi: 10.1016/j.celrep.2015.03.038.

67. Zhang H, Liu H, Chen Y, Yang X, Wang P, Liu T, Deng M, Qin B, Correia C, Lee S, Kim J, Sparks M, Nair AA, et al. A cell cycle-dependent BRCA1-UHRF1 cascade regulates DNA double-strand break repair pathway choice. Nat Commun. 2016; 7: 10201. doi: 10.1038/ncomms10201.

68. Liang CC, Zhan B, Yoshikawa Y, Haas W, Gygi SP, Cohn MA. UHRF1 is a sensor for DNA interstrand crosslinks and recruits FANCD2 to initiate the Fanconi anemia pathway. Cell Rep. 2015; 10: 1947-56. doi: 10.1016/j.celrep.2015.02.053.

69. Wang KY, Chen CC, Tsai SF, Shen CJ. Epigenetic enhancement of the post-replicative DNA mismatch repair of mammalian genomes by a hemi-mCpG-Np95-Dnmt1 axis. Sci Rep. 2016; 6: 37490. doi: 10.1038/srep37490.

70. Park SA, Platt J, Lee JW, Lopez-Giraldez F, Herbst RS, Koo JS. E2F8 as a novel therapeutic target for lung cancer. J Natl Cancer Inst. 2015; 107: djv151. doi: 10.1093/jnci/djv151.

71. Wu SM, Cheng WL, Liao CJ, Chi HC, Lin YH, Tseng YH, Tsai CY, Chen CY, Lin SL, Chen WJ, Yeh YH, Huang CY, Chen MH, et al. Negative modulation of the epigenetic regulator, UHRF1, by thyroid hormone receptors suppresses liver cancer cell growth. Int J Cancer. 2015; 137: 37-49. doi: 10.1002/ijc.29368.

72. Sanders DA, Gormally MV, Marsico G, Beraldi D, Tannahill D, Balasubramanian S. FOXM1 binds directly to non-consensus sequences in the human genome. Genome Biol. 2015; 16: 130. doi: 10.1186/s13059-015-0696-z.

73. Kim KB, Son HJ, Choi S, Hahm JY, Jung H, Baek HJ, Kook H, Hahn Y, Kook H, Seo SB. H3K9 methyltransferase G9a negatively regulates UHRF1 transcription during leukemia cell differentiation. Nucleic Acids Res. 2015; 43: 3509-23. doi: 10.1093/nar/gkv183.

74. Zhou L, Zhao X, Han Y, Lu Y, Shang Y, Liu C, Li T, Jin Z, Fan D, Wu K. Regulation of UHRF1 by miR-146a/b modulates gastric cancer invasion and metastasis. FASEB J. 2013; 27: 4929-39. doi: 10.1096/fj.13-233387.

75. Zhu M, Xu Y, Ge M, Gui Z, Yan F. Regulation of UHRF1 by microRNA-9 modulates colorectal cancer cell proliferation and apoptosis. Cancer Sci. 2015; 106: 833-9. doi: 10.1111/cas.12689.

76. Matsushita R, Yoshino H, Enokida H, Goto Y, Miyamoto K, Yonemori M, Inoguchi S, Nakagawa M, Seki N. Regulation of UHRF1 by dual-strand tumor-suppressor microRNA-145 (miR-145-5p and miR-145-3p): Inhibition of bladder cancer cell aggressiveness. Oncotarget. 2016; 7: 28460-87. doi: 10.18632/oncotarget.8668.

77. Wang X, Wu Q, Xu B, Wang P, Fan W, Cai Y, Gu X, Meng F. MiR-124 exerts tumor suppressive functions on the cell

proliferation, motility and angiogenesis of bladder cancer by fine-tuning UHRF1. FEBS J. 2015; 282: 4376-88. doi: 10.1111/febs.13502.

78. Goto Y, Kurozumi A, Nohata N, Kojima S, Matsushita R, Yoshino H, Yamazaki K, Ishida Y, Ichikawa T, Naya Y, Seki N. The microRNA signature of patients with sunitinib failure: regulation of UHRF1 pathways by microRNA-101 in renal cell carcinoma. Oncotarget. 2016; 7: 59070-86. doi: 10.18632/oncotarget.10887.
79. Deng W, Yan M, Yu T, Ge H, Lin H, Li J, Liu Y, Geng Q, Zhu M, Liu L, He X, Yao M. Quantitative proteomic analysis of the metastasis-inhibitory mechanism of miR-193a-3p in non-small cell lung cancer. Cell Physiol Biochem. 2015; 35: 1677-88. doi: 10.1159/000373981.
80. Zhang ZM, Rothbart SB, Allison DF, Cai Q, Harrison JS, Li L, Wang Y, Strahl BD, Wang GG, Song J. An allosteric interaction links USP7 to deubiquitination and chromatin targeting of UHRF1. Cell Rep. 2015; 12: 1400-6. doi: 10.1016/j.celrep.2015.07.046.
81. Zhao GY, Lin ZW, Lu CL, Gu J, Yuan YF, Xu FK, Liu RH, Ge D, Ding JY. USP7 overexpression predicts a poor prognosis in lung squamous cell carcinoma and large cell carcinoma. Tumour Biol. 2015; 36: 1721-9. doi: 10.1007/s13277-014-2773-4.
82. Song MS, Salmena L, Carracedo A, Egia A, Lo-Coco F, Teruya-Feldstein J, Pandolfi PP. The deubiquitinylation and localization of PTEN are regulated by a HAUSP-PML network. Nature. 2008; 455: 813-7. doi: 10.1038/nature07290.
83. Nicholson B, Suresh Kumar KG. The multifaceted roles of USP7: new therapeutic opportunities. Cell Biochem Biophys. 2011; 60: 61-8. doi: 10.1007/s12013-011-9185-5.
84. Taniue K, Kurimoto A, Sugimasa H, Nasu E, Takeda Y, Iwasaki K, Nagashima T, Okada-Hatakeyama M, Oyama M, Kozuka-Hata H, Hiyoshi M, Kitayama J, Negishi L, et al. Long noncoding RNA UPAT promotes colon tumorigenesis by inhibiting degradation of UHRF1. Proc Natl Acad Sci U S A. 2016; 113: 1273-8. doi: 10.1073/pnas.1500992113.
85. Ding G, Chen P, Zhang H, Huang X, Zang Y, Li J, Li J, Wong J. Regulation of Ubiquitin-like with plant homeodomain and RING finger domain 1 (UHRF1) protein stability by heat shock protein 90 chaperone machinery. J Biol Chem. 2016; 291: 20125-35. doi: 10.1074/jbc.M116.727214.
86. Ferlay J, Soerjomataram I, Dikshit R, Eser S, Mathers C, Rebelo M, Parkin DM, Forman D, Bray F. Cancer incidence and mortality worldwide: sources, methods and major patterns in GLOBOCAN 2012. Int J Cancer. 2015; 136: E359-86. doi: 10.1002/ijc.29210.
87. Unoki M, Daigo Y, Koinuma J, Tsuchiya E, Hamamoto R, Nakamura Y. UHRF1 is a novel diagnostic marker of lung cancer. Br J Cancer. 2010; 103: 217-22. doi: 10.1038/sj.bjc.6605717.
88. Huang P, Cheng CL, Chang YH, Liu CH, Hsu YC, Chen JS, Chang GC, Ho BC, Su KY, Chen HY, Yu SL. Molecular gene signature and prognosis of non-small cell lung cancer. Oncotarget. 2016; 7: 51898-907. doi: 10.18632/oncotarget.10622.
89. Daskalos A, Oleksiewicz U, Filia A, Nikolaidis G, Xinarianos G, Gosney JR, Malliri A, Field JK, Liloglou T. UHRF1-mediated tumor suppressor gene inactivation in nonsmall cell lung cancer. Cancer. 2011; 117: 1027-37. doi: 10.1002/cncr.25531.
90. Liang D, Xue H, Yu Y, Lv F, You W, Zhang B. Elevated expression of UHRF1 predicts unfavorable prognosis for patients with hepatocellular carcinoma. Int J Clin Exp Pathol. 2015; 8: 9416-21.
91. Chen X, Cheung ST, So S, Fan ST, Barry C, Higgins J, Lai KM, Ji J, Dudoit S, Ng IO, Van De Rijn M, Botstein D, Brown PO. Gene expression patterns in human liver cancers. Mol Biol Cell. 2002; 13: 1929-39. doi: 10.1091/mbc.02-02-0023.
92. Liu X, Ou H, Xiang L, Li X, Huang Y, Yang D. Elevated UHRF1 expression contributes to poor prognosis by promoting cell proliferation and metastasis in hepatocellular carcinoma. Oncotarget. 2017; 8: 10510-22. doi: 10.18632/oncotarget.14446.
93. Chang L, Wang G, Jia T, Zhang L, Li Y, Han Y, Zhang K, Lin G, Zhang R, Li J, Wang L. Armored long non-coding RNA MEG3 targeting EGFR based on recombinant MS2 bacteriophage virus-like particles against hepatocellular carcinoma. Oncotarget. 2016; 7: 23988-4004. doi: 10.18632/oncotarget.8115.
94. Shen L, Toyota M, Kondo Y, Lin E, Zhang L, Guo Y, Hernandez NS, Chen X, Ahmed S, Konishi K, Hamilton SR, Issa JP. Integrated genetic and epigenetic analysis identifies three different subclasses of colon cancer. Proc Natl Acad Sci U S A. 2007; 104: 18654-9. doi: 10.1073/pnas.0704652104.
95. Sabatino L, Fucci A, Pancione M, Carafa V, Nebbioso A, Pistore C, Babbio F, Votino C, Laudanna C, Ceccarelli M, Altucci L, Bonapace IM, Colantuoni V. UHRF1 coordinates peroxisome proliferator activated receptor gamma (PPARG) epigenetic silencing and mediates colorectal cancer progression. Oncogene. 2012; 31: 5061-72. doi: 10.1038/onc.2012.3.
96. Kofunato Y, Kumamoto K, Saitou K, Hayase S, Okayama H, Miyamoto K, Sato Y, Katakura K, Nakamura I, Ohki S, Koyama Y, Unoki M, Takenoshita S. UHRF1 expression is upregulated and associated with cellular proliferation in colorectal cancer. Oncol Rep. 2012; 28: 1997-2002. doi: 10.3892/or.2012.2064.
97. Geng Y, Gao Y, Ju H, Yan F. Diagnostic and prognostic value of plasma and tissue ubiquitin-like, containing PHD and RING finger domains 1 in breast cancer patients. Cancer Sci. 2013; 104: 194-9. doi: 10.1111/cas.12052.
98. Macaluso M, Montanari M, Noto PB, Gregorio V, Bronner C, Giordano A. Epigenetic modulation of estrogen receptor-

alpha by pRb family proteins: a novel mechanism in breast cancer. Cancer Res. 2007; 67: 7731-7. doi: 10.1158/0008-5472.CAN-07-1476.

99. Li XL, Xu JH, Nie JH, Fan SJ. Exogenous expression of UHRF1 promotes proliferation and metastasis of breast cancer cells. Oncol Rep. 2012; 28: 375-83. doi: 10.3892/or.2012.1792.

100. Li X, Meng Q, Rosen EM, Fan S. UHRF1 confers radioresistance to human breast cancer cells. Int J Radiat Biol. 2011; 87: 263-73. doi: 10.3109/09553002.2011.530335.

101. Yan F, Tan XY, Geng Y, Ju HX, Gao YF, Zhu MC. Inhibition effect of siRNA-downregulated UHRF1 on breast cancer growth. Cancer Biother Radiopharm. 2011; 26: 183-9. doi: 10.1089/cbr.2010.0886.

102. Fang L, Shanqu L, Ping G, Ting H, Xi W, Ke D, Min L, Junxia W, Huizhong Z. Gene therapy with RNAi targeting UHRF1 driven by tumor-specific promoter inhibits tumor growth and enhances the sensitivity of chemotherapeutic drug in breast cancer in vitro and in vivo. Cancer Chemother Pharmacol. 2012; 69: 1079-87. doi: 10.1007/s00280-011-1801-y.

103. Lorenzato M, Caudroy S, Bronner C, Evrard G, Simon M, Durlach A, Birembaut P, Clavel C. Cell cycle and/or proliferation markers: what is the best method to discriminate cervical high-grade lesions? Hum Pathol. 2005; 36: 1101-7. doi: 10.1016/j.humpath.2005.07.016.

104. Ge TT, Yang M, Chen Z, Lou G, Gu T. UHRF1 gene silencing inhibits cell proliferation and promotes cell apoptosis in human cervical squamous cell carcinoma CaSki cells. J Ovarian Res. 2016; 9: 42. doi: 10.1186/s13048-016-0253-8.

105. Li XL, Meng QH, Fan SJ. Adenovirus-mediated expression of UHRF1 reduces the radiosensitivity of cervical cancer HeLa cells to gamma-irradiation. Acta Pharmacol Sin. 2009; 30: 458-66. doi: 10.1038/aps.2009.18.

106. Yan F, Wang X, Shao L, Ge M, Hu X. Analysis of UHRF1 expression in human ovarian cancer tissues and its regulation in cancer cell growth. Tumour Biol. 2015; 36: 8887-93. doi: 10.1007/s13277-015-3638-1.

107. Adjakly M, Ngollo M, Dagdemir A, Judes G, Pajon A, Karsli-Ceppioglu S, Penault-Llorca F, Boiteux JP, Bignon YJ, Guy L, Bernard-Gallon D. Prostate cancer: the main risk and protective factors-Epigenetic modifications. Ann Endocrinol (Paris). 2015; 76: 25-41. doi: 10.1016/j.ando.2014.09.001.

108. Babbio F, Pistore C, Curti L, Castiglioni I, Kunderfranco P, Brino L, Oudet P, Seiler R, Thalman GN, Roggero E, Sarti M, Pinton S, Mello-Grand M, et al. The SRA protein UHRF1 promotes epigenetic crosstalks and is involved in prostate cancer progression. Oncogene. 2012; 31: 4878-87. doi: 10.1038/onc.2011.641.

109. Wan X, Yang S, Huang W, Wu D, Chen H, Wu M, Li J, Li T, Li Y. UHRF1 overexpression is involved in cell proliferation and biochemical recurrence in prostate cancer after radical prostatectomy. J Exp Clin Cancer Res. 2016; 35: 34. doi: 10.1186/s13046-016-0308-0.

110. Unoki M, Kelly JD, Neal DE, Ponder BA, Nakamura Y, Hamamoto R. UHRF1 is a novel molecular marker for diagnosis and the prognosis of bladder cancer. Br J Cancer. 2009; 101: 98-105. doi: 10.1038/sj.bjc.6605123.

111. Yang GL, Zhang LH, Bo JJ, Chen HG, Cao M, Liu DM, Huang YR. UHRF1 is associated with tumor recurrence in non-muscle-invasive bladder cancer. Med Oncol. 2012; 29: 842-7. doi: 10.1007/s12032-011-9983-z.

112. Ying L, Lin J, Qiu F, Cao M, Chen H, Liu Z, Huang Y. Epigenetic repression of regulator of G-protein signaling 2 by ubiquitin-like with PHD and ring-finger domain 1 promotes bladder cancer progression. FEBS J. 2015; 282: 174-82. doi: 10.1111/febs.13116.

113. Saidi S, Popov Z, Janevska V, Panov S. Overexpression of UHRF1 gene correlates with the major clinicopathological parameters in urinary bladder cancer. Int Braz J Urol. 2017; 43: 224-9. doi: 10.1590/S1677-5538.IBJU.2016.0126.

114. Ma J, Peng J, Mo R, Ma S, Wang J, Zang L, Li W, Fan J. Ubiquitin E3 ligase UHRF1 regulates p53 ubiquitination and p53-dependent cell apoptosis in clear cell Renal Cell Carcinoma. Biochem Biophys Res Commun. 2015; 464: 147-53. doi: 10.1016/j.bbrc.2015.06.104.

115. Wotschofsky Z, Gummlich L, Liep J, Stephan C, Kilic E, Jung K, Billaud JN, Meyer HA. Integrated microRNA and mRNA signature associated with the transition from the locally confined to the metastasized clear cell renal cell carcinoma exemplified by miR-146-5p. PLoS One. 2016; 11: e0148746. doi: 10.1371/journal.pone.0148746.

116. Oba-Shinjo SM, Bengtson MH, Winnischofer SM, Colin C, Vedoy CG, de Mendonca Z, Marie SK, Sogayar MC. Identification of novel differentially expressed genes in human astrocytomas by cDNA representational difference analysis. Brain Res Mol Brain Res. 2005; 140: 25-33. doi: 10.1016/j.molbrainres.2005.06.015.

117. Zhang ZY, Cai JJ, Hong J, Li KK, Ping Z, Wang Y, Ng HK, Yao Y, Mao Y. Clinicopathological analysis of UHRF1 expression in medulloblastoma tissues and its regulation on tumor cell proliferation. Med Oncol. 2016; 33: 99. doi: 10.1007/s12032-016-0799-8.

118. Qin Y, Wang J, Gong W, Zhang M, Tang Z, Zhang J, Quan Z. UHRF1 depletion suppresses growth of gallbladder cancer cells through induction of apoptosis and cell cycle arrest. Oncol Rep. 2014; 31: 2635-43. doi: 10.3892/or.2014.3145.

119. Abbady AQ, Bronner C, Trotzier MA, Hopfner R, Bathami K, Muller CD, Jeanblanc M, Mousli M. ICBP90 expression is downregulated in apoptosis-induced Jurkat cells. Ann N Y Acad Sci. 2003; 1010: 300-3.

120. Pi JT, Lin Y, Quan Q, Chen LL, Jiang LZ, Chi W, Chen HY. Overexpression of UHRF1 is significantly associated with poor prognosis in laryngeal squamous cell carcinoma.

Med Oncol. 2013; 30: 613. doi: 10.1007/s12032-013-0613-9.

121. Yang C, Wang Y, Zhang F, Sun G, Li C, Jing S, Liu Q, Cheng Y. Inhibiting UHRF1 expression enhances radiosensitivity in human esophageal squamous cell carcinoma. Mol Biol Rep. 2013; 40: 5225-35. doi: 10.1007/s11033-013-2559-6.

122. Nakamura K, Baba Y, Kosumi K, Harada K, Shigaki H, Miyake K, Kiyozumi Y, Ohuchi M, Kurashige J, Ishimoto T, Iwatsuki M, Sakamoto Y, Yoshida N, et al. UHRF1 regulates global DNA hypomethylation and is associated with poor prognosis in esophageal squamous cell carcinoma. Oncotarget. 2016; 7: 57821-31. doi: 10.18632/oncotarget.11067.

123. Crnogorac-Jurcevic T, Gangeswaran R, Bhakta V, Capurso G, Lattimore S, Akada M, Sunamura M, Prime W, Campbell F, Brentnall TA, Costello E, Neoptolemos J, Lemoine NR. Proteomic analysis of chronic pancreatitis and pancreatic adenocarcinoma. Gastroenterology. 2005; 129: 1454-63. doi: 10.1053/j.gastro.2005.08.012.

124. Abu-Alainin W, Gana T, Liloglou T, Olayanju A, Barrera LN, Ferguson R, Campbell F, Andrews T, Goldring C, Kitteringham N, Park BK, Nedjadi T, Schmid MC, et al. UHRF1 regulation of the Keap1-Nrf2 pathway in pancreatic cancer contributes to oncogenesis. J Pathol. 2016; 238: 423-33. doi: 10.1002/path.4665.

125. Cui L, Chen J, Zhang Q, Wang X, Qu J, Zhang J, Dang S. Up-regulation of UHRF1 by oncogenic Ras promoted the growth, migration, and metastasis of pancreatic cancer cells. Mol Cell Biochem. 2015; 400: 223-32. doi: 10.1007/s11010-014-2279-9.

126. Pita JM, Banito A, Cavaco BM, Leite V. Gene expression profiling associated with the progression to poorly differentiated thyroid carcinomas. Br J Cancer. 2009; 101: 1782-91. doi: 10.1038/sj.bjc.6605340.

127. Wang BC, Lin GH, Wang B, Yan M, He B, Zhang W, Yang AK, Long ZJ, Liu Q. UHRF1 suppression promotes cell differentiation and reduces inflammatory reaction in anaplastic thyroid cancer. Oncotarget. 2016 Jul 18. doi: 10.18632/oncotarget.10674. [Epub ahead of print].

128. Myrianthopoulos V, Cartron PF, Liutkeviciute Z, Klimasauskas S, Matulis D, Bronner C, Martinet N, Mikros E. Tandem virtual screening targeting the SRA domain of UHRF1 identifies a novel chemical tool modulating DNA methylation. Eur J Med Chem. 2016; 114: 390-6. doi: 10.1016/j.ejmech.2016.02.043.

PART 2
Materials and Methods

Biophysical experimentation

1- Materials:

1.1- Compounds and buffers:

All compounds were dissolved in DMSO at concentration of 50 mM. For experimental usage, the compounds were diluted to 10mM or 1mM. Their storage temperature is -20°C. The buffer used in the majority of experiments is a 20 mM phosphate buffer pH 7.5 containing 50 mM NaCl, 2.5 mM TCEP (Tris(2-carboxyethyl) phosphine)), 1 mM EDTA (Ethylenediaminetetraacetic acid), PEG 0.4% (it will be referred as the PBS buffer). The PBS buffer was stored at +4°C and used for one-week maximum.

1.2- Protein production and purification

For our studies, Wild-type SRA (**Fig 26**) and one SRA mutant (**Fig 27**) were used. The SRA domain of UHRF1 (residues 408-643) and its mutant was expressed and purified in *Escherichia coli* BL21-pLysS (DE3) 3839 [223] by the team of Catherine Birck of the Department of Structural Biology Integrative of IGBMC.

GHM ^{408}*KEC TIVPS NHYGP IPGIP VGTMW RFRVQ VSESG VHRPH VAGIH GRSND*

GAYSL VLAGG YEDDV DHGNF FTYTG SGGRD LSGNK RTAEQ SCDQK LTNTN

RALAL NCFAP INDQE GAEAK DWRSG KPVRV VRNVK GGKNS KYAPA EGNRY

DGIYK VVKYW PEKGK SGFLV WRYLL RRDDD EPGPW TKEGK DRIKK LGLTM

QYPEG YLEAL ANRER EKENS KREEE EQQEG GFASP RTG^{643}

Figure 26. Sequence of SRA binding domain (408-643) of UHRF1 protein

GHM [408]*KEC TIVPS NHYGP IPGIP VGTMW RFRVQ VSESG VHRPH VA**D**IH GRSND*

GAYSL VLAGG YEDDV DHGNF FTYTG SGGRD LSGNK RTAEQ SCDQK LTNTN

RALAL NCFAP INDQE GAEAK DWRSG KPVRV VRNVK GGKNS KYAPA EGNRY

DGIYK VVKYW PEKGK SGFLV WRYLL RRDDD EPGPW TKEGK DRIKK LGLTM

QYPEG YLEAL ANRER EKENS KREEE EQQEG GFASP RTG[643]

***Figure 27**. **Sequence of the SRA G448D mutant.** The glycine at position 448 was replaced with aspartic acid (in black).*

1.3- Storage of SRA

To store the SRA protein, glycerol was added as a cryoprotectant, and the method of "shock freezing" of the protein solution was applied. The solution of SRA protein was frozen by immersing aliquots (150µL) into liquid nitrogen. Samples contained in storage buffer (PB 20 mM, pH 7.5, NaCl 50mM, 2.5 mM TCEP) and 5% glycerol were stored at -20°C.

1.4- Buffer exchange of the SRA

The SRA stock solution was thawed and was added to 15 mL of 20mM PB, pH 7.5, NaCl 50mM, TCEP 2.5 mM, 1 mM EDTA. In order to perform the buffer exchange Amicon Ultro-15 centrifugal filters were loaded in the centrifuge Sigma3k10 (Avantec) equipped with the Nr11133 rotor. The speed was set to 4500 rpm for 30 minutes. The procedure was repeated several times to achieve a 10 000- fold dilution of the initial buffer. Its concentration was calculated by using extinction coefficient of 43,890 $M^{-1}cm^{-1}$ at 280 nm.

1.5- DNA duplexes

The following sequence of the 12-bp duplex was used **5'-GGGCCXGCAGGG-3' / 5'-CCCTGCGGGCCC-3'** with a single CpG site that was either non-methylated (X = C) or hemi-methylated (X = 5mC). Unlabeled oligonucleotides were purchased from IBA GmbH Nucleic Acids Product Supply (Germany) in a HPLC-purified form. Labeled oligonucleotides with ^{th}G at position 7 within the duplex were purchased from TriLink Biotechnologies (USA). Extinction coefficients for the non-labeled sequences 5'-GGGCCCGCAGGG-3' and 5'-CCCTGCGGGCCC-3' were 112,500 $M^{-1}cm^{-1}$ and 97,300 $M^{-1}cm^{-1}$, respectively. Extinction coefficients for single strand DNA

sequence labeled with thG at position 7 was 103,000 $M^{-1}cm^{-1}$. All experiments were performed at 20°C in 20 mM phosphate buffer pH 7.5 containing 50 mM NaCl.

1.6- Hybridization of the DNA

DNA duplexes were made by hybridization of complementary oligonucleotides in equal molar amounts and were annealed by heating to 90°C for 5 min, and then cooling slowly at room temperature. Duplex samples were then kept at +4° C for a few weeks.

2- Physical measurements

2.1- Absorption spectroscopy

Absorption spectra were recorded using Cary400 spectrophotometer or Cary4000 based on double beam principle. The measurements allow determining the fraction of the incident light transmitted through a solution in quartz cuvettes. In order to quantify the absorbance and determine the concentration of used materials Beer-Lambert law is used:

$$A = \log \frac{I_0}{I} = \varepsilon.c.l \qquad (1)$$

Where A is the absorbance of light through the solution, I_0 and I represent the intensities of the incident and transmitted light, ε is the coefficient extinction of the solution, l is the pathlength and C is the concentration. The coefficient extinctions were used at 280 nm for proteins, and at 260 nm for ODNs.

2.2- Steady state fluorescence spectroscopy

Fluorescence spectra were recorded using Fluorolog (Jobin Yvon) or Fluoromax 4 spectrofluorometers equipped with thermostated cell compartement. The spectra were corrected from buffer fluorescence, lamp fluctuations, and instrumental wavelength dependent bias. Excitation wavelength was fixed at 330 nm.

2.3- Screening test:

- ***Principle of the base flipping assay***

The base flipping assay is a fluorescent based test that ensures the sensitive monitoring of the binding of the SRA domain to DNA and the successive flipping process. In order to study SRA-

DNA interactions and the subsequent induced flipping of the methylated cytosine, we used in our study a 12 bp hemimethylated DNA duplex labeled by thG, an isomorphic guanosine fluorescent derivative that substitutes perfectly the guanine in the DNA [224]. thG was incorporated at the vicinity of the methylcytosine to monitor the SRA-induced base flipping (**Fig 28**). The environment sensitive thG was shown to respond with an increase in the fluorescence intensity of approximately 4 folds [225] whenever SRA domain of UHRF1 was added to labeled hemimethylated DNA. This is explained by the binding of SRA to DNA and flipping of the methylated cytosine (**Fig 28**). Accordingly, we speculate that an active compound able to inhibit SRA domain, will lead to a decrease in fluorescence intensity by preventing the binding and the flipping of the methylcytosine. Thus, this test represents a robust tool to screen for UHRF1-SRA inhibitors.

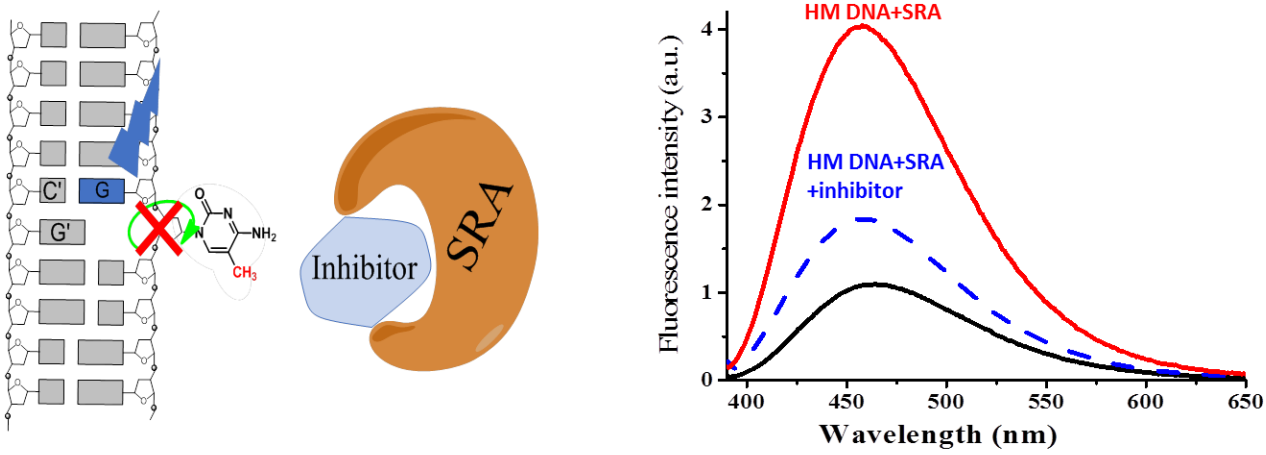

Figure 28. Principle of the base flipping assay by the SRA domain of UHRF1*. The hemimethylated DNA is labeled with the thG fluorescent base, which substitutes the Guanine neighboring the methylated cytosine. The binding of SRA which induces the flipping of the methylated cytosine leads to a strong increase in the fluorescence of thG. The perturbation of the binding between the SRA domain and the hemimethylated DNA by the active molecules must prevent the flipping of the methylated cytosine and thus induce a decrease in the fluorescence intensity.*

- ***Screening protocol and analysis of data***

The screening was performed in the PBS buffer at 20°C in presence of 1µM of hemimethylated DNA and 3µM of SRA. At first, the compounds were tested at two concentrations 10µM and 100µM. Fluorescence spectra were recorded with Fluorolog or with Fluoromax 4 with an excitation

wavelength of 330nm and emission wavelength starting from 340nm to 640nm. The compounds were also tested in buffer alone to check their intrinsic fluorescence and in presence of the labeled DNA to track any interference with the duplex. Absorbance measurements were done to check any aggregation. In the case of an absorbance value higher than 0.1 at the excitation wavelength (330 nm), the emissions spectra were corrected from the inner filter effect by using the equation:

$$I_0 = I \times 10^{\frac{(A_{ex}+A_{em})}{2}} \quad (2)$$

Where A_{ex} and A_{em} correspond to the absorbance at the excitation and emission wavelengths. I_0 and I are the corrected and the measured fluorescence signals respectively.

In order to determine the percentage of inhibition for the positive compounds the corrected spectra were used upon the following formula:

$$\% \text{ inhibition} = \frac{I_{(DNA+SRA)} - I_{(DNA+SRA+inhibitor)}}{I_{(DNA+SRA)} - I_{DNA}} \quad (3)$$

Where $I_{(DNA)}$ corresponds to the fluorescence intensity of DNA alone, $I_{(DNA+SRA)}$ corresponds to the one in presence of SRA and $I_{(DNA+SRA+inhibitor)}$ corresponds to the DNA/SRA mixture with inhibitor.

Next, IC_{50} titrations were performed with the compound that shows a positive response without interfering with the DNA, with no autofluorescence and no aggregation. The IC_{50} value was considered the concentration at which the SRA activity is 50% inhibited. For this, increasing amounts of the molecules were added to the DNA/SRA mixture and the fluorescence and absorbance spectra were recorded in the same parameters and conditions.

After calculation of the percentage of inhibition for each concentration using the listed equation above, this percentage was plotted versus the concentration of the inhibitor to generate a dose-response curve using the Origin 8.6 with the equation of:

$$\% \text{ inhibition} = A1 + \frac{(A2-A1)}{1+10^{((\log(IC50)-C)\times p)}} \quad (4)$$

Where A1 and A2 correspond to the percentage of inhibition in the absence and at saturating concentration of the compound respectively, C is the concentration of the compound, IC_{50} corresponds to half maximal inhibitory concentration and *p* the Hill coefficient is the slope factor.

2.4- Anisotropy

Fluorescence anisotropy method is considered as a powerful tool to study protein/ligand interactions. When a sample is excited by a vertically polarized light, the excitation occurs preferentially on fluorophores with vectors that are aligned parallel to the polarization plane of the light, and subsequently these fluorophores will emit light. The ones with perpendicular vectors do not get excited. This process creates a biased population of excited molecules. The measurement of the emission light is done on a vertical and horizontal plane. The extent by which a molecule can depolarize the polarized light can be described as anisotropy *r* that can be calculated by the following equation:

$$r = \frac{I_{\parallel} + I_{\perp}}{I_{\parallel} + 2I_{\perp}} \quad (5)$$

where $I_{\parallel}$ and $I_{\perp}$ corresponds to the fluorescence intensities measured respectively in the parallel and in the perpendicular plane to the polarization of the excitation light.

The anisotropy measurements provide information about the shape, size, and flexibility of the molecules. The excited state of a small molecule leads it to tumble rapidly and have a high rotational diffusion, and thus upon emission, have low polarization values and low anisotropy. In contrast, in a complex where a small molecule is bound with a larger one at the excited state, the rotation is slow, and consequently it will have high polarization values and high anisotropy (**Fig 29**). For competition experiments, the anisotropy measurements were performed by Fluorolog spectrofluorometer (Horiba Jobin Yvon) equipped with a Peltier thermostated cell at 20°C. For titrations, 1 µM of thG labeled non-methylated DNA was titrated with increasing concentrations of SRA in absence or in presence of 10µM of the compounds in PBS buffer. The anisotropy was monitored through thG fluorescence where excitation and emission wavelengths were set at 330 nm and 460 nm respectively, using the single point mode. The value of each point represents the average of 10 consecutive measurements.

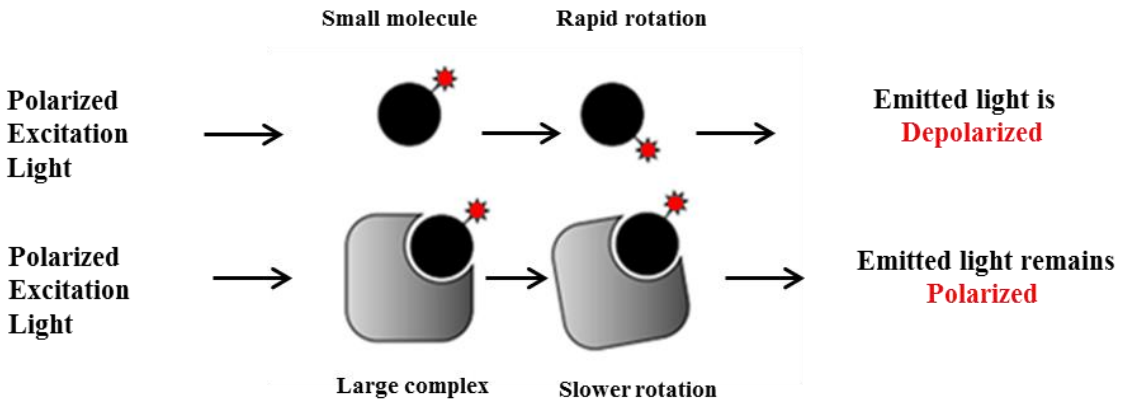

Figure 29. Scheme of fluorescence polarization between small and large complexes.

2.5- Stopped Flow Analysis

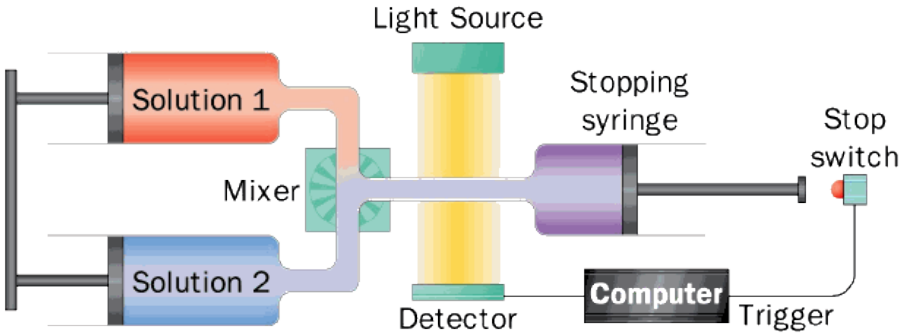

Figure 30. Schematic view of the stopped flow instrument.

The stopped flow technique is a kinetic method to analyze fast rate reactions in solutions. The schematic view of a stopped-flow apparatus is shown in **(Fig 30**). After loading the sample and the reagents solutions into separate drive syringes, the apparatus rapidly fires the two solutions together into a mixing device. The solutions then flow into the observation cell removing the previous contents with freshly mixed reagents. A stop syringe is used to abruptly stop the flow of sample and reagent. The fresh reactants in the observation cell are illuminated by a light source and the changes in function of time, are monitored spectrophotometrically. The measurement is performed by the detector. The time resolution of this method is limited by the "dead time" of the instrument which corresponds to the time needed for the reactants to flow from the final point of mixing to the observation cell. This time is typically around the order of 1-4 ms.

To determine the kinetics of SRA's induced flipping in the thG labeled duplex, a stopped flow apparatus was used (SFM-3, Bio-Logic, Claix, France). The experiments were performed in absence and in presence of the compound at 10 µM and 25 µM. The compound was mixed with the SRA. The thG excitation wavelength was set to 360 nm, a long-pass filter (Kodak Wratten) was used to record its fluorescence intensity. The data recording frequency was 20 kHz. The dead time of the set-up was 2 ms. The kinetic curves were recorded after fast mixing of 100 µL of each solution. The final concentration of labeled DNA and SRA was adjusted to have 80% of DNA bound to protein. Blank experiments in absence of SRA were performed under the same conditions. Data acquisition and processing were done with the Biokine software from the instrument manufacturer. In our case the mechanism itself suggests that the kinetics should obey a single exponential.

2.6- Isothermal Calorimetry (ITC)

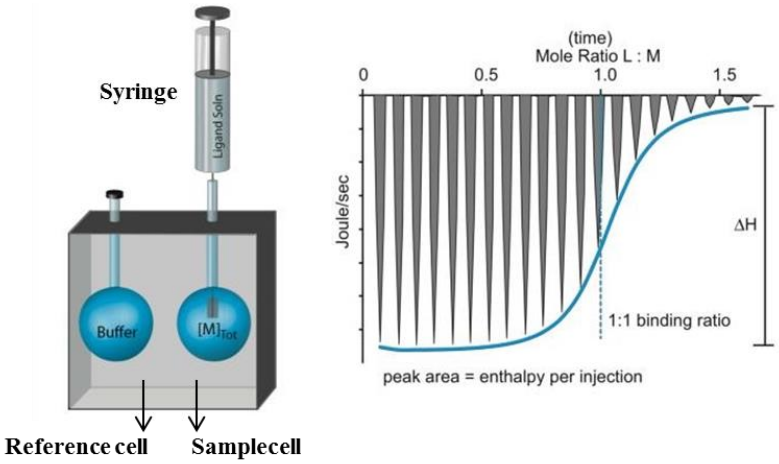

Figure 31. Scheme of the isothermal titration calorimeter.

Isothermal calorimetric titration (ITC) is a technique used for the quantitative study of a wide variety of interactions between biomolecules such as protein-ligands binding. It is based on a direct measurement of the heat released or absorbed during a binding reaction between biomolecules. The measured heat allows an accurate determination of the binding affinities and of the thermodynamic profile. The parameters include binding constants (K_d), the stoichiometry (n), the enthalpy (ΔH) which represents the heat absorbed or released of the reaction and the entropy (ΔS) which refers to the disorder in the system.

The ITC instrument is constituted of two cells (**Fig 31**): the reference and the sample cell. The reagent is loaded into the sample cell while the ligand in the syringe. Small aliquots of ligand are added into the solution and in presence of binding; a heat change is detected and measured. Initially, as the first injections are made, there is a large excess of reagent versus ligand, allowing all the ligand to be in a bound state with a lot of absorbed or released heat. Through the next series of ligand injection, the reagent will be more saturated till it gives the heat corresponding to the dilution of the ligand. Later, the quantity of heat is calculated from each peak and fitted versus the molar ratio of the reagents.

To determine the binding affinity of SRA/molecules and DNA/molecules, ITC was performed using a Nano ITC microcalorimeter (TA instruments). Experiments were performed at 20°C in 20 mM phosphate buffer pH 7.5 containing 50 mM NaCl and 1 mM EDTA. Solutions were prepared in a buffer containing less than 0.1% DMSO. A fixed concentration of 80 µM of SRA contained in a syringe was titrated into 8µM of each of the compounds contained in the compartment cell. In the second experiment, 80µM of hemimethylated duplex was titrated into 8µM of the compounds. The heat flow resulting from the reaction between the two partners was recorded. Instrument control, data acquisition, and analysis were done with NanoAnalyze and ITC run software provided by the manufacturer. The molar heat of binding ΔH^0 and the equilibrium dissociation constant K_d were obtained by fitting the differential heat dQ/dX_{tot} [226] as a function of the total compound concentration ($[SRA]_{tot}$) to equation (7):

$$\frac{1}{V0\left(\frac{dQ}{dX_{tot}}\right)} = \Delta H^0 \left(\frac{1}{2} + \frac{1-\frac{(1+r)}{2}-X_r/2}{(X_r^2-2X_r(1-r)+(1+r)^2)^{1/2}}\right) \quad (6)$$

With $\frac{1}{r}$ = c = $[Hit]_{tot}$ / K_d and $X_r = X_{tot}/[Hit]_{tot}$ where X_{tot} is the SRA concentration in the reaction cell of volume V_0.

2.7- DNA thermal stability analysis

The “melting” is a phenomenon that occurs during a DNA heating process, where duplexes are dissociated to form single strands due to break of hydrogen bonds. When melting occurs, the absorption at 260nm is increased. By measuring the absorbance at 260 nm in function of the temperature, a metling curve is generated. At the melting temperature (Tm), the ratio of double

strands to single strands of DNA is equal. Tm is an indicator of the thermal stability of a duplex, and it varies based on many factors such as base sequence, number of nucleotides, nucleic acid concentration, solvent conditions and others.

In our DNA thermal stability measurements, melting curves were recorded by following the absorbance changes at 260 nm in a temperature-dependent manner ranging from 20 to 80° C on a Cary 4000 spectrophotometer equipped with a Peltier thermostated cell holder. The optical path length of the cell was 1 cm. The heating speed of 0.5°C/min. The concentration of DNA was 1 µM and the concentration of UM63 was 10 µM. Experiments were performed in PBS buffer.

Biological experimentation

1- Materials:

1.1- Cell lines

- **HeLa:** This human cell line name comes from the first two letters of the person from whom the first sample was taken “Henrietta Lacks” and it is derived from cervical cancer cells. This was the first aneuploid line derived from human tissue maintained in continuous cell culture.
- **A375:** It is a human cell line taken originally from a 54-year-old female and it is derived from malignant melanoma.
- **Huh7:** It is a differentiated hepatocyte derived cellular carcinoma cell line that was originally taken from a liver tumor in a 57-year-old Japanese male in 1982.

1.2- Plasmid Construct

For *in vivo* HeLa cell transfection, UHRF1 was cloned into pCMV-mCherry vector to express UHRF1-mCherry protein while the DNMT1 wild type was cloned into pEGFP-N1 plasmid to express DNMT1-eGFP proteins in cells.

1.3- Antibodies

Name	Organism	Source	Type
anti-UHRF1	mouse	Engineered in lab as described previously in [81]	monoclonal
anti-DNMT1	mouse	Stressgen, Canada & Proteogenix, France (PTG-MAB0079)	monoclonal
anti-eGFP	mouse	Thermo Fisher ScientificA-11120 & Proteintech 66002-1-Ig	monoclonal
anti-p73	mouse	BD Biosciences Pharmingen (558785)	monoclonal
anti-p53	mouse	BD Biosciences Pharmingen (554293)	monoclonal
anti-GAPDH	mouse	Merck Millipore (MAB 374)	monoclonal
anti-caspase 3	rabbit	Cell Signaling Technology, Danvers, MA, USA (9661)	polyclonal
anti-PARP	mouse	BD Biosciences Pharmingen (51-6639GR)	monoclonal
Anti-5mC	mouse	Actif Motif (39649)	monoclonal
anti-Bcl2	mouse	Merck-Millipore (05-826)	monoclonal

2- Methods:

2.1- Cell culture

The human cervical cancer cell line HeLa (ATCC, CCL-2 Amp) and Huh7 cell line, was grown in DMEM (Dulbecco's Modified Eagle's Medium) which was supplemented with GlutaMAX (Gibco, Lifetech, France), 10% FBS (fetal bovine serum), in addition to penicillin (100 U/ml) and streptomycin (100 U/ml) (penicillin/streptomycin: Invitrogen Corporation Pontoise, France). Cells were maintained in a humid atmosphere with 5% CO2 at 37°C. The transfection of the plasmids in HeLa cells was carried by the jetPEI™ reagent (Life Technologies, Saint Aubin, France) according to the manufacturer's protocol.

2.2- Transfection protocol

Transfection consists of introducing foreign nucleic acids into mammalian cells. In our experiments, the transient transfection was done by using jetPEI® (Polyplus) DNA transfection reagent. jetPEI is a linear polyethylenimine derivative , known for its minimal toxicity towards the mammalian cells. It covers up the DNA and forms positively charged particles that interact with anionic proteoglycans on cell surface that are later internalized via endocytosis. Afterward, PEI releases the DNA into cytoplasm for transportation to nucleus and a subsequent transcription.

The transfection was performed according to manufacturer's protocol by preparing two solutions one that contains the DNA (plasmid) in 150 mM of NaCl while the other contains JetPEI in 150 mM of NaCl. Then, JetPEI solution was added to DNA following by 20 min incubation. Later, DNA-PEI particles were added drop by drop into the culture media. Cells were transfected with equal amount of DNA.

2.3- Cell proliferation and viability by MTT assay

The MTT (3-[4,5-dimethylthiazol-2-yl]-2,5 diphenyl tetrazolium bromide) assay is based on the reduction of yellow MTT into purple formazan crystals by metabolically active cells, which reflects mitochondrial activity. The formazan is solubilized and quantified by spectrophotometric means.

MTT assay was used in order to assess the proliferation state of cells after treatment with the molecules. HeLa cells were seeded in 96-wells plate at a density of 0.5×10^4 cells/well and treated first with 10 µM of each compound. The positive hits were later tested with various concentrations (0, 0.1, 0.3, 1, 3, 10, 30,100 µM) for 24 hours. Each concentration was tested in triplicate. 100µl of MTT reagent (5mg/10ml) dissolved in medium was added to each well followed with an incubation for 4 hours at 37°C. The medium was discarded and 100µL of dimethylsulfoxide (DMSO) was added to each well. The plates were mixed gently until the dissolution of the formazan crystals. MTT reading was performed by measuring the optical density at 570 nm using Xenius plate reader. Each experiment was repeated three times. The percentage of inhibition was calculated as following:

$$\%\text{inhibition} = \frac{(Control\ value - Compound\ value)}{Control\ value} \qquad (7)$$

The calculation of IC_{50} was done based on the equation (4).

2.4- Protein quantification by Bradford assay

The Bradford assay is a colorimetric method used to determine the quantity of proteins present in a sample. It is based on the change in absorbance due to the change of Coomassie blue color upon interaction of the aromatic amino acids (tryptophan, tyrosine and phenylalanine) and the hydrophobic residues of the amino acids present in the proteins. In order to obtain the working reagent 2mL of BioRad protein Assay reagent (ref:5000006) solution is diluted in 8 ml of water. The reference range is made with increasing amounts of BSA (Bovine Serum Albumin). 5 µL of each test sample are added to 95 µL of reagent. Assays are performed in triplicates. The absorbance of each well was measured at 525nm with respect to the "blank" protein free control. Absorbance measurements are made by a spectrophotometer Safas FLX- Xenius.

Volumes (µL)	1	2	3	4	5
Bradford	200	195	190	185	180
BSA (1.44 mg/mL)	0	5	10	15	20

2.5- Western blot analysis

HeLa, Huh7 and A375 cells (0.15×10^6) were seeded into 6-well cell plates and grown for 24 hours. Cells were treated with different concentrations of compounds for 24 hours. After that cells were harvested, and washed with PBS. Proteins were extracted by resuspending in ice cold lysis buffer (10 mM Tris-HCl pH 7.5, 150 mM NaCl, 1 mM EDTA and 1% NP40) containing protease inhibitors (complete mini EDTA free protease inhibitor cocktail tablets, Roche Germany 11836170001). Cellular protein was quantified by Bradford method and 40 µg of proteins from cell lysate were separated on 10% SDS- polyacrylamide gel by electrophoresis after a 5 min denaturation step in Lammeli sample buffer (Bio-Rad Laboratories USA 1610747). After that, separated proteins are transferred to a (PVDF) membrane and 3% of non-fat dried milk was used to block the membrane at room temperature for 1 hour. Incubation with primary antibodies a mouse monoclonal anti-UHRF1, anti-p53, anti-DNMT1, anti-p73, anti-Bcl2, anti-PARP, anti-caspase3, anti-GAPDH overnight at 4°C was followed. Primary antibodies were labeled with Horseradish Peroxidase conjugated secondary antibody. Signals were visualized by the chemiluminescent ECL

system (Clarity™ ECL western blotting substrate, Biorad, 170-5060) on Image Quant LAS 4000 apparatus. Images were analyzed using Image Studio Lite (Li-Core Biosciences USA).

2.6- Cell Cycle and Apoptosis analysis

Cell cycle analysis is based on a quantification of DNA after staining it with fluorescent dyes. These dyes bind stoichiometrically to DNA, which means they are proportional to the amount of DNA present in cell allowing to determine the different phases of the cell cycle.

Apoptosis is a normal physiologic process of programmed cell death, characterized by a number of morphological and biochemical features. In contrary to normal cells, apoptotic ones include a translocation of membrane phosphatidylserine (PS) from the inner side of the plasma membrane to the surface (**Fig 32**). Annexin V, a phospholipid-binding protein, presents a high affinity for PS. Thus, a labeled Annexin V can be used for the detection of exposed PS using flow cytometry.

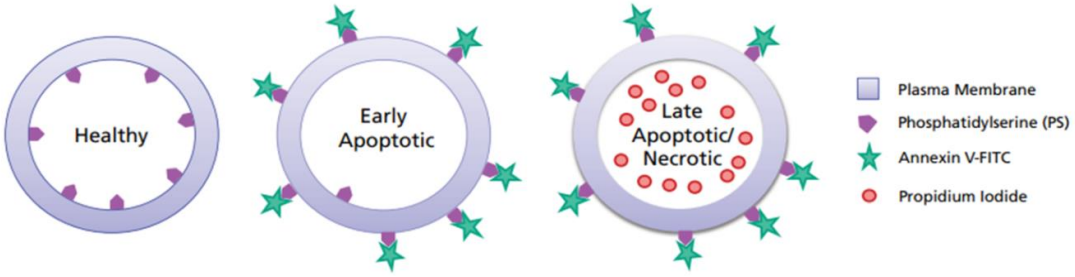

Figure 32. Difference between healthy and apoptotic cells with the corresponding detection markers of apoptosis.

Flow cytometry was used to analyze cell cycle distribution and apoptosis. HeLa cells at a density of 0.15×10^6 cells/well were seeded into a 6-well plate and treated with a concentration of 10 µM for cell cycle and with different concentrations for apoptosis. Treated cells were compared to non-treated HeLa cells that served as control. For cell cycle, the cells were washed once with PBS, trypsinized and fixed with BD cellfix (BD Biosciences) reagent and incubated with FxCycle™ (Thermo Fisher Scientific F10797) PI/RNase staining solution for 20 min. After that cells were fixed and cellular DNA content was done by guava easyCyte™ flow cytometer (Merck Millipore) and population percentages were determined by analyzing the results using InCyte Software for Guava® (Merck Millipore. For apoptosis, the cells were trypsinized and were incubated with PI (Miltenyi Biotec) and annexin V- FITC conjugate (Miltenyi Biotec). The analysis was done using guava easyCyte™ flow cytometer (Merck Millipore).

2.7- Quantification of DNA methylation

HeLa cells were treated with 10 µM of UM 63 and with 10µM of 5-Azacytindine (Sigma-Aldrich), a specific demethylating agent. QIAamp® DNA Kit was used for DNA purification. Methylated DNA was assessed by using 200 ng of DNA extracted from non-treated cells, treated cells, as described by the manufacturer; Sigma's Imprint® Methylated DNA Quantification Kit.

2.9- Fluorescence Lifetime Imaging Microscopy (FLIM)

Fluorescence lifetime imaging (FLIM) is considered to be one of the main fluorescence microscopy methods used to study interaction of specific probes in living cells. FLIM has been used to detect Förster Resonance Energy Transfer (FRET) in order to determine protein interactions or conformational changes in cell biology.

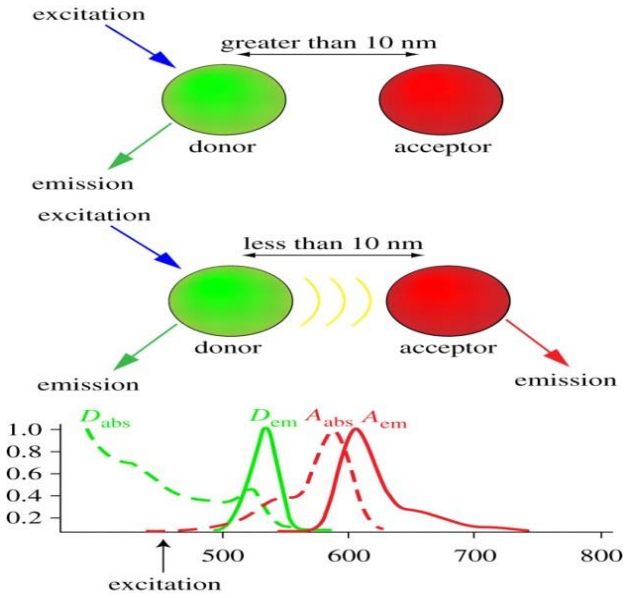

***Figure 33. Schematic representation of FRET**. The realization of FRET occurs when the donor and the acceptor are in close proximity and when there is a spectral overlap between emission of the donor and absorption of the acceptor.*

FRET involves the energy transfer through dipole-dipole coupling of a donor and acceptor chromophores. To be able to realize FRET between 2 fluorophores, the following rules should be respected 1) the emission spectrum of the donor must overlap the excitation spectrum of the acceptor 2) the fluorescent molecules should be close to one another with a distance that corresponds approximately in less than 5-8 nm (Förster distance) (**Fig 33**). In order to have a

possible energy transfer between the donor and acceptor, the labeled proteins must be in very close proximity and random interactions must be excluded. The most popular used couple is eGFP as donor and mCherry or mRFP as acceptor.

The used FLIM approach is based on the Time-correlated single-photon counting (TCSPC). TCSPC allows to record the fluorescent lifetime decay at each pixel of the image. Following donor excitation, fluorescence decay is recorded through TCSPC and fluorescence lifetime measurement is performed. In presence of the acceptor, FRET is measured by the variation of the fluorescence lifetime of the donor fluorophore.

Therefore, the FRET efficiency can be directly determined by the equation: τ

$$\mathrm{E} = 1 - \frac{\tau_D^A}{\tau_D}$$

Where τ_D^A is the fluorescence lifetime of the donor in the presence of an acceptor, and τ_D in the abscence of an acceptor. Evidently, the lower lifetime of donor corresponds to more FRET between the two partners.

To study the interaction between UHRF and DNMT1 we performed the FLIM technique. For this, 10^5 cells were seeded in a µ-dish (Ibidi) with 35 mm wells and were co-transfected with 1 µg DNMT1-eGFP and 1 µg UHRF1-mCherry plasmids by using jetPEI™ reagent as described. After 24 hours of transfection, HeLa cells were treated with the selected compounds. Cells were fixed with 4% paraformaldehyde. After fixation, cells were analyzed on a homemade two-photon excitation scanning microscope based on an Olympus IX70 inverted microscope with an Olympus 60× 1.2NA water immersion objective operating in the descanned fluorescence collection mode [227]. Two-photon excitation at 900nm is provided by a mode-locked titanium-sapphire laser (Tsunami;SpectraPhysics) or an Insight DeepSee (Spectra Physics) laser. Photons are collected using a set of two filters: a shortpass filter with a cutoff wavelength of 680nm (F75-680; AHF,Germany) and a band-pass filter of 520 ± 17 nm (F37-520; AHF, Germany). The fluorescence is directed to a fiber-coupled APD (SPCM-AQR-14-FC; PerkinElmer), which is connected to a time-correlated single photon counting module (SPC830; Becker & Hickl, Germany). A fluorescence lifetime image is visualized by using an arbitrary color coded scale (shorter lifetime in blue and longer lifetime in red) at each pixel. An interaction between the two tagged proteins was considered to occur when FRET efficiency was indicating a minimum of 5%.

2.10- Confocal microscopy

Confocal Microscopy is proving to be one of the most main advances ever reached in optical microscopy and that has been used in applications of cell biology. The advantages of this technique consists of its ability to control depth of field, minimizing the background information away from the focal plane (that leads to image degradation), and the ability to collect serial optical sections from thick specimen.

To analyze the global methylation levels, HeLa cells were seeded on cover glass and then treated for 24 hours with the selected compounds and with 5-Azacytidine as control for demethylation. 4% paraformaldehyde was used for 15 minutes to fix the cells followed by permeabilization with 0.2% Triton X-100 for 15 min. Then DNA was denaturated using 4N HCl for 20 min and neutralized with 100mM Tris HCl pH = 8.5 for 10 min. Next, cells were blocked using 1% BSA and 0.05% Tween in PBS for 1 hour and then pre-incubated with primary antibody anti 5mc (Actif Motif) overnight at 4°C. After washing three times with PBS, an incubation with secondary antibodies was followed with Alexa Fluor 488 (goat anti-mouse). Cells were washed three times and images were visualized by confocal microscopy with a Leica SPE equipped with a 20× 0.7N.A air immersion objective.The images were further processed with Image J software.

Aim of PhD thesis

During the past decade, the recognition of the epigenetic profile of cancer along with the greater understanding of the underlying mechanisms, have led to emergence of new therapeutic avenues.

UHRF1, a key epigenetic player, operates the function of the methylation machinery. During replication, UHRF1 via its SRA domain, helps the inheritance of methylation tags by recognizing hemimethylated DNA and guiding DNMT1 to the newly formed strands [97, 98]. Along with this function, UHRF1 holds an oncogenic potential and is strongly involved in tumorogenesis [178]. UHRF1 plays a role in silencing several tumor suppressor genes through their promoter hypermethylation and controls cellular proliferation [214, 216]. However, it is well documented that UHRF1 is overexpressed in different tumors, and its level correlates with poor prognosis and cancer invasiveness [178].

Given these reasons, UHRF1 was chosen as a candidate in our work specially that till present there is no UHRF1 inhibitor that reached the clinical phase. Thus, the main objective of my research is to identify new UHRF1 inhibitors that target SRA domain in order to prevent abnormal DNA methylation and to demonstrate that targeting UHRF1 can hold a promise as an anti-tumor therapy. More specifically the aims were:

- To rationally select the candidates by screening the molecules with a highly sensitive fluorescent tool “the base flipping assay” that reflects the dynamics of the SRA/DNA complex. The positive hits will be explored further at the molecular level and the mechanism of action will be characterized by various biophysical methods as steady state fluorescence and spectroscopy, kinetics, anisotropy, isothermal calorimetry, FRET analysis.
- To assess anti-tumoral characteristics of these candidates on different cancer cell lines. To investigate their impact on proliferation, apoptosis and cell cycle with the possible related pathways.
- To evaluate the DNA methylation changes upon treatment with an active hit. To measure the interaction *in vivo* in cells between UHRF1 and DNMT1 by FRET-FLIM technique.

This work will help to disclose new clues for anti-cancer therapy and to develop methods to therapeutically target the abnormalities related to UHRF1 in cancer, which will shed more light on the role of UHRF1 in the replication of the epigenetic code.

PART 3
Results and discussions

Strategy for identifying novel UHRF1 inhibitors

In order to identify novel UHRF1 inhibitors, we adopted a multidisciplinary strategy that ranges from virtual screening, to biophysical analysis and biological experimentation.

Our approach was firstly based on an *in silico* virtual screening realized by a collaborator Dr Mattia Mori from Siena University, Italy. For this purpose, a library of commercially available compounds was screened based on several properties (predicted binding mode, theoretical affinity, pharmacophoric features, SAR within the SRA domain of UHRF1). As a result of the virtual screening, we received three batches with 71 total number of molecules as following:
The first batch consisted of 39 molecules representing different chemical structures and families while the second one had 26 molecules sharing the common aniline substructure. The third batch comprised of 6 molecules from the anthraquinone family that were selected based on an active hit identified in the second batch.

Following this screening, my work aimed to evaluate the selected compounds using a variety of biophysical and biological approaches (**Fig 34)** to determine the mechanism of action of active hits and their effect on cellular levels.
As a start, the primary evaluation of the 71 compounds was performed *in vitro* by using two tests:

- **The base flipping assay:** For this test (discussed in Materials and Methods section), two concentrations of each compound were used: 10 µM and 100 µM. A compound is considered positive whenever there is a decrease in fluorescence intensity.
- **The proliferation test:** All compounds studied in the previous assay were also tested at 10 µM for their proliferation-inhibitory potential of cancer cells. The most active ones were then proceeded for further analysis. (It should be noted that this cell line was used due to its availability and usage in our laboratory).

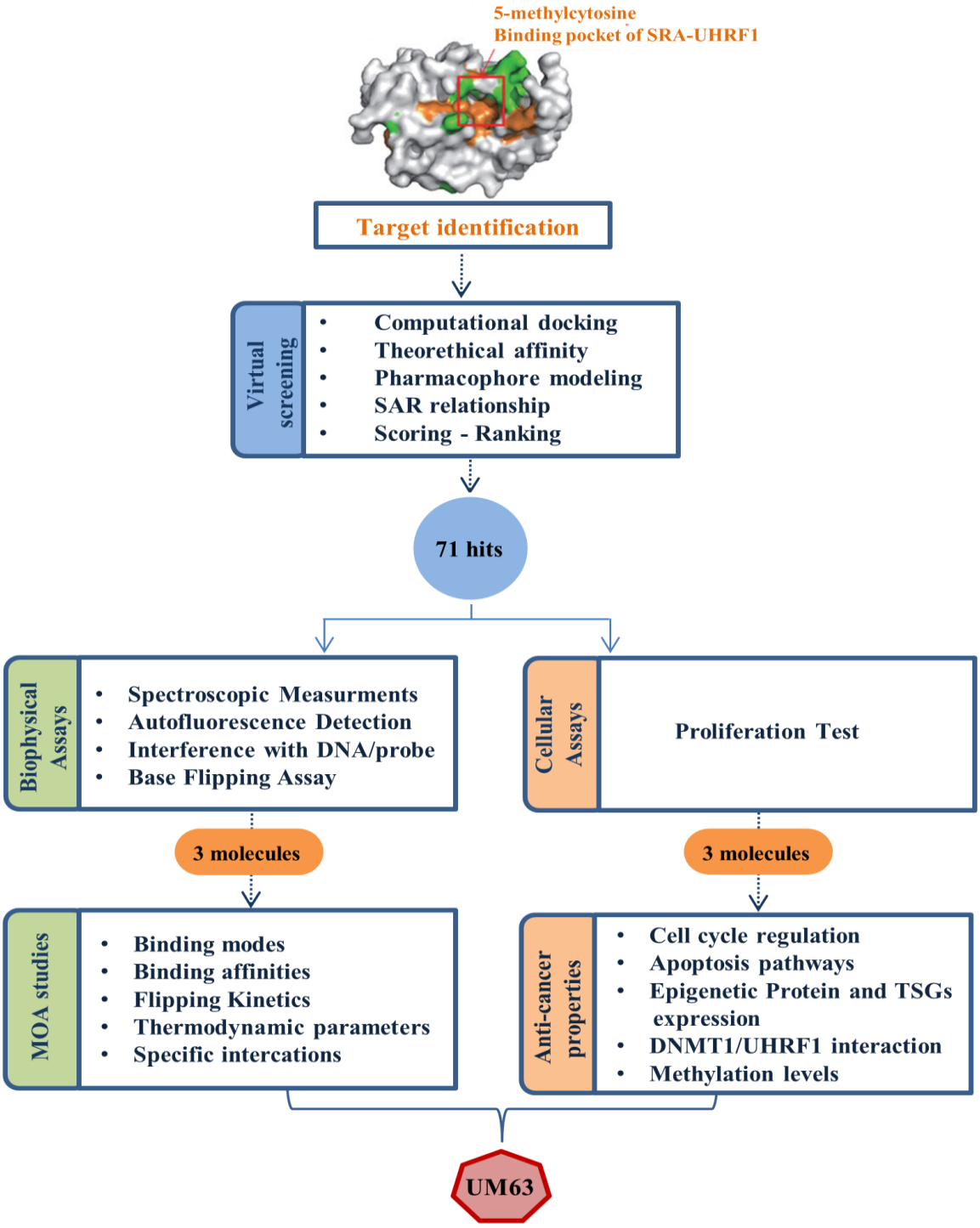

Figure 34. Schematic representation of the work flow used for the evaluation of all compounds. *Three molecules were active in biophysical assays and three were active in biological assays. UM63 is the compound that proved an activity on both levels.*

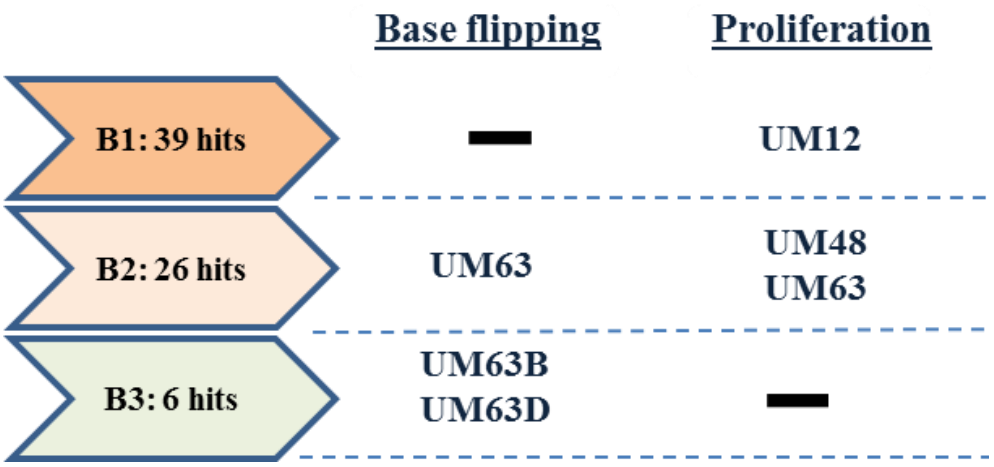

Figure 35. Summary of the results of screening of the 71 molecules. *The molecules are named as "UM" for "Unknown Molecule" with their corresponding number. "B" corresponds to batch followed by the number of the batch.*

"UM63", an anthraquinone analog, with the chemical name of 2-amino-3-hydroxyanthraquinone (AHAQ) inhibited the binding and flipping of the SRA domain to hemimethylated DNA and affected cell viability in HeLa cancer cells (**Fig 35**). Later, this hit served as a lead for optimization to select 6 compounds of anthraquinone family, among which two hits "UM63B" and "UM63D" gave a positive response on the base flipping assay with an efficacy comparable to the parent hit UM63. Unfortunately, in our cellular assays, these two molecules did not show any efficient response, perhaps due to their limited capacity to enter the cell and penetrate inside the nucleus to inhibit UHRF1.

Finally, only UM63 was found of interest and was carefully characterized for its mechanism of action in UHRF1 inhibition, which will be discussed in ***Manuscript I*** and for its UHRF1-related anti-cancer effects in different cancer cell lines, which will be described in ***Manuscript II***.

Additionally, two more compounds "UM12" and "UM48" from 1st and 2nd batch of molecules showed inhibitory effect on proliferation of cancer cells. These compounds were later proceeded in biological experiments to explore their effects on UHRF1 related cellular functions. Contrary to UM12, UM48 exerted its effect only in preliminary studies and didn't pass the tests which are more specific to UHRF1. Activity of these molecules will be described in the last part of results section.

Manuscript 1

Identification of a new molecule targeting UHRF1 and disrupting its interaction with DNMT1

Liliyana Zaayter[1,#], Mattia Mori[3,#], Waseem Ashraf[1], Christian Boudier[1], Vasyl Kilin[1], Krishna Gavvala[1], Tanveer Ahmad[1], Maurizio Botta[3], Christian Bronner[2], Marc Ruff[4], Sylvia Eiler[4], Marc Mousli[1,*], Yves Mély[1,*]

[1] Laboratoire de Bioimagerie et Pathologies, UMR 7021 CNRS, Université de Strasbourg, Faculté de Pharmacie, Illkirch-France

[2] Institut de Génétique et de Biologie Moléculaire et Cellulaire (IGBMC), INSERM U964 CNRS UMR 7104, Université de Strasbourg, Illkirch-France.

[3] Dipartimento di Biotecnologie, Chimica e Farmacia, Università degli Studi di Siena, Via Aldo Moro 2, 53100, Siena, Italy.

[4]Institut de Génétique et de Biologie Moléculaire et Cellulaire (IGBMC), INSERM U964 CNRS UMR 7104, Université de Strasbourg, Illkirch, France.

[#] LZ and MM equally contributed to this work

*Authors to whom correspondence should be addressed: Marc Mousli, mousli@unistra.fr; Yves Mély, yves.mely@unistra.fr

Abstract:

Abnormal DNA methylation is recognized as one of the major cancer signatures. During replication, Ubiquitin-like, containing PHD and RING fingers domains (UHRF1) plays a key role in the inheritance of methylation patterns to daughter strands by recognizing through its set and ring (SRA) domain the methylated CpGs and recruiting DNMT1. Besides its role as an epigenetic regulator, UHRF1 is implicated in tumorogenesis, by modulating the expression of tumor suppressor genes and promoting cancer growth through various mechanisms. Accordingly, one promising strategy in anti-cancer therapy is to develop molecules able to inhibit UHRF1 activity. Herein, our aim is to identify new UHRF1 inhibitors that target the SRA domain in order to prevent methylation aberrancies and thus, develop leads for cancer treatment. For this, we conducted a multidisciplinary strategy that integrates virtual screening with biophysical studies and cellular assays. Our screen identified one active compound from the anthraquinone family, with a dose-response in the micromolar range (4.4 ±0.5 µM) that was able to bind to the SRA domain cavity and inhibit the flipping of the methylated cytosine. Our results also showed that this hit impaired the interaction between UHRF1 and DNMT1 and exhibited a demethylating effect in cancer cells. This study provides a proof of concept that small molecules targeting UHRF1 can hold a potential for anti-cancer therapy.

A- Introduction:

During the lifespan of an organism, the genome undergoes a chain of epigenetic processes that shape the function and morphology of a cell in a very diverse manner. These epigenetic processes direct the gene expression patterns, establishing the identity of a cell that could be heritable for future generations. DNA methylation is considered to be a major epigenetic modification that controls the cell identity and fate, being responsible for many fundamental processes such as differentiation, genome imprinting and X chromosome inactivation [1-3]. This mark is also strongly involved in cancer [4, 5], as it is well recognized that DNA hypermethylation is one of the hallmarks of tumorigenesis. Indeed, abnormal gain of DNA methylation in promoter regions of tumor suppressor genes plays a key role in gene silencing and transcriptional repression [6, 7]. Interestingly, epigenetic mechanisms are reversible and dynamic, unlike genetic mechanisms, which has given epigenetic mediators great attention as pharmaceutical targets.

Different ways can be used to target DNA methylation as numerous actors are involved in this epigenetic process. In order to achieve a faithful transmission of the epigenetic code, the DNA methylation machinery is coordinated by a macro-molecular protein complex [8, 9], in which UHRF1 (Ubiquitin-like, containing PHD and RING fingers domains) is an essential epigenetic regulator. UHRF1 is a multifunctional protein that ensures recognition of both DNA methylation status and histone modification status and connects them. UHRF1 binds specifically to CpG motifs in hemi-methylated (HM) DNA via its SET and RING-associated domain (SRA) and flips out the methylated cytosine (5mC) from the DNA helix [10, 11]. X-ray crystallography studies revealed the structure of SRA in complex with HM DNA, which helped to propose a model of DNA recognition and base flipping [10, 12, 13]. In this structure, SRA acts as a hand grasping the DNA duplex in its palm. Through its NKR finger and its thumb, the SRA domain flips out the methylcytosine into a binding pocket located in the “palm”. The flipped out 5mC is stabilized by pi-stacking interactions with two aromatic residues (Y478, Y466) [13]. Besides this, UHRF1 also binds to histone H3K9me3 via its tandem Tudor and PHD domain [14, 15]. These functions facilitate the recruitment of DNA methyltransferase1 (DNMT1) to replication forks in the S phase of the cell cycle in order to ensure the maintenance of the methylation patterns in the newly formed DNA [11, 15, 16]. Moreover, via the E3 ligase activity of its RING domain, UHRF1, can also mediate the ubiquitylation of H3K23 and H3K18, creating binding sites for DNMT1 [17, 18].

Numerous emerging therapeutic strategies focus on targeting DNA methylation [19], but till date, only demethylating agents targeting DNMT1 have been disclosed. These agents include FDA-approved nucleoside analogs (Azacytidine and Decitabine) [20, 21] and non-nucleoside inhibitors such as Hydralazine and Procainamide [22]. Several limitations upon their usage such as chemical instability, cytotoxicity and poor selectivity [23-25] stimulated the development of alternative treatments with better therapeutic effect and fewer side effects. Due to its key role in DNA methylation and its overexpression in almost every type of tumors [26], UHRF1 is perceived as a major target for anti-cancer therapy [27, 28]. Till date, several natural compounds have been reported to act on UHRF1 signaling pathways [9, 29, 30], but only two inhibitors have been identified to directly target the protein. One of these inhibitors is a uracil derivative that targets the SRA domain and perturbs the interaction with DNMT1 [31], while the second one, 4-benzylpiperidine-1-carboximidamide, targets the TTD groove and alters the binding of UHRF1 to H3K9me3 [32]. Finally, mitoxantrone, a topoisomerase II inhibitor, has also been reported to alter the binding of the SRA domain to HM DNA and to induce hypomethylation with subsequent reexpression of tumor suppressor genes (TSGs) [33, 34].

In this context, our aim was to disclose small molecule inhibitors of UHRF1 that can fit into the 5mC binding pocket of the SRA domain. This binding mechanism is expected to impair the interaction of SRA to HM DNA and the related flipping of 5mC, which may prevent transmission of the methylation marks, and enhance the control of aberrant DNA methylation. To this aim, we established a multidisciplinary strategy that includes virtual screening, biophysical assays and cellular studies. We discovered one active compound, UM63 that shares some chemical features with mitoxantrone [35, 36]. UM63 altered the binding of SRA with HM DNA and prevented base flipping with an IC_{50} value in the low micromolar range. Cellular assays further showed that this compound prevented the DNMT1/UHRF1 interaction and altered the DNA methylation status in HeLa cells, thus emerging as a valuable UHRF1 inhibitor tool as well as a starting point for hit-to-lead optimization.

B- Materials and methods:

All compounds were dissolved in pure DMSO (Sigma Aldrich) and kept at -20°C. 4-Amino-1-(β-D-ribofuranosyl)-1,3,5-triazin-2(1*H*)-one (5-Azacitidine) ≥98 % (HPLC) was purchased from Sigma Aldrich. Wild-type SRA (residues 408-643) and SRA mutant (G488D) were expressed and purified in Escherichia coli BL21-pLysS (DE3) 3839 as previously described [37, 38]. Their concentration was calculated by using an extinction coefficient of 43,890 $M^{-1}cm^{-1}$ at 280 nm. DNA duplexes were obtained by annealing equal molar amounts of complementary oligonucleotides, and heating to 90°C for 5 min, and then cooling slowly down to room temperature. The following 12-bp duplex sequence was used **5'-GGGCCXGCAGGG-3' / 5'-CCCTGCGGGCCC-3'** with a single CpG site that was either non-methylated (X = C) or hemi-methylated (X = 5mC). Unlabeled oligonucleotides were purchased from IBA GmbH Nucleic Acids Product Supply (Germany) in a HPLC-purified form. Labeled 5'-GGGCCXGCAGGG-3' oligonucleotides with thG at position 7 were purchased from TriLink Biotechnologies (USA). Extinction coefficients for the non-labeled sequences 5'-GGGCCCGCAGGG-3' and 5'-CCCTGCGGGCCC-3' were 112,500 $M^{-1}cm^{-1}$ and 97,300 $M^{-1}cm^{-1}$, respectively. Extinction coefficient for the single strand DNA sequence labeled with thG at position 7 was 103,000 $M^{-1}cm^{-1}$. The majority of experiments was performed at 20°C in 20 mM phosphate buffer pH 7.5 containing 50 mM NaCl and 1 mM EDTA, 2.5 mM TCEP and PEG 0.05%. Absorption spectra were recorded on a Cary 400 spectrophotometer (Varian).

1- Molecular modeling.

The MolPort commercial library of compounds containing 6,504,839 entries at April 2015 was downloaded in SMILES format. Filtration was performed with the FILTER application implemented in OMEGA (version 2.5.1.4) from OpenEye [39, 40] using the SMARTS string corresponding to the aniline substructure as query: c1ccccc1[NH2]. Filtration of the initial library let to 30,947 molecules, whose protonation state was assigned by QUACPAC from OpenEye (version 1.6.3.1) [41]. Conformational analysis was performed with OMEGA (version 2.5.1.4) keeping all default settings and allowing the storage of up to 600 conformers per molecule. The crystallographic structure of the SRA domain of UHRF1 bound to methylated DNA was retrieved from the Protein Data Bank under the accession code PDB: 3CLZ and used as rigid receptor in molecular docking simulations [10]. Docking-based virtual screening was performed with FRED from OpenEye (version 3.0.1)[42, 43] using default settings and retaining only the best pose of each

docked molecule. In-depth docking investigation of UM63 was carried out with FRED, using the highest docking resolution settings and retaining 10 poses.

2- Steady-state fluorescence spectroscopy

Fluorescence spectra were recorded at 20°C on a FluoroLog (Jobin Yvon) or a Fluoromax 4 spectrofluorometer equipped with a thermostated cell compartment. Excitation was set at 330 nm. Spectra were corrected for buffer fluorescence, lamp fluctuations, and detector spectral sensitivity. To determine the percentage of inhibition for a given compound, the following formula was used:

$$\% \text{ inhibition} = \frac{I_{(DNA+SRA)} - I_{(DNA+SRA+inhibitor)}}{I_{(DNA+SRA)} - I_{(DNA)}} \quad (1)$$

where I_{DNA}, $I_{(DNA+SRA)}$ and $I_{(DNA+SRA+inhibitor)}$ correspond to the fluorescence intensity of DNA alone, DNA/SRA complex and DNA/SRA complex in the presence of inhibitor, respectively. For positive hits, the percentage of inhibition was measured at several hit concentrations in order to generate a dose-response curve. This curve was then fitted using:

$$\% \text{ inhibition} = A1 + \frac{(A2 - A1)}{1 + 10^{((\log(IC50) - C) \times p)}} \quad (2)$$

where A1 and A2 correspond to the percentage of inhibition in the absence and at saturating concentration of the hit, respectively. C is the concentration of the hit, IC_{50} corresponds to half maximal inhibitory concentration and p is the Hill coefficient. From the IC_{50} value, the inhibition constant of the compound (K_i) was then determined based on the Cheng and Prussof equation:

$$Ki = \frac{IC_{50}}{1 + \frac{[DNA]}{K_{d_{(SRA/DNA)}}}} \quad (3)$$

where $K_{d_{(SRA/DNA)}}$ is the dissociation constant of SRA to the duplex and [DNA] is the DNA concentration.

In order to determine the binding constant of SRA to DNA in presence of the hits, a titration was performed by monitoring the changes in fluorescence anisotropy of a fixed amount of labeled duplex in the presence of increasing concentrations of SRA. This titration was performed in the absence and in the presence of 10 µM of the positive hit. Anisotropy values were the average of 10

measurements. Excitation wavelength for thG was at 330 nm and emission was collected at 460 nm. The affinity constants were determined by fitting the fluorescence anisotropy changes to the following equation:

$$r = \frac{vRr_t - r_d(v-1)}{1+R_v-v} \quad (4)$$

where r and r_d are the anisotropy values in the presence and absence of SRA, and r_t is the anisotropy at a saturating SRA concentration. R is the ratio of fluorescence intensity of the bound to the free forms, K_a is the apparent affinity constant, v is the fraction of bound SRA calculated as:

$$v = \frac{(K_a^{-1}+nL_t+P_t) - \sqrt{(K_a^{-1}+nL_t+P_t)^2 - 4nP_tL_t}}{2L_t} \quad (5)$$

where Pt and Lt represent the total concentrations of SRA and thG-labeled duplex, respectively, and n represents the number of DNA binding sites per SRA [44].

3- Isothermal Titration Calorimetry

To determine the binding affinity of the hits to SRA or DNA, ITC was performed using a Nano ITC microcalorimeter (TA instruments). Experiments were performed at 20°C in 20 mM phosphate buffer pH 7.5, 50 mM NaCl. Solutions were prepared in a buffer containing less than 0.1% DMSO. Aliquots of 2.5 µL of 80 µM of SRA or HM duplex solution contained in a syringe was titrated into 8 µM of tested compound contained in the reaction cell. The heat flow (µcal ×s $^{-1}$) resulting from the reaction between the two partners was recorded. Instrument control, data acquisition, and analysis were done with the NanoAnalyze and ITC runsoftware provided by the manufacturer. The molar heat of binding ΔH^0 and the equilibrium dissociation constant K_d were obtained by fitting the differential heat dQ/dX_{tot} [45] as a function of the total compound concentration ($[SRA]_{tot}$) to equation (7):

$$\frac{1}{V0(\frac{dQ}{dX_{tot}})} = \Delta H^0 \left(\frac{1}{2} + \frac{1-\frac{(1+r)}{2} - X_r/2}{(X_r^2-2X_r(1-r)+(1+r)^2)^{1/2}}\right) \quad (6)$$

With $\frac{1}{r}$ = c = $[Hit]_{tot}$ / K_d and $X_r = X_{tot}/[Hit]_{tot}$ where X_{tot} is the SRA concentration in the reaction cell of volume V_0.

4- Stopped Flow

The kinetics of SRA-induced base flipping in the thG-labeled duplex was monitored using a stopped-flow apparatus (SFM-3, Bio-Logic, Claix, France). The thG excitation wavelength was set to 360 nm. Fluorescence intensity was followed above 425 nm using a long-pass filter (Kodak Wratten). The data recording frequency was 20 kHz. The dead time of the set-up was 2 ms. The kinetic curves were recorded after fast mixing of 100 µL of labeled DNA in one syringe and SRA in the absence or presence of UM63 in the other syringe. The final concentration of labeled DNA was 0.2 µM and the concentration of SRA was 1.5 µM. UM63 was tested at 10 µM and 25 µM. For dissociation experiments, 10 µM or 25 µM UM63 was added to a pre-formed DNA/SRA complex. Same parameters were used for both experiments. Data acquisition and processing were done with the Biokine software from the instrument manufacturer.

5- Cell culture

HeLa cells (ATCC, CCL-2) were grown in DMEM (Dulbecco's Modified Eagle's Medium) which was supplemented with 10% FBS (fetal bovine serum), in addition to penicillin (100 U/ml) and streptomycin (100 U/ml) (Invitrogen Corporation Pontoise, France). Cells were maintained in a humid atmosphere with 5% CO_2 at 37°C. The transfection of the plasmids in HeLa cells was carried out with jetPEI™ (Life Technologies, Saint Aubin, France) according to the manufacturer's protocol.

6- Immunofluorescence Assay

HeLa cells were seeded on a cover glass and then treated for 24 h with UM63 or 5-Azacytidine (5-Aza), used as control. Cells were fixed with 4% paraformaldehyde for 15 minutes and then, permeabilized with 0.2% Triton X-100 for 15 min. Then, 4M HCl was added for 20 min to denature DNA. The medium was then neutralized with 100 mM Tris HCl pH = 8.5 for 10 min. Next, cells were blocked using 1% BSA and 0.05% Tween in PBS for 1 hour, before incubation with a primary antibody against 5mC (Actif Motif) overnight at 4°C. After washing three times with PBS, cells were incubated with secondary antibodies labeled with Alexa Fluor 488 (goat anti-mouse) for 20 min. Finally, cells were washed three times and imaged with a confocal Leica SPE microscope equipped with a 20x 0.7 N.A air immersion lens objective. The images were further processed with Image J software.

7- Fluorescence Lifetime Imaging Microscopy (FLIM)

For FLIM experiments, 10^5 cells were seeded in a µ-dish (Ibidi) with 35 mm wells and were co-transfected with 1 µg DNMT1-eGFP and 1 µg UHRF1-mCherry plasmids by using jetPEI™ reagent. After transfection, cells were treated with 10 µM of UM63 for 24 h. At the end of the treatment, cells were fixed with 4% paraformaldehyde. After fixation, cells were analyzed with a homemade two-photon excitation scanning microscope based on an Olympus IX70 inverted microscope with an 60X 1.2 NA water immersion objective operating in the descanned fluorescence collection mode as described [46, 47]. Two-photon excitation at 930 nm was provided by an Insight DeepSee laser (Spectra Physics). Fluorescence photons were collected using a short-pass filter with a cut-off wavelength of 680 nm (F75-680, AHF, Germany) and a band-pass filter of 520 ± 17 nm (F37-520, AHF, Germany). The fluorescence was directed to a fiber coupled APD (SPCM-AQR-14-FC, Perkin Elmer), which was connected to a time-correlated single photon counting module (SPC830, Becker & Hickl, Germany). FLIM data were analyzed using SPCImage v 4.9.7 (Becker & Hickel) and the Förster resonance energy transfer (FRET) efficiency was calculated according to $E=1-(\tau_{DA}/\tau_D)$, where τ_{DA} is the lifetime of the donor (eGFP) in the presence of acceptor (mCherry) and τ_D is the lifetime of eGFP in the absence of acceptor.

C- Results:

1- Selection of hits by virtual screening

With the aim to identify different chemotypes of UHRF1 inhibitors that target the 5mC binding pocket of the SRA domain, and based on structural information available from X-ray crystallography studies [10, 12, 13, 48], a diversity-oriented and structure-based virtual screening approach was established. To this aim, the high resolution crystallographic structure of the human SRA domain of UHRF1 bound to methylated DNA [10] was used as a rigid receptor in virtual screening. Analysis of the interactions established by the flipped 5mC in its narrow binding site on SRA revealed key pharmacophoric features such as the aromatic ring, which is pi-pi stacked to the side chain of Tyr478 in a parallel displaced geometry, and a number of polar groups able to establish H-bonds with the protein. These features were exploited to pre-screen the MolPort database of commercially available compounds (https://www.molport.com/shop/index, around 6.5M compounds at April 2015), and to enrich the test-set with compounds endowed with a high probability to mimic the binding of 5mC within the SRA binding site. In particular, the aniline substructure was selected for filtration of the database, which was accomplished through a SMARTS-based query with the FILTER application of OMEGA from OpenEye [39, 40]. This operation decreased the overall size of the screening library up to around 31K molecules, which were submitted to conformational analysis with OMEGA (OpenEye) [39, 40] and were subsequently docked within the 5mC binding site of methylcytosine by FRED docking program from OpenEye [42, 43]. Top ranking 1,000 compounds were further selected for visual inspection. Moreover, to maximize chemical diversity, these molecules were clustered based on fingerprints and substructure search through a cheminformatics approach [49-51]. The combination between visual inspection and chemical diversity led to the selection of 26 small molecules for *in vitro* testing (Fig. S1).

2- Selection of hits by using an in vitro "base flipping assay"

To test the 26 compounds selected by virtual screening, we used a fluorescence-based assay highly sensitive to 5mC base flipping. This assay is based on the use of a HM DNA labeled by thG (Fig. 2A), an isomorphic guanosine derivative that has been shown to perfectly replace the guanine residue next to the methylated cytosine in the CpG motif [52, 53]. Addition of SRA to this labeled DNA is accompanied by a 4-fold increase in the fluorescence intensity, as a result of the SRA-

induced flipping of the methylated cytosine (Fig. 2) [53]. Among the 26 compounds, UM63 was the most promising hit candidate, as it induced a concentration-dependent decrease in fluorescence intensity, suggesting that it could inhibit the SRA-induced base flipping. IC_{50} calculation for this compound indicated a value of 4.4 ±0.5 µM (Fig. 2B). Moreover, to substantiate the quality of the selected scaffold, a number of commercially available chemical derivatives of UM63, namely UM63A-F (Fig. 1) were selected and tested as well.

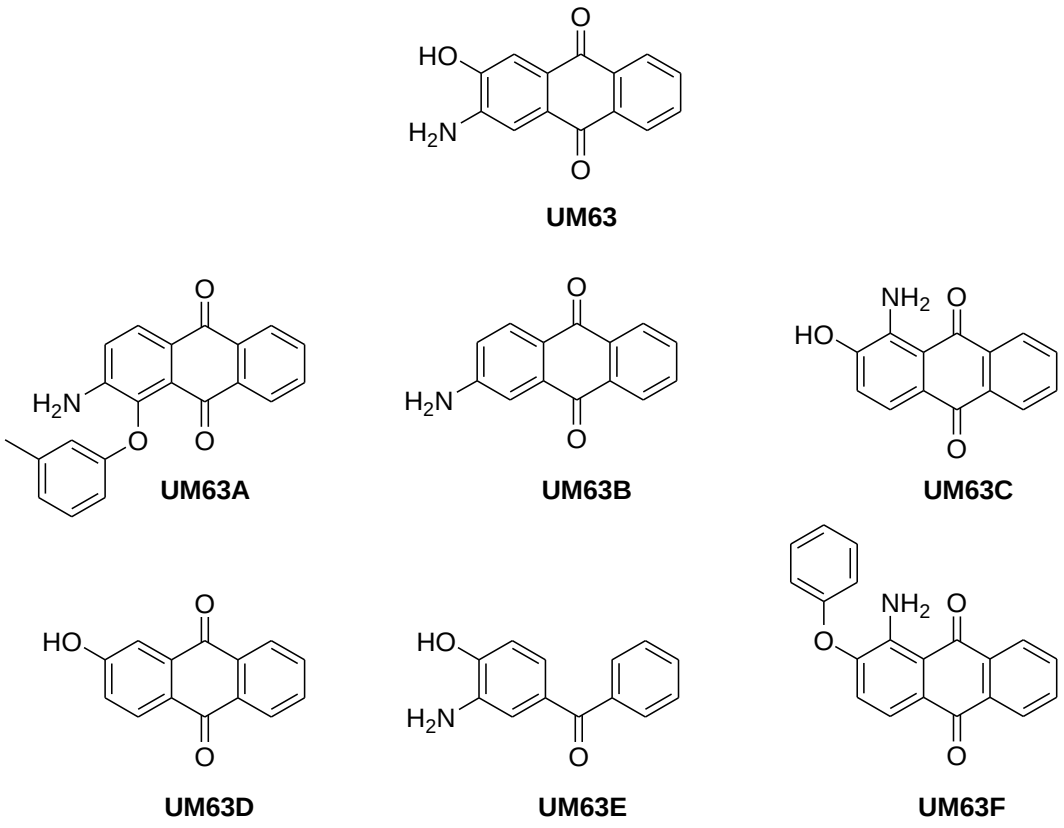

Figure 1. Chemical structure of the hit UM63 identified by virtual screening and seven commercially available analogues of UM63 selected for *in vitro* tests.

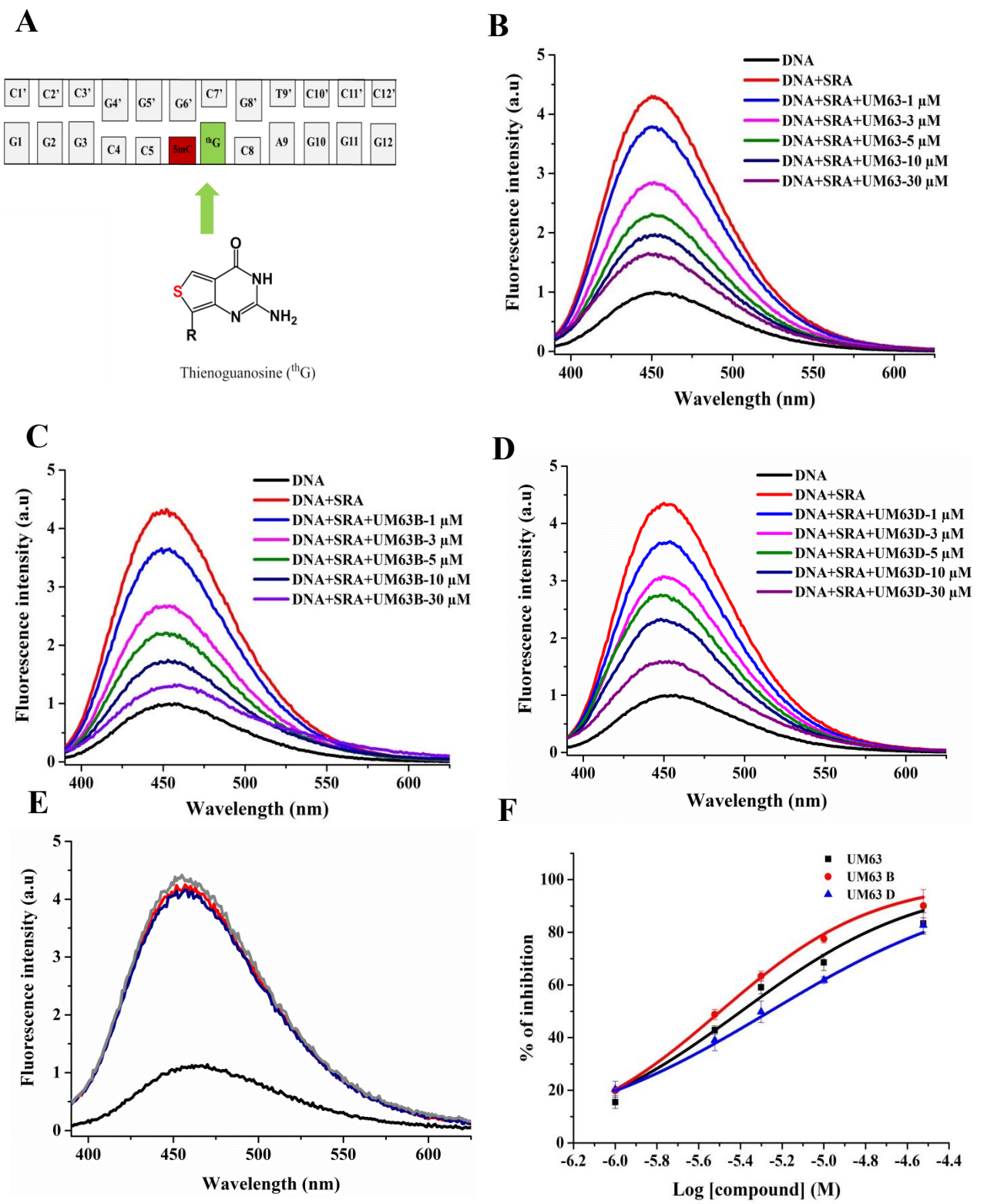

Figure 2. **Effects of the selected compounds on the base flipping assay**. (**A**) Structure of the HM thG-labeled duplex. The guanosine at position 7 is substituted by thG and highlighted in green , the

methylayed cytosine is highlighted in red. Emission spectra of HM thG-labeled DNA (1 µM) were recorded in the absence (black) and in the presence of SRA (3 µM) before (red) and after addition of 1 µM (blue) , 3 µM (magenta) , 5 µM (green) , 10 µM (dark blue) or 30 µM (purple) of (**B**) UM63 (**C**) UM63B and (**D**) UM63D. (**E**) Emission spectra of HM thG-labeled DNA (1 µM) were recorded in the absence (black) and in the presence of SRA (3 µM) before (red) and after addition of 10 µM (dark blue) and 100 µM (grey) of UM63E. (**F**) Dose-response curve representing the inhibition of SRA activity by the selected compounds. The solid lines correspond to the fits of the experimental points by eq. (2). The IC_{50} values given in the text were obtained from the mean ± S.E.M. of three independent experiments. Experiments were performed in phosphate buffer 20 mM, NaCl 50 mM, 1mM EDTA, TCEP 2.5 mM, PEG 0.05%, pH 7.5.

Only two of the tested UM63 analogs, namely UM63B and UM63D, were able to inhibit the SRA-induced base flipping (Fig. 2C, D). Similarly, to UM63, UM63B and UM63D inhibited the 5mC flipping in a concentration-dependent manner with IC_{50} values of 3.3 ±0.3 µM and 6.1 ±0.7 µM, respectively (Fig. 2C, D). Noticeably, this decrease in fluorescence was not due to a quenching of thG fluorescence by these compounds, since none of them was found to modify the fluorescence of the labeled duplexes in the absence of SRA (Fig. S2). The corresponding K_i values as calculated from eq. (3) were respectively 1.45 ±0.15, 1.05 ±0.1 and 2.0 ±0.2 µM for UM63, UM63B and UM63D, indicating that the three compounds have similar potency in inhibiting the SRA-induced base flipping. As the three compounds have similar chemical structures, this strongly suggests that their activity is related to a specific pharmacophore. As UM63B has been reported to be carcinogenic [54], this compound was discontinued and the subsequent assays were performed only with UM63 and UM63D.

3- Binding parameters of the positive hits to SRA and HM DNA

In order to determine whether the inhibitory effect of UM63 and UM63D on SRA-induced base flipping is related to their binding to SRA, we analyzed by ITC the thermodynamic binding parameters of UM63 and UM63D for SRA. ITC titration of UM63 by SRA (Fig. 3A) showed that the reaction is exothermic (ΔH= -10.9 KJ/mol), with a K_d value of 0.73 ± 0.03 µM and a 1:1 stoichiometry. The reaction was also characterized by a positive entropy ΔS, suggesting that SRA/UM63 complex formation may be partly driven by release of ions and water molecules. In

contrast, the interaction of UM63D with wild-type SRA was heat-silent (data not shown), preventing the determination of its K_d value.

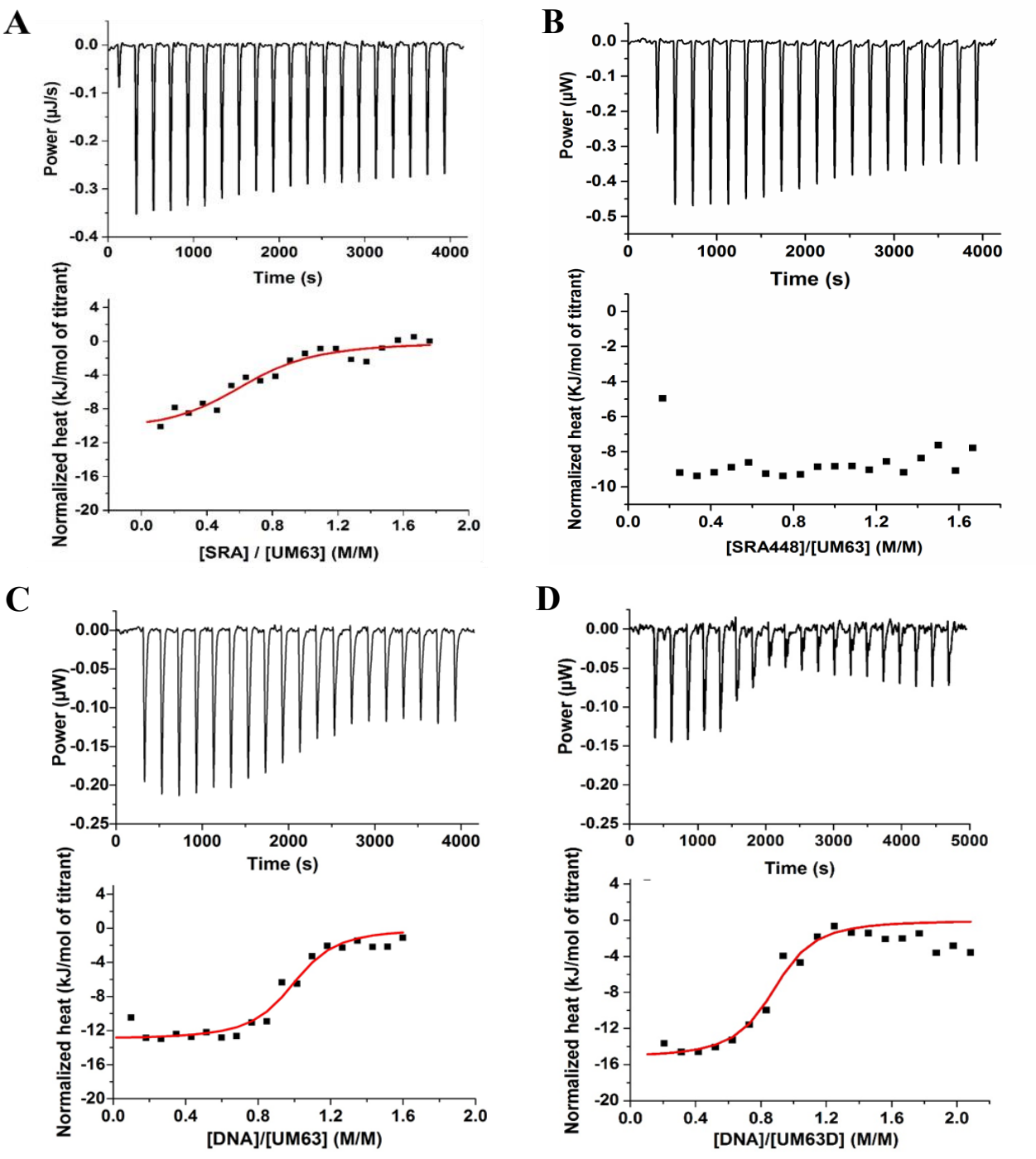

Figure 3. Binding of UM63 and UM63D to SRA and DNA, as monitored by Isothermal Titration Calorimetry. Representative ITC titration curves of 8 µM UM63 by (**A**) SRA and (**B**)

SRA-G448D. The protein concentration in the syringe was 80 µM. Titration of 8 µM of (**C**) UM63 and (**D**) UM63D by HM DNA. The DNA concentration in the syringe was 80 µM. During titration, the area of the peak regularly decreases, reaching a plateau value that corresponds to the dilution heats of (**A**) SRA, (**B**) SRA-G448D or (**C, D**) DNA into the buffer alone. The red curves were fitted to the experimental heat quantities using equation (6). Experiments were performed at 20°C in 20 mM phosphate buffer, NaCl 50 mM, pH=7.4.

In a next step, we examined the possible interaction of UM63 and UM63D with DNA (Fig. 3B, C) to check whether this interaction may also contribute to their inhibitory effect. The binding of both compounds to DNA was found to be exothermic (ΔH= -13.03 and –15.25 kJ/mol for UM63 and UM63D, respectively) with K_d values of 0.13± 0.01 µM and and 0.15 ± 0.08 µM for UM63 and UM63D, respectively. These strong affinities could be explained by the fact that anthraquinones are DNA intercalators [55]. UM63 was clearly confirmed to be a DNA intercalator by its ability to displace ethidium bromide (EtBr) from DNA (Fig. S5). However, the contribution of the DNA binding component of these compounds appears to be marginal in the inhibition of base flipping, since UM63E which is unable to prevent base flipping (Fig. 2D), binds to DNA with a comparable affinity to UM63 and UM63D (Fig. S6). From the demonstration of its binding to the SRA binding pocket, UM63 was selected for more detailed studies.

4- UM63 binds to the SRA binding pocket and competes with DNA binding to SRA

To determine whether UM63 may target the 5mC binding pocket on SRA, we replaced the wild-type SRA with a SRA G448D mutant where the glycine 448 residue is replaced by a more bulky aspartic acid at the entry of the binding pocket to prevent base flipping [10, 53]. Only marginal heat exchange could be observed with this mutant (Fig. 3B), indicating that this mutation prevents UM63 binding to SRA, and thus, that the 5mC binding pocket of SRA is the target of UM63, in line with molecular modeling predictions.

To further explore the base flipping inhibition by UM63, we investigated by the stopped-flow technique how UM63 alters the kinetics of SRA-induced 5mC flipping in the thG-labeled DNA [53]. In line with our previous study [53], the kinetic trace of the thG-labeled DNA in the presence of SRA showed a slow component with a rate constant of ~ 6.5 s^{-1} attributed to the 5mC base flipping

process (Fig. 4, red curve). Addition of UM63 only marginally decreases the kinetic rate constant, but efficiently reduces the final fluorescence level in a concentration-dependent manner (Fig. 4 compare blue and magenta curves with the red curve). This decrease in the final fluorescence is in line with the spectra in Figure 2 and is consistent with the co-existence of a SRA population bound to UM63 that is unable to flip the 5mC base with a population of free SRA that flips 5mC with unaltered kinetics. With increasing UM63 concentrations, the population of free active SRA decreases, explaining the decrease in the final plateau. As expected, the negative compound UM63E did not induce any change in the kinetics or the final plateau (Fig. S3).

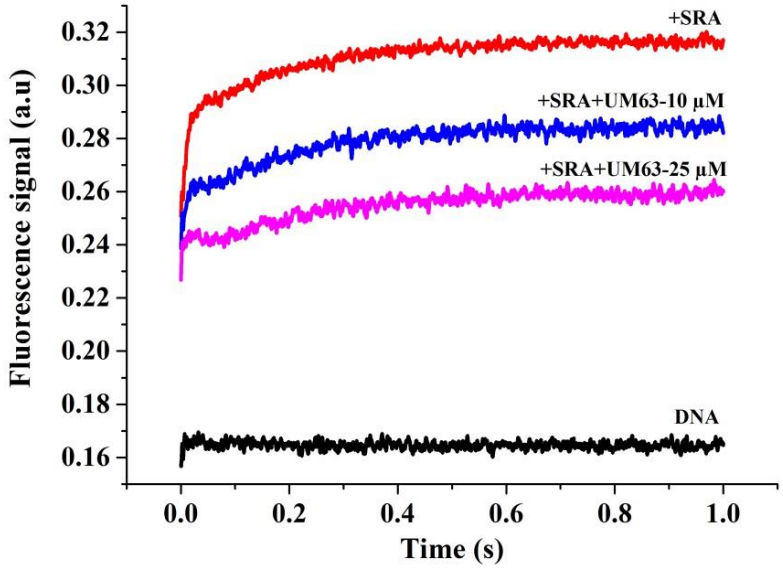

Figure 4. Effect of UM63 on the base flipping kinetics of the SRA domain. Kinetic traces were monitored by the stopped-flow technique. The black trace corresponds to the thG-labeled HM duplex mixed with buffer. The red trace describes the interaction of the thG-labeled duplex with SRA. The blue and magenta traces describe the kinetics of interaction of thG-labeled duplex with SRA in the presence of 10 µM and 25 µM of UM63. The final concentrations of thG-labeled HM DNA and SRA were 0.2 µM and 1.5 µM, respectively. Experiments were performed in phosphate buffer 20 mM, NaCl 50 mM, TCEP 2.5 mM, pH 7.5.

To determine whether the binding of UM63 to the SRA binding pocket may alter the DNA binding properties of SRA, we performed competition experiments using the non methylated version of the DNA duplex in Fig 2A. As no base flipping occurs with this non-methylated duplex [53], the effect

of UM63 on the binding process only can be explored. Accordingly, we titrated by fluorescence anisotropy the non-methylated thG-labeled DNA with increasing concentrations of SRA in the absence or in the presence of 10 µM UM63. In the absence of UM63, the dissociation constant K_d of SRA to DNA was found to be 0.43 ±0.04 µM, close to the previously reported value [53]. Addition of UM63 shifted the titration curve to higher SRA concentrations (Fig. 5A), indicating that UM63 compete with DNA for binding to SRA with an apparent dissociation constant $K_{d_{(app)}}$ = 1.04 ± 0.15 µM. In contrast, no competition was observed when the thG-labeled DNA was titrated by the SRA-G448D mutant (Fig. 5B), confirming that UM63 is unable to bind to this SRA mutant.

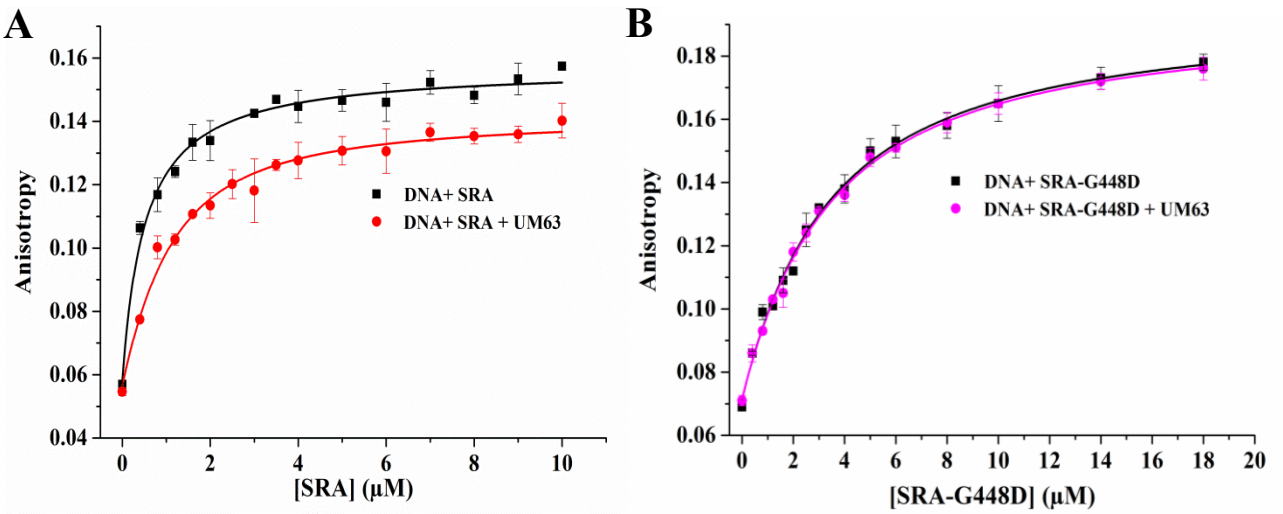

Figure 5. Effect of UM63 on the binding of SRA and SRAG448D to DNA, as monitored by fluorescence anisotropy. (A) Titration of 1 µM DNA with SRA in the absence (black) or in the presence of 10 µM UM63 (red). (**B**) Titration of 1 µM DNA with SRAG448D in the absence (black) or in the presence of 10 µM UM63 (magenta). Experimental points are represented as means ± S.E.M for n=3 independent experiments. The solid lines correspond to the fits of the experimental data to equation (4).

To confirm the competition of UM63 with DNA for binding to SRA, we investigated the ability of UM63 to dissociate the SRA/DNA complex. For this purpose, 10 µM and 25 µM concentrations of UM63 were added to the preformed complex of SRA with the thG-labeled HM duplex (Fig. 6). With both concentrations, the time-dependent decrease in the thG fluorescence intensity indicated the flipping back of the 5mC residue and the dissociation of the complex [53]. Independently of the UM63 concentration, a dissociation rate constant of 8 s^{-1} was observed, in good agreement with the

3 s^{-1} rate constant reported for the dissociation of the same complex by an excess of unlabeled DNA [53]. As expected, the negative compound UM63E that has no effect on base flipping (Fig. 2E) was unable to dissociate the DNA/SRA complex (Fig. S4), when added at a 10 µM concentration.

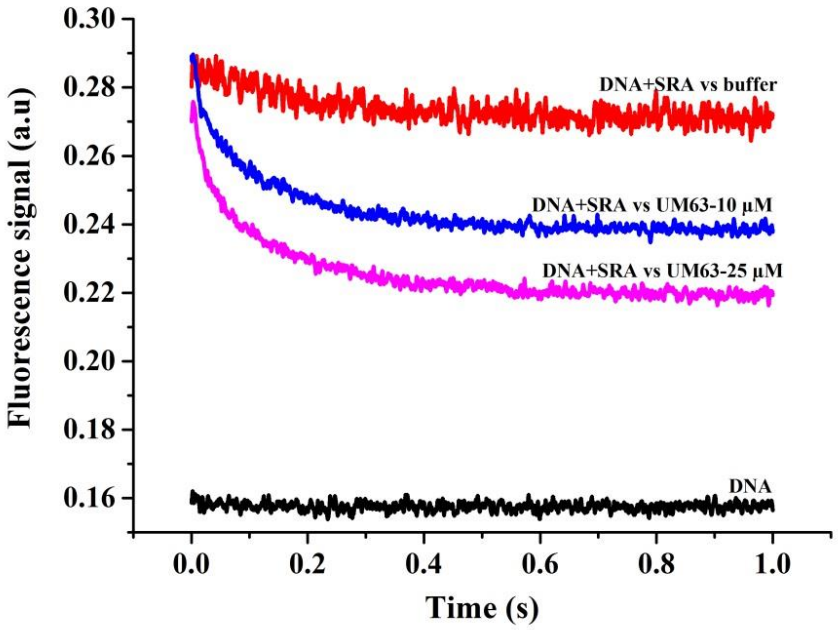

Figure 6. Dissociation kinetics of the DNA/SRA complex by UM63. The dissociation curves were measured by the stopped-flow technique after addition of 10 µM (blue curve) and 25 µM (magenta curve) of UM63 to a complex formed by 0.2 µM of thG-labeled HM duplex and 1.5 µM SRA. The red and black curve correspond respectively, to the DNA/SRA complex and the DNA alone mixed with buffer.

5- Binding mode of UM63 to SRA binding pocket

The interaction of UM63 within the binding site of 5mC on SRA was also investigated by molecular modeling simulations. Compared to the virtual screening setting, a more accurate docking simulation was carried out with the FRED docking program to predict the possible binding mode of UM63. Results of this study clearly show that UM63 acts as 5mC mimetic, being pi-pi stacked with the side chain of Tyr478 and H-bonded to key residues that are also contacted by methylated DNA [10] such as Asp469, Thr479, Gly448, Gly465 and Ala463 (Fig. 7). It is worth noting that the distal phenyl ring of the anthraquinone core occupies a region near the entrance of

the binding site and seems not involved in direct binding to the SRA residues, thus becoming the ideal candidate for chemical modifications in the further hit-to-lead optimization step. An additional site for chemical modification is also the phenol group, which is not directly involved in H-bond and points to partially accessible sub-pockets of the 5mC binding site. In contrast, the amino group and the quinone moiety are well adapted to interact with SRA residues and no replacement or substitution seem allowed. Overall, the binding mode of UM63 predicted by molecular docking is highly comparable to the crystallographic binding mode of 5mC, and is also consistent with the lack of detectable binding of UM63 to the G448D mutant of SRA. Indeed, it is expected that the Asp488 side chain in the mutant SRA occupies the binding site and thus prevents UM63 interaction by steric hindrance

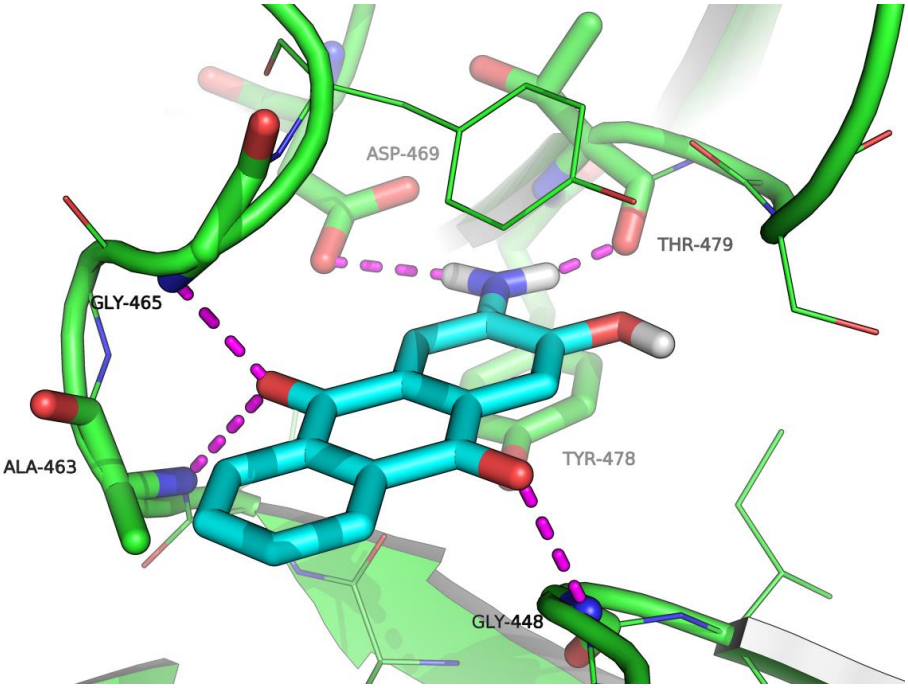

Figure 7. Docking-based binding mode of UM63 within the 5mC binding site of SRA. UM63 is shown as cyan sticks, and the crystallographic structure of SRA (PDB 3CLZ) is show as green cartoon. Residues within 5 Å from UM63 are shown as lines, while residues contacted by UM63 via H-bond or pi-pi stacking are shown in sticks and are labeled (residue numbering corresponds to the scheme adopted in the crystallographic structure). H-bonds are highlighted by magenta dashed lines.

6- Inhibition of SRA activity by UM63 is associated with a decrease in global DNA methylation

As our *in vitro* experiments and molecular modeling revealed that UM63 competes with the binding of SRA to the HM DNA and inhibits the flipping of the 5mC base, we hypothesized that UM63 should induce genomic DNA demethylation. Global DNA methylation was estimated by an immunofluorescence assay using a specific monoclonal antibody against 5mC and Alexa488-labeled secondary antibodies (Fig 8A). Based on the mean fluorescence intensity of Alexa488, the global DNA methylation level was found to decrease after 24 h treatment with UM63 at 10 µM (Fig. 8B). The decrease in fluorescence (37%) was comparable to that induced by 10 µM of Azacytidine (44%), a DNMT1 inhibitor taken as a positive control. This decrease in global genomic methylation may tentatively be related to the effect of UM63 on the SRA/HM DNA complexes.

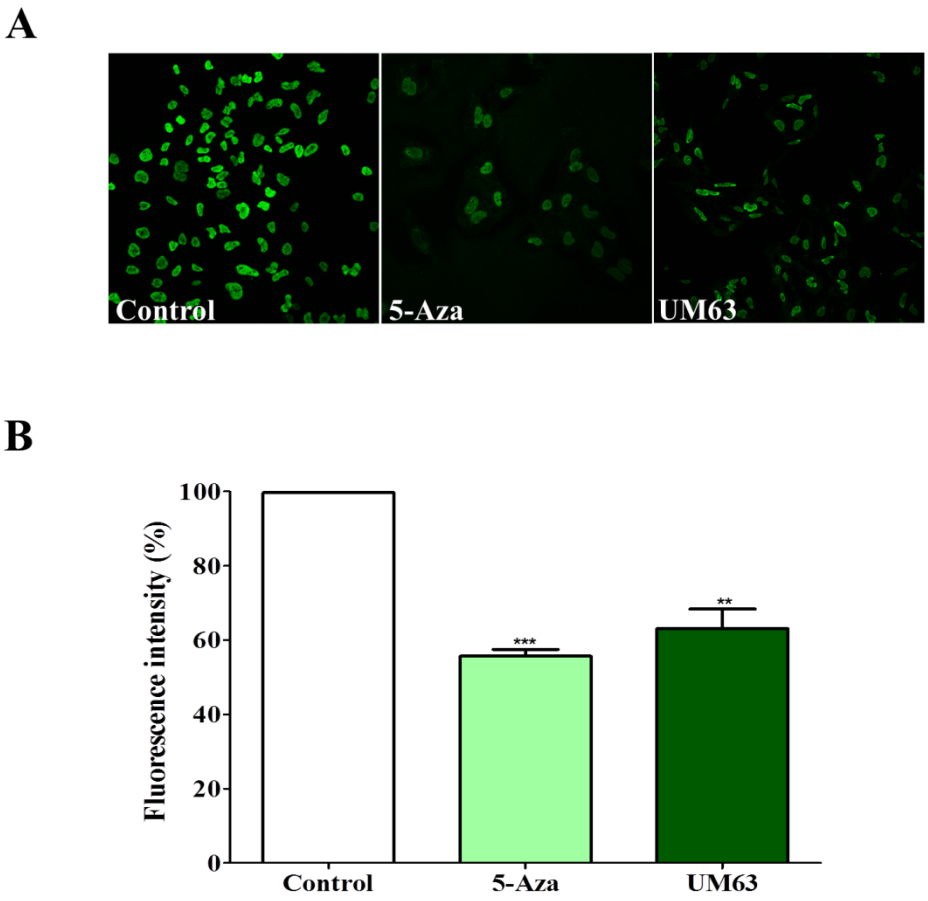

Figure 8. Effect of UM63 on global DNA methylation in HeLa cells. (**A**) Immunostaining of 5-mC in HeLa cells. Non treated HeLa cells served as negative control, while cells treated with 10 µM 5-Azacytidine were used as a positive control and were compared to cells treated with 10 µM

of UM63. The cells were fixed after treatment and labeled by anti-5mC antibodies and Alexa488-labeled secondary antibodies before visualization in confocal microscopy (**B**) Mean fluorescence intensities representing the amount of methylated cytosines in genomic DNA. Values are means ±S.E.M. for three independent experiments; statistically significant: * $p < 0.05$; ** $p < 0.01$; *** $p < 0.001$ (versus untreated group).

7- UM63 prevents the interaction between UHRF1 and DNMT1 in cells

The observed inhibition of DNA methylation by UM63 could be the result of the inhibition of 5mC flipping by UHRF1, which in turn prevents the recruitment of DNMT1 that is responsible of DNA methylation. To test this hypothesis, we used the FRET-FLIM technique to monitor the interaction between DNMT1 and UHRF1 inside the nucleus, after transfection of HeLa cells with DNMT1-eGFP and UHRF1-mCherry (Fig. 9). FRET between eGFP and mCherry only occurs when they are less than 8 nm apart, a distance corresponding to intermolecular protein–protein interactions [46–48]. By measuring the fluorescence decay at each pixel of the cell, the FLIM technique allows extracting the fluorescence lifetime (τ) that, in contrast to fluorescence intensity, does not depend on the instrumentation or the concentration of fluorophores. The lifetime of the DNMT1-eGFP was 2.54 ± 0.01 ns in cells transfected with DNMT1-eGFP alone. The lifetime of eGFP was reduced to 2.19 ± 0.02 ns when DNMT1-eGFP was co-transfected with UHRF1-mCherry (Fig.9B). This corresponds to a FRET efficiency of 13.7 ± 0.8%, clearly indicating that UHRF1 and DNMT1 interact in the cell nucleus (Fig. 9B). In the same conditions, the lifetime of DNMT1-eGFP in cells treated with 10 µM UM63 was 2.44 ± 0.01 ns, corresponding to a FRET efficiency of only 3.4 ± 0.3% (Fig. 9A, B,C), a value considered as non-significant [56]. This strong decrease in FRET strongly suggests that UM63 efficiently prevents the interaction of UHRF1 with DNMT1, in full line with our hypothesis. Thus, by interacting with the 5mC binding pocket of SRA, UM63 may inhibit base flipping and thus the recruitment of DNMT1.

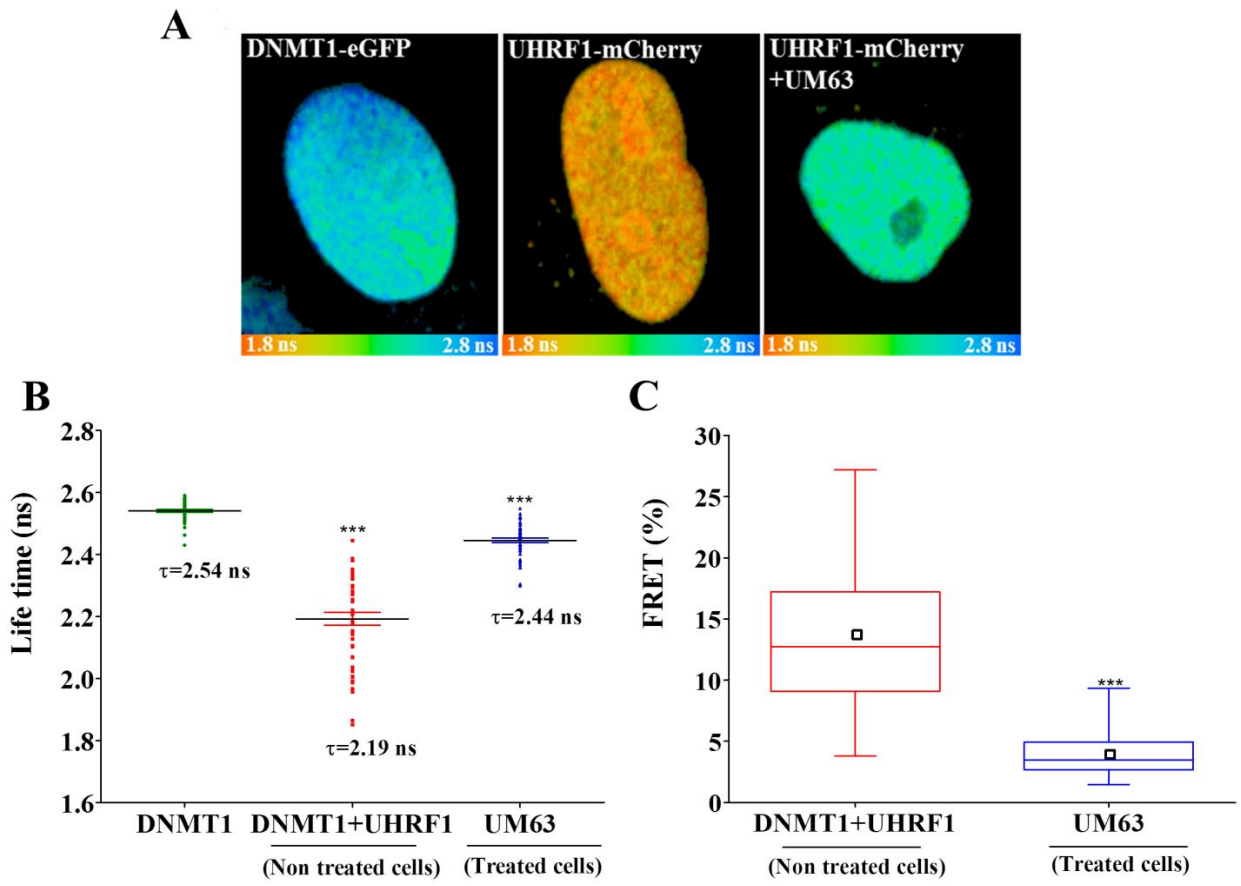

Figure 9. Effect of UM63 on DNMT1/UHRF1 interaction, as assessed by FRET-FLIM. (**A**) 30 µm x 30 µm FLIM images of HeLa cells transfected with DNMT1-eGFP or co-transfected with UHRF1-mCherry without or with UM63 treatment. The lifetime values are determined by using color coded images ranging from red (1.8 ns) to blue (2.8 ns). (**B**, **C**) Effect of UM63 on FRET efficiency**. (B)** Distribution of lifetimes expressed as means ±S.E.M. of three independent experiments in treated and non-treated samples. The horizontal lines show the mean values. **(C)** FRET efficiencies calculated from the average lifetime values of at least 50 cells in three independent experiments. Box-and-whiskers plots represent the FRET efficiency in non-treated and treated cells. Whiskers represent the minimum and maximum values. The boxes define the interquartile range that extends from the 25th to the 75th percentile, whereas the horizontal lines and square show the median values and the mean, respectively. Statistical significance: * $p < 0.05$; ** $p < 0.01$; *** $p < 0.001$ (versus untreated group).

D- Discussion:

UHRF1 plays a key role in the inheritance of methylation marks during DNA replication by reading the DNA sequence, recognizing the CpG motifs and promoting the flipping of 5mC residues. Base flipping induced by the SRA domain of UHRF1 is thought to be the key event for recruiting the DNMT1 enzyme that will methylate the opposite cytosine on the daughter strand. In this context, the aim of the present work was to probe the druggability of UHRF1 by identifying small molecules that can inhibit its activity and thus regulate the inheritance of the methylation patterns during cell replication. To reach this aim we combined virtual screening to select molecules able to bind to the 5mC binding pocket on the SRA domain and a fluorescence-based screening assay monitoring the SRA-induced base flipping to evaluate the molecules selected by virtual screening. Through this approach we selected three molecules from the anthraquinone family (UM63, UM63B and UM63D) that were observed to inhibit the SRA-induced based flipping with *K*i values in the low µM range. From these 3 compounds, we discarded UM63B that was reported to be carcinogenic. The two others were tested by ITC for their binding to SRA and DNA. UM63 was found to be the most interesting compound, as its binding to the wild-type SRA but not to the G448D mutant confirmed its binding to the 5mC binding pocket of SRA. This conclusion was further rationalized by molecular modeling, which indicates that UM63 mimics 5mC in the SRA pocket, being stabilized through a pi-pi stacking with the side chain of Tyr478 and several H-bonds to key SRA residues also contacted by methylated DNA. UM63 can also bind to DNA with a 0.1 µM dissociation constant, likely through intercalation (Fig. S5). However, as a similar high affinity for DNA was observed with UM63E, a compound structurally related to UM63 that has no effect on base flipping, the inhibitory effect of UM63 is thought to be mainly the consequence of its binding to the 5mC binding pocket of SRA. The binding of UM63 to the 5mC binding pocket was further shown to prevent the binding of SRA to DNA, as supported by the competition between UM63 and DNA for binding to SRA (Fig. 5A) and the dissociation of the SRA/DNA complexes by UM63 (Fig. 6). In addition, the inability of UM63 to hinder the binding of the G448D SRA mutant to DNA further confirmed that the intercalation of UM63 into the DNA has only a marginal effect on the binding of SRA (Fig. 5B).

Interestingly, treatment of HeLa cells with UM63 was found to prevent the interaction between UHRF1 and DNMT1 (Fig. 9). This is likely a direct consequence of the binding of UM63 to the SRA domain of UHRF1, which prevents UHRF1 to recognize the methylated sites and recruit

DNMT1, through a direct interaction between SRA and the replication foci targeting sequence (RFTS) domain of DNMT1 [57]. Indeed, the interaction of the SRA domain of UHRF1 with the CpG site is mandatory to trigger the conversion of the "closed form" of UHRF1 protein to its "open form" which is able to interact with DNMT1 [58]. By preventing the binding of UHRF1 to HM DNA, UM63 keeps thus this protein in its closed form, unable to interact with DNMT1.

By altering two crucial steps in the replication of DNA methylation, namely the interaction of UHRF1 with HM DNA and the recruitment of DNMT1, UM63 is thought to regulate the DNA methylation status of the cell. In line with this hypothesis, UM63 was found to decrease the global DNA methylation level by about 40% in HeLa cells. A similar effect was observed when UHRF1 was knockdown with shRNAs in HeLa cells [59], highlighting the key role of UHRF1 in the maintenance of the DNA methylation level. These findings strongly suggest that UM63 is pharmacologically able to target UHRF1 and could thus prevent aberrant DNA methylation, such as hypermethylation of TSG promoters that is frequently observed in cancer development. UM63 may thus have the same effect than interference RNAs that knockdown UHRF1, which reactivates the expression of TSGs and inhibits oncogenesis [30, 61] [62]. Similarly, natural products such as flavonoids derived from *Limoniastrum guyonianum* and luteolin have been shown to downregulate UHRF1 and subsequently reduce the global methylation levels in cervical cancer cells, with a reexpression of TSGs and inhibition of cell proliferation [63].

Altogether, these findings suggest that UM63 acts as an UHRF1 inhibitor that binds to the 5mC binding pocket of the SRA domain, and prevents the binding of UHRF1 to DNA and the recruitment of DNMT1 to the DNA replication foci. As a result, UM63 induces a decrease in the global methylation of DNA in the cell. This compound appears thus as a potential candidate that could serve as a starting point for designing more selective and efficient UHRF1 inhibitors, which could be used in pathologies such as cancers where UHRF1 is highly expressed and contributes in tumor development and progression by epigenetically silencing the tumor suppressor genes.

Acknowledgements

We thank Ludovic Richert for his help in FLIM experiments. We thank the ANR (SMFLUONA, ANR-17-CE11-0036-01) for financial support. LZ and KG were supported by fellowships from Lebanese government and FRM. W.A. and T.A. were supported by fellowships from HEC (Pakistan).

References:

1. Ehrlich M: **Expression of various genes is controlled by DNA methylation during mammalian development**. *Journal of cellular biochemistry* 2003, **88**(5):899-910.
2. Okamoto I, Otte AP, Allis CD, Reinberg D, Heard E: **Epigenetic dynamics of imprinted X inactivation during early mouse development**. *Science* 2004, **303**(5658):644-649.
3. Murphy SK, Jirtle RL: **Imprinting evolution and the price of silence**. *BioEssays : news and reviews in molecular, cellular and developmental biology* 2003, **25**(6):577-588.
4. Feinberg AP, Ohlsson R, Henikoff S: **The epigenetic progenitor origin of human cancer**. *Nature reviews Genetics* 2006, **7**(1):21-33.
5. Klose RJ, Bird AP: **Genomic DNA methylation: the mark and its mediators**. *Trends in biochemical sciences* 2006, **31**(2):89-97.
6. Baylin SB, Jones PA: **A decade of exploring the cancer epigenome - biological and translational implications**. *Nature reviews Cancer* 2011, **11**(10):726-734.
7. Sandoval J, Esteller M: **Cancer epigenomics: beyond genomics**. *Current opinion in genetics & development* 2012, **22**(1):50-55.
8. Bronner C, Krifa M, Mousli M: **Increasing role of UHRF1 in the reading and inheritance of the epigenetic code as well as in tumorogenesis**. *Biochemical pharmacology* 2013, **86**(12):1643-1649.
9. Alhosin M, Sharif T, Mousli M, Etienne-Selloum N, Fuhrmann G, Schini-Kerth VB, Bronner C: **Down-regulation of UHRF1, associated with re-expression of tumor suppressor genes, is a common feature of natural compounds exhibiting anti-cancer properties**. *Journal of experimental & clinical cancer research : CR* 2011, **30**:41.
10. Avvakumov GV, Walker JR, Xue S, Li Y, Duan S, Bronner C, Arrowsmith CH, Dhe-Paganon S: **Structural basis for recognition of hemi-methylated DNA by the SRA domain of human UHRF1**. *Nature* 2008, **455**(7214):822-825.
11. Sharif J, Muto M, Takebayashi S, Suetake I, Iwamatsu A, Endo TA, Shinga J, Mizutani-Koseki Y, Toyoda T, Okamura K *et al*: **The SRA protein Np95 mediates epigenetic inheritance by recruiting Dnmt1 to methylated DNA**. *Nature* 2007, **450**(7171):908-912.
12. Arita K, Ariyoshi M, Tochio H, Nakamura Y, Shirakawa M: **Recognition of hemi-methylated DNA by the SRA protein UHRF1 by a base-flipping mechanism**. *Nature* 2008, **455**(7214):818-821.
13. Hashimoto H, Horton JR, Zhang X, Bostick M, Jacobsen SE, Cheng X: **The SRA domain of UHRF1 flips 5-methylcytosine out of the DNA helix**. *Nature* 2008, **455**(7214):826-829.
14. Cheng J, Yang Y, Fang J, Xiao J, Zhu T, Chen F, Wang P, Li Z, Yang H, Xu Y: **Structural insight into coordinated recognition of trimethylated histone H3 lysine 9 (H3K9me3) by the plant homeodomain (PHD) and tandem tudor domain (TTD) of UHRF1 (ubiquitin-like, containing PHD and RING finger domains, 1) protein**. *The Journal of biological chemistry* 2013, **288**(2):1329-1339.
15. Liu X, Gao Q, Li P, Zhao Q, Zhang J, Li J, Koseki H, Wong J: **UHRF1 targets DNMT1 for DNA methylation through cooperative binding of hemi-methylated DNA and methylated H3K9**. *Nature communications* 2013, **4**:1563.
16. Bostick M, Kim JK, Esteve PO, Clark A, Pradhan S, Jacobsen SE: **UHRF1 plays a role in maintaining DNA methylation in mammalian cells**. *Science* 2007, **317**(5845):1760-1764.
17. Nishiyama A, Yamaguchi L, Sharif J, Johmura Y, Kawamura T, Nakanishi K, Shimamura S, Arita K, Kodama T, Ishikawa F *et al*: **Uhrf1-dependent H3K23 ubiquitylation couples maintenance DNA methylation and replication**. *Nature* 2013, **502**(7470):249-253.
18. Qin W, Wolf P, Liu N, Link S, Smets M, La Mastra F, Forne I, Pichler G, Horl D, Fellinger K *et al*: **DNA methylation requires a DNMT1 ubiquitin interacting motif (UIM) and histone ubiquitination**. *Cell research* 2015, **25**(8):911-929.

19. Yang X, Lay F, Han H, Jones PA: **Targeting DNA methylation for epigenetic therapy**. *Trends in pharmacological sciences* 2010, **31**(11):536-546.
20. Issa JP, Kantarjian H: **Azacitidine**. *Nature reviews Drug discovery* 2005, **Suppl**:S6-7.
21. Kantarjian H, Issa JP, Rosenfeld CS, Bennett JM, Albitar M, DiPersio J, Klimek V, Slack J, de Castro C, Ravandi F *et al*: **Decitabine improves patient outcomes in myelodysplastic syndromes: results of a phase III randomized study**. *Cancer* 2006, **106**(8):1794-1803.
22. Chuang JC, Yoo CB, Kwan JM, Li TW, Liang G, Yang AS, Jones PA: **Comparison of biological effects of non-nucleoside DNA methylation inhibitors versus 5-aza-2'-deoxycytidine**. *Molecular cancer therapeutics* 2005, **4**(10):1515-1520.
23. Foulks JM, Parnell KM, Nix RN, Chau S, Swierczek K, Saunders M, Wright K, Hendrickson TF, Ho KK, McCullar MV *et al*: **Epigenetic drug discovery: targeting DNA methyltransferases**. *Journal of biomolecular screening* 2012, **17**(1):2-17.
24. Jung Y, Park J, Kim TY, Park JH, Jong HS, Im SA, Robertson KD, Bang YJ, Kim TY: **Potential advantages of DNA methyltransferase 1 (DNMT1)-targeted inhibition for cancer therapy**. *Journal of molecular medicine* 2007, **85**(10):1137-1148.
25. Palii SS, Van Emburgh BO, Sankpal UT, Brown KD, Robertson KD: **DNA methylation inhibitor 5-Aza-2'-deoxycytidine induces reversible genome-wide DNA damage that is distinctly influenced by DNA methyltransferases 1 and 3B**. *Molecular and cellular biology* 2008, **28**(2):752-771.
26. Ashraf W, Ibrahim A, Alhosin M, Zaayter L, Ouararhni K, Papin C, Ahmad T, Hamiche A, Mely Y, Bronner C *et al*: **The epigenetic integrator UHRF1: on the road to become a universal biomarker for cancer**. *Oncotarget* 2017.
27. Bronner C, Achour M, Arima Y, Chataigneau T, Saya H, Schini-Kerth VB: **The UHRF family: oncogenes that are drugable targets for cancer therapy in the near future?** *Pharmacology & therapeutics* 2007, **115**(3):419-434.
28. Unoki M: **Current and potential anticancer drugs targeting members of the UHRF1 complex including epigenetic modifiers**. *Recent patents on anti-cancer drug discovery* 2011, **6**(1):116-130.
29. Alhosin M, Abusnina A, Achour M, Sharif T, Muller C, Peluso J, Chataigneau T, Lugnier C, Schini-Kerth VB, Bronner C *et al*: **Induction of apoptosis by thymoquinone in lymphoblastic leukemia Jurkat cells is mediated by a p73-dependent pathway which targets the epigenetic integrator UHRF1**. *Biochemical pharmacology* 2010, **79**(9):1251-1260.
30. Alhosin M, Omran Z, Zamzami MA, Al-Malki AL, Choudhry H, Mousli M, Bronner C: **Signalling pathways in UHRF1-dependent regulation of tumor suppressor genes in cancer**. *Journal of experimental & clinical cancer research : CR* 2016, **35**(1):174.
31. Myrianthopoulos V, Cartron PF, Liutkeviciute Z, Klimasauskas S, Matulis D, Bronner C, Martinet N, Mikros E: **Tandem virtual screening targeting the SRA domain of UHRF1 identifies a novel chemical tool modulating DNA methylation**. *European journal of medicinal chemistry* 2016, **114**:390-396.
32. Houliston RS, Lemak A, Iqbal A, Ivanochko D, Duan S, Kaustov L, Ong MS, Fan L, Senisterra G, Brown PJ *et al*: **Conformational dynamics of the TTD-PHD histone reader module of UHRF1 reveals multiple histone binding states, allosteric regulation and druggability**. *The Journal of biological chemistry* 2017.
33. Parker BS, Cutts SM, Nudelman A, Rephaeli A, Phillips DR, Sukumar S: **Mitoxantrone mediates demethylation and reexpression of cyclin d2, estrogen receptor and 14.3.3sigma in breast cancer cells**. *Cancer biology & therapy* 2003, **2**(3):259-263.
34. Walker DA, Wyhs N, Giovinazzo H, Yegnasubramanian S, Nelson WG: **Abstract 5390: Development of a high-throughput screening assay to identify UHRF1 inhibitors via time-resolved fluorescence resonance energy transfer (TR-FRET)**. *Cancer research* 2014, **74**(19 Supplement):5390-5390.

35. Evison BJ, Sleebs BE, Watson KG, Phillips DR, Cutts SM: **Mitoxantrone, More than Just Another Topoisomerase II Poison**. *Medicinal research reviews* 2016, **36**(2):248-299.
36. Das A, Roy S, Mondal P, Datta A, Mahali K, Loganathan G, Dharumadurai D, Sengupta PS, Akbarsha MA, Guin PS: **Studies on the interaction of 2-amino-3-hydroxy-anthraquinone with surfactant micelles reveal its nucleation in human MDA-MB-231 breast adinocarcinoma cells**. *RSC Advances* 2016, **6**(34):28200-28212.
37. Delagoutte B, Lallous N, Birck C, Oudet P, Samama JP: **Expression, purification, crystallization and preliminary crystallographic study of the SRA domain of the human UHRF1 protein**. *Acta crystallographica Section F, Structural biology and crystallization communications* 2008, **64**(Pt 10):922-925.
38. Achour M, Mousli M, Alhosin M, Ibrahim A, Peluso J, Muller CD, Schini-Kerth VB, Hamiche A, Dhe-Paganon S, Bronner C: **Epigallocatechin-3-gallate up-regulates tumor suppressor gene expression via a reactive oxygen species-dependent down-regulation of UHRF1**. *Biochemical and biophysical research communications* 2013, **430**(1):208-212.
39. Hawkins PC, Skillman AG, Warren GL, Ellingson BA, Stahl MT: **Conformer generation with OMEGA: algorithm and validation using high quality structures from the Protein Databank and Cambridge Structural Database**. *J Chem Inf Model* 2010, **50**(4):572-584.
40. **OMEGA 2.5.1.4: OpenEye Scientific Software, Santa Fe, NM. http://www.eyesopen.com**.
41. **QUACPAC 1.6.3.1: OpenEye Scientific Software, Santa Fe, NM. http://www.eyesopen.com.** In.
42. McGann M: **FRED pose prediction and virtual screening accuracy**. *J Chem Inf Model* 2011, **51**(3):578-596.
43. **FRED 3.0.1 OpenEye Scientific Software, Santa Fe, NM. http://www.eyesopen.com**.
44. Rochel N, Ciesielski F, Godet J, Moman E, Roessle M, Peluso-Iltis C, Moulin M, Haertlein M, Callow P, Mely Y *et al*: **Common architecture of nuclear receptor heterodimers on DNA direct repeat elements with different spacings**. *Nature structural & molecular biology* 2011, **18**(5):564-570.
45. Wiseman T, Williston S, Brandts JF, Lin LN: **Rapid measurement of binding constants and heats of binding using a new titration calorimeter**. *Analytical biochemistry* 1989, **179**(1):131-137.
46. El Meshri SE, Dujardin D, Godet J, Richert L, Boudier C, Darlix JL, Didier P, Mely Y, de Rocquigny H: **Role of the nucleocapsid domain in HIV-1 Gag oligomerization and trafficking to the plasma membrane: a fluorescence lifetime imaging microscopy investigation**. *Journal of molecular biology* 2015, **427**(6 Pt B):1480-1494.
47. Clamme JP, Azoulay J, Mely Y: **Monitoring of the formation and dissociation of polyethylenimine/DNA complexes by two photon fluorescence correlation spectroscopy**. *Biophysical journal* 2003, **84**(3):1960-1968.
48. Qian C, Li S, Jakoncic J, Zeng L, Walsh MJ, Zhou MM: **Structure and hemimethylated CpG binding of the SRA domain from human UHRF1**. *J Biol Chem* 2008, **283**(50):34490-34494.
49. Stahl M, Mauser H: **Database clustering with a combination of fingerprint and maximum common substructure methods**. *J Chem Inf Model* 2005, **45**(3):542-548.
50. Mori M, Tottone L, Quaglio D, Zhdanovskaya N, Ingallina C, Fusto M, Ghirga F, Peruzzi G, Crestoni ME, Simeoni F *et al*: **Identification of a novel chalcone derivative that inhibits Notch signaling in T-cell acute lymphoblastic leukemia**. *Sci Rep* 2017, **7**(1):2213.
51. Mori M, Kovalenko L, Malancona S, Saladini F, De Forni D, Pires M, Humbert N, Real E, Botzanowski T, Cianferani S *et al*: **Structure-Based Identification of HIV-1 Nucleocapsid Protein Inhibitors Active against Wild-Type and Drug-Resistant HIV-1 Strains**. *ACS Chem Biol* 2018, **13**(1):253-266.
52. Shin D, Sinkeldam RW, Tor Y: **Emissive RNA alphabet**. *Journal of the American Chemical Society* 2011, **133**(38):14912-14915.

53. Kilin V, Gavvala K, Barthes NP, Michel BY, Shin D, Boudier C, Mauffret O, Yashchuk V, Mousli M, Ruff M *et al*: **Dynamics of Methylated Cytosine Flipping by UHRF1**. *Journal of the American Chemical Society* 2017, **139**(6):2520-2528.
54. National Toxicology P: **Bioassay of 2-aminoanthraquinone for possible carcinogenicity**. *National Cancer Institute carcinogenesis technical report series* 1978, **144**:1-117.
55. Hsin LW, Wang HP, Kao PH, Lee O, Chen WR, Chen HW, Guh JH, Chan YL, His CP, Yang MS *et al*: **Synthesis, DNA binding, and cytotoxicity of 1,4-bis(2-amino-ethylamino)anthraquinone-amino acid conjugates**. *Bioorganic & medicinal chemistry* 2008, **16**(2):1006-1014.
56. Becker W: **The Bh TCSPC Handbook**: Becker & Hickl; 2014.
57. Bashtrykov P, Jankevicius G, Jurkowska RZ, Ragozin S, Jeltsch A: **The UHRF1 protein stimulates the activity and specificity of the maintenance DNA methyltransferase DNMT1 by an allosteric mechanism**. *The Journal of biological chemistry* 2014, **289**(7):4106-4115.
58. Fang J, Cheng J, Wang J, Zhang Q, Liu M, Gong R, Wang P, Zhang X, Feng Y, Lan W *et al*: **Hemi-methylated DNA opens a closed conformation of UHRF1 to facilitate its histone recognition**. *Nature communications* 2016, **7**:11197.
59. Rothbart SB, Krajewski K, Nady N, Tempel W, Xue S, Badeaux AI, Barsyte-Lovejoy D, Martinez JY, Bedford MT, Fuchs SM *et al*: **Association of UHRF1 with methylated H3K9 directs the maintenance of DNA methylation**. *Nature structural & molecular biology* 2012, **19**(11):1155-1160.
60. Unoki M, Nishidate T, Nakamura Y: **ICBP90, an E2F-1 target, recruits HDAC1 and binds to methyl-CpG through its SRA domain**. *Oncogene* 2004, **23**(46):7601-7610.
61. Zhou L, Shang Y, Jin Z, Zhang W, Lv C, Zhao X, Liu Y, Li N, Liang J: **UHRF1 promotes proliferation of gastric cancer via mediating tumor suppressor gene hypermethylation**. *Cancer biology & therapy* 2015, **16**(8):1241-1251.
62. Jin W, Chen L, Chen Y, Xu SG, Di GH, Yin WJ, Wu J, Shao ZM: **UHRF1 is associated with epigenetic silencing of BRCA1 in sporadic breast cancer**. *Breast cancer research and treatment* 2010, **123**(2):359-373.
63. Krifa M, Pizzi A, Mousli M, Chekir-Ghedira L, Leloup L, Ghedira K: **Limoniastrum guyonianum aqueous gall extract induces apoptosis in colorectal cancer cells by inhibiting calpain activity**. *Tumour biology : the journal of the International Society for Oncodevelopmental Biology and Medicine* 2014, **35**(8):7877-7885.

Supporting Information

Identification of a new molecule targeting UHRF1 and disrupting its interaction with DNMT1

Liliyana Zaayter[1,#], Mattia Mori[3,#], Waseem Ashraf[1], Christian Boudier[1], Vasyl Kilin[1], Krishna Gavvala[1], Tanveer Ahmad[1], Maurizio Botta[3], Christian Bronner[2], Marc Ruff[4], Sylvia Eiler[4], Marc Mousli[1,*], Yves Mély[1,*]

[1] Laboratoire de Bioimagerie et Pathologies, UMR 7021 CNRS, Université de Strasbourg, Faculté de Pharmacie, Illkirch-France

[2] Institut de Génétique et de Biologie Moléculaire et Cellulaire (IGBMC), INSERM U964 CNRS UMR 7104, Université de Strasbourg, Illkirch-France.

[3] Dipartimento di Biotecnologie, Chimica e Farmacia, Università degli Studi di Siena, Via Aldo Moro 2, 53100, Siena, Italy.

[4]Institut de Génétique et de Biologie Moléculaire et Cellulaire (IGBMC), INSERM U964 CNRS UMR 7104, Université de Strasbourg, Illkirch, France.

[#] LZ and MM equally contributed to this work

*Authors to whom correspondence should be addressed: Marc Mousli, mousli@unistra.fr; Yves Mély, yves.mely@unistra.fr

- **Hits selection in silico**

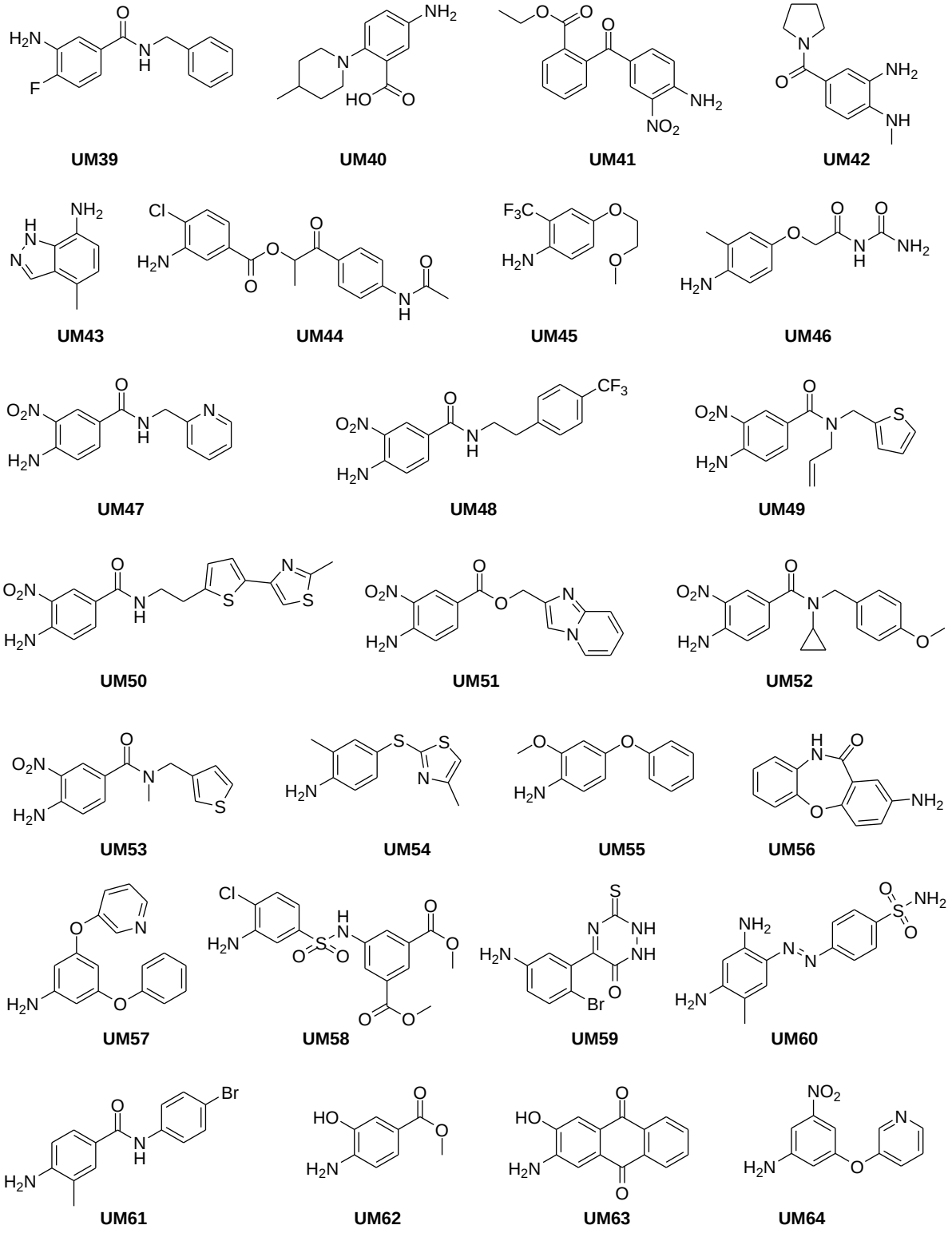

Figure S1. Chemical structure of putative hits UM39–UM64 selected by virtual screening.

- **Effect of UM63, UM63B and UM63D on the fluorescence of thG-labeled HM duplexes**

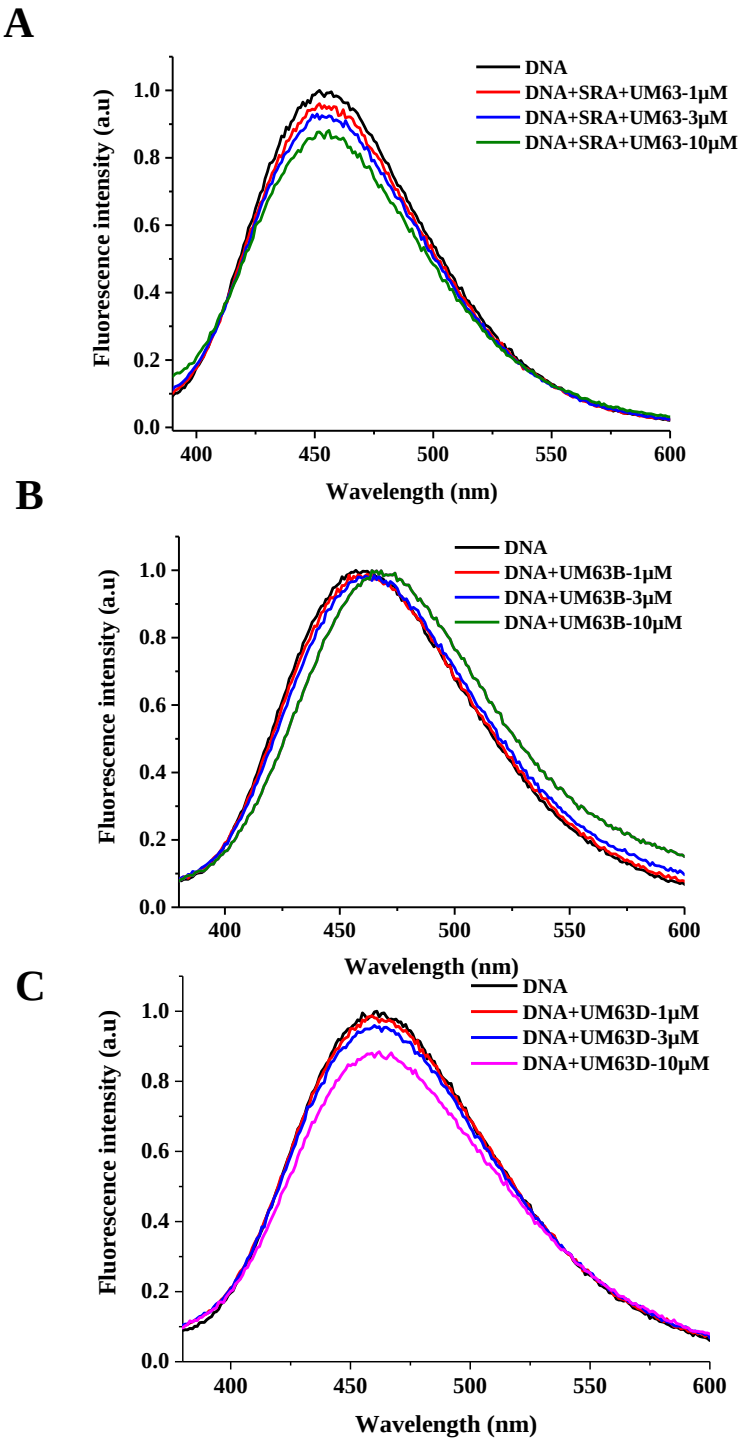

Figure S2. Effect of UM63, UM63B and UM63D on the emission spectrum of the thG-labeled HM duplex. Emission spectra of 1 μM thG-labeled duplex were recorded in the absence (black) and in the presence of different concentrations of (**A**) UM63 (**B**) UM63B (**C**) UM63D. Excitation was at 330 nm.

- **Effect of UM63E on the base flipping kinetics of the SRA domain**

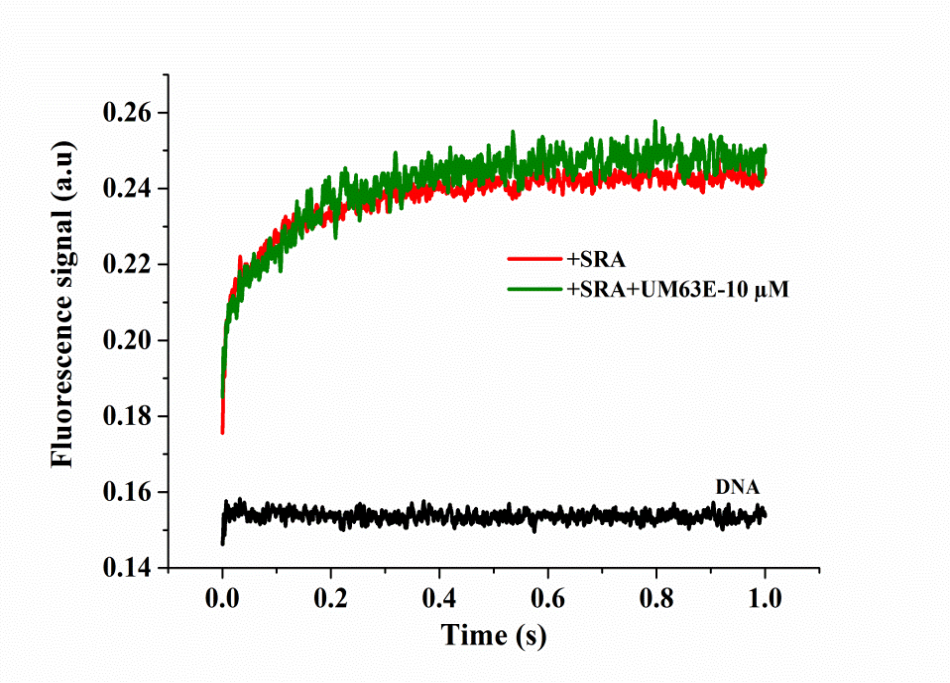

Figure S3. Effect of UM63E on the base flipping kinetics of the SRA domain. Kinetic curves were obtained by the stopped flow technique, monitoring the fluorescence of the thG-labeled HM duplex. The black curve corresponds to 0.2 µM HM duplex mixed with buffer. The red and green traces correspond to the mixing of 0.2 µM HM duplex with 1.5 µM SRA, respectively in the absence and the presence of 10 µM UM63E.

- **Effect of UM63E on the SRA/HM DNA complex**

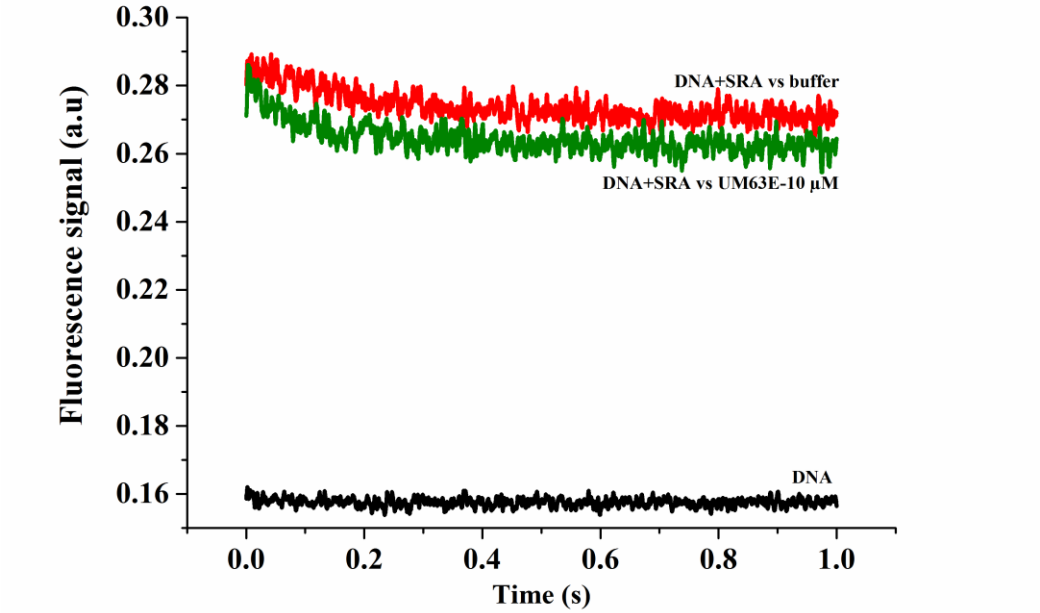

Figure S4. **Effect of UM63E on the SRA/HM DNA complex.** The dissociation of the SRA/HM DNA complex was monitored by the stopped flow technique after addition of 10 µM (green curve) of UM63E to the complex. The black curve corresponds to the DNA alone mixed with buffer. The concentrations of SRA and thG-labeled DNA were 0.2 µM and 1.5 µM, respectively.

- **UM63 competes with Ethidium bromide (EtBr) to bind to DNA:**

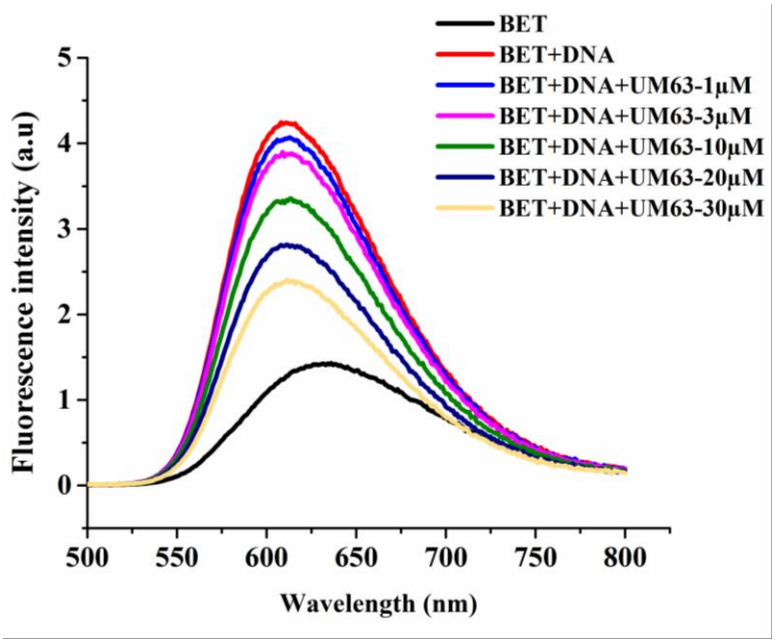

Figure S5. **UM63 competition with EtBr for DNA intercalation**. Fluorescence emission spectra of 1 µM EtBr free (black line) or bound to 1 µM DNA before (red) and after addition of different concentrations of UM63.

- **Binding of UM63E to HM DNA**

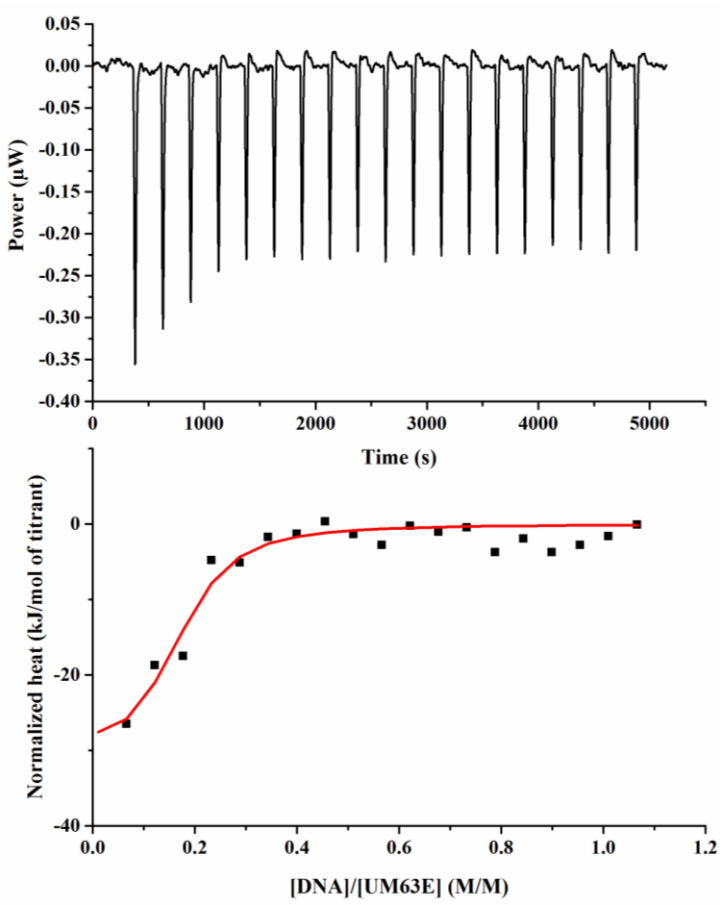

Figure S6. Binding of UM63E to HM duplexe as monitored by Isothermal Titration Calorimetry. Representative ITC titration curve of 80 µM of HM DNA in syringe into 12 µM of UM63E in measurement cell. The red curve was fitted to the experimental heat quantities using equation (6) giving a K_d value of 0.25 µM and a (ΔH=-31.48 kJ/mol).

Additional experiments 1: Biophysical aspects of UM63 interaction with DNA and its analog mitoxantrone

The interaction of small molecules with DNA can be categorized into three types : 1) intercalation into the base pairs of the DNA 2) binding to minor or major groove of DNA 3) external binding from the outside of the DNA helix [228]. UM63, an anthraquinone analog, proved in our previous results to be a DNA binder and it has moderate affinity for DNA. To confirm our findings, and for a further understanding of the UM63-DNA binding mode we used a series of techniques which reveal more details about the molecular mechanism of this interaction.

1- Displacement assay:

In the previous section, a displacement assay was performed in order to have an insight of the interaction between UM63 and DNA. For this, Ethidium bromide (EtBr) was chosen as our reporter by tracking its displacement from the DNA by fluorescence spectroscopy. It is known that EtBr is a DNA binder through intercalation [229]. After addition of DNA to EtBr, an important increase in fluorescence intensity was observed due to its strong intercalation between the base pairs (**Fig S5**), which is in perfect agreement with previous findings. The EtBr fluorescence intensity was quenched after titrating with different concentrations of UM63, leading to a progressive decrease which reflects a competition between UM63 and EtBr to bind to DNA with a displacement from the intercalation site. Thus, this indicates that UM63 is inserted into the DNA through an intercalative mechanism which results in the EtBr out of DNA.

2- Time resolved studies

Unsurprisingly, the measurement of fluorescence lifetimes confirmed the binding scenario of UM63 to DNA. The lifetime component of EtBr in its unbound form was 1.7 ns, a value matching with previous reports [230]. This value of lifetime was notably increased after addition of DNA to 18.5 ns indicating that the EtBr forms a complex with the nucleic acids. The outcome of UM63 addition results in a significant reduction of the lifetime (**Fig 1A**) which supports the results observed in the fluorescence spectroscopy that UM63 intercalates into DNA.

A

	τ1 (ns)	α1	τ2 (ns)	α2	τ3 (ns)	α3	τ (ns)
EtBr			**1.70**				**1.70**
EtBr-DNA			**1.82**	**0.12**	**20.83**	**0.88**	**18.54**
EtBr-DNA+UM63-10µM	**0.17**	**0.37**	**2.42**	**0.08**	**20.29**	**0.55**	**11.4**
EtBr-DNA+UM63-30µM	**0.15**	**0.40**	**2.56**	**0.11**	**20.29**	**0.49**	**10.28**

B

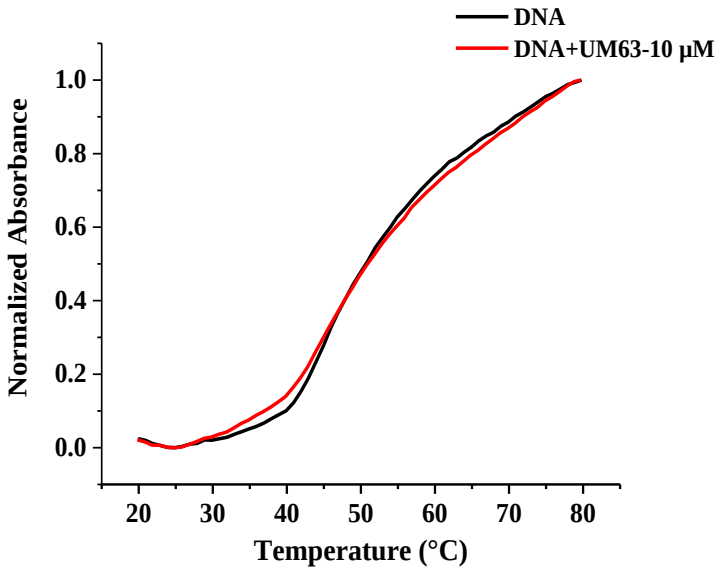

Figure 1. *(**A**) Time-resolved fluorescence decay parameters of ethidium bromide in absence or in presence of 10 µM and 30 µM of UM63. (**B**) Melting curve analysis of DNA in presence and absence of UM63. Absorbance of 1µM wild type DNA without (black) and with 10µM of UM63 (red) was collected at 260 nm.*

3- Melting Temperature

To validate the possibility whether UM63 binding to the DNA duplex can provoke any structural stabilization, we performed thermal denaturation assay for free DNA and bound DNA with UM63. After thermal denaturation, usually compounds able to interact with DNA increase the stability of DNA duplex which consequently increases the midpoint melting temperature. Addition of 10µM of UM63 did not change significantly the melting temperature curve showing that UM63 intercalation contributes in a negligible change in the stability (**Fig 1B**).

4- (ITC) titration

In order to characterize the thermodynamic parameters of UM63 binding to DNA, (ITC) studies were carried out. The reaction between UM63 and DNA is

UM63+DNA ‹—› UM63-DNA complex

As shown previously, the dissociation constant (K_d) value is 0.1 µM. The binding stoichiometry (n) which reflects the binding site indicated n=1. Moreover, the fitting of the titration curve of DNA with UM63 revealed that this binding process is enthalpically driven (ΔH = -13.03 kJ/mol) with a high entropic contribution (ΔS = 88 J/mol.K) suggesting that this complex is entropically governed. The important enthalpy could probably be the reason behind the intercalation of the aromatic rings of UM63 in the DNA helix. The positive entropy demonstrates that followed the intercalation there is a release of water molecules. Thus, this titration is important to have a clue about of the nature of the binding as well as the driving forces of this interaction.

Taken together, these findings provide knowledge about the possible scenario of a physical interaction between UM63 and DNA. Certainly, UM63 acts through an intercalative mechanism with a moderate affinity to DNA that is in micromolar range, and this process is favoured entropically and enthalipacally. However, as many anti-cancer drugs, anthraquinone family seems to depend totally or partially on the intercalation that is favored by its tricyclic structure. This data offers interesting insights for further investigation by analyzing structural properties of the UM63 and understanding their role in the DNA binding step. Hence, it will help us to elaborate the molecular basis of the mechanism of UM63 and monitor its therapeutic benefits or any possible toxicity related to it when used as anti-tumor agent.

5- Mitoxantrone:

Another drug that binds to DNA and shares pharmacophoric features with UM63 is mitoxantrone (MTX). MTX is an anthracene derivative that contains the planar anthraquinone ring (**Fig 2**). This feature makes mitoxantrone able to bind to DNA and perform its anti-tumoral activity by inhibiting replication of DNA and RNA transcription [231, 232]. Mitoxantrone is an anti-cancer agent that is approved for clinical usage and that has been used in a range of various cancers, such as acute leukemia, breast cancer, prostate cancer [233].

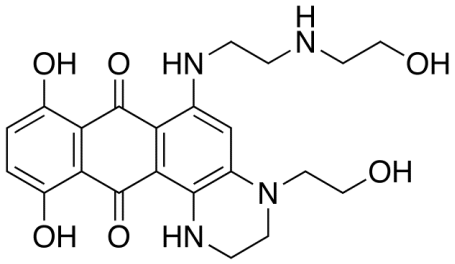

Figure 2. Structure of mitoxantrone.

Recently, a report proposed that MTX could interfere at the level of DNA UHRF1-SRA binding [234]. However, the exact mechanism is not elucidated. Based on the analogy in structure with UM63, we performed a control experiment to compare UM63 with the MTX in terms of binding with SRA. For this, (ITC) experiments were carried out. SRA was titrated into mitoxantrone, and after fitting the curve of the heat flow, K_d was indicating a good affinity between MTX and the protein with a value of 4.5 µM (**Fig 3**) versus 0.71 µM of the K_d between SRA and UM63. Unfortunately, we couldn't study further SRA binding with DNA in presence of MTX and track for a possible effect on the methylcytosine flipping by fluorescence methods since MTX results in a strong quenching of the thG fluorophore incorporated the DNA duplex.

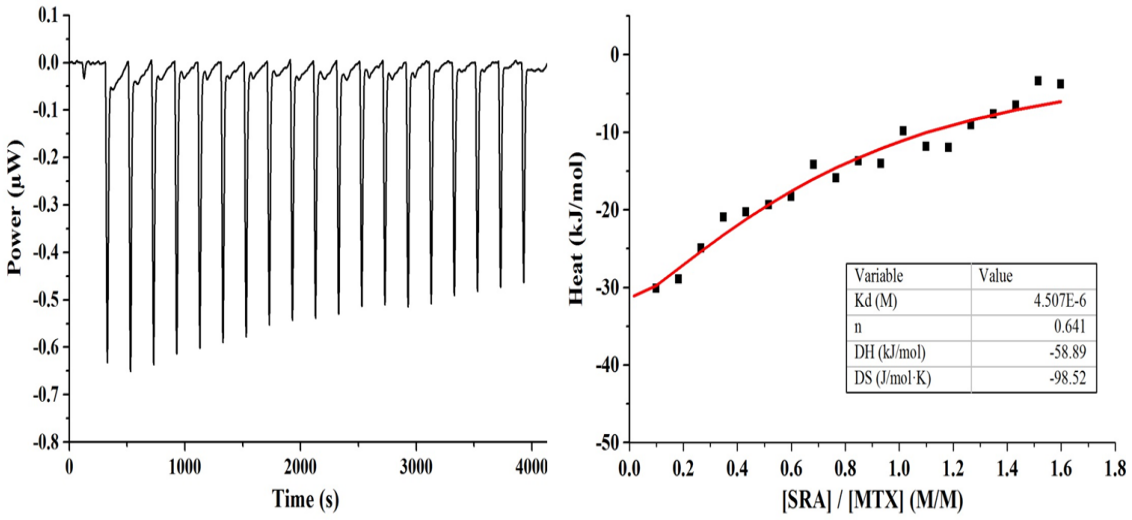

Figure 3. Binding of mitoxantrone to SRA domain as monitored by ITC. *80 µM of SRA in syringe was titrated into 8 µM of mitoxantrone in the measurement cell (left panel). Fitting of the titration curve provided a K_d value of 4.5 µM (right panel). Experiments were performed at 20°C in 20 mM phosphate buffer, 50 mM NaCl, pH= 7.5.*

It is worthy to point that the same report proposed that mitoxantrone exposure also induced DNA demethylation in DU145 cells [234]. Another report also suggested that mitoxantrone as mono treatment or combination treatment, facilitates hypomethylation and contributes in reactivation of silenced genes in breast cancer cells [235, 236].

The results obtained in this work with UM63 and the test performed with mitoxantrone opens the road to reconsider the anthraquinone family for further optimization and displays their potential in correcting epigenetic mistakes. Especially that mitoxantrone and UM63 possess the same structural ring and are shown to influence the methylation status in cancer cells.

Manuscript 2

Epigenetic dysregulation mechanism of 2-amino-3-hydroxyanthraquinone (AHAQ) induces cell cycle arrest and apoptosis in cervical cancer cells

Liliyana Zaayter [1], Waseem Ashraf [1], Tanveer Ahmad [1], Mattia Mori [3,] Christian D. Muller [4], Christina Bronner [2,*], Yves Mély [1], Marc Mousli [1,*]

[1]Laboratoire de Bioimagerie et Pathologies, UMR 7021 CNRS, Université de Strasbourg, Faculté de Pharmacie, Illkirch-France

[2]Institut de Génétique et de Biologie Moléculaire et Cellulaire (IGBMC), INSERM U964 CNRS UMR 7104, Université de Strasbourg, Illkirch-France

[3]Dipartimento di Biotecnologie, Chimica e Farmacia, Università degli Studi di Siena, Via Aldo Moro 2, Siena, Italy

[4]UMR 7200 CNRS, Laboratoire d'Innovation Thérapeutique, Université de Strasbourg, Faculte´ de Pharmacie, Illkirch, France

Corresponding author: Dr. Marc Mousli, Laboratoire de Biophotonique et Pharmacologie, UMR 7213 CNRS, Université de Strasbourg, Faculté de Pharmacie, 74 Route du Rhin, 67400, Illkirch-France

E-mail: marc.mousli@unistra.fr

Abbreviations : AHAQ, 2-amino-3-hydroxyanthraquinone ; DNMT1, DNA Methyltransferase 1 ; ICBP90, Inverted CCAAT box Binding Protein of 90 kDa ; TSG, Tumor suppressor gene; UHRF1,Ubiquitin-like containing PHD and RING finger domains 1.

Keywords: Cancer, anthraquinones, apoptosis, cell cycle, epigenetics, UHRF1, DNMT1, p53.

ZAAYTER et al., ANTI-CANCER PROPERTIES OF 2-AMINO-3 HYDROXYANTHRAQUINONE (AHAQ)

Abstract. Anthraquinone family contains many natural and synthetic compounds that have displayed a remarkable anti-tumor profile. Yet, there is an urge to identify new derivatives in order to effectively target the cancer cells. Recently, 2-amino-3-hydroxyanthraquinone (AHAQ) has been reported as a candidate of UHRF1 inhibitor that blocks SRA domain and leads to a decrease in global methylation levels. This compound also was shown to target human breast cancer cells (MDA-MB-231) and induce death in these cells. The aim of the study is to investigate the antitumor potential of AHAQ on different types of cancer cells and to propose an underlying mechanism for these antitumor properties. In the present study, we evaluated the anti-proliferative activity of AHAQ by MTT assay on three different cancer cell lines (HeLa, A375, and Huh7) and non-cancerous fibroblasts. AHAQ significantly inhibited the HeLa cell growth (IC_{50} = 2.4 ± 0.5 µM) whereas other cell lines were less sensitive to AHAQ treatment. The flow cytometry cell cycle analysis shows that AHAQ induces cell cycle arrest at G0/G1 phase. Treatment with AHAQ induces apoptosis in HeLa cells which is accompanied by re-activation of caspase3, PARP, the tumor suppressor gene p53 and deactivation of Bcl2 protein. These findings were associated with a downregulation of UHRF1 and DNMT1 which subsequently induced a global genomic demethylation. Our results suggest that AHAQ can be an interesting candidate for treatment of cervical cancer. It exerts its anti-cancer activity through induction of apoptosis and cell cycle arrest besides epigenetic modulation via UHRF1 and DNMT1. Antitumor properties of AHAQ can be further characterized for its possible application in preclinical and clinical studies.

A- Introduction

Anthraquinones, a family of aromatic compounds, with a planar tricyclic structure has gained considerable interest in past due to its wide anti-cancer profile (1). Doxorubicin and mitoxantrone are the two exemplified members of this family that have been widely used as chemotherapeutic agents (2). These agents are frequently recommended to treat a large variety of tumors such as multiple myeloma, breast cancers and solid tumors (2). New analogs of these anthraquinones are emerging in an attempt to improve the potency and safety of these drugs. Anthraquinones mainly exert their anti-cancer activity by interacting with DNA and interfering with the cellular machinery. In this way they target the cell proliferation by inducing apoptosis and cell cycle arrest (3). Recently, 2-amino-3-hydroxyanthraquinone (AHAQ), an anthraquinone derivative was described as an UHRF1 inhibitor that targets SRA domain and affects DNA methylation levels in cervical cancer cells. Another study of this compound has shown a possibility of AHAQ to mimic the known anthracycline drugs in terms of their anticancer effect (4). AHAQ's permeability to biological membrane is comparable to other anthracyclines and the compound exhibits antitumor effect in breast cancer cells MDAMB 231 by inhibiting cell growth and inducing of cell death (4). However, the exact mechanism of action of this anticancer effect is not well defined.

A programmed cell death is a common strategy for an anti-tumoral effect, that many anti-cancer therapies either anthraquinones-based or others proved to exert (3, 5, 6). The p53 tumor suppressor gene, a gatekeeper and caretaker of genome prevents tumorigenesis, and it is considered to be a crucial player in the cell death machinery. In response to stress, p53 controls many physiological processes through cell cycle arrest, apoptosis activation and DNA damage repair (7). An activated p53 may induce various pro-apoptotic genes that may promote intrinsic and extrinsic apoptotic pathways (8).

It is noteworthy that epigenetic abnormalities are one of the recent uncovered cancer signatures that play a crucial role in developing multiple tumors (9). Besides genetic mutations, different epimutations have also been associated with almost every step of cancer progression (10). However, the epigenetic network is not so simple and it is driven by interplay between varieties of epigenetic integrators.

Ubiquitin-like containing PHD and RING finger domains 1, (UHRF1), is a multi-domain protein recognized as one of the main epigenetic regulators. UHRF1 plays a pivotal role in faithful

transmission of DNA methylation mark from the parent strand to the daughter strand during the DNA replication by preferentially binding to hemimethylated DNA through its SRA domain and then recruiting the DNA methyltransferase (DNMT1) (11-13). In addition to this normal function, UHRF1 can play a critical role as a tumor promoter, since its levels are found to be highly expressed in majority of cancers such as hepatocellular carcinoma (14), breast cancer (15), gastric cancer (16),colorectal cancer (17), gallbladder cancer (18), and its abundance seems to correlate with tumor aggressiveness (19). The regulation of UHRF1 expression is cell cycle dependent in normal cells, but this expression remains high throughout the cell cycle in multiple tumors (20, 21). The oncogenic property of UHRF1 is also favored through regulating the function of some of tumor suppressor genes (TSGs) (22). It silences many of them including $p16^{INK4A}$ (23), HlC1 (24), RB1 (25), after DNMT1 and HDAC1 recruitment (26) leading to their promoter hypermethylation. Thus, through this repressive mechanism UHRF1 compromises the role of these genes in turmorogenesis prevention. Many studies have also underlined involvement of UHRF1 in promoting the proliferation of cancer cells by facilitating their passage through the cell cycle checkpoints (18, 27). All this highlights the putative role of UHRF1 in human malignancies (19) from where the growing interest in reconsidering UHRF1 for tumor treatments.

Accordingly, numerous investigations clearly indicate that targeting UHRF1 by si-RNA, small molecules, and natural compounds in various human cancer cell lines show anti-tumor activities (28, 29). The observed consequences of UHRF1 knockdown that include upregulation of TSGs (p14, p16, and RB), inhibition of proliferation, cell cycle regulation and apoptosis initiation (22) encouraged to investigate the effect of natural compounds on UHRF1-mediated epigenetic regulation. One noted example, is when a natural polyphenolic compound thymoquinone intensively downregulated UHRF1 in Jurkat cells. Thus, leading to an arrest at G0/G1 phase of the cell cycle and induction of apoptosis through reactivation of p73 (30). However, other compounds targeting UHRF1 in human breast cancer cells, cervical cells, and leukemia cancer cells proved to inhibit cell growth through reactivation of genes such as *p21*, *p16*, *p53* and consequently induce cell cycle arrest and apoptosis in these cells through their pathways (23, 31-33).

Given that AHAQ, the anthraquinone derivative is an UHRF1 inhibitor, our work aimed to investigate whether this compound exerts an anti-cancer activity related to UHRF1 inhibition. In our study we evaluate the anti-proliferative effect of AHAQ on different cell lines by using cervical carcinoma cells (HeLa), melanoma cells (A375) and hepatocarcinoma cells (Huh7) and we

determine whether AHAQ targets UHRF1 and DNMT1 expression in HeLa cells. We found that AHAQ induced apoptosis and cell cycle arrest in cervical cancer cells via reactivation of tumor suppressive p53 and downregulation of UHRF1 and DNMT1.

B- Material and Methods

Cell culture. HeLa (ATCC, CCL-2), A375, Huh7 and fibroblast were grown in DMEM (Dulbecco's Modified Eagle's Medium) which was supplemented with 10% FBS (fetal bovine serum), in addition to penicillin (100 U/ml) and streptomycin (100 U/ml) (penicillin/streptomycin: Invitrogen Corporation Pontoise, France). Cells were maintained in a humid atmosphere with 5% CO_2 at 37°C.

Antibodies. Antibodies used in this study include mouse monoclonal anti-UHRF1 which was engineered as described previously (34), mouse monoclonal anti-DNMT1 (Stressgen Canada), mouse monoclonal anti-PARP (BD Biosciences Pharmingen), mouse monoclonal anti-Bcl-2 (Merck-Millipore), rabbit polyclonal anti-caspase3 (Cell Signaling Technology, Danvers, MA, USA), mouse monoclonal anti-p53 (Delta Biolabs DB018), and mouse monoclonal anti-GAPDH (Merck Millipore MAB 374).

Cell proliferation by MTT assay. MTT assay was used in order to assess the proliferation state of cells after treatment with the molecules. HeLa cells were seeded in 96-well plates at a density of 5×10^3 cells/well and treated with various concentrations (0; 0.1; 0.3; 1; 3; 10; 30; 50; 100 µM) of AHAQ for 24 h. Each concentration was tested in triplicate. 100 µl of MTT reagent (5mg/10ml) dissolved in medium was added to each well and followed with incubation for 4 h at 37°C. The medium was discarded and 100µL of dimethylsulfoxide (DMSO) was added to each well. The plates were mixed gently until the dissolution of the formazan crystals. MTT reading was performed by measuring the optical density at 570 nm using Xenius plate reader. Each experiment was repeated three times and IC_{50} was calculated.

Cell Cycle and Apoptosis analysis. Flow cytometry was used to analyze cell cycle distribution and apoptosis. HeLa cells at a density of 1.5×10^5 cells/well were seeded into a 6-well plate and treated with a concentration of 10 µM for cell cycle and with different concentrations for apoptosis. Treated cells were compared to non-treated HeLa cells that served as control. For cell cycle, the cells were washed once with PBS, trypsinized and fixed with BD cellfix (BD Biosciences) reagent and incubated with FxCycle™ (Thermo Fisher Scientific F10797) PI/RNase staining solution for 20

min. After that DNA content was analyzed by guava easyCyte™ flow cytometer (Merck Millipore) and population percentages were determined by analyzing the results using InCyte Software for Guava® (Merck Millipore). For apoptosis, the cells were trypsinized and were incubated with PI (Miltenyi Biotec) and annexin V- FITC conjugate (Miltenyi Biotec) for 20 min. The apoptotic cells were analyzed using guava easyCyte™ flow cytometer provided with InCyte software (Merck Millipore).

Quantification of DNA methylation. HeLa cells were treated with 10 µM of AHAQ and 5-Azacytindine (Sigma-Aldrich), a specific demethylating agent serving as positive control. QIAamp® DNA Kit was used for DNA purification. Methylated DNA was assessed by using 200 ng of extracted DNA from non-treated cells and treated cells by using Sigma's Imprint® Methylated DNA Quantification Kit according to the manufacturer's protocol.

Western blot analysis. HeLa cells (1.5×10^5) were seeded into 6-well cell plates and grown for 24 h. Cells were treated with different concentrations of AHAQ for 24 h. Proteins were extracted by resuspending in ice cold lysis buffer (10 mM Tris-HCl pH 7.5, 150 mM NaCl, 1 mM EDTA and 1% NP40) containing protease inhibitors (complete mini EDTA free protease inhibitor cocktail tablets, Roche Germany). Cellular protein was quantified by Bradford method and 40 µg of proteins from cell lysate were separated on 10% SDS- polyacrylamide gel by electrophoresis after a 5 min denaturation step in Laemmli sample buffer (Bio-Rad Laboratories USA). After that, separated proteins are transferred to a (PVDF) membrane and 3% of non-fat dried milk was used to block the membrane at room temperature for 1 h. Incubation with primary antibodies a mouse monoclonal anti-UHRF1 (dilution 1:2000), anti-p53 (dilution 1:10000) , anti-DNMT1 (dilution 1:5000), anti-GAPDH (dilution 1:5000), anti-Caspase3 (dilution 1:2000), anti-BCl2 (dilution 1:2000), anti-PARP (dilution 1:10000) overnight at 4°C was followed. Primary antibodies were labeled with Horseradish Peroxidase conjugated secondary antibody. Signals were visualized by the chemiluminescent ECL system (Clarity™ ECL western blotting substrate, Biorad-USA) on Image Quant LAS 4000 apparatus. Images were analyzed and quantified by using Image Studio Lite (Li-Core Biosciences USA).

Statistical analysis. Data presented from at least three independent experiments and were statistically analyzed by t-Student test using GraphPadPrism (version 5.04) and Origin (version 8.6).

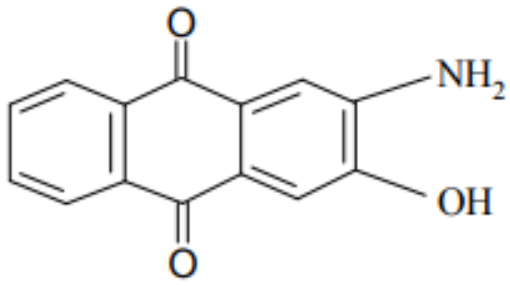

Figure 1. Chemical structure of AHAQ.

C- Results

1- AHAQ inhibits cell growth of cancer cells.

In order to evaluate AHAQ (Fig.1) as a potential hit for anti-proliferative activity, AHAQ was assessed by MTT assay. Following a 24 h treatment with AHAQ, cell proliferation was significantly decreased in a dose-dependent manner in HeLa cancer cells (Fig. 2A). In contrast, cell proliferation was less affected in A375 cells (Fig. 2B) where the percentage of proliferation started to effectively decrease at a higher concentration than in HeLa (3 µM). In Huh7 cells (Fig. 2C), the proliferation was slightly decreased comparing to the two other cell lines, and the effect started at 10 µM of treatment. Interestingly, AHAQ exerted a less significant effect on normal (fibroblast) cells after 24 h of exposure to AHAQ (Fig. 2D). The IC_{50} values were determined graphically indicating values of 2.4±0.5 µM, 18±0.8 µM and 25±0.6 µM for HeLa, A375 and Huh7 cells respectively. These results suggest that AHAQ is controlling cell proliferation in different cancer cells. For the next experiments of our work, we chose HeLa cells as referential model.

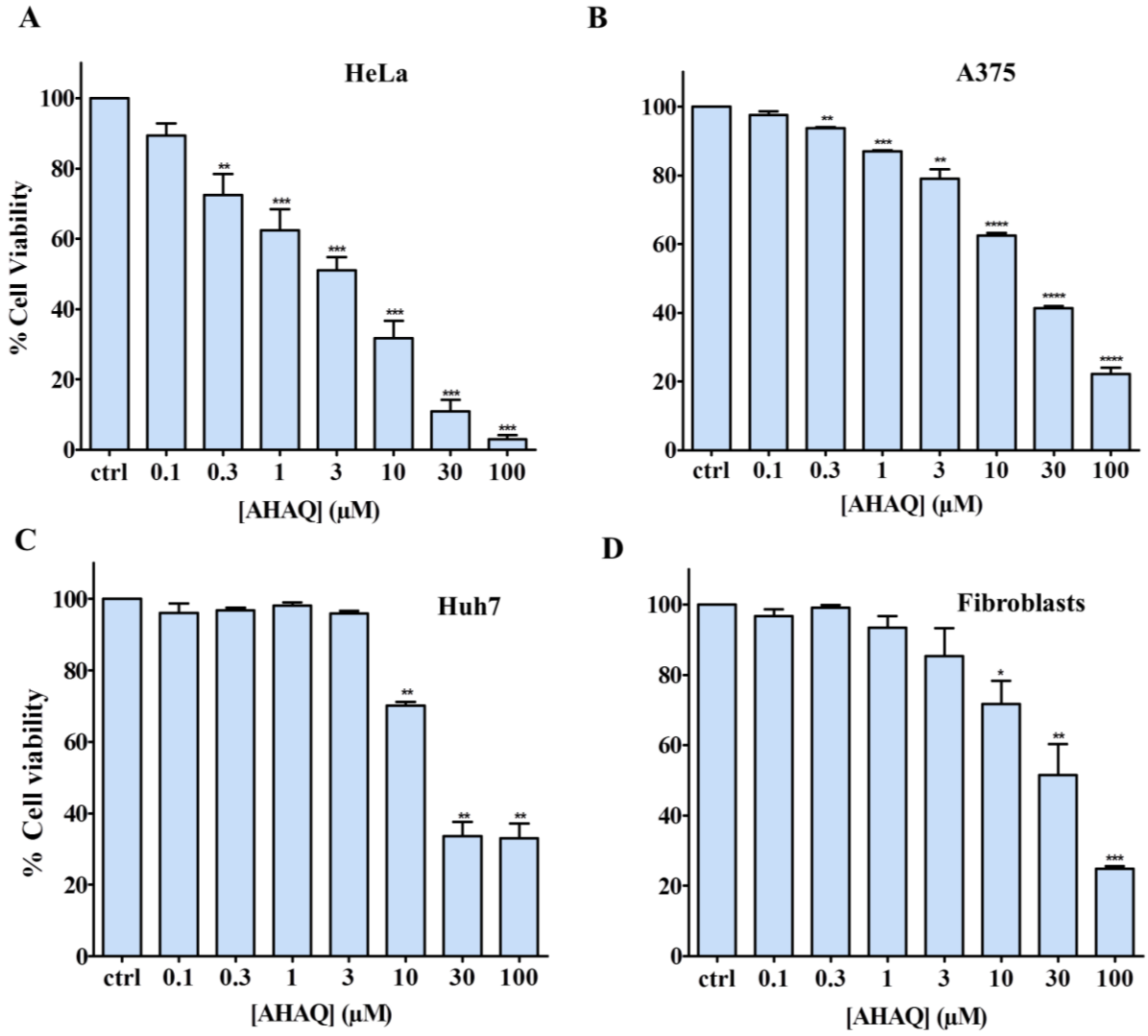

Figure 2. Concentration-dependent effect on cell viability of the AHAQ on different cancer cell lines and normal fibroblasts. (A) HeLa (B) A375 (C) Huh7 and (D) Fibroblasts cells were treated with AHAQ at the indicated concentrations for 24 h. Cell proliferation rate was assessed by colorimetry using the MTT assay. The absolute value obtained for each treated sample is expressed in a second step as percent relative to the corresponding absolute value obtained for the untreated sample and set at 100%. Values are means ±S.E.M. of three independent experiments; statistically significant * $p < 0.05$; ** $p < 0.01$; *** $p < 0.001$ (versus the corresponding untreated group).

2- AHAQ arrests HeLa cells on G0/G1 phase.

Because cell proliferation is the process when cells progress through the different phases of the cell cycle, we next evaluated the effects of AHAQ on the cell cycle distribution.

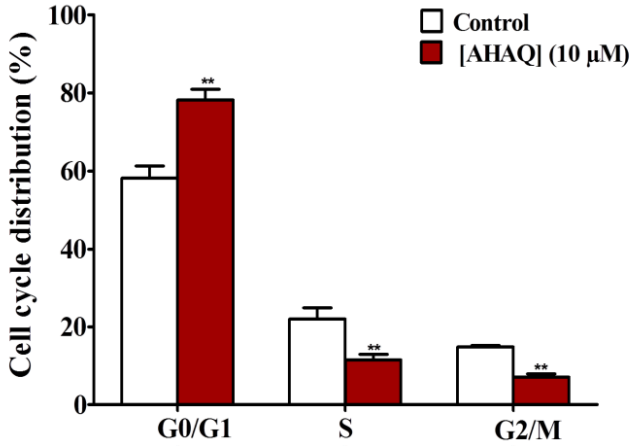

Figure 3. Effect of AHAQ on the cell cycle progression. Cells were treated with AHAQ for 24h and cell cycle distribution was assessed by a capillary cytometry detection assay. The graph shows the distribution of cells in G0/G1, S or G2/M phase; the number of cells in each phase was determined and expressed as percent relative to the total cell number. Values are means ±S.E.M. of three independent experiments; statistically significant: * $p < 0.05$; ** $p < 0.01$; *** $p < 0.001$ (versus the corresponding untreated group).

Treatment with AHAQ at 10 µM for 24 h induced an obvious cell cycle arrest at G0/G1 phase and the percentages of cells at S and G2 phase were correspondingly decreased. The percentage of G0/G1 cells increased from 58.14% to 78.23% following a decrease in G2/M population from 14.8% to 7.12% (Fig. 3). Therefore, this data suggests that AHAQ is able to inhibit the growth of HeLa cells within 24 h by promoting cell cycle arrest at the G0/G1 phase.

3- AHAQ induces apoptosis in HeLa cancer cells through caspase-3 and PARP activation and Bcl2 deactivation.

Given that one of the mechanisms that lead to growth inhibition of tumor cells is by undergoing apoptosis through the reactivation of signaling pathways, we investigated whether AHAQ induces an apoptotic response in HeLa cancer cells. As shown in (Fig. 4A), AHAQ increased the number of apoptotic cells in a concentration-dependent manner. At the highest tested concentration 20 µM, AHAQ showed a significant increase in apoptosis 29%. These findings were confirmed further by

western blot results that show an activation of pro-apoptotic proteins. Non treated cells show undetectable levels of cleaved caspase3; these levels start to increase after exposure to AHAQ in a dose-dependent manner (Fig. 4B). In addition, treatment with AHAQ was followed by a downregulation of PARP with a significant increase in its cleaved form (Fig. 4D). Then, we determined the levels of the pro-survival marker Bcl2 (Fig. 4C), where the levels of the protein decreased significantly starting 2 µM. Altogether, our results suggest that the exposure of HeLa cancer cells to AHAQ induces a caspase3-dependant apoptosis.

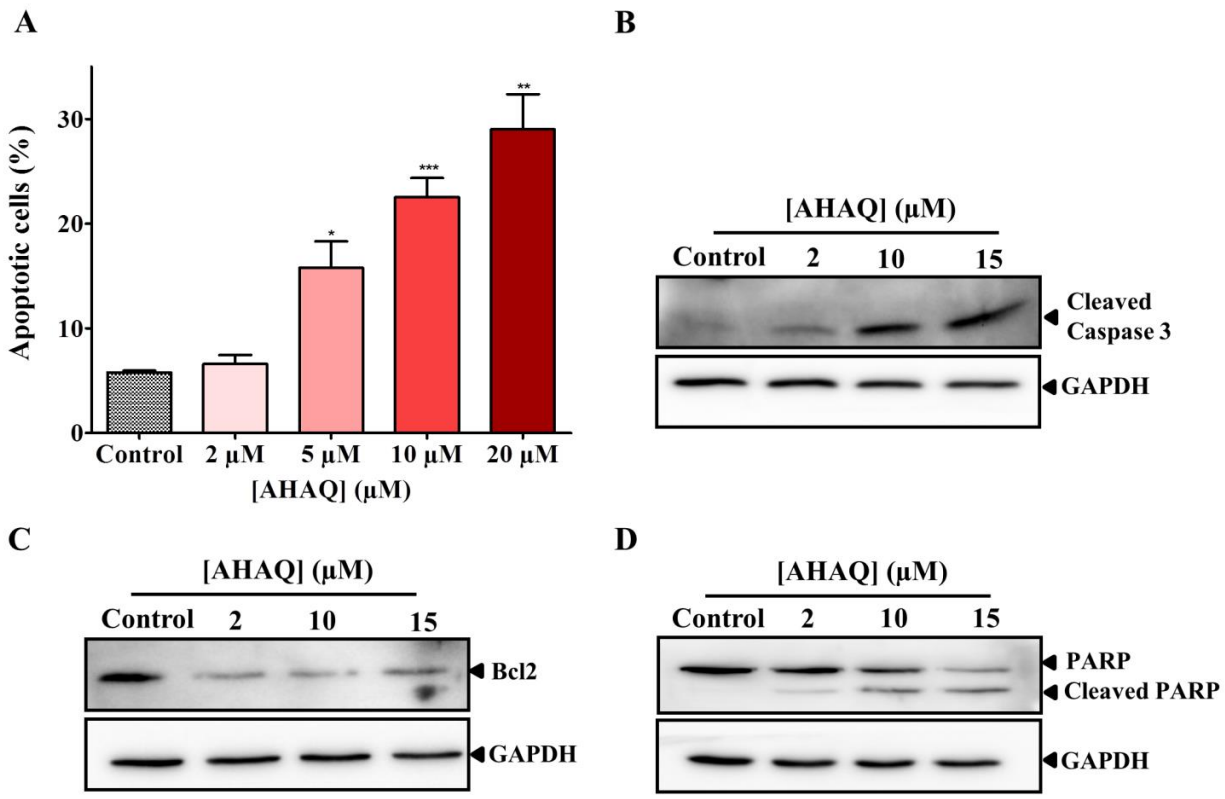

Figure 4. Effect of AHAQ on apoptosis and on expression of apoptotic protein levels in HeLa cells. Cells were treated with AHAQ at the indicated concentrations and incubated for 24 h. Cell apoptosis rate was assessed by cytometry using the Annexin V-FITC staining assay. (A) Recapitulates the number of apoptotic cells expressed as percent relative to the total cell number. Effect of AHAQ on expression levels of (B) cleaved caspase-3 (C) Bcl2 and (D) PARP. Values are means ±S.E.M. of three independent experiments; statistically significant: * $p < 0.05$; ** $p < 0.01$; *** $p < 0.001$ (versus the corresponding untreated group).

4- AHAQ induces p53 reactivation and down-regulation of UHRF1 and DNMT1 and in HeLa cells.

In order to determine more precisely the molecular events activated in response to the treatment, we wanted to investigate if apoptosis is induced by activation of a tumor suppressor gene. For this we analyzed the effect of AHAQ on the expression of p53. Treatment of HeLa cells with AHAQ, reactivated p53 in an evident manner (Fig. 5) suggesting that previous results in apoptosis could be triggered through a p53-dependant pathway.

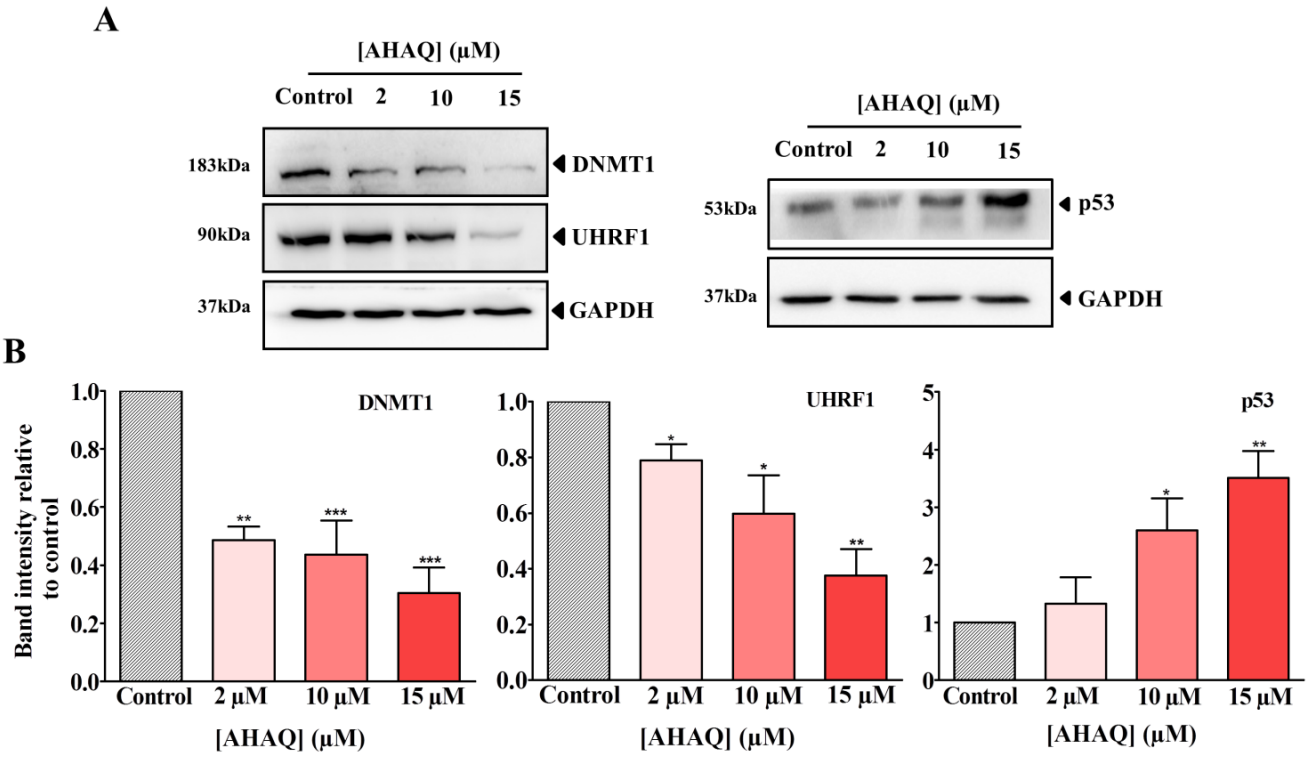

Figure 5. Concentration-dependent effects of AHAQ on the expression levels of DNMT1/ UHRF1 and on the levels of tumor suppressor p53 in HeLa cells. Cells were treated with AHAQ at the indicated concentrations and incubated for 24 h. (A) shows a representative western blot results of DNMT1/UHRF1 expression (left panel) and p53 expression (right panel). (B) shows the normalized signal for AHAQ treatment. GAPDH was used for the normalization of the expression levels of the different indicated proteins. Values are means ±S.E.M. of three independent experiments; statistically significant: * $p < 0.05$; ** $p < 0.01$; *** $p < 0.001$ (versus untreated group).

UHRF1 has been identified to be targeted by TSGs such p53 and p73, and any dysregulation of these TSGs modulates the expression of UHRF1, that can also itself control the expression of these genes by a negative feedback (22). For this, further analysis was carried out to study UHRF1 and DNMT1 proteins which are primarily involved in epigenetic modulation. HeLa cells were treated with different concentrations of AHAQ (2 µM, 10 µM, 15 µM) respectively in order to evaluate the effect on UHRF1 and DNMT1 expression in a concentration-dependent manner (Fig. 5). HeLa cells incubation with AHAQ for 24 h induced a significant reduction in DNMT1 levels. Similarly, UHRF1 expression was downregulated gradually in the same conditions of treatment.

5- UHRF1 and DNMT1 down-regulation is associated with a decrease in global DNA methylation.

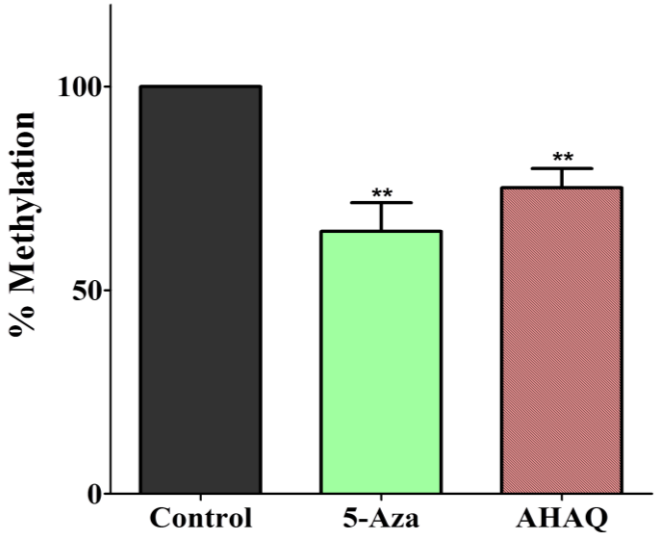

Figure 6. Effect of AHAQ on the global DNA methylation in HeLa cells. DNA was extracted from treated and non-treated cells. The graph illustrates the absorbance representing the content of methylated DNA. Values are means ±S.E.M. of three independent experiments; statistically significant: * $p < 0.05$; ** $p < 0.01$; *** $p < 0.001$ (versus untreated group).

We wanted to uncover whether the epigenetic alteration shown in our western blot result, is associated with an effect on genomic DNA methylation. For that, 5-Azacytidine, a known DNMT1 inhibitor with a demethylating effect, was used as positive control. Global DNA methylation was estimated by using Imprint Methylated DNA quantification assay after extracting the DNA from

treated and untreated HeLa cells (Fig. 6). Comparing to non-treated cells, cells treated with AHAQ showed a 25.1% decrease versus a 35.7% decrease in 5-Azacytidine treated samples which is in agreement with our previously reported finding. Altogether, this data demonstrates that AHAQ leads to a reduced methylation level in the genome.

D- Discussion

Anthraquinones have shown a great potential to be used as anti-tumor agents in different studies, however so far, their use in therapeutics is limited because of their high toxicity, poor selectivity and other side effects. Therefore, there is a need to develop new analogues which can safely and selectively target cancer cells.

Anthraquinones mostly exerts their cytotoxic effects by their ability to intercalate into the DNA bases (35), a property that has been exploited by variety of chemotherapeutic agents. A lot of natural and synthetic anthraquinone compounds such Rhein, emodin and 1,3-dihydroxy-9,10-anthraquinone-2- carboxylic acid (DHAQC) have been reported to target various cancer cell lines (HeLa, A375, MOLT-4,MCF-7) (1, 36, 37). A recent study described that 2-amino-3-hydroxyanthraquinone AHAQ, a derivative from 9, 10 anthraquinone, impaired the cell viability of breast cancer cells (4). In this study, we also observed an evident inhibiting effect of AHAQ on proliferation of cervical cancer (HeLa), melanoma (A375) and hepatocarcinoma (Huh7). It is interesting to note that AHAQ seems not to exert evident anti-proliferative effect on non-cancer (fibroblasts) cells, which holds an opportunity for its application in chemotherapy with fewer side effects. Anyhow, further investigations should be carried out to validate this finding.

Treatment of cancer cells with AHAQ resulted in cell cycle arrest at G0/G1 phase. Anticancer drugs tend to inhibit the cell cycle progression by activation of different tumor suppressor genes and cell cycle checkpoints. For example, HeLa cells treated with aloe emodin, a natural anthraquinone, induced a G2/M arrest (38). However, the same compound arrested the hepatoma cells in G0/G1 phase after the p53 induced activation of p21 (39). Moreover, FACS analysis showed that the treatment with AHAQ also induced apoptosis in HeLa cells. Activation of apoptotic machinery is a mechanism induced in response of many anticancer drugs to kill tumors. In our study, by investigating the apoptosis related proteins, we found that the apoptotic effect is mechanistically mediated by a caspase-3 signaling pathway, which is followed by a prominent PARP cleavage. In

the same context, upon AHAQ exposure, Bcl2, an anti-apoptotic protein involved in mitochondrial pathway and necessary for cell survival was also found to be reduced.

p53 is an important tumor suppressor gene coordinating DNA repair, cell cycle arrest and apoptosis in cells (40). Studies have shown that in majority of the human malignancies, p53 is either mutated or suppressed to overcome its tumor preventive role in cancer (41). Upon treatment with different chemotherapeutic drugs, p53 gets activated and induces cell cycle arrest or apoptosis depending on the activating stimuli and downstream signaling initiated in response to p53 activation. Our western blot analysis demonstrated that p53 is reactivated in response to treatment with AHAQ and can be the reason for cell cycle arrest and apoptosis induction.

UHRF1, an overexpressed epigenetic regulator in cancers, plays a critical role as tumor promoter by disrupting the function of various TSGs (19, 22). Previously, it has been reported that UHRF1 promotes oncogenesis by negatively regulating the p53 activity and suppressing p53 mediated transactivation (42). Therefore, we examined UHRF1 expression and our results showed that UHRF1 levels were down-regulated in HeLa cells after treatment with AHAQ. Accordingly, a reasonable explanation indicates the possibility of AHAQ to activate the p53 pathway by downregulation of UHRF1. Altogether, these findings show that AHAQ probably acts by a mechanism that controls tumor suppressor genes and UHRF1.

It is important to note that DNMT1 levels were also downregulated after treatment with AHAQ and over all global methylation reduced by 25% in these cells. DNMT1 is found upregulated in many cancers (43) and is currently being targeted by different epigenetic drugs such as azacytidine and decitabine to improve the therapeutic outcome in cancer patients. Till present, three chemical molecules have been suggested to act as UHRF1 inhibitors, but their anti-cancer effect has never been evaluated in a cellular system. However, only the effect of natural extracts that target UHRF1's signaling pathways or of the usage of siRNAs has been described to have a favorable antitumor response in various human cancer cell lines (28-30, 44, 45). The consequences of UHRF1 downregulation were upregulation of TSGs, inhibition of the proliferation, cell cycle arrest and apoptosis initiation (22, 44, 46). For instance, the proliferation of MDAMB 231 cells was shown to be promoted through UHRF1 activity (47) and it is interesting to note that in a previous study treatment of AHAQ induced apoptosis of these cells (4), a finding that could be associated with UHRF1 inhibition. However, since AHAQ has been reported as an UHRF1-SRA inhibitor, it is

expected to have comparable effects to those of UHRF1 downregulation. Furthermore, treatment with AHAQ downregulated UHRF1 and DNMT1 proteins, induced global hypomethylation, thus reactivated the p53 to induce cell cycle arrest and apoptosis. Taken the mode of action reported in our previous study, the mechanism underlying the process of demethylation by AHAQ can be attributed to not only the decreased levels of both proteins upon treatment , but additionally to the inhibition of flipping of the methylated cytosine and the impairment of DNMT1/UHRF1 interaction.

In conclusion, our study describes for the first time the anti-tumoral properties of a small chemical molecule that targets UHRF1. Our findings clearly demonstrate that AHAQ has an anti-proliferative activity which is mediated through cell cycle arrest and apoptosis induction in HeLa cancer cells. Our results also suggest that AHAQ is able to target the expression of epigenetic modulators UHRF1 and DNMT1 with a subsequent global DNA demethylation. Overall, these results indicate the potential of AHAQ as an UHRF1 inhibitor and as a candidate for anti-cancer research, as well as a useful reference for further investigations in order to characterize and understand the exact mechanism.

References:

1. Hussain H, Al-Harrasi A, Al-Rawahi A, et al.: A fruitful decade from 2005 to 2014 for anthraquinone patents. Expert opinion on therapeutic patents 25: 1053-1064, 2015.
2. Evison BJ, Sleebs BE, Watson KG, Phillips DR and Cutts SM: Mitoxantrone, More than Just Another Topoisomerase II Poison. Medicinal research reviews 36: 248-299, 2016.
3. Huang Q, Lu G, Shen HM, Chung MC and Ong CN: Anti-cancer properties of anthraquinones from rhubarb. Medicinal research reviews 27: 609-630, 2007.
4. Das A, Roy S, Mondal P, et al.: Studies on the interaction of 2-amino-3-hydroxy-anthraquinone with surfactant micelles reveal its nucleation in human MDA-MB-231 breast adinocarcinoma cells. RSC Advances 6: 28200-28212, 2016.
5. Koceva-Chyla A, Jedrzejczak M, Skierski J, Kania K and Jozwiak Z: Mechanisms of induction of apoptosis by anthraquinone anticancer drugs aclarubicin and mitoxantrone in comparison with doxorubicin: relation to drug cytotoxicity and caspase-3 activation. Apoptosis : an international journal on programmed cell death 10: 1497-1514, 2005.
6. Hickman JA: Apoptosis induced by anticancer drugs. Cancer metastasis reviews 11: 121-139, 1992.
7. Harris SL and Levine AJ: The p53 pathway: positive and negative feedback loops. Oncogene 24: 2899-2908, 2005.
8. el-Deiry WS: Regulation of p53 downstream genes. Seminars in cancer biology 8: 345-357, 1998.
9. Nakamura K, Nakabayashi K, Htet Aung K, et al.: DNA methyltransferase inhibitor zebularine induces human cholangiocarcinoma cell death through alteration of DNA methylation status. PloS one 10: e0120545, 2015.
10. Timp W and Feinberg AP: Cancer as a dysregulated epigenome allowing cellular growth advantage at the expense of the host. Nature reviews. Cancer 13: 497-510, 2013.
11. Arita K, Ariyoshi M, Tochio H, Nakamura Y and Shirakawa M: Recognition of hemi-methylated DNA by the SRA protein UHRF1 by a base-flipping mechanism. Nature 455: 818-821, 2008.
12. Avvakumov GV, Walker JR, Xue S, et al.: Structural basis for recognition of hemi-methylated DNA by the SRA domain of human UHRF1. Nature 455: 822-825, 2008.
13. Sharif J, Muto M, Takebayashi S, et al.: The SRA protein Np95 mediates epigenetic inheritance by recruiting Dnmt1 to methylated DNA. Nature 450: 908-912, 2007.
14. Liang D, Xue H, Yu Y, Lv F, You W and Zhang B: Elevated expression of UHRF1 predicts unfavorable prognosis for patients with hepatocellular carcinoma. International journal of clinical and experimental pathology 8: 9416-9421, 2015.
15. Geng Y, Gao Y, Ju H and Yan F: Diagnostic and prognostic value of plasma and tissue ubiquitin-like, containing PHD and RING finger domains 1 in breast cancer patients. Cancer science 104: 194-199, 2013.

16. Zhou L, Zhao X, Han Y, et al.: Regulation of UHRF1 by miR-146a/b modulates gastric cancer invasion and metastasis. FASEB journal : official publication of the Federation of American Societies for Experimental Biology 27: 4929-4939, 2013.
17. Wang F, Yang YZ, Shi CZ, et al.: UHRF1 promotes cell growth and metastasis through repression of p16(ink(4)a) in colorectal cancer. Annals of surgical oncology 19: 2753-2762, 2012.
18. Qin Y, Wang J, Gong W, et al.: UHRF1 depletion suppresses growth of gallbladder cancer cells through induction of apoptosis and cell cycle arrest. Oncology reports 31: 2635-2643, 2014.
19. Ashraf W, Ibrahim A, Alhosin M, et al.: The epigenetic integrator UHRF1: on the road to become a universal biomarker for cancer. Oncotarget, 2017.
20. Mousli M, Hopfner R, Abbady AQ, et al.: ICBP90 belongs to a new family of proteins with an expression that is deregulated in cancer cells. British journal of cancer 89: 120-127, 2003.
21. Jeanblanc M, Mousli M, Hopfner R, et al.: The retinoblastoma gene and its product are targeted by ICBP90: a key mechanism in the G1/S transition during the cell cycle. Oncogene 24: 7337-7345, 2005.
22. Alhosin M, Omran Z, Zamzami MA, et al.: Signalling pathways in UHRF1-dependent regulation of tumor suppressor genes in cancer. Journal of experimental & clinical cancer research : CR 35: 174, 2016.
23. Achour M, Mousli M, Alhosin M, et al.: Epigallocatechin-3-gallate up-regulates tumor suppressor gene expression via a reactive oxygen species-dependent down-regulation of UHRF1. Biochemical and biophysical research communications 430: 208-212, 2013.
24. Fleuriel C, Touka M, Boulay G, Guerardel C, Rood BR and Leprince D: HIC1 (Hypermethylated in Cancer 1) epigenetic silencing in tumors. The international journal of biochemistry & cell biology 41: 26-33, 2009.
25. Alhosin M, Sharif T, Mousli M, et al.: Down-regulation of UHRF1, associated with re-expression of tumor suppressor genes, is a common feature of natural compounds exhibiting anti-cancer properties. Journal of experimental & clinical cancer research : CR 30: 41, 2011.
26. Hashimoto H, Horton JR, Zhang X, Bostick M, Jacobsen SE and Cheng X: The SRA domain of UHRF1 flips 5-methylcytosine out of the DNA helix. Nature 455: 826-829, 2008.
27. Bronner C, Krifa M and Mousli M: Increasing role of UHRF1 in the reading and inheritance of the epigenetic code as well as in tumorogenesis. Biochemical pharmacology 86: 1643-1649, 2013.
28. Krifa M, Pizzi A, Mousli M, Chekir-Ghedira L, Leloup L and Ghedira K: Limoniastrum guyonianum aqueous gall extract induces apoptosis in colorectal cancer cells by inhibiting calpain activity. Tumour biology : the journal of the International Society for Oncodevelopmental Biology and Medicine 35: 7877-7885, 2014.
29. Unoki M: Current and potential anticancer drugs targeting members of the UHRF1 complex including epigenetic modifiers. Recent patents on anti-cancer drug discovery 6: 116-130, 2011.
30. Alhosin M, Abusnina A, Achour M, et al.: Induction of apoptosis by thymoquinone in lymphoblastic leukemia Jurkat cells is mediated by a p73-dependent pathway which targets the epigenetic integrator UHRF1. Biochemical pharmacology 79: 1251-1260, 2010.

31. Jang SY, Hong D, Jeong SY and Kim JH: Shikonin causes apoptosis by up-regulating p73 and down-regulating ICBP90 in human cancer cells. Biochemical and biophysical research communications 465: 71-76, 2015.
32. Kim MY, Park SJ, Shim JW, Yang K, Kang HS and Heo K: Naphthazarin enhances ionizing radiation-induced cell cycle arrest and apoptosis in human breast cancer cells. International journal of oncology 46: 1659-1666, 2015.
33. Sharif T, Auger C, Alhosin M, et al.: Red wine polyphenols cause growth inhibition and apoptosis in acute lymphoblastic leukaemia cells by inducing a redox-sensitive up-regulation of p73 and down-regulation of UHRF1. European journal of cancer 46: 983-994, 2010.
34. Hopfner R, Mousli M, Jeltsch J-M, et al.: ICBP90, a novel human CCAAT binding protein, involved in the regulation of topoisomerase IIα expression. Cancer research 60: 121-128, 2000.
35. Hsin LW, Wang HP, Kao PH, et al.: Synthesis, DNA binding, and cytotoxicity of 1,4-bis(2-amino-ethylamino)anthraquinone-amino acid conjugates. Bioorganic & medicinal chemistry 16: 1006-1014, 2008.
36. Yeap S, Akhtar MN, Lim KL, et al.: Synthesis of an anthraquinone derivative (DHAQC) and its effect on induction of G2/M arrest and apoptosis in breast cancer MCF-7 cell line. Drug design, development and therapy 9: 983-992, 2015.
37. Genov M, Kreiseder B, Nagl M, et al.: Tetrahydroanthraquinone Derivative (+/-)-4-Deoxyaustrocortilutein Induces Cell Cycle Arrest and Apoptosis in Melanoma Cells via Upregulation of p21 and p53 and Downregulation of NF-kappaB. Journal of Cancer 7: 555-568, 2016.
38. Guo JM, Xiao BX, Liu Q, Zhang S, Liu DH and Gong ZH: Anticancer effect of aloe-emodin on cervical cancer cells involves G2/M arrest and induction of differentiation. Acta pharmacologica Sinica 28: 1991-1995, 2007.
39. Kuo PL, Lin TC and Lin CC: The antiproliferative activity of aloe-emodin is through p53-dependent and p21-dependent apoptotic pathway in human hepatoma cell lines. Life sciences 71: 1879-1892, 2002.
40. Kruse JP and Gu W: Modes of p53 regulation. Cell 137: 609-622, 2009.
41. Hainaut P and Hollstein M: p53 and human cancer: the first ten thousand mutations. Advances in cancer research 77: 81-137, 2000.
42. Ma J, Peng J, Mo R, et al.: Ubiquitin E3 ligase UHRF1 regulates p53 ubiquitination and p53-dependent cell apoptosis in clear cell Renal Cell Carcinoma. Biochemical and biophysical research communications 464: 147-153, 2015.
43. Subramaniam D, Thombre R, Dhar A and Anant S: DNA methyltransferases: a novel target for prevention and therapy. Frontiers in oncology 4: 80, 2014.
44. Seo JS, Choi YH, Moon JW, Kim HS and Park SH: Hinokitiol induces DNA demethylation via DNMT1 and UHRF1 inhibition in colon cancer cells. BMC cell biology 18: 14, 2017.
45. Kofunato Y, Kumamoto K, Saitou K, et al.: UHRF1 expression is upregulated and associated with cellular proliferation in colorectal cancer. Oncology reports 28: 1997-2002, 2012.
46. Esteller M: Epigenetics in cancer. The New England journal of medicine 358: 1148-1159, 2008.

47. Li XL, Xu JH, Nie JH and Fan SJ: Exogenous expression of UHRF1 promotes proliferation and metastasis of breast cancer cells. Oncology reports 28: 375-383, 2012.

Additional experiments 2: Molecules positive only in cellular assays

During the selection process, molecules were evaluated by base flipping assay and by MTT. In the previous sections, we discussed the results of compounds that were positive in base flipping assay. Herein, we will provide additional experiments that were performed on the two positive molecules in MTT assay "UM12" and "UM48". Despite being not active on biophysical experiments, we thought to continue with our investigations to check whether the effect observed on proliferation is related to UHRF1 or to some other pathway. Additionally, we thought to use these molecules as "control" for our experiments.

1- Selection of biologically active compounds:

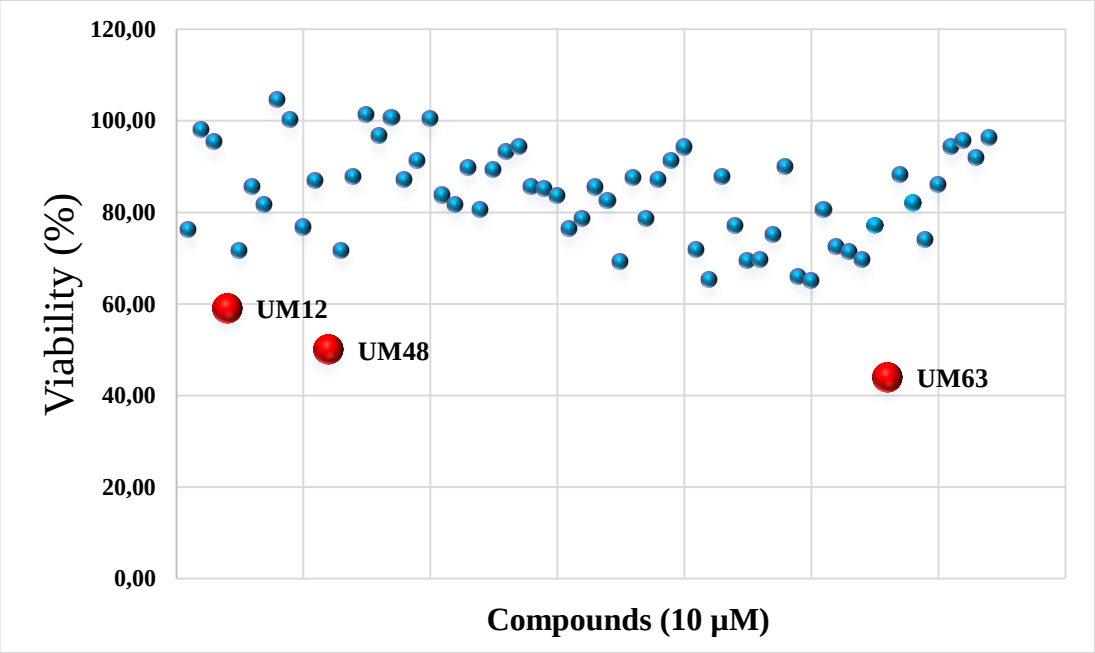

Figure 1. Evaluation of first two batches of molecules by using MTT assay. *Cell proliferation was assessed after 24 h treatment of each compound at 10 µM. The molecules in blue correspond to not active ones at the indicated concentration, while the molecules in red correspond to the active ones*.

MTT assay is considered to be an easy and rapid method for preliminary evaluation of anticancer activity for drug discovery. This test allows studying the sensitivity of cancer cells towards anti-tumor agents. Firstly, we thought to test all compounds for 24 h on cervical cancer cell line (HeLa), and to follow their effect on cell viability (Fig.1). At 10 µM, UM12 and UM48 were able to slow proliferation of HeLa cells. Based on this observation, we further performed a chain of experiments that could help us to have a clue on the activity of these compounds on the molecular level.

Given that we are looking for potential candidates with anti-cancer effect that could target UHRF1/DNMT1 complex, we assessed the anti-prolifrative activity in HeLa cells. Following treatment with UM12 and UM48, cell proliferation was decreased in a concentration-dependent manner (Fig. 2). The IC_{50} values after 24 h were determined graphically. The values were 13.3 µM and 11.3 µM for UM12 and UM48 respectively. These results suggest that UM12 and UM48 control cell proliferation in HeLa cells.

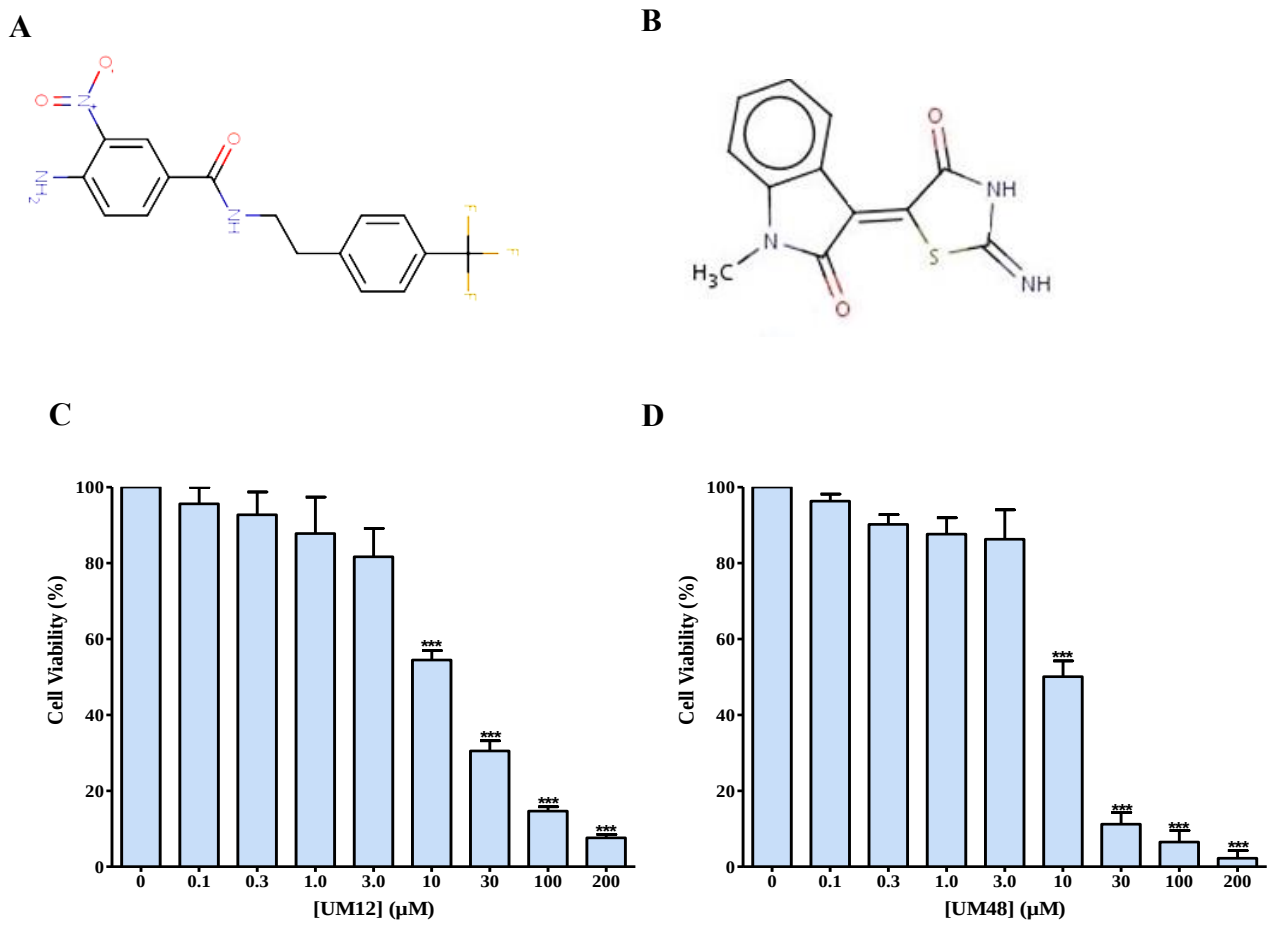

Figure 2. The two positive hits in MTT assay UM12 and UM48. *Chemical structure of (**A**) UM12 and (**B**) UM48. Concentration-dependent effect on cell viability of UM12 and UM48 on HeLa cancer cell line. Cells were treated with (**C**) UM12 (**D**) UM48 at the indicated concentrations and incubated for 24 h. Cell proliferation rate was assessed by colorimetry using the MTT assay.*

2- Cell cycle Analysis:

Next, to examine the possible mechanism by which UM12 and UM48 change the growth profile of HeLa, we performed cell cycle analysis. Following treatment with UM12, the percentage of population in G0/G1 phase was increased from 62.64% in control to 76.43% in treated cells (Fig. 3A). After treatment with UM48, G0/G1 population increased from 69.8% in control to 76.4% in treated cells, while G2/M population significantly decreased from 13.35% to 6.82% (Fig. 3B). This shows that UM12 and UM48 inhibit the growth of HeLa cells within 24 h by promoting cell cycle arrest at the G0/G1 phase.

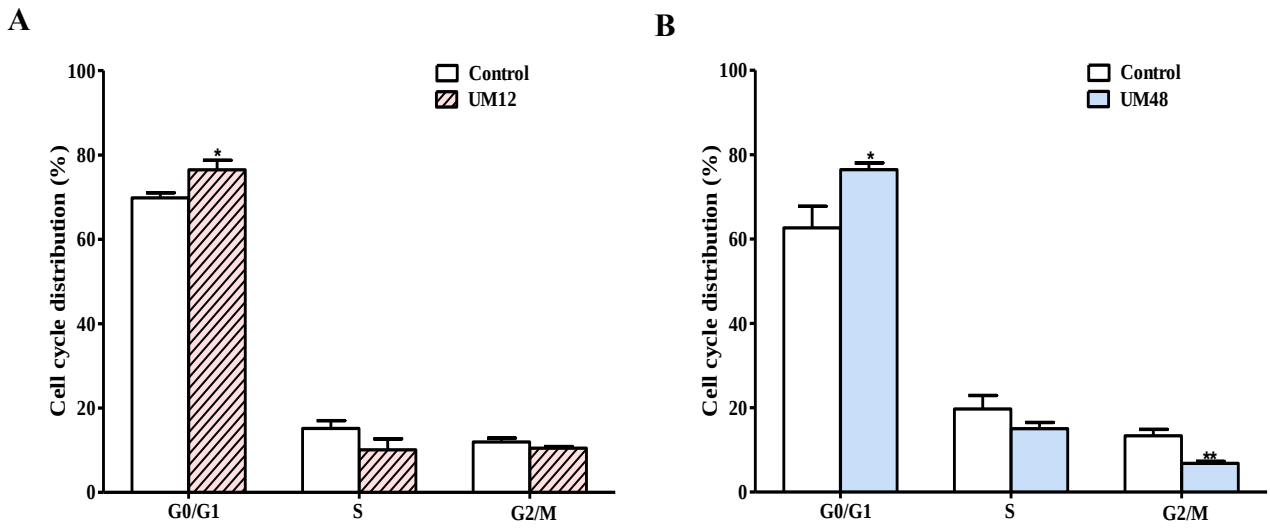

Figure 3. Effect of UM12 and UM48 on the cell cycle regulation of HeLa cells. *Cells were treated with (**A**) UM12 (**B**) UM48 at their IC_{50} concentration for 24 h.*

3- Western Blot Analysis:

In order to see the effect of the selected molecules on the proteins of the targeting complex DNMT1/UHRF1, and to determine more precisely the molecular events which could be activated in response to their treatment, HeLa cells were treated with UM12 and UM48 for 24 h. Cells treated with UM48 didn't shown a decrease in DNMT/UHRF1 levels neither any upregulation of the TSGs. In contrast, UM12 induced a significant reduction in DNMT1 and UHRF1 expression.

UHRF1 has been identified to be targeted by TSGs such p53 and p73, and any dysregulation of these TSGs modulates the expression of UHRF1. To check the tumor suppressor pathway, we analyzed the expression levels of p53 and p73. After 24 h of treatment with different concentrations, only UM12 induced a significant upregulation of the p53 and p73. Next, we performed cytometric analysis to test the hypothesis that these molecules may induce apoptosis.

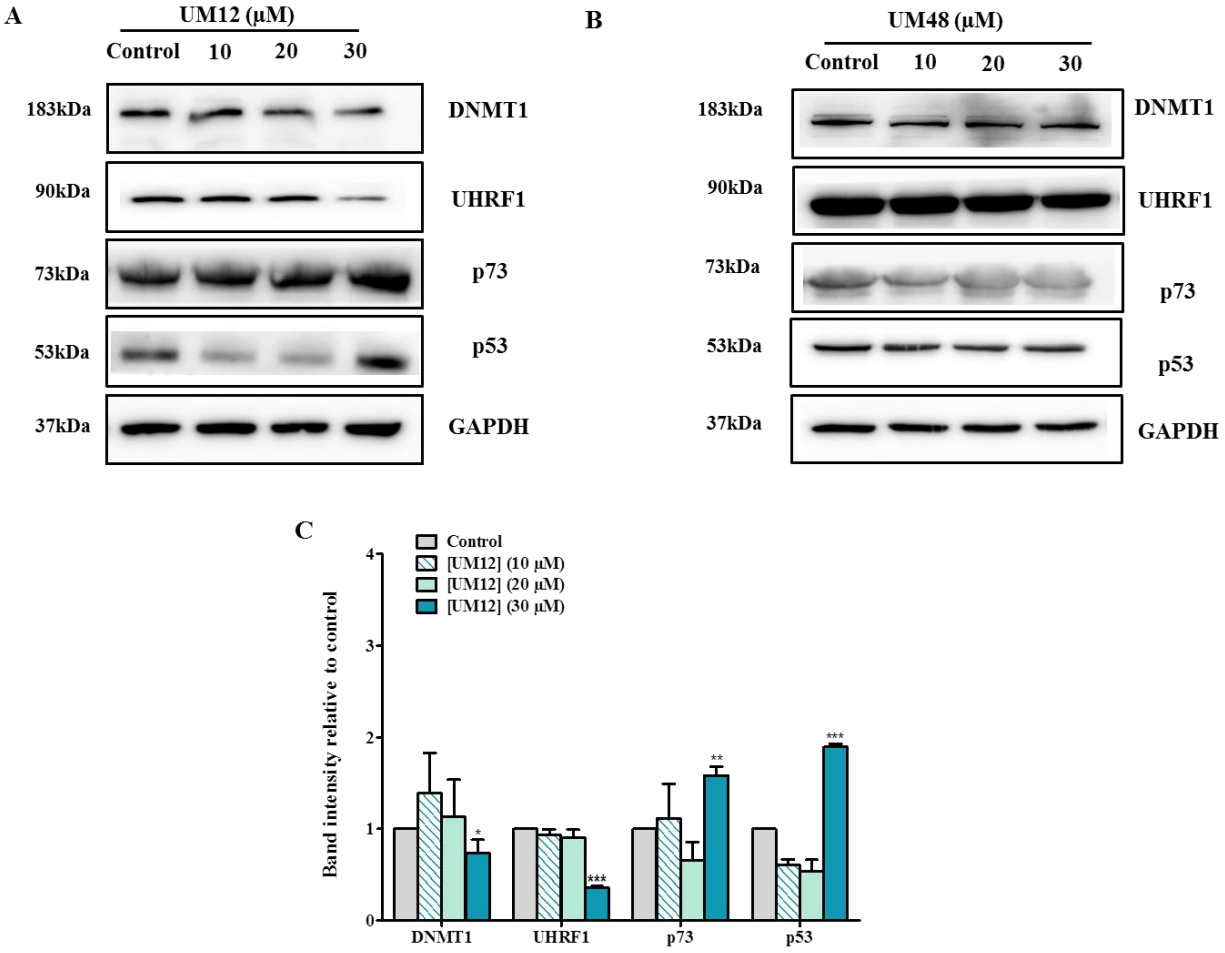

Figure 4. Concentration-dependent effects of the UM12 and UM48 on the expression levels of DNMT1/ UHRF1 and on tumor suppressors p53 and p73 in HeLa cells*. Cells were treated with UM12 and UM48 at the indicated concentrations and incubated for 24 h. (**A**) shows a representative western blot results after UM12 treatment (**B**) shows a representative western blot results after UM48 treatment (**C**) shows normalized signal for UM12 treatment. GAPDH was used for the normalization of the expression levels of the different proteins.*

4- Apoptosis analysis :

Given that inhibition of UHRF1 expression leads cancer cells to undergo apoptosis through the reactivation of the TSGs, we investigated whether UM12 induce an apoptotic response in HeLa cancer cells upon its activation of p53 and p73. As shown in (Fig. 4), UM12 increased the number of apoptotic cells in a concentration-dependent manner. At the highest tested concentration 60µM, UM12 showed a significant increase in apoptosis 38.3%. These findings suggest that the exposure of HeLa cancer cells to UM12 induces the occurrence of a p53 and p73-dependant apoptosis.

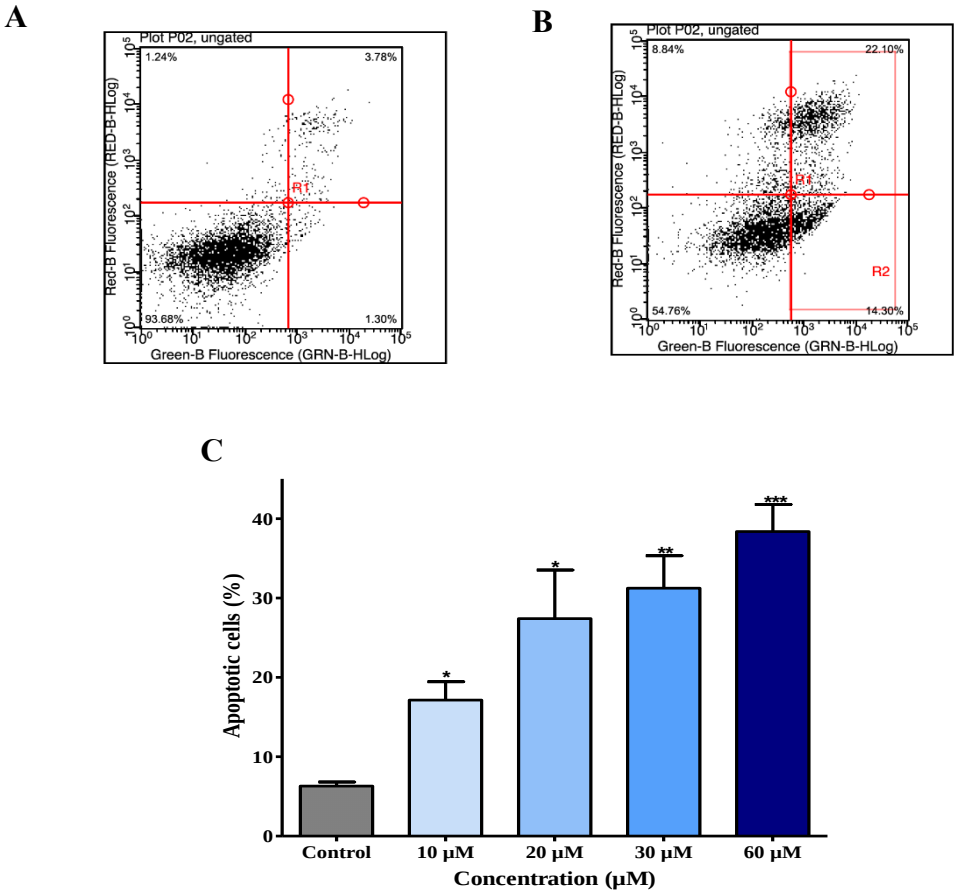

Figure 5. Concentration-dependent effect of UM12 on the apoptosis rate of HeLa cells. *(**A**) non treated samples (**B**) UM12 treated samples and (**C**) recapitulates the number of apoptotic cells after exposure to UM12, expressed as percent relative to the total cell number.*

5- Methylation assay by (IF):

We wanted to uncover whether the epigenetic alteration shown in our western blot results, is associated with an effect on genomic DNA methylation. Global DNA methylation was estimated by using immunofluorescence assay. As shown in (Fig. 5A and B) the global DNA methylation levels decreased to 60.5% with respect to untreated cells after a 24h treatment with UM12 while UM48 didn't show any significant decrease in methylation which is consistent with previous results of western blot where no change in DNMT1 or UHRF1 levels are detectable.

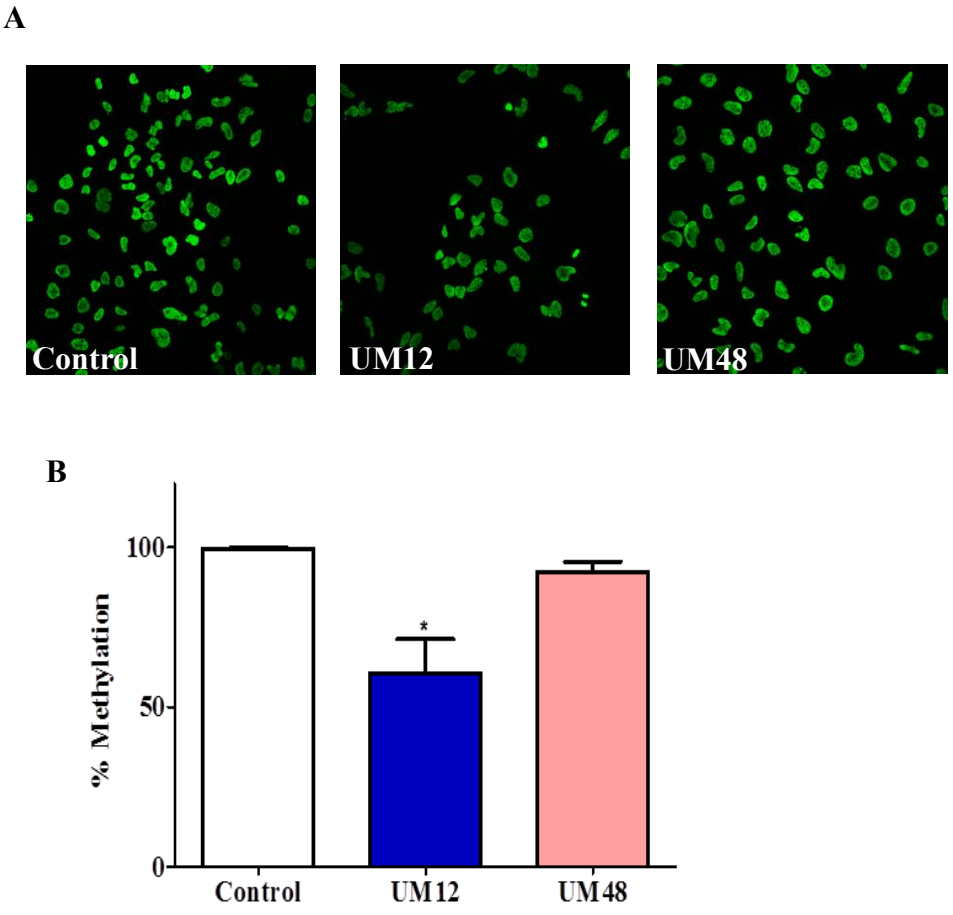

Figure 6. Effect of UM12 and UM48 on global DNA methylation in HeLa cells. *(**A**) Immunostaining analysis of 5-mC upon the treatment of HeLa cells with UM12 UM48. (**B**) The quantitative measurement of the mean intensity of fluorescence representing the 5-mC in genomic DNA.*

6- FLIM Analysis:

After transfection of HeLa cells with DNMT1-eGFP and UHRF1-mCherry, the interaction between DNMT1 and UHRF1 inside the nucleus was tested by the FLIM technique. The lifetime of the DNMT1-eGFP was 2.54 ± 0.005 ns in the cells transfected with DNMT1-eGFP alone. However the lifetime of eGFP was significantly reduced from 2.54 ± 0.005 to 2.19 ± 0.02 when DNMT1-eGFP was co-trasnsfected with UHRF1-mCherry (Fig.8A). This result was due to a FRET efficiency of 13.75 ± 0.8% (Fig. 7B). Next, cells were treated with UM12 to verify the effect of the molecules on the interaction. When cells were treated with UM12, the lifetime of the DNMT1-eGFP was 2.35±0.03 ns resulting in a FRET efficiency of 9.2 ±1.6% (Fig. 8A,B) indicating the occurrence of the interaction between the two proteins. These results clearly suggest that UM12 do not alter the interaction of UHRF1/DNMT1 complex.

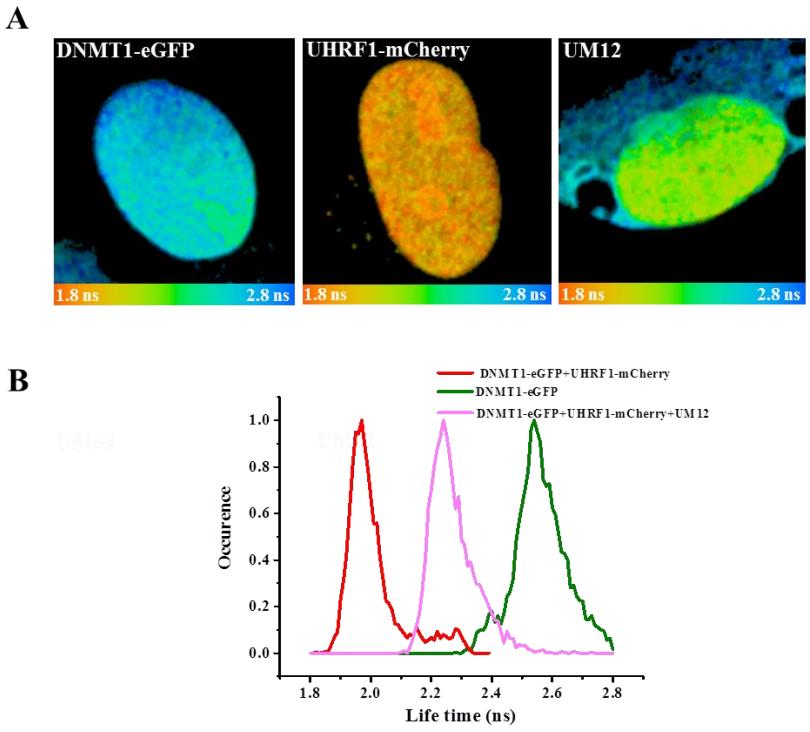

Figure 7. Effect of UM12 on DNMT1/UHRF1 interaction. *The interaction between DNMT1 and UHRF1 was assessed by FLIM. (**A**) 30µm x 30µm FLIM images for the HeLa cells transfected with DNMT1-eGFP or co-transfected with DNMT1-eGFP and UHRF1-mCherry in presence and in absence of UM12 treatment.The lifetime values are determined by using color coded images ranging from red (1.8 ns) to blue (2.8 ns). (**B**) The life time distribution curve of each sample.*

Summary:

Finally, UM12 and UM48 inhibit the proliferation of HeLa cells. Both compounds lead cancer cells to undergo apoptosis apparently through different pathways as UM12 induce the re-expression of p53 and p73 which can activate apoptotic pathway in cells. The decrease of DNA methylation along with DNMT1 and UHRF1 downregulation shows the potential of UM12 to target the DNA methylation maintenance machinery.

Conclusion and perspectives

UHRF1 is considered to be an essential player in the transmission of the epigenetic code. The structural diversity ensures to the protein a variety of tasks that bridges DNA methylation and histone modifications. However, UHRF1 coordinates these functions through the interaction with many proteins such as DNMT1, Tip60, USP7, and HDAC1. Altogether, these proteins constitute the members of a large macromolecular protein complex "epigenetic code replication machinery" (ECREM) that serves as a guardian of the epigenome [198, 237]. The implication of UHRF1 in cancerogenesis has been well recognized lately since UHRF1 is overexpressed in cancer cells and it promotes tumor by blocking the activity of TSGs thus inducing cell proliferation and escape from apoptosis. Taken together, UHRF1 deserves a plausible attention as therapeutic target.

UHRF1 can be targeted through its various domains: SRA domain which is responsible to bind hemimethylated DNA [96], the TTD domain that is able to bind the methylated histone H3K9 [238, 239], and the RING domain that has E3 ligase activity [240]. The identification of molecules that act on one of these parts can exhibit a pharmacological potential that can be used in therapeutical applications. In this context, the focus of our project was to target SRA domain of UHRF1 mainly for three criteria:

- The importance of this domain in inheritance of abnormal methylation marks.
- The availability of the crystallographic structure of SRA domain that opened the road to design molecules able to fit into its 5mC binding pocket.
- The presence of a fluorescent method that has been developed in our laboratory and allows to sensitively monitor the base flipping activity of SRA domain.

During my project, we tested 71 different compounds by two approaches, biophysical and biological one.

In our first approach, by utilizing fluorescence based tools, we mimic some major steps involved in transmission of DNA methylation including recognition of hemimethylated DNA by SRA domain of UHRF1, flipping of methylcystosine by SRA and later recruitment of DNMT1 by UHRF1 [98]. The key evaluation point was set by using the "base flipping assay" which is a novel test that allows us to have a dynamic picture of the SRA/DNA complex including the flipping of the mC, in presence of the molecules. It should be noted that this test is applied for the first time and the obtained results highlight the potential of this method to screen in the future for more small

molecules of UHRF1/SRA inhibitors. The limitation of this test was the absence of a positive control since till date there is no commercially available UHRF1/SRA inhibitor. The first active hit "UM63" from the second batch and the two other active ones "UM63B" and "UM63D" from the third batch inhibited the flipping of mC with an IC_{50} values in the micromolar range. However, among these hits, UM63 was the most interesting one and was further characterized.

During division, binding of SRA domain to hemimethylated DNA causes the flipping of methylcytosine which is considered to be a critical step for the recruitment of DNMT1 that is responsible for maintenance of DNA methylation. UM63 clearly interferes at this level and hinders SRA binding to DNA and flipping of the methylated cytosine. Moving further, with the help of SRA mutant G488D, we succeeded to demonstrate that UM63 binds to SRA in a specific manner at the level of the 5 methylcytosine binding pocket. Moreover, the biophysical aspects of the binding mode of UM63 with DNA were investigated where we provided the binding and thermodynamic parameters of the interaction. Additionally the displacement assay performed with the EtBr demonstrates that UM63 has an intercalative property, which correlates with its anthraquinone moiety. However, more work should be done for a robust validation and characterization.

Many anti-cancer compounds act by blocking the activity of DNA-interacting proteins, yet this mechanism remains a double edged sword, and its effect on cellular levels need to be explored and considered. Taken that UM63 is a DNA binder; the question that we addressed is whether UM63 inhibits the flipping through blocking SRA or through DNA binding? To answer this question, we performed experiments with an analog "UM63E" that is able to bind DNA with a comparable affinity to UM63/DNA binding. UM63E was unable to bind SRA domain and didn't show any response on the base flipping assay. Notably, UM63E structure has bulky side chain, which makes it difficult to fit into the binding cavity of SRA domain. This leads to a greater understanding of the MOA of UM63 by supporting the point that the property of binding DNA alone is not sufficient to hinder SRA/DNA interaction.

UHRF1 via its SRA domain is known to recruit DNMT1 for the methylation step, by interacting with its RFTS domain. Our work clearly shows that treatment with UM63 that blocks SRA domain of UHRF1 results in a defective UHRF1/DNMT1 interaction in HeLa cells. Collectively, the inhibition of different key processes related to DNA methylation by UM63, like binding of SRA to hemimethylated DNA, flipping of the methylcytosine and DNMT1/UHRF1 interaction explains the

UM63-induced global demethylation in treated HeLa cells. For further work, it would be interesting to explore if the demethylation is favored as a function of the treatment duration, since it is known that the methylation could be diluted after certain cell division.

Moving to the second approach in cultured cells, cervical carcinoma cells (HeLa) were chosen as a referential model in our experiments. Among the 71 molecules that were evaluated on HeLa cells viability for 24 h, three molecules "UM12", "UM48" and "UM63" exerted an impact on cell proliferation. UM48 quit the race at early steps with no effect on UHRF1/DNMT1 levels neither on methylation status in HeLa cells. On the other hand, UM12 exerted a global demethylating effect without affecting the DNMT1/UHRF1 interaction indicating that it could be involved in the inhibition of a different pathway.

Although using UM63 on various cell systems (HeLa, A375, Huh7, and fibroblasts), the anti-proliferative activity of UM63 varied in "cell line-dependent manner". UM63 inhibited the proliferation in HeLa, A375 and Huh7 cells with an IC_{50} in the micromolar range. The usage of multiple cell line systems and observing different effects propose to decipher more the characteristics of this molecule in order to question the factors (membrane permeability, selectivity, non-specific protein binding) that could affect the pharmacological activity of UM63. Time-dependent analysis can be included to track a long term impact of UM63 on cell proliferation and other cellular processes.

Whilst evidences describe that decreased UHRF1 expression by using natural compounds that target UHRF1 is linked to apoptosis induction, cell cycle arrest and reactivation of TSGs, our work shows that UM63 treatment reactivated the expression of p53, with a subsequent cell cycle arrest at G0/G1 phase and induced apoptosis through a caspase-3 pathway. It would be also valuable to check other TSGs since it is very well known that UHRF1 along with DNMT1 is able to deactivate the genes involved in tumor suppression.

Also, it can be interesting to push further the pharmacological investigations for UM63 in order to study its potential *in cellulo* as combination treatment with other anti-cancer therapies in an attempt to ameliorate the anti-cancer effects. The complementary functions of UHRF1 and DNMT1 suggest that a combination with DNMT inhibitors leads to a synergistic effect on tumor cells.

Starting from all the gathered results about UM63 and its mode of action, this could be a solid basis for future work that can serve to develop and improve the characteristics of next generation of UHRF1 inhibitors by performing a number of chemical modifications to the UM63 for the purpose of:

- Increasing the affinity for the SRA domain
- Enhancing the inhibitory effect on UHRF1
- Decreasing cytotoxicity, *i.e.*, by decreasing the binding affinity to nonspecific DNA sequences
- Helping to determine pharmacokinetic properties, for example by increasing the solubility in water and modulating the metabolic stability of the new compounds.

Finally, *in vitro* identification of new inhibitors of UHRF1 remains a big challenge, since it is hard to predict their effect on cells especially if inhibiting a functional domain could lead to undesirable events at other molecular levels. This work was satisfying for us since we identified a SRA inhibitor and for the first time we characterized broadly its mechanism of action *in vitro* and in cellular levels. For future directions, these findings could be used as groundwork in the discovery of UHRF1 inhibitors that can contribute in epigenetic-based cancer therapy.

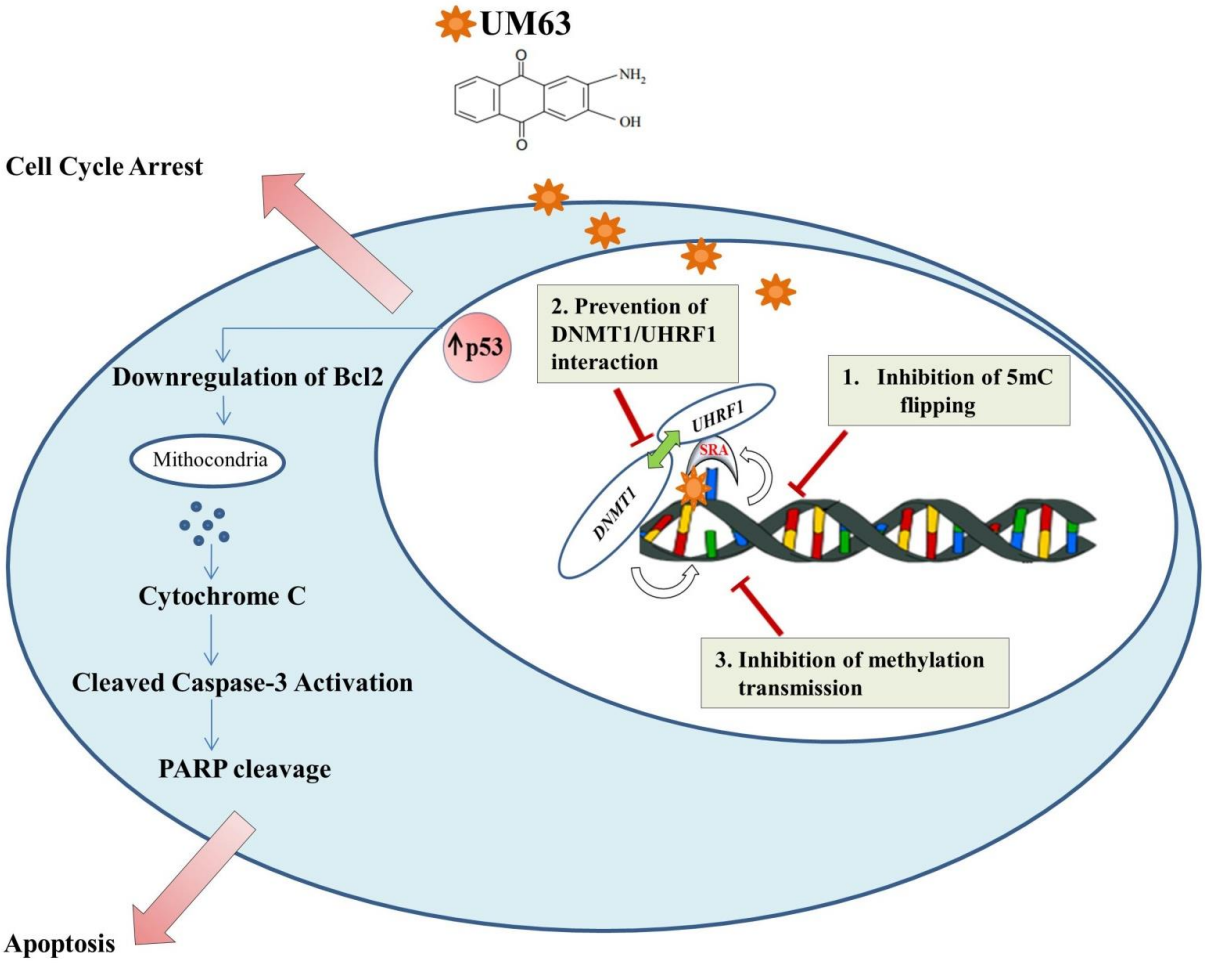

Schematic model summarizing the mechanism of action of UM63.

References

1. Bird A: **Perceptions of epigenetics**. *Nature* 2007, **447**(7143):396-398.

2. Esteller M: **Epigenetics in cancer**. *The New England journal of medicine* 2008, **358**(11):1148-1159.

3. Luger K, Mader AW, Richmond RK, Sargent DF, Richmond TJ: **Crystal structure of the nucleosome core particle at 2.8 A resolution**. *Nature* 1997, **389**(6648):251-260.

4. Woodcock CL, Ghosh RP: **Chromatin higher-order structure and dynamics**. *Cold Spring Harbor perspectives in biology* 2010, **2**(5):a000596.

5. Trojer P, Reinberg D: **Facultative heterochromatin: is there a distinctive molecular signature?** *Molecular cell* 2007, **28**(1):1-13.

6. Jurkowska RZ, Jurkowski TP, Jeltsch A: **Structure and function of mammalian DNA methyltransferases**. *Chembiochem : a European journal of chemical biology* 2011, **12**(2):206-222.

7. Bird A: **DNA methylation patterns and epigenetic memory**. *Genes & development* 2002, **16**(1):6-21.

8. Li E: **Chromatin modification and epigenetic reprogramming in mammalian development**. *Nature reviews Genetics* 2002, **3**(9):662-673.

9. Ehrlich M: **Expression of various genes is controlled by DNA methylation during mammalian development**. *Journal of cellular biochemistry* 2003, **88**(5):899-910.

10. Okamoto I, Otte AP, Allis CD, Reinberg D, Heard E: **Epigenetic dynamics of imprinted X inactivation during early mouse development**. *Science* 2004, **303**(5658):644-649.

11. Murphy SK, Jirtle RL: **Imprinting evolution and the price of silence**. *BioEssays : news and reviews in molecular, cellular and developmental biology* 2003, **25**(6):577-588.

12. Fitzpatrick DR, Wilson CB: **Methylation and demethylation in the regulation of genes, cells, and responses in the immune system**. *Clinical immunology* 2003, **109**(1):37-45.

13. Reik W: **Stability and flexibility of epigenetic gene regulation in mammalian development**. *Nature* 2007, **447**(7143):425-432.

14. Yoder JA, Soman NS, Verdine GL, Bestor TH: **DNA (cytosine-5)-methyltransferases in mouse cells and tissues. Studies with a mechanism-based probe**. *Journal of molecular biology* 1997, **270**(3):385-395.

15. Feinberg AP: **Phenotypic plasticity and the epigenetics of human disease**. *Nature* 2007, **447**(7143):433-440.

16. Robertson KD: **DNA methylation and human disease**. *Nature reviews Genetics* 2005, **6**(8):597-610.

17. Feinberg AP, Tycko B: **The history of cancer epigenetics**. *Nature reviews Cancer* 2004, **4**(2):143-153.

18. Richardson B: **Impact of aging on DNA methylation**. *Ageing research reviews* 2003, **2**(3):245-261.

19. Sharma S, Kelly TK, Jones PA: **Epigenetics in cancer**. *Carcinogenesis* 2010, **31**(1):27-36.

20. Garzon R, Fabbri M, Cimmino A, Calin GA, Croce CM: **MicroRNA expression and function in cancer**. *Trends in molecular medicine* 2006, **12**(12):580-587.

21. Morita S, Horii T, Kimura M, Ochiya T, Tajima S, Hatada I: **miR-29 represses the activities of DNA methyltransferases and DNA demethylases**. *International journal of molecular sciences* 2013, **14**(7):14647-14658.

22. Varambally S, Cao Q, Mani RS, Shankar S, Wang X, Ateeq B, Laxman B, Cao X, Jing X, Ramnarayanan K *et al*: **Genomic loss of microRNA-101 leads to overexpression of histone methyltransferase EZH2 in cancer**. *Science* 2008, **322**(5908):1695-1699.

23. Chen JF, Mandel EM, Thomson JM, Wu Q, Callis TE, Hammond SM, Conlon FL, Wang DZ: **The role of microRNA-1 and microRNA-133 in skeletal muscle proliferation and differentiation**. *Nature genetics* 2006, **38**(2):228-233.

24. Noonan EJ, Place RF, Pookot D, Basak S, Whitson JM, Hirata H, Giardina C, Dahiya R: **miR-449a targets HDAC-1 and induces growth arrest in prostate cancer**. *Oncogene* 2009, **28**(14):1714-1724.

25. Ramakrishnan V: **Histone structure and the organization of the nucleosome**. *Annual review of biophysics and biomolecular structure* 1997, **26**:83-112.

26. Kouzarides T: **Chromatin modifications and their function**. *Cell* 2007, **128**(4):693-705.

27. Biswas S, Rao CM: **Epigenetics in cancer: Fundamentals and Beyond**. *Pharmacology & therapeutics* 2017, **173**:118-134.

28. Xu Y, Zhang S, Lin S, Guo Y, Deng W, Zhang Y, Xue Y: **WERAM: a database of writers, erasers and readers of histone acetylation and methylation in eukaryotes**. *Nucleic acids research* 2017, **45**(D1):D264-D270.

29. Liang G, Lin JC, Wei V, Yoo C, Cheng JC, Nguyen CT, Weisenberger DJ, Egger G, Takai D, Gonzales FA *et al*: **Distinct localization of histone H3 acetylation and H3-K4 methylation to the transcription start sites in the human genome**. *Proceedings of the National Academy of Sciences of the United States of America* 2004, **101**(19):7357-7362.

30. Hebbes TR, Thorne AW, Crane-Robinson C: **A direct link between core histone acetylation and transcriptionally active chromatin**. *The EMBO journal* 1988, **7**(5):1395-1402.

31. Shahbazian MD, Grunstein M: **Functions of site-specific histone acetylation and deacetylation**. *Annual review of biochemistry* 2007, **76**:75-100.

32. Lehnertz B, Ueda Y, Derijck AA, Braunschweig U, Perez-Burgos L, Kubicek S, Chen T, Li E, Jenuwein T, Peters AH: **Suv39h-mediated histone H3 lysine 9 methylation directs DNA methylation to major satellite repeats at pericentric heterochromatin**. *Current biology : CB* 2003, **13**(14):1192-1200.

33. Tachibana M, Matsumura Y, Fukuda M, Kimura H, Shinkai Y: **G9a/GLP complexes independently mediate H3K9 and DNA methylation to silence transcription**. *The EMBO journal* 2008, **27**(20):2681-2690.

34. Zhao Q, Rank G, Tan YT, Li H, Moritz RL, Simpson RJ, Cerruti L, Curtis DJ, Patel DJ, Allis CD *et al*: **PRMT5-mediated methylation of histone H4R3 recruits DNMT3A, coupling histone and DNA methylation in gene silencing**. *Nature structural & molecular biology* 2009, **16**(3):304-311.

35. Wang J, Hevi S, Kurash JK, Lei H, Gay F, Bajko J, Su H, Sun W, Chang H, Xu G *et al*: **The lysine demethylase LSD1 (KDM1) is required for maintenance of global DNA methylation**. *Nature genetics* 2009, **41**(1):125-129.

36. Esteve PO, Chin HG, Benner J, Feehery GR, Samaranayake M, Horwitz GA, Jacobsen SE, Pradhan S: **Regulation of DNMT1 stability through SET7-mediated lysine methylation in mammalian cells**. *Proceedings of the National Academy of Sciences of the United States of America* 2009, **106**(13):5076-5081.

37. Izzo A, Schneider R: **Chatting histone modifications in mammals**. *Briefings in functional genomics* 2010, **9**(5-6):429-443.

38. Takai D, Jones PA: **Comprehensive analysis of CpG islands in human chromosomes 21 and 22**. *Proceedings of the National Academy of Sciences of the United States of America* 2002, **99**(6):3740-3745.

39. Wang Y, Leung FC: **An evaluation of new criteria for CpG islands in the human genome as gene markers**. *Bioinformatics* 2004, **20**(7):1170-1177.

40. Illingworth RS, Bird AP: **CpG islands--'a rough guide'**. *FEBS letters* 2009, **583**(11):1713-1720.

41. Wade PA: **Methyl CpG-binding proteins and transcriptional repression**. *BioEssays : news and reviews in molecular, cellular and developmental biology* 2001, **23**(12):1131-1137.

42. Watt F, Molloy PL: **Cytosine methylation prevents binding to DNA of a HeLa cell transcription factor required for optimal expression of the adenovirus major late promoter**. *Genes & development* 1988, **2**(9):1136-1143.

43. Santoro R, Grummt I: **Molecular mechanisms mediating methylation-dependent silencing of ribosomal gene transcription**. *Molecular cell* 2001, **8**(3):719-725.

44. Jeltsch A: **On the enzymatic properties of Dnmt1: specificity, processivity, mechanism of linear diffusion and allosteric regulation of the enzyme**. *Epigenetics* 2006, **1**(2):63-66.

45. Jurkowska RZ, Jeltsch A: **Enzymology of Mammalian DNA Methyltransferases**. *Advances in experimental medicine and biology* 2016, **945**:87-122.

46. Rondelet G, Wouters J: **Human DNA (cytosine-5)-methyltransferases: A functional and structural perspective for epigenetic cancer therapy**. *Biochimie* 2017.

47. Song J, Teplova M, Ishibe-Murakami S, Patel DJ: **Structure-based mechanistic insights into DNMT1-mediated maintenance DNA methylation**. *Science* 2012, **335**(6069):709-712.

48. Jeltsch A: **Beyond Watson and Crick: DNA methylation and molecular enzymology of DNA methyltransferases**. *Chembiochem : a European journal of chemical biology* 2002, **3**(4):274-293.

49. Leonhardt H, Page AW, Weier HU, Bestor TH: **A targeting sequence directs DNA methyltransferase to sites of DNA replication in mammalian nuclei**. *Cell* 1992, **71**(5):865-873.

50. Fatemi M, Hermann A, Pradhan S, Jeltsch A: **The activity of the murine DNA methyltransferase Dnmt1 is controlled by interaction of the catalytic domain with the N-terminal part of the enzyme leading to an allosteric activation of the enzyme after binding to methylated DNA**. *Journal of molecular biology* 2001, **309**(5):1189-1199.

51. Li E, Bestor TH, Jaenisch R: **Targeted mutation of the DNA methyltransferase gene results in embryonic lethality**. *Cell* 1992, **69**(6):915-926.

52. Jeltsch A, Jurkowska RZ: **Allosteric control of mammalian DNA methyltransferases - a new regulatory paradigm**. *Nucleic acids research* 2016, **44**(18):8556-8575.

53. Ding F, Chaillet JR: **In vivo stabilization of the Dnmt1 (cytosine-5)- methyltransferase protein**. *Proceedings of the National Academy of Sciences of the United States of America* 2002, **99**(23):14861-14866.

54. Chuang LS, Ian HI, Koh TW, Ng HH, Xu G, Li BF: **Human DNA-(cytosine-5) methyltransferase-PCNA complex as a target for p21WAF1**. *Science* 1997, **277**(5334):1996-2000.

55. Egger G, Jeong S, Escobar SG, Cortez CC, Li TW, Saito Y, Yoo CB, Jones PA, Liang G: **Identification of DNMT1 (DNA methyltransferase 1) hypomorphs in somatic knockouts suggests an essential role for DNMT1 in cell survival**. *Proceedings of the National Academy of Sciences of the United States of America* 2006, **103**(38):14080-14085.

56. Easwaran HP, Schermelleh L, Leonhardt H, Cardoso MC: **Replication-independent chromatin loading of Dnmt1 during G2 and M phases**. *EMBO reports* 2004, **5**(12):1181-1186.

57. Bashtrykov P, Jankevicius G, Jurkowska RZ, Ragozin S, Jeltsch A: **The UHRF1 protein stimulates the activity and specificity of the maintenance DNA methyltransferase DNMT1 by an allosteric mechanism**. *The Journal of biological chemistry* 2014, **289**(7):4106-4115.

58. Berkyurek AC, Suetake I, Arita K, Takeshita K, Nakagawa A, Shirakawa M, Tajima S: **The DNA methyltransferase Dnmt1 directly interacts with the SET and RING finger-associated (SRA) domain of the multifunctional protein Uhrf1 to facilitate accession of the catalytic center to hemi-methylated DNA**. *The Journal of biological chemistry* 2014, **289**(1):379-386.

59. Bashtrykov P, Jankevicius G, Smarandache A, Jurkowska RZ, Ragozin S, Jeltsch A: **Specificity of Dnmt1 for methylation of hemimethylated CpG sites resides in its catalytic domain**. *Chemistry & biology* 2012, **19**(5):572-578.

60. Robertson KD, Uzvolgyi E, Liang G, Talmadge C, Sumegi J, Gonzales FA, Jones PA: **The human DNA methyltransferases (DNMTs) 1, 3a and 3b: coordinate mRNA expression in normal tissues and overexpression in tumors**. *Nucleic acids research* 1999, **27**(11):2291-2298.

61. Szyf M, Bozovic V, Tanigawa G: **Growth regulation of mouse DNA methyltransferase gene expression**. *The Journal of biological chemistry* 1991, **266**(16):10027-10030.

62. Bigey P, Ramchandani S, Theberge J, Araujo FD, Szyf M: **Transcriptional regulation of the human DNA Methyltransferase (dnmt1) gene**. *Gene* 2000, **242**(1-2):407-418.

63. Jung JK, Arora P, Pagano JS, Jang KL: **Expression of DNA methyltransferase 1 is activated by hepatitis B virus X protein via a regulatory circuit involving the p16INK4a-cyclin D1-CDK 4/6-pRb-E2F1 pathway**. *Cancer research* 2007, **67**(12):5771-5778.

64. Hermann A, Goyal R, Jeltsch A: **The Dnmt1 DNA-(cytosine-C5)-methyltransferase methylates DNA processively with high preference for hemimethylated target sites**. *The Journal of biological chemistry* 2004, **279**(46):48350-48359.

65. Song J, Rechkoblit O, Bestor TH, Patel DJ: **Structure of DNMT1-DNA complex reveals a role for autoinhibition in maintenance DNA methylation**. *Science* 2011, **331**(6020):1036-1040.

66. Nicolas P.F Barthes BYM, Janah Shaya , Nadine Martinet, Alain Burget: **Génétique et épigenetique Un code au-dessus du code !** *L'actualité chimique* 2016, **412**.

67. Takeshita K, Suetake I, Yamashita E, Suga M, Narita H, Nakagawa A, Tajima S: **Structural insight into maintenance methylation by mouse DNA methyltransferase 1 (Dnmt1)**.

Proceedings of the National Academy of Sciences of the United States of America 2011, **108**(22):9055-9059.

68. Schermelleh L, Haemmer A, Spada F, Rosing N, Meilinger D, Rothbauer U, Cardoso MC, Leonhardt H: **Dynamics of Dnmt1 interaction with the replication machinery and its role in postreplicative maintenance of DNA methylation**. *Nucleic acids research* 2007, **35**(13):4301-4312.

69. Hermann A, Schmitt S, Jeltsch A: **The human Dnmt2 has residual DNA-(cytosine-C5) methyltransferase activity**. *The Journal of biological chemistry* 2003, **278**(34):31717-31721.

70. Okano M, Xie S, Li E: **Dnmt2 is not required for de novo and maintenance methylation of viral DNA in embryonic stem cells**. *Nucleic acids research* 1998, **26**(11):2536-2540.

71. Jones PA, Liang G: **Rethinking how DNA methylation patterns are maintained**. *Nature reviews Genetics* 2009, **10**(11):805-811.

72. Sykes M, Szot GL, Swenson K, Pearson DA, Wekerle T: **Separate regulation of peripheral hematopoietic and thymic engraftment**. *Experimental hematology* 1998, **26**(6):457-465.

73. Kim GD, Ni J, Kelesoglu N, Roberts RJ, Pradhan S: **Co-operation and communication between the human maintenance and de novo DNA (cytosine-5) methyltransferases**. *The EMBO journal* 2002, **21**(15):4183-4195.

74. Okano M, Bell DW, Haber DA, Li E: **DNA methyltransferases Dnmt3a and Dnmt3b are essential for de novo methylation and mammalian development**. *Cell* 1999, **99**(3):247-257.

75. Kohli RM, Zhang Y: **TET enzymes, TDG and the dynamics of DNA demethylation**. *Nature* 2013, **502**(7472):472-479.

76. Parry L, Clarke AR: **The Roles of the Methyl-CpG Binding Proteins in Cancer**. *Genes & cancer* 2011, **2**(6):618-630.

77. Buck-Koehntop BA, Defossez PA: **On how mammalian transcription factors recognize methylated DNA**. *Epigenetics* 2013, **8**(2):131-137.

78. Rottach A, Leonhardt H, Spada F: **DNA methylation-mediated epigenetic control**. *Journal of cellular biochemistry* 2009, **108**(1):43-51.

79. Mazzio EA, Soliman KF: **Basic concepts of epigenetics: impact of environmental signals on gene expression**. *Epigenetics* 2012, **7**(2):119-130.

80. Bronner C, Achour M, Arima Y, Chataigneau T, Saya H, Schini-Kerth VB: **The UHRF family: oncogenes that are drugable targets for cancer therapy in the near future?** *Pharmacology & therapeutics* 2007, **115**(3):419-434.

81. Hopfner R, Mousli M, Jeltsch JM, Voulgaris A, Lutz Y, Marin C, Bellocq JP, Oudet P, Bronner C: **ICBP90, a novel human CCAAT binding protein, involved in the regulation of topoisomerase IIalpha expression**. *Cancer research* 2000, **60**(1):121-128.

82. Hopfner R, Mousli M, Garnier JM, Redon R, du Manoir S, Chatton B, Ghyselinck N, Oudet P, Bronner C: **Genomic structure and chromosomal mapping of the gene coding for ICBP90, a protein involved in the regulation of the topoisomerase IIalpha gene expression**. *Gene* 2001, **266**(1-2):15-23.

83. Unoki M, Bronner C, Mousli M: **A concern regarding the current confusion with the human homolog of mouse Np95, ICBP90/UHRF1**. *Radiation research* 2008, **169**(2):240-244.

84. Mori T, Ikeda DD, Yamaguchi Y, Unoki M, Project N: **NIRF/UHRF2 occupies a central position in the cell cycle network and allows coupling with the epigenetic landscape**. *FEBS letters* 2012, **586**(11):1570-1583.

85. Pichler G, Wolf P, Schmidt CS, Meilinger D, Schneider K, Frauer C, Fellinger K, Rottach A, Leonhardt H: **Cooperative DNA and histone binding by Uhrf2 links the two major repressive epigenetic pathways**. *Journal of cellular biochemistry* 2011, **112**(9):2585-2593.

86. Li Y, Mori T, Hata H, Homma Y, Kochi H: **NIRF induces G1 arrest and associates with Cdk2**. *Biochemical and biophysical research communications* 2004, **319**(2):464-468.

87. Mori T, Ikeda DD, Fukushima T, Takenoshita S, Kochi H: **NIRF constitutes a nodal point in the cell cycle network and is a candidate tumor suppressor**. *Cell cycle* 2011, **10**(19):3284-3299.

88. Zhou T, Xiong J, Wang M, Yang N, Wong J, Zhu B, Xu RM: **Structural basis for hydroxymethylcytosine recognition by the SRA domain of UHRF2**. *Molecular cell* 2014, **54**(5):879-886.

89. Zhang J, Gao Q, Li P, Liu X, Jia Y, Wu W, Li J, Dong S, Koseki H, Wong J: **S phase-dependent interaction with DNMT1 dictates the role of UHRF1 but not UHRF2 in DNA methylation maintenance**. *Cell research* 2011, **21**(12):1723-1739.

90. Lu R, Wang GG: **Tudor: a versatile family of histone methylation 'readers'**. *Trends in biochemical sciences* 2013, **38**(11):546-555.

91. Tauber M, Fischle W: **Conserved linker regions and their regulation determine multiple chromatin-binding modes of UHRF1**. *Nucleus* 2015, **6**(2):123-132.

92. Rajakumara E, Wang Z, Ma H, Hu L, Chen H, Lin Y, Guo R, Wu F, Li H, Lan F *et al*: **PHD finger recognition of unmodified histone H3R2 links UHRF1 to regulation of euchromatic gene expression**. *Molecular cell* 2011, **43**(2):275-284.

93. Lallous N, Legrand P, McEwen AG, Ramon-Maiques S, Samama JP, Birck C: **The PHD finger of human UHRF1 reveals a new subgroup of unmethylated histone H3 tail readers**. *PloS one* 2011, **6**(11):e27599.

94. Nishiyama A, Yamaguchi L, Sharif J, Johmura Y, Kawamura T, Nakanishi K, Shimamura S, Arita K, Kodama T, Ishikawa F *et al*: **Uhrf1-dependent H3K23 ubiquitylation couples maintenance DNA methylation and replication**. *Nature* 2013, **502**(7470):249-253.

95. Qin W, Wolf P, Liu N, Link S, Smets M, La Mastra F, Forne I, Pichler G, Horl D, Fellinger K *et al*: **DNA methylation requires a DNMT1 ubiquitin interacting motif (UIM) and histone ubiquitination**. *Cell research* 2015, **25**(8):911-929.

96. Hashimoto H, Horton JR, Zhang X, Bostick M, Jacobsen SE, Cheng X: **The SRA domain of UHRF1 flips 5-methylcytosine out of the DNA helix**. *Nature* 2008, **455**(7214):826-829.

97. Arita K, Ariyoshi M, Tochio H, Nakamura Y, Shirakawa M: **Recognition of hemi-methylated DNA by the SRA protein UHRF1 by a base-flipping mechanism**. *Nature* 2008, **455**(7214):818-821.

98. Avvakumov GV, Walker JR, Xue S, Li Y, Duan S, Bronner C, Arrowsmith CH, Dhe-Paganon S: **Structural basis for recognition of hemi-methylated DNA by the SRA domain of human UHRF1**. *Nature* 2008, **455**(7214):822-825.

99. Felle M, Joppien S, Nemeth A, Diermeier S, Thalhammer V, Dobner T, Kremmer E, Kappler R, Langst G: **The USP7/Dnmt1 complex stimulates the DNA methylation activity of Dnmt1 and regulates the stability of UHRF1**. *Nucleic acids research* 2011, **39**(19):8355-8365.

100. Unoki M, Nishidate T, Nakamura Y: **ICBP90, an E2F-1 target, recruits HDAC1 and binds to methyl-CpG through its SRA domain**. *Oncogene* 2004, **23**(46):7601-7610.

101. Kim JK, Esteve PO, Jacobsen SE, Pradhan S: **UHRF1 binds G9a and participates in p21 transcriptional regulation in mammalian cells**. *Nucleic acids research* 2009, **37**(2):493-505.

102. Roberts RJ, Cheng X: **Base flipping**. *Annual review of biochemistry* 1998, **67**:181-198.

103. Kriaucionis S, Heintz N: **The nuclear DNA base 5-hydroxymethylcytosine is present in Purkinje neurons and the brain**. *Science* 2009, **324**(5929):929-930.

104. Tahiliani M, Koh KP, Shen Y, Pastor WA, Bandukwala H, Brudno Y, Agarwal S, Iyer LM, Liu DR, Aravind L *et al*: **Conversion of 5-methylcytosine to 5-hydroxymethylcytosine in mammalian DNA by MLL partner TET1**. *Science* 2009, **324**(5929):930-935.

105. Frauer C, Hoffmann T, Bultmann S, Casa V, Cardoso MC, Antes I, Leonhardt H: **Recognition of 5-hydroxymethylcytosine by the Uhrf1 SRA domain**. *PloS one* 2011, **6**(6):e21306.

106. Bostick M, Kim JK, Esteve PO, Clark A, Pradhan S, Jacobsen SE: **UHRF1 plays a role in maintaining DNA methylation in mammalian cells**. *Science* 2007, **317**(5845):1760-1764.

107. Sharif J, Muto M, Takebayashi S, Suetake I, Iwamatsu A, Endo TA, Shinga J, Mizutani-Koseki Y, Toyoda T, Okamura K *et al*: **The SRA protein Np95 mediates epigenetic inheritance by recruiting Dnmt1 to methylated DNA**. *Nature* 2007, **450**(7171):908-912.

108. Nady N, Lemak A, Walker JR, Avvakumov GV, Kareta MS, Achour M, Xue S, Duan S, Allali-Hassani A, Zuo X *et al*: **Recognition of multivalent histone states associated with heterochromatin by UHRF1 protein**. *The Journal of biological chemistry* 2011, **286**(27):24300-24311.

109. Rothbart SB, Krajewski K, Nady N, Tempel W, Xue S, Badeaux AI, Barsyte-Lovejoy D, Martinez JY, Bedford MT, Fuchs SM *et al*: **Association of UHRF1 with methylated H3K9 directs the maintenance of DNA methylation**. *Nature structural & molecular biology* 2012, **19**(11):1155-1160.

110. Wang C, Shen J, Yang Z, Chen P, Zhao B, Hu W, Lan W, Tong X, Wu H, Li G *et al*: **Structural basis for site-specific reading of unmodified R2 of histone H3 tail by UHRF1 PHD finger**. *Cell research* 2011, **21**(9):1379-1382.

111. Hu L, Li Z, Wang P, Lin Y, Xu Y: **Crystal structure of PHD domain of UHRF1 and insights into recognition of unmodified histone H3 arginine residue 2**. *Cell research* 2011, **21**(9):1374-1378.

112. von Meyenn F, Iurlaro M, Habibi E, Liu NQ, Salehzadeh-Yazdi A, Santos F, Petrini E, Milagre I, Yu M, Xie Z *et al*: **Impairment of DNA Methylation Maintenance Is the Main Cause of Global Demethylation in Naive Embryonic Stem Cells**. *Molecular cell* 2016, **62**(6):848-861.

113. Fang J, Cheng J, Wang J, Zhang Q, Liu M, Gong R, Wang P, Zhang X, Feng Y, Lan W *et al*: **Hemi-methylated DNA opens a closed conformation of UHRF1 to facilitate its histone recognition**. *Nature communications* 2016, **7**:11197.

114. Gelato KA, Tauber M, Ong MS, Winter S, Hiragami-Hamada K, Sindlinger J, Lemak A, Bultsma Y, Houliston S, Schwarzer D *et al*: **Accessibility of different histone H3-binding domains of UHRF1 is allosterically regulated by phosphatidylinositol 5-phosphate**. *Molecular cell* 2014, **54**(6):905-919.

115. Zhang ZM, Rothbart SB, Allison DF, Cai Q, Harrison JS, Li L, Wang Y, Strahl BD, Wang GG, Song J: **An Allosteric Interaction Links USP7 to Deubiquitination and Chromatin Targeting of UHRF1**. *Cell reports* 2015, **12**(9):1400-1406.

116. Karagianni P, Amazit L, Qin J, Wong J: **ICBP90, a novel methyl K9 H3 binding protein linking protein ubiquitination with heterochromatin formation**. *Molecular and cellular biology* 2008, **28**(2):705-717.

117. Geng Y, Gao Y, Ju H, Yan F: **Diagnostic and prognostic value of plasma and tissue ubiquitin-like, containing PHD and RING finger domains 1 in breast cancer patients**. *Cancer science* 2013, **104**(2):194-199.

118. Qin W, Leonhardt H, Spada F: **Usp7 and Uhrf1 control ubiquitination and stability of the maintenance DNA methyltransferase Dnmt1**. *Journal of cellular biochemistry* 2011, **112**(2):439-444.

119. Bronner C: **Control of DNMT1 abundance in epigenetic inheritance by acetylation, ubiquitylation, and the histone code**. *Science signaling* 2011, **4**(157):pe3.

120. Du Z, Song J, Wang Y, Zhao Y, Guda K, Yang S, Kao HY, Xu Y, Willis J, Markowitz SD *et al*: **DNMT1 stability is regulated by proteins coordinating deubiquitination and acetylation-driven ubiquitination**. *Science signaling* 2010, **3**(146):ra80.

121. Ma H, Chen H, Guo X, Wang Z, Sowa ME, Zheng L, Hu S, Zeng P, Guo R, Diao J *et al*: **M phase phosphorylation of the epigenetic regulator UHRF1 regulates its physical association with the deubiquitylase USP7 and stability**. *Proceedings of the National Academy of Sciences of the United States of America* 2012, **109**(13):4828-4833.

122. Liang D, Xue H, Yu Y, Lv F, You W, Zhang B: **Elevated expression of UHRF1 predicts unfavorable prognosis for patients with hepatocellular carcinoma**. *International journal of clinical and experimental pathology* 2015, **8**(8):9416-9421.

123. Lawley PD, Phillips DH: **DNA adducts from chemotherapeutic agents**. *Mutation research* 1996, **355**(1-2):13-40.

124. Muto M, Kanari Y, Kubo E, Takabe T, Kurihara T, Fujimori A, Tatsumi K: **Targeted disruption of Np95 gene renders murine embryonic stem cells hypersensitive to DNA damaging agents and DNA replication blocks**. *The Journal of biological chemistry* 2002, **277**(37):34549-34555.

125. Mistry H, Gibson L, Yun JW, Sarras H, Tamblyn L, McPherson JP: **Interplay between Np95 and Eme1 in the DNA damage response**. *Biochemical and biophysical research communications* 2008, **375**(3):321-325.

126. Liang CC, Zhan B, Yoshikawa Y, Haas W, Gygi SP, Cohn MA: **UHRF1 is a sensor for DNA interstrand crosslinks and recruits FANCD2 to initiate the Fanconi anemia pathway**. *Cell reports* 2015, **10**(12):1947-1956.

127. Tian Y, Paramasivam M, Ghosal G, Chen D, Shen X, Huang Y, Akhter S, Legerski R, Chen J, Seidman MM *et al*: **UHRF1 contributes to DNA damage repair as a lesion recognition factor and nuclease scaffold**. *Cell reports* 2015, **10**(12):1957-1966.

128. Jeanblanc M, Mousli M, Hopfner R, Bathami K, Martinet N, Abbady AQ, Siffert JC, Mathieu E, Muller CD, Bronner C: **The retinoblastoma gene and its product are targeted by ICBP90: a key mechanism in the G1/S transition during the cell cycle**. *Oncogene* 2005, **24**(49):7337-7345.

129. Mousli M, Hopfner R, Abbady AQ, Monte D, Jeanblanc M, Oudet P, Louis B, Bronner C: **ICBP90 belongs to a new family of proteins with an expression that is deregulated in cancer cells**. *British journal of cancer* 2003, **89**(1):120-127.

130. Zhou L, Zhao X, Han Y, Lu Y, Shang Y, Liu C, Li T, Jin Z, Fan D, Wu K: **Regulation of UHRF1 by miR-146a/b modulates gastric cancer invasion and metastasis**. *FASEB journal : official publication of the Federation of American Societies for Experimental Biology* 2013, **27**(12):4929-4939.

131. Wang F, Yang YZ, Shi CZ, Zhang P, Moyer MP, Zhang HZ, Zou Y, Qin HL: **UHRF1 promotes cell growth and metastasis through repression of p16(ink(4)a) in colorectal cancer**. *Annals of surgical oncology* 2012, **19**(8):2753-2762.

132. Qin Y, Wang J, Gong W, Zhang M, Tang Z, Zhang J, Quan Z: **UHRF1 depletion suppresses growth of gallbladder cancer cells through induction of apoptosis and cell cycle arrest**. *Oncology reports* 2014, **31**(6):2635-2643.

133. Yang GL, Zhang LH, Bo JJ, Chen HG, Cao M, Liu DM, Huang YR: **UHRF1 is associated with tumor recurrence in non-muscle-invasive bladder cancer**. *Medical oncology* 2012, **29**(2):842-847.

134. Babbio F, Pistore C, Curti L, Castiglioni I, Kunderfranco P, Brino L, Oudet P, Seiler R, Thalman GN, Roggero E *et al*: **The SRA protein UHRF1 promotes epigenetic crosstalks and is involved in prostate cancer progression**. *Oncogene* 2012, **31**(46):4878-4887.

135. Daskalos A, Oleksiewicz U, Filia A, Nikolaidis G, Xinarianos G, Gosney JR, Malliri A, Field JK, Liloglou T: **UHRF1-mediated tumor suppressor gene inactivation in nonsmall cell lung cancer**. *Cancer* 2011, **117**(5):1027-1037.

136. Pi JT, Lin Y, Quan Q, Chen LL, Jiang LZ, Chi W, Chen HY: **Overexpression of UHRF1 is significantly associated with poor prognosis in laryngeal squamous cell carcinoma**. *Medical oncology* 2013, **30**(4):613.

137. Fang Z, Xing F, Bronner C, Teng Z, Guo Z: **ICBP90 mediates the ERK1/2 signaling to regulate the proliferation of Jurkat T cells**. *Cellular immunology* 2009, **257**(1-2):80-87.

138. Alhosin M, Abusnina A, Achour M, Sharif T, Muller C, Peluso J, Chataigneau T, Lugnier C, Schini-Kerth VB, Bronner C *et al*: **Induction of apoptosis by thymoquinone in lymphoblastic leukemia Jurkat cells is mediated by a p73-dependent pathway which targets the epigenetic integrator UHRF1**. *Biochemical pharmacology* 2010, **79**(9):1251-1260.

139. Abbady AQ, Bronner C, Bathami K, Muller CD, Jeanblanc M, Mathieu E, Klein JP, Candolfi E, Mousli M: **TCR pathway involves ICBP90 gene down-regulation via E2F binding sites**. *Biochemical pharmacology* 2005, **70**(4):570-579.

140. Arima Y, Hirota T, Bronner C, Mousli M, Fujiwara T, Niwa S, Ishikawa H, Saya H: **Down-regulation of nuclear protein ICBP90 by p53/p21Cip1/WAF1-dependent DNA-damage**

checkpoint signals contributes to cell cycle arrest at G1/S transition. *Genes to cells : devoted to molecular & cellular mechanisms* 2004, **9**(2):131-142.

141. Trotzier MA, Bronner C, Bathami K, Mathieu E, Abbady AQ, Jeanblanc M, Muller CD, Rochette-Egly C, Mousli M: **Phosphorylation of ICBP90 by protein kinase A enhances topoisomerase IIalpha expression**. *Biochemical and biophysical research communications* 2004, **319**(2):590-595.

142. Sidhu H, Capalash N: **UHRF1: The key regulator of epigenetics and molecular target for cancer therapeutics**. *Tumour biology : the journal of the International Society for Oncodevelopmental Biology and Medicine* 2017, **39**(2):1010428317692205.

143. Choudhry H, Zamzami MA, Omran Z, Wu W, Mousli M, Bronner C, Alhosin M: **Targeting microRNA/UHRF1 pathways as a novel strategy for cancer therapy**. *Oncology letters* 2018, **15**(1):3-10.

144. Yu T, Li J, Yan M, Liu L, Lin H, Zhao F, Sun L, Zhang Y, Cui Y, Zhang F *et al*: **MicroRNA-193a-3p and -5p suppress the metastasis of human non-small-cell lung cancer by downregulating the ERBB4/PIK3R3/mTOR/S6K2 signaling pathway**. *Oncogene* 2014, **34**:413.

145. Achour M, Fuhrmann G, Alhosin M, Ronde P, Chataigneau T, Mousli M, Schini-Kerth VB, Bronner C: **UHRF1 recruits the histone acetyltransferase Tip60 and controls its expression and activity**. *Biochemical and biophysical research communications* 2009, **390**(3):523-528.

146. Kamine J, Elangovan B, Subramanian T, Coleman D, Chinnadurai G: **Identification of a cellular protein that specifically interacts with the essential cysteine region of the HIV-1 Tat transactivator**. *Virology* 1996, **216**(2):357-366.

147. Sapountzi V, Logan IR, Robson CN: **Cellular functions of TIP60**. *The international journal of biochemistry & cell biology* 2006, **38**(9):1496-1509.

148. Kim CH, Kim JW, Jang SM, An JH, Seo SB, Choi KH: **The chromodomain-containing histone acetyltransferase TIP60 acts as a code reader, recognizing the epigenetic codes for initiating transcription**. *Bioscience, biotechnology, and biochemistry* 2015, **79**(4):532-538.

149. Sun Y, Jiang X, Price BD: **Tip60: connecting chromatin to DNA damage signaling**. *Cell cycle* 2010, **9**(5):930-936.

150. Jang SM, Kim JW, Kim CH, An JH, Johnson A, Song PI, Rhee S, Choi KH: **KAT5-mediated SOX4 acetylation orchestrates chromatin remodeling during myoblast differentiation**. *Cell Death &Amp; Disease* 2015, **6**:e1857.

151. Dai C, Shi D, Gu W: **Negative regulation of the acetyltransferase TIP60-p53 interplay by UHRF1 (ubiquitin-like with PHD and RING finger domains 1)**. *The Journal of biological chemistry* 2013, **288**(27):19581-19592.

152. Jemal A, Center MM, DeSantis C, Ward EM: **Global patterns of cancer incidence and mortality rates and trends**. *Cancer epidemiology, biomarkers & prevention : a publication of the American Association for Cancer Research, cosponsored by the American Society of Preventive Oncology* 2010, **19**(8):1893-1907.

153. Kreeger PK, Lauffenburger DA: **Cancer systems biology: a network modeling perspective**. *Carcinogenesis* 2010, **31**(1):2-8.

154. Laget S, Defossez PA: **[Master and servant: epigenetic deregulations as a cause and a consequence of cancer]**. *Medecine sciences : M/S* 2008, **24**(8-9):725-730.

155. Vogelstein B, Kinzler KW: **Cancer genes and the pathways they control**. *Nature medicine* 2004, **10**(8):789-799.

156. Croce CM: **Causes and consequences of microRNA dysregulation in cancer**. *Nature reviews Genetics* 2009, **10**(10):704-714.

157. Jones PA, Issa JP, Baylin S: **Targeting the cancer epigenome for therapy**. *Nature reviews Genetics* 2016, **17**(10):630-641.

158. Fabbri M, Garzon R, Cimmino A, Liu Z, Zanesi N, Callegari E, Liu S, Alder H, Costinean S, Fernandez-Cymering C *et al*: **MicroRNA-29 family reverts aberrant methylation in lung cancer by targeting DNA methyltransferases 3A and 3B**. *Proceedings of the National Academy of Sciences of the United States of America* 2007, **104**(40):15805-15810.

159. Fraga MF, Ballestar E, Villar-Garea A, Boix-Chornet M, Espada J, Schotta G, Bonaldi T, Haydon C, Ropero S, Petrie K *et al*: **Loss of acetylation at Lys16 and trimethylation at Lys20 of histone H4 is a common hallmark of human cancer**. *Nature genetics* 2005, **37**(4):391-400.

160. Halkidou K, Gaughan L, Cook S, Leung HY, Neal DE, Robson CN: **Upregulation and nuclear recruitment of HDAC1 in hormone refractory prostate cancer**. *The Prostate* 2004, **59**(2):177-189.

161. Song J, Noh JH, Lee JH, Eun JW, Ahn YM, Kim SY, Lee SH, Park WS, Yoo NJ, Lee JY *et al*: **Increased expression of histone deacetylase 2 is found in human gastric cancer**. *APMIS : acta pathologica, microbiologica, et immunologica Scandinavica* 2005, **113**(4):264-268.

162. Nguyen CT, Weisenberger DJ, Velicescu M, Gonzales FA, Lin JC, Liang G, Jones PA: **Histone H3-lysine 9 methylation is associated with aberrant gene silencing in cancer cells and is rapidly reversed by 5-aza-2'-deoxycytidine**. *Cancer research* 2002, **62**(22):6456-6461.

163. Kondo Y, Shen L, Ahmed S, Boumber Y, Sekido Y, Haddad BR, Issa JP: **Downregulation of histone H3 lysine 9 methyltransferase G9a induces centrosome disruption and chromosome instability in cancer cells**. *PloS one* 2008, **3**(4):e2037.

164. Kondo Y, Shen L, Suzuki S, Kurokawa T, Masuko K, Tanaka Y, Kato H, Mizuno Y, Yokoe M, Sugauchi F *et al*: **Alterations of DNA methylation and histone modifications contribute to gene silencing in hepatocellular carcinomas**. *Hepatology research : the official journal of the Japan Society of Hepatology* 2007, **37**(11):974-983.

165. Valk-Lingbeek ME, Bruggeman SW, van Lohuizen M: **Stem cells and cancer; the polycomb connection**. *Cell* 2004, **118**(4):409-418.

166. Rodriguez J, Frigola J, Vendrell E, Risques RA, Fraga MF, Morales C, Moreno V, Esteller M, Capella G, Ribas M *et al*: **Chromosomal instability correlates with genome-wide DNA demethylation in human primary colorectal cancers**. *Cancer research* 2006, **66**(17):8462-9468.

167. Kim YI, Giuliano A, Hatch KD, Schneider A, Nour MA, Dallal GE, Selhub J, Mason JB: **Global DNA hypomethylation increases progressively in cervical dysplasia and carcinoma**. *Cancer* 1994, **74**(3):893-899.

168. Lin CH, Hsieh SY, Sheen IS, Lee WC, Chen TC, Shyu WC, Liaw YF: **Genome-wide hypomethylation in hepatocellular carcinogenesis**. *Cancer research* 2001, **61**(10):4238-4243.

169. Bedford MT, van Helden PD: **Hypomethylation of DNA in pathological conditions of the human prostate**. *Cancer research* 1987, **47**(20):5274-5276.

170. Cadieux B, Ching TT, VandenBerg SR, Costello JF: **Genome-wide hypomethylation in human glioblastomas associated with specific copy number alteration, methylenetetrahydrofolate reductase allele status, and increased proliferation**. *Cancer research* 2006, **66**(17):8469-8476.

171. Feinberg AP, Vogelstein B: **Hypomethylation of ras oncogenes in primary human cancers**. *Biochemical and biophysical research communications* 1983, **111**(1):47-54.

172. Szyf M, Pakneshan P, Rabbani SA: **DNA methylation and breast cancer**. *Biochemical pharmacology* 2004, **68**(6):1187-1197.

173. Greger V, Passarge E, Hopping W, Messmer E, Horsthemke B: **Epigenetic changes may contribute to the formation and spontaneous regression of retinoblastoma**. *Human genetics* 1989, **83**(2):155-158.

174. Baylin SB: **DNA methylation and gene silencing in cancer**. *Nature clinical practice Oncology* 2005, **2 Suppl 1**:S4-11.

175. Pei JH, Luo SQ, Zhong Y, Chen JH, Xiao HW, Hu WX: **The association between non-Hodgkin lymphoma and methylation of p73**. *Tumour biology : the journal of the International Society for Oncodevelopmental Biology and Medicine* 2011, **32**(6):1133-1138.

176. Dawson MA, Kouzarides T: **Cancer epigenetics: from mechanism to therapy**. *Cell* 2012, **150**(1):12-27.

177. Sandoval J, Esteller M: **Cancer epigenomics: beyond genomics**. *Current opinion in genetics & development* 2012, **22**(1):50-55.

178. Ashraf W, Ibrahim A, Alhosin M, Zaayter L, Ouararhni K, Papin C, Ahmad T, Hamiche A, Mely Y, Bronner C *et al*: **The epigenetic integrator UHRF1: on the road to become a universal biomarker for cancer**. *Oncotarget* 2017.

179. Unoki M: **Current and potential anticancer drugs targeting members of the UHRF1 complex including epigenetic modifiers**. *Recent patents on anti-cancer drug discovery* 2011, **6**(1):116-130.

180. Khan O, La Thangue NB: **HDAC inhibitors in cancer biology: emerging mechanisms and clinical applications**. *Immunology and cell biology* 2012, **90**(1):85-94.

181. Joseph J, Mudduluru G, Antony S, Vashistha S, Ajitkumar P, Somasundaram K: **Expression profiling of sodium butyrate (NaB)-treated cells: identification of regulation of genes related to cytokine signaling and cancer metastasis by NaB**. *Oncogene* 2004, **23**(37):6304-6315.

182. Witt O, Lindemann R: **HDAC inhibitors: magic bullets, dirty drugs or just another targeted therapy**. *Cancer letters* 2009, **280**(2):123-124.

183. Zahnow CA, Topper M, Stone M, Murray-Stewart T, Li H, Baylin SB, Casero RA, Jr.: **Inhibitors of DNA Methylation, Histone Deacetylation, and Histone Demethylation: A Perfect Combination for Cancer Therapy**. *Advances in cancer research* 2016, **130**:55-111.

184. Stresemann C, Lyko F: **Modes of action of the DNA methyltransferase inhibitors azacytidine and decitabine**. *International journal of cancer* 2008, **123**(1):8-13.

185. Egger G, Liang G, Aparicio A, Jones PA: **Epigenetics in human disease and prospects for epigenetic therapy**. *Nature* 2004, **429**(6990):457-463.

186. Li LH, Olin EJ, Buskirk HH, Reineke LM: **Cytotoxicity and mode of action of 5-azacytidine on L1210 leukemia**. *Cancer research* 1970, **30**(11):2760-2769.

187. Ghoshal K, Datta J, Majumder S, Bai S, Kutay H, Motiwala T, Jacob ST: **5-Aza-deoxycytidine induces selective degradation of DNA methyltransferase 1 by a proteasomal pathway that requires the KEN box, bromo-adjacent homology domain, and nuclear localization signal**. *Molecular and cellular biology* 2005, **25**(11):4727-4741.

188. Yoo CB, Jones PA: **Epigenetic therapy of cancer: past, present and future**. *Nature reviews Drug discovery* 2006, **5**(1):37-50.

189. Nakamura K, Nakabayashi K, Htet Aung K, Aizawa K, Hori N, Yamauchi J, Hata K, Tanoue A: **DNA methyltransferase inhibitor zebularine induces human cholangiocarcinoma cell death through alteration of DNA methylation status**. *PloS one* 2015, **10**(3):e0120545.

190. Holleran JL, Parise RA, Joseph E, Eiseman JL, Covey JM, Glaze ER, Lyubimov AV, Chen YF, D'Argenio DZ, Egorin MJ: **Plasma pharmacokinetics, oral bioavailability, and interspecies scaling of the DNA methyltransferase inhibitor, zebularine**. *Clinical cancer research : an official journal of the American Association for Cancer Research* 2005, **11**(10):3862-3868.

191. Lyko F, Brown R: **DNA methyltransferase inhibitors and the development of epigenetic cancer therapies**. *Journal of the National Cancer Institute* 2005, **97**(20):1498-1506.

192. Chuang JC, Yoo CB, Kwan JM, Li TW, Liang G, Yang AS, Jones PA: **Comparison of biological effects of non-nucleoside DNA methylation inhibitors versus 5-aza-2'-deoxycytidine**. *Molecular cancer therapeutics* 2005, **4**(10):1515-1520.

193. Fang MZ, Wang Y, Ai N, Hou Z, Sun Y, Lu H, Welsh W, Yang CS: **Tea polyphenol (-)-epigallocatechin-3-gallate inhibits DNA methyltransferase and reactivates methylation-silenced genes in cancer cell lines**. *Cancer research* 2003, **63**(22):7563-7570.

194. Amato RJ: **Inhibition of DNA methylation by antisense oligonucleotide MG98 as cancer therapy**. *Clinical genitourinary cancer* 2007, **5**(7):422-426.

195. Ren J, Singh BN, Huang Q, Li Z, Gao Y, Mishra P, Hwa YL, Li J, Dowdy SC, Jiang SW: **DNA hypermethylation as a chemotherapy target**. *Cellular signalling* 2011, **23**(7):1082-1093.

196. Wan X, Yang S, Huang W, Wu D, Chen H, Wu M, Li J, Li T, Li Y: **UHRF1 overexpression is involved in cell proliferation and biochemical recurrence in prostate cancer after radical prostatectomy**. *Journal of experimental & clinical cancer research : CR* 2016, **35**:34.

197. Zhou L, Shang Y, Jin Z, Zhang W, Lv C, Zhao X, Liu Y, Li N, Liang J: **UHRF1 promotes proliferation of gastric cancer via mediating tumor suppressor gene hypermethylation**. *Cancer biology & therapy* 2015, **16**(8):1241-1251.

198. Bronner C, Krifa M, Mousli M: **Increasing role of UHRF1 in the reading and inheritance of the epigenetic code as well as in tumorogenesis**. *Biochemical pharmacology* 2013, **86**(12):1643-1649.

199. Citterio E, Papait R, Nicassio F, Vecchi M, Gomiero P, Mantovani R, Di Fiore PP, Bonapace IM: **Np95 is a histone-binding protein endowed with ubiquitin ligase activity**. *Molecular and cellular biology* 2004, **24**(6):2526-2535.

200. Parashar G, Capalash N: **Promoter methylation-independent reactivation of PAX1 by curcumin and resveratrol is mediated by UHRF1**. *Clinical and experimental medicine* 2016, **16**(3):471-478.

201. Zhang Y, Huang Z, Zhu Z, Zheng X, Liu J, Han Z, Ma X, Zhang Y: **Upregulated UHRF1 promotes bladder cancer cell invasion by epigenetic silencing of KiSS1**. *PloS one* 2014, **9**(10):e104252.

202. Sabatino L, Fucci A, Pancione M, Carafa V, Nebbioso A, Pistore C, Babbio F, Votino C, Laudanna C, Ceccarelli M *et al*: **UHRF1 coordinates peroxisome proliferator activated receptor gamma (PPARG) epigenetic silencing and mediates colorectal cancer progression**. *Oncogene* 2012, **31**(49):5061-5072.

203. Jin W, Chen L, Chen Y, Xu SG, Di GH, Yin WJ, Wu J, Shao ZM: **UHRF1 is associated with epigenetic silencing of BRCA1 in sporadic breast cancer**. *Breast cancer research and treatment* 2010, **123**(2):359-373.

204. Myrianthopoulos V, Cartron PF, Liutkeviciute Z, Klimasauskas S, Matulis D, Bronner C, Martinet N, Mikros E: **Tandem virtual screening targeting the SRA domain of UHRF1 identifies a novel chemical tool modulating DNA methylation**. *European journal of medicinal chemistry* 2016, **114**:390-396.

205. Ding G, Chen P, Zhang H, Huang X, Zang Y, Li J, Li J, Wong J: **Regulation of Ubiquitin-like with Plant Homeodomain and RING Finger Domain 1 (UHRF1) Protein Stability by Heat Shock Protein 90 Chaperone Machinery**. *The Journal of biological chemistry* 2016, **291**(38):20125-20135.

206. Houliston RS, Lemak A, Iqbal A, Ivanochko D, Duan S, Kaustov L, Ong MS, Fan L, Senisterra G, Brown PJ *et al*: **Conformational dynamics of the TTD-PHD histone reader module of UHRF1 reveals multiple histone binding states, allosteric regulation and druggability**. *The Journal of biological chemistry* 2017.

207. Krifa M, Leloup L, Ghedira K, Mousli M, Chekir-Ghedira L: **Luteolin induces apoptosis in BE colorectal cancer cells by downregulating calpain, UHRF1, and DNMT1 expressions**. *Nutrition and cancer* 2014, **66**(7):1220-1227.

208. Krifa M, Pizzi A, Mousli M, Chekir-Ghedira L, Leloup L, Ghedira K: **Limoniastrum guyonianum aqueous gall extract induces apoptosis in colorectal cancer cells by inhibiting calpain activity**. *Tumour biology : the journal of the International Society for Oncodevelopmental Biology and Medicine* 2014, **35**(8):7877-7885.

209. Achour M, Mousli M, Alhosin M, Ibrahim A, Peluso J, Muller CD, Schini-Kerth VB, Hamiche A, Dhe-Paganon S, Bronner C: **Epigallocatechin-3-gallate up-regulates tumor suppressor gene expression via a reactive oxygen species-dependent down-regulation of UHRF1**. *Biochemical and biophysical research communications* 2013, **430**(1):208-212.

210. Gali-Muhtasib H, Roessner A, Schneider-Stock R: **Thymoquinone: a promising anti-cancer drug from natural sources**. *The international journal of biochemistry & cell biology* 2006, **38**(8):1249-1253.

211. Shoieb AM, Elgayyar M, Dudrick PS, Bell JL, Tithof PK: **In vitro inhibition of growth and induction of apoptosis in cancer cell lines by thymoquinone**. *International journal of oncology* 2003, **22**(1):107-113.

212. Gali-Muhtasib HU, Abou Kheir WG, Kheir LA, Darwiche N, Crooks PA: **Molecular pathway for thymoquinone-induced cell-cycle arrest and apoptosis in neoplastic keratinocytes**. *Anti-cancer drugs* 2004, **15**(4):389-399.

213. Gali-Muhtasib H, Diab-Assaf M, Boltze C, Al-Hmaira J, Hartig R, Roessner A, Schneider-Stock R: **Thymoquinone extracted from black seed triggers apoptotic cell death in human colorectal cancer cells via a p53-dependent mechanism**. *International journal of oncology* 2004, **25**(4):857-866.

214. Alhosin M, Omran Z, Zamzami MA, Al-Malki AL, Choudhry H, Mousli M, Bronner C: **Signalling pathways in UHRF1-dependent regulation of tumor suppressor genes in cancer**. *Journal of experimental & clinical cancer research : CR* 2016, **35**(1):174.

215. Sharif T, Auger C, Alhosin M, Ebel C, Achour M, Etienne-Selloum N, Fuhrmann G, Bronner C, Schini-Kerth VB: **Red wine polyphenols cause growth inhibition and apoptosis in acute lymphoblastic leukaemia cells by inducing a redox-sensitive up-regulation of p73 and down-regulation of UHRF1**. *European journal of cancer* 2010, **46**(5):983-994.

216. Alhosin M, Sharif T, Mousli M, Etienne-Selloum N, Fuhrmann G, Schini-Kerth VB, Bronner C: **Down-regulation of UHRF1, associated with re-expression of tumor suppressor genes, is a common feature of natural compounds exhibiting anti-cancer properties**. *Journal of experimental & clinical cancer research : CR* 2011, **30**:41.

217. Mauray A, Milenkovic D, Besson C, Caccia N, Morand C, Michel F, Mazur A, Scalbert A, Felgines C: **Atheroprotective effects of bilberry extracts in apo E-deficient mice**. *Journal of agricultural and food chemistry* 2009, **57**(23):11106-11111.

218. Alhosin M, Leon-Gonzalez AJ, Dandache I, Lelay A, Rashid SK, Kevers C, Pincemail J, Fornecker LM, Mauvieux L, Herbrecht R *et al*: **Bilberry extract (Antho 50) selectively induces redox-sensitive caspase 3-related apoptosis in chronic lymphocytic leukemia cells by targeting the Bcl-2/Bad pathway**. *Scientific reports* 2015, **5**:8996.

219. Kim MY, Park SJ, Shim JW, Yang K, Kang HS, Heo K: **Naphthazarin enhances ionizing radiation-induced cell cycle arrest and apoptosis in human breast cancer cells**. *International journal of oncology* 2015, **46**(4):1659-1666.

220. Jang SY, Hong D, Jeong SY, Kim JH: **Shikonin causes apoptosis by up-regulating p73 and down-regulating ICBP90 in human cancer cells**. *Biochemical and biophysical research communications* 2015, **465**(1):71-76.

221. Seo JS, Choi YH, Moon JW, Kim HS, Park SH: **Hinokitiol induces DNA demethylation via DNMT1 and UHRF1 inhibition in colon cancer cells**. *BMC cell biology* 2017, **18**(1):14.

222. Mikeska T, Craig JM: **DNA methylation biomarkers: cancer and beyond**. *Genes* 2014, **5**(3):821-864.

223. Delagoutte B, Lallous N, Birck C, Oudet P, Samama JP: **Expression, purification, crystallization and preliminary crystallographic study of the SRA domain of the human UHRF1 protein**. *Acta crystallographica Section F, Structural biology and crystallization communications* 2008, **64**(Pt 10):922-925.

224. Shin D, Sinkeldam RW, Tor Y: **Emissive RNA alphabet**. *Journal of the American Chemical Society* 2011, **133**(38):14912-14915.

225. Kilin V, Gavvala K, Barthes NP, Michel BY, Shin D, Boudier C, Mauffret O, Yashchuk V, Mousli M, Ruff M *et al*: **Dynamics of Methylated Cytosine Flipping by UHRF1**. *Journal of the American Chemical Society* 2017, **139**(6):2520-2528.

226. Wiseman T, Williston S, Brandts JF, Lin LN: **Rapid measurement of binding constants and heats of binding using a new titration calorimeter**. *Analytical biochemistry* 1989, **179**(1):131-137.

227. Clamme JP, Azoulay J, Mely Y: **Monitoring of the formation and dissociation of polyethylenimine/DNA complexes by two photon fluorescence correlation spectroscopy**. *Biophysical journal* 2003, **84**(3):1960-1968.

228. Sirajuddin M, Ali S, Badshah A: **Drug-DNA interactions and their study by UV-Visible, fluorescence spectroscopies and cyclic voltametry**. *Journal of photochemistry and photobiology B, Biology* 2013, **124**:1-19.

229. Palchaudhuri R, Hergenrother PJ: **DNA as a target for anticancer compounds: methods to determine the mode of binding and the mechanism of action**. *Current opinion in biotechnology* 2007, **18**(6):497-503.

230. Heller DP, Greenstock CL: **Fluorescence lifetime analysis of DNA intercalated ethidium bromide and quenching by free dye**. *Biophysical chemistry* 1994, **50**(3):305-312.

231. White RJ, Durr FE: **Development of mitoxantrone**. *Investigational new drugs* 1985, **3**(2):85-93.

232. Shenkenberg TD, Von Hoff DD: **Mitoxantrone: a new anticancer drug with significant clinical activity**. *Annals of internal medicine* 1986, **105**(1):67-81.

233. Evison BJ, Sleebs BE, Watson KG, Phillips DR, Cutts SM: **Mitoxantrone, More than Just Another Topoisomerase II Poison**. *Medicinal research reviews* 2016, **36**(2):248-299.

234. Walker DA, Wyhs N, Giovinazzo H, Yegnasubramanian S, Nelson WG: **Abstract 5390: Development of a high-throughput screening assay to identify UHRF1 inhibitors via time-resolved fluorescence resonance energy transfer (TR-FRET)**. *Cancer research* 2014, **74**(19 Supplement):5390-5390.

235. Parker BS, Cutts SM, Nudelman A, Rephaeli A, Phillips DR, Sukumar S: **Mitoxantrone mediates demethylation and reexpression of cyclin d2, estrogen receptor and 14.3.3sigma in breast cancer cells**. *Cancer biology & therapy* 2003, **2**(3):259-263.

236. Yang AS, Issa JP: **Mitoxantrone: a hypomethylating agent?** *Cancer biology & therapy* 2003, **2**(3):264-265.

237. Bronner C, Chataigneau T, Schini-Kerth VB, Landry Y: **The "Epigenetic Code Replication Machinery", ECREM: a promising drugable target of the epigenetic cell memory**. *Current medicinal chemistry* 2007, **14**(25):2629-2641.

238. Hashimoto H, Horton JR, Zhang X, Cheng X: **UHRF1, a modular multi-domain protein, regulates replication-coupled crosstalk between DNA methylation and histone modifications**. *Epigenetics* 2009, **4**(1):8-14.

239. Rottach A, Frauer C, Pichler G, Bonapace IM, Spada F, Leonhardt H: **The multi-domain protein Np95 connects DNA methylation and histone modification**. *Nucleic acids research* 2010, **38**(6):1796-1804.

240. Jenkins Y, Markovtsov V, Lang W, Sharma P, Pearsall D, Warner J, Franci C, Huang B, Huang J, Yam GC *et al*: **Critical role of the ubiquitin ligase activity of UHRF1, a nuclear RING finger protein, in tumor cell growth**. *Molecular biology of the cell* 2005, **16**(12):5621-5629.

241. Zhang X, Wu J, Luan Y: **Tip60: Main Functions and Its Inhibitors**. *Mini reviews in medicinal chemistry* 2017, **17**(8):675-682.

List of publications

1- **Liliyana Zaayter,** Mattia Mori, Waseem Ashraf, Christian Boudier, Vasyl Kilin, Krishna Gavvala, Tanveer Ahmad, Maurizio Botta, Christian Bronner, Marc Ruff, Sylvia Eiler, Marc Mousli, Yves Mély. Identification of a new molecule targeting UHRF1 and disrupting its interaction with DNMT1. (*in preparation*)

2- **Liliyana Zaayter**, Waseem Ashraf, Tanveer Ahmad, Mattia Mori, Christian D. Muller, Christina Bronner, Yves Mély, Marc Mousli. Epigenetic dysregulation mechanism of 2-amino-3-hydroxyanthraquinone (AHAQ) induces cell cycle arrest and apoptosis in cervical cancer cells. *(in preparation)*

3- Waseem Ashraf, Christian Bronner, **Liliyana Zaayter**, Tanveer Ahmad, Christian D. Muller,Ludovic Richert, Ali Hamich, Yves Mely and Marc Mousli. "Interaction of the Epigenetic Integrator UHRF1 with Tip60 through MYST domain during S Phase in Living Cells". *Journal of experimental & clinical cancer research 2017.*

4- Waseem Ashraf, Abdulkhaleg Ibrahim, Mahmoud Alhosin, **Liliyana Zaayter**, Khalid Ouararhni, Christophe Papin, Tanveer Ahmad, Ali Hamiche, Yves Mely, Christian Bronner, Marc Mousli. UHRF1: on the road to become a universal biomarker for cancer". *Oncotarget 2017*

Annex 1

Interaction of the epigenetic integrator UHRF1 with the MYST domain of TIP60 inside the cell

During my PhD thesis, I had the opportunity to collaborate on another project, that is presented in the following published paper and that will be shortly introduced here below.

Tip60 is an important acetyltransferase enzyme that plays a key role in transcriptional regulation, DNA damage repair, cell cycle regulation and apoptosis. It is also multi-domain protein composed of N-terminal chromodomain (CRD) and central MYST domain which itself is made up of a Zinc finger domain and a catalytic histone acetyltransferase (HAT) domain by which it can acetylate various proteins including histones (H2AK5, H3K14, and H4K), p53, ATM, DNMT1 [241]. It is an important partner of UHRF1. Indeed, the interaction between UHRF1 and Tip60 is believed to be responsible for regulation of DNMT1 activity and suppression of p53-mediated growth arrest and apoptosis [120, 151].

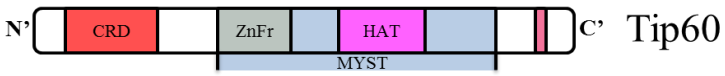

Schematic diagram of TIP60

The main questions addressed in this work are how these two proteins interact with each other? Which domains are involved in this interaction? At which phase of the cell cycle this interaction takes place?

The results suggest that TIP60 interacts with UHRF1 through its MYST domain and this interaction is more pronounced in S phase of cell cycle. Overexpression of Tip60 downregulates UHRF1 in cancer cells and induces apoptosis thus predicting a role of Tip60 in the regulation of UHRF1, which can be further explored to overcome the oncogenic potential of UHRF1 in cancer by using Tip60.

Ashraf et al. Journal of Experimental & Clinical Cancer Research (2017) 36:188
DOI 10.1186/s13046-017-0659-1

Journal of Experimental & Clinical Cancer Research

RESEARCH Open Access

Interaction of the epigenetic integrator UHRF1 with the MYST domain of TIP60 inside the cell

Waseem Ashraf[1], Christian Bronner[2], Liliyana Zaayter[1], Tanveer Ahmad[1], Ludovic Richert[1], Mahmoud Alhosin[3,4], Abdulkhaleg Ibrahim[2,5], Ali Hamiche[2], Yves Mely[1] and Marc Mousli[1*]

Abstract

Background: The nuclear epigenetic integrator UHRF1 is known to play a key role with DNMT1 in maintaining the DNA methylation patterns during cell division. Among UHRF1 partners, TIP60 takes part in epigenetic regulations through its acetyltransferase activity. Both proteins are involved in multiple cellular functions such as chromatin remodeling, DNA damage repair and regulation of stability and activity of other proteins. The aim of this work was to investigate the interaction between UHRF1 and TIP60 in order to elucidate the dialogue between these two proteins.

Methods: Biochemical (immunoprecipitation and pull-down assays) and microscopic (confocal and fluorescence lifetime imaging microscopy; FLIM) techniques were used to analyze the interaction between TIP60 and UHRF1 in vitro and in vivo. Global methylation levels were assessed by using a specific kit. The results were statistically analyzed using Graphpad prism and Origin.

Results: Our study shows that UHRF1, TIP60 and DNMT1 were found in the same epigenetic macro-molecular complex. In vitro pull-down assay showed that deletion of either the zinc finger in MYST domain or deletion of whole MYST domain from TIP60 significantly reduced its interaction with UHRF1. Confocal and FLIM microscopy showed that UHRF1 co-localized with TIP60 in the nucleus and confirmed that both proteins interacted together through the MYST domain of TIP60. Moreover, overexpression of TIP60 reduced the DNA methylation levels in HeLa cells along with downregulation of UHRF1 and DNMT1.

Conclusion: Our data demonstrate for the first time that TIP60 through its MYST domain directly interacts with UHRF1 which might be of high interest for the development of novel oncogenic inhibitors targeting this interaction.

Keywords: Cancer, Epigenetics, Fluorescence lifetime imaging microscopy (FLIM), Fluorescence resonance energy transfer (FRET), Protein-protein interaction, TIP60, UHRF1, Cell cycle

Background

Ubiquitin-like containing PHD and RING Finger domains 1 (UHRF1) is a multi-domain nuclear protein that plays an important role in epigenetics through the maintenance of DNA methylation patterns during DNA replication [1, 2]. UHRF1 senses hemi-methylated strand through its SRA domain and then recruits the DNA methyltransferase 1 (DNMT1) to duplicate the methylation patterns on the newly formed daughter strand [3–5]. Besides the readout of DNA methylation marks, UHRF1 also reads histone post-translational modifications (H3K9me2/3) via its tandem tudor and PHD domains and ubiquitinylates histone H3 at lysine 23 by its C-terminal RING domain [6–9]. UHRF1 is highly expressed in proliferating cells as compared with differentiated cells and its level peaks during the G1/S phase transition and G2/M phase of the cell cycle [1, 10]. In cancer cells, UHRF1 is mostly up-regulated and its levels are maintained constant throughout the cell cycle. The high levels of UHRF1 found in variety of cancers are often

* Correspondence: marc.mousli@unistra.fr
[1]Laboratoire de Biophotonique et Pharmacologie, UMR 7213 CNRS, Faculté de Pharmacie, Université de Strasbourg, 74, Route du Rhin, 67401 Illkirch Cedex, France
Full list of author information is available at the end of the article

BioMed Central

© The Author(s). 2017 **Open Access** This article is distributed under the terms of the Creative Commons Attribution 4.0 International License (http://creativecommons.org/licenses/by/4.0/), which permits unrestricted use, distribution, and reproduction in any medium, provided you give appropriate credit to the original author(s) and the source, provide a link to the Creative Commons license, and indicate if changes were made. The Creative Commons Public Domain Dedication waiver (http://creativecommons.org/publicdomain/zero/1.0/) applies to the data made available in this article, unless otherwise stated.

correlated to the epigenetically silencing of tumor suppressor genes, poor prognosis and aggressiveness of the tumor [11–15]. UHRF1 is stabilized in the cells by its association with the ubiquitin specific protease 7 (USP7 or HAUSP) which prevents the proteasomal degradation of UHRF1 [16]. UHRF1 also plays an important role in regulating the stability and functions of other proteins such as DNMT1, promyelocytic leukemia protein (PML) and p53 through its interaction with other proteins such as the Tat-interacting protein 60 kDa (TIP60), USP7 and histone deacetylase 1 (HDAC1) [17–20]. UHRF1 and TIP60 were shown to be in the same epigenetic complex and to play an important role in regulating the stability and activity of DNMT1 [19, 21]. DNMT1 is acetylated by TIP60 which allows UHRF1 to ubiquitinylate DNMT1 and induce its down-regulation [19].

TIP60, initially identified as a partner of the HIV-1 Tat protein, is an evolutionary conserved and ubiquitously expressed acetyltransferase of the MYST family [22–25]. The TIP60 protein contains several domains (Fig. 1a, (i)), including a chromodomain and MYST domain endowed with acetyltransferase activity. Through these domains, TIP60 acetylates both histone and non-histone proteins. Tip60 also interacts with androgenic receptors and transcription factors and is involved in a variety of cellular activities including DNA damage response, chromatin remodeling, gene transcription, cell cycle regulation and apoptosis [26–29]. It also mediates the progression of the cell cycle by facilitating the G1/S phase transition, maintaining the genome integrity during the G1 and S phase and ensuring the faithful chromatin segregation during the M phase [30–33]. TIP60 also plays a role in regulating the activities of p53 in an acetylation-dependent and independent manner [18]. TIP60 mediated K120 acetylation in DNA binding region of p53 is necessary for the induction of apoptosis through Bcl 2-associated X protein (BAX) and p53 upregulated modulator of apoptosis (PUMA) pathway. The knockdown of TIP60 has been shown to abrogate the p21-induced cell cycle arrest after the activation of the tumor suppressor gene p53 in response to DNA damage [34–36]. Of note, UHRF1 by its direct interaction with TIP60 through the SRA and RING domains is thought to perturb the association between TIP60 and p53, preventing this latter from an acetylation-dependent activation and antitumor response [18]. Thus, a new anticancer strategy would be to restore p53 function by hindering UHRF1 to interact with TIP60. Although, the literature [18, 21] clearly suggests the occurrence of such an interaction in cells, its final demonstration is still lacking.

In order to further explore this interaction in cells and identify its determinants, we performed Fluoresecence Lifetime Imaging Microscopy (FLIM) experiments to demonstrate that UHRF1 and TIP60 physically interacts inside the cells. Through the use of deletion mutants of TIP60, we identified the key role of the MYST domain in its interaction with the UHRF1. This interaction also occurs in the S phase of the cell cycle during DNA replication.

Methods

Cell cultures

HeLa cells (ATCC, CCL-2 Amp, HeLa; Cervical Adenocarcinoma; Human) were cultured in Dulbecco's modified Eagle's medium (DMEM + GlutaMAX, Gibco, Lifetech, France) supplemented with 10% of heat inactivated fetal bovine serum and mixture of penicillin (100 U/ml) and streptomycin (100 U/ml) (penicillin/streptomycin: Invitrogen Corporation Pontoise, France) at 37 °C in 5% CO_2. Transfection of the plasmids in HeLa cells was carried by the jetPEI™ reagent (Life Technologies, Saint Aubin, France) according to the manufacturer's protocol.

Plasmid constructs

For HeLa cell transfection, UHRF1 was cloned into pCMV-mCherry vector to express UHRF1-mCherry protein while the TIP60 wild-type and mutants were cloned into a pEGFP-N1 plasmid to express eGFP-labeled TIP60 proteins in cells. For protein purification, UHRF1 was cloned into pGEX-4 T-1 to get the recombinant GST-UHRF1 fusion protein as described in [1]. For in vitro studies, TIP60 wild-type (TIP60-WT) and mutant TIP60 proteins were cloned into pET15b vector with XhoI and BamHI restriction sites to purify His tagged TIP60WT/mutants from bacteria.

Antibodies

Antibodies used in this study include the mouse monoclonal anti-UHRF1 engineered as described previously [1], mouse monoclonal anti-DNMT1 (Stressgen Canada), rabbit polyclonal anti-TIP60 (Genetex GTX 112197), rabbit polyclonal anti-mCherry (Genetex GTX 59788), mouse monoclonal anti-eGFP (Thermo Fisher Scientific A-11120 & Proteintech 66,002–1-Ig), and mouse monoclonal anti-GAPDH (Merck Millipore MAB 374). Mouse monoclonal anti-His and mouse monoclonal anti-GST antibodies were engineered in our core facilities (IGBMC, Illkirch, France).

Protein purification and pull-down assays

For protein purification, the plasmids were transfected in BL21 cells and cells were allowed to grow at 37 °C until the absorbance of the culture reached 0.5–0.6. Expression of the proteins was induced by the addition of 1 mM isopropyl-1-thio-β-D-galactopyranoside (IPTG) and the cells were further incubated at 25 °C for 4 h before collecting the proteins. GST-tagged UHRF1 protein

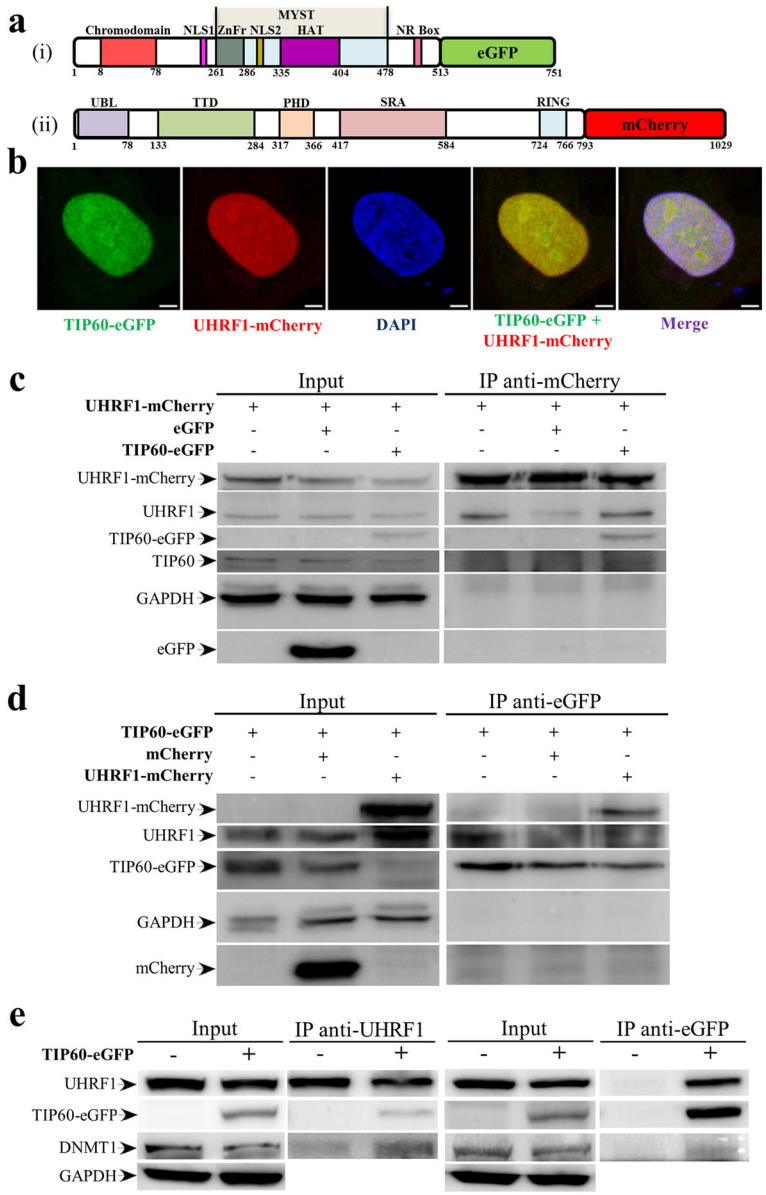

Fig. 1 TIP60 interacts with UHRF1 and DNMT1 in HeLa cells. **a** Schematic diagram of TIP60 wild type tagged with eGFP (i) and UHRF1 tagged with mCherry (ii) at their C-terminus. **b** Transfection of TIP60-eGFP and UHRF1-mCherry in the nucleus of HeLa cells. White bar indicates size of 5 μm. **c** Immunoprecipitation of UHRF1-mCherry with anti-mCherry antibody co-immunoprecipitating exogenous TIP60-eGFP and endogenous TIP60. **d** Reciprocal immunoprecipitation of TIP60-eGFP with anti-eGFP antibody co-immunoprecipitating exogenous UHRF1-mCherry and endogenous UHRF1. **e** DNMT1 co-immunoprecipitate with UHRF1 and TIP60-eGFP using anti-UHRF1 and anti-eGFP antibody respectively

was purified from the cell lysate using Glutathione Sepharose 4B beads (GE Healthcare Life Sciences 17–0756-05) while the His-tagged wild-type and mutant TIP60 proteins were purified using Ni-NTA agarose beads (Qiagen 30,230) in appropriate buffers. Wild-type and mutant TIP60 proteins were immobilized on the Ni-NTA agarose beads and equal quantity of GST-UHRF1 was added in PBS containing 30 mM imidazole and 0.1% triton to study protein-protein interaction. The immobilized beads were washed five times before being analyzed by SDS-PAGE.

Fluorescence lifetime imaging microscopy (FLIM)

For FLIM measurements, 10^5 cells were seeded in a μ-dish 35 mm, glass bottom grid-50 (Ibidi 81,148) wells and were co-transfected with 0.75 μg TIP60-eGFP and 0.75 μg UHRF1-mCherry plasmids by using jetPEI™ reagent as described in manufacturer's protocol. After 24 h of transfection, cells were incubated for 20 min with 10 μM 5-ethynyl-2′-deoxyuridine (EdU) containing media before fixation with 3.7% paraformaldehyde. After fixation, cells were analyzed with a homemade two-photon excitation

scanning microscope based on an Olympus IX70 inverted microscope with an Olympus 60X 1.2 NA water immersion objective operating in the descanned fluorescence collection mode as described [37]. Two-photon excitation at 930 nm was provided by an Insight DeepSee laser (Spectra Physics). Photons were collected using a short pass filter with a cut-off wavelength of 680 nm (F75–680, AHF, Germany) and a band-pass filter of 520 ± 17 nm (F37–520, AHF, Germany). The fluorescence was directed to a fiber coupled APD (SPCM-AQR-14-FC, Perkin Elmer), which was connected to a time-correlated single photon counting module (SPC830, Becker & Hickl, Germany). FLIM data were analyzed using the SPCImage v 4.0.6 (Becker & Hickel) software. The Förster resonance energy transfer (FRET) efficiency was calculated according to $E = 1- (\tau_{DA}/\tau_{D})$, where τ_{DA} is lifetime of donor (eGFP) in the presence of acceptor (mCherry) and τ_{D} is the lifetime of donor in the absence of acceptor.

Confocal microscopy

The cells imaged by FLIM were also imaged by confocal microscopy. The same cells could be imaged by both techniques, by locating the cells with the help of coordinates on the ibidi well. Prior to confocal microscopy the cells in S phase were labeled with the Click-iT® EdU Alexa Fluor® 647 Imaging Kit (Thermo Fisher Scientific USA C10340) according to the manufacturer's protocol. For transfection and localization analysis, cells were co-transfected with TIP60-eGFP WT/mutants and UHRF1-mCherry and were labeled with DAPI after fixation to stain the nucleus. All samples were imaged with a Leica SPE equipped with a 63× 1.4NA oil immersion objective (HXC PL APO 63×/1.40 OIL CS). The images were further processed with Image J software.

Immunoprecipitation and western blotting

For Western blot, cells were harvested 24 h post-transfection by mild trypsinization. After washing with PBS, cells were lysed by ice cold lysis buffer 10 mM Tris-HCl pH 7.5, 150 mM NaCl, 1 mM EDTA and 1% NP40 supplemented with protease inhibitors (complete mini EDTA free protease inhibitor cocktail tablets, Roche Germany 11,836,170,001). Cell lysates (40 μg of the protein) were loaded onto 10% SDS-PAGE gels after denaturation for 5 min in Laemmli sample buffer (Bio-Rad Laboratories USA 1610747). The proteins were identified by anti-UHRF1, anti-eGFP, anti-DNMT1 and anti-GAPDH antibodies with overnight incubation at 4 °C. Primary antibodies were labeled with secondary anti-mouse (Promega, W402B) or anti-rabbit antibodies (Promega, W401B) conjugated with horseradish peroxidase and were visualized with the chemiluminescent ECL system (Clarity™ ECL western blotting substrate, Biorad, 170–5060) on an Image Quant LAS 4000 apparatus. Images were analyzed using the Image Studio Lite (Li-Core Biosciences, USA). For co-immunoprecipitation, the cells were collected and lysed by freeze shock and sonication in PBS supplemented with protease inhibitor cocktail tablet. A fraction of 40 μg of protein from each lysate was saved to serve as input control while 800 μg to 1 mg of protein lysate was incubated with appropriate antibodies for 4 h at 4 °C for subsequent immunoprecipitation. After washing and equilibration, 50 μL of Dynabeads® Protein A (Thermo Fisher Scientific Norway 10002D) were added to the lysate-antibody mixture and incubated for 1 h at 4 °C. Beads were collected later and washed five times in lysis buffer. They were then resuspended in Laemmli sample buffer (Bio-Rad Laboratories, USA). Proteins denatured by heating at 95 °C for 5 min were analyzed through Western blotting.

Global DNA Methylation analysis

HeLa cells were transiently transfected with TIP60-eGFP and mutants and were analyzed for global methylation levels by using Sigma's Imprint® Methylated DNA Quantification Kit Sigma-Aldrich). Briefly DNA was extracted from the cells using QIAamp® DNA Kit (Qiagen) and 200 ng of purified DNA were used for global DNA methylation level analysis according to the manufacturer's protocol.

Statistical analysis

The results were statistically analyzed using GraphPadPrism (version 5.04) and Origin (version 8.6).

Results

UHRF1 and TIP60 interaction inside the cells

In order to study the interaction between TIP60 and UHRF1, we expressed eGFP-tagged TIP60 (Fig. 1a, (i)) and mCherry-tagged UHRF1 (Fig. 1a, (ii)) in HeLa cells. The two proteins were expressed and co-localized with DAPI inside the nucleus of HeLa cells as seen by the merge (Fig. 1b). The interaction between UHRF1 and TIP60 proteins was assessed in vitro by co-immunoprecipitation experiments. Immunoprecipitating UHRF1-mCherry by using anti-mCherry antibody led to the co-immunoprecipitation of both endogenous TIP60 and exogenous TIP60-eGFP while free eGFP which was co-transfected with UHRF1-mCherry did not co-immunoprecipitate with it (Fig. 1c). This shows specific interaction of UHRF1-mCherry with endogenous TIP60 and exogenous TIP60-eGFP. Similarly, reciprocal co-immunoprecipitation experiments were performed by immunoprecipitating TIP60-eGFP with anti-eGFP antibody in cells (Fig. 1d). Immunoprecipitation of TIP60-eGFP led to co-immunoprecipitation of UHRF1-mCherry and endogenous UHRF1 while it did not immunoprecipitate free mCherry suggesting specific interaction between UHRF1 and TIP60 in the cells. Therefore, we can

assume that tagged proteins correctly localize in the nucleus of HeLa cells and can mimic the interaction pattern of endogenous proteins. It is interesting to note that UHRF1-mCherry co-expression resulted in lower levels of TIP60-eGFP recombinant protein (Fig. 1d) as compared with cells transfected with TIP60-eGFP or co-transfected with mCherry alone.

LikeTIP60, DNMT1 has also been reported to be associated with UHRF1 in the same protein complex [21]. So, in order to check the presence of DNMT1 in UHRF1/TIP60 complex, we also performed co-immunoprecipitation experiments. DNMT1 co-immunoprecipitated with the UHRF1 in normal HeLa cells or cells with overexpressed TIP60-eGFP (Fig. 1e). Overexpressed TIP60-eGFP also interacted with endogenous DNMT1 as DNMT1 co-immunoprecipitated with TIP60-eGFP along with UHRF1 showing the presence of the three proteins together in the same complex (Fig. 1e). This supports that the tag of TIP60-eGFP does not hinder it to adequately interact with its partners like DNMT1.

However, the results obtained with immunoprecipitation cannot confirm the interaction of proteins in vivo and do not explain the presence or absence of a close dialogue between the two proteins inside the cell.

Therefore, we studied the interaction between UHRF1 and TIP60 in cells using the FLIM-FRET technique which allows monitoring of very close contact (< 10 nm) between two proteins inside a cell. TIP60-eGFP served as the FRET pair donor because of the mono-exponential decay and high quantum yield of eGFP while the UHRF1-mCherry served as the FRET pair acceptor in these experiments as the absorption spectrum of mCherry falls in the emission spectrum of the eGFP. FRET occurs only when the two fluorophores are in close proximity to each other and can be unambiguously evidenced by a decrease of lifetime of the donor. By using FLIM microscopy, the lifetime of eGFP is calculated and color coded in each pixel of the image. The red to blue color covers lifetime ranging from 1.8 ns to 2.8 ns. FLIM images were recorded for TIP60-eGFP transfected cells (Fig. 2a, (i)) and cells co-transfected with TIP60-eGFP and UHRF1-mCherry (Fig. 2a, (ii)). The resulting distributions of fluorescent lifetimes are given in (Fig. 2a, (iii)). The average lifetime of TIP60-eGFP was 2.52 ± 0.01 ns in the cells transfected with TIP60-eGFP alone (Fig. 2b) or co-transfected with free mCherry (data not shown). However, the lifetime of eGFP was significantly reduced when TIP60-eGFP was co-transfected with UHRF1-mCherry in 1:1 ratio (Fig. 2b). The average lifetime of eGFP in co-transfected cells was 2.15 ± 0.02 ns, which corresponds to a mean FRET efficiency of 14.3 ± 0.6% (Fig. 2b). Altogether, these findings demonstrate that TIP60-eGFP interacts with UHRF1-mCherry in HeLa cells.

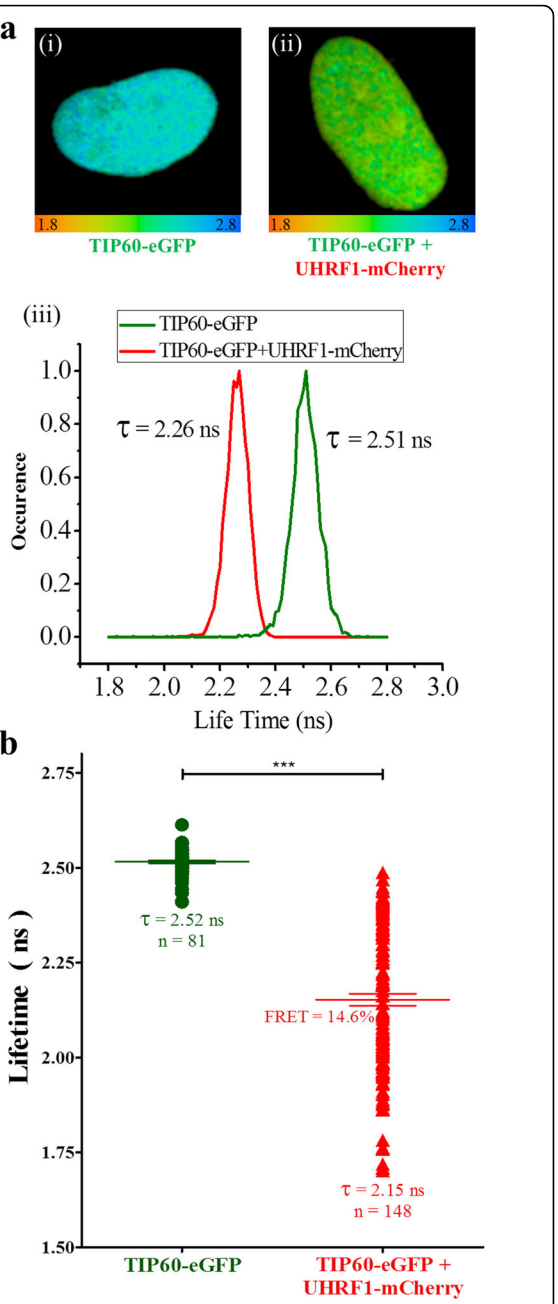

Fig. 2 Interaction of TIP60-eGFP with UHRF1-mCherry evidenced by FRET-FLIM. **a** 25 μm × 25 μm FLIM images of HeLa cells transfected with TIP60eGFP (i) or co-transfected with TIP60-eGFP and UHRF1-mCherry (ii) and lifetime distribution curve (iii). Color coded images indicate the fluorescence lifetime of TIP60-eGFP at each pixel. Color scale codes for lifetimes ranging from 1.8 ns (red) to 2.8 ns (blue). **b** Fluorescence lifetimes in TIP60-eGFP (●) and TIP60-eGFP + UHRF1-mCherry co-transfected cells (▲). Values are means ± SEM from five independent experiments. For statistical analysis, a Student's *t*-test was performed (*** $P < 0.001$)

UHRF1 and TIP60 interaction occurs during S phase of the cell cycle

UHRF1 localization and its association with other proteins dynamically changes during the cell cycle. NP95, the murine homologue of UHRF1 associates with PCNA and chromatin in early and mid S phase of cell cycle. Moreover UHRF1 interaction with DNMT1 for maintenance of DNA methylation pattern is also dependent on the S phase of cell cycle and is more pronounced in mid and late S phase of cell cycle [38–40]. Since both UHRF1 and TIP60 are also regulating the DNMT1 levels [19] and TIP60 is also playing important roles during the G1/S phase transition and S phase of the cell cycle [30, 33], we focused on S phase to decipher the interaction between UHRF1 and TIP60. Therefore, we labeled S phase cells undergoing DNA replication with EdU (thymidine analogue) for 15 min before fixation and then, we performed FLIM analysis (Fig. 3). After this, S phase cells were identified using alexa 647 labeling for confocal microscopy study. Different sub-phases of S phase were identified by the characteristic staining of EdU which gets incorporated into the genome at the sites of active replication [41]. Early S phase cells have numerous replication foci in the nucleus as evident by bright and abundant EdU labeling in nucleus of HeLa cells (Fig. 3a). In mid S phase the replication foci are more localized to periphery of nucleus and surrounding the nucleolus (Fig. 3b) while in late S phase, very few irregular replication foci are found in nucleus at heterochromatin regions of genome (Fig. 3c). The lifetime of the TIP60-eGFP was found to be decreased in the different sub-phases of the S phase (Fig. 3a-c). When the average lifetime of TIP60-eGFP in S phase cells was compared to the total cells, it was decreased to 2.12 ± 0.03 ns and the overall FRET efficiency increased to 16.0 ± 1.2% in the S phase positive cells (Fig. 3d). These results confirm UHRF1/ TIP60 interaction during the S phase of cell cycle.

TIP60 interacts with UHRF1 through its MYST domain

It is known that UHRF1 interacts with TIP60 through its SRA and RING domains and hinders the association of TIP60 with p53 and K120 acetylation of p53 [18]. However, the TIP60 domain responsible for its interaction with UHRF1 remains to be determined. Therefore, in this study we performed in vitro pull-down assay to identify the domain of TIP60 that is responsible for interaction with UHRF1. For this, we used His-tagged mutants of the TIP60 (Fig. 4a) immobilized on Nickel NTA agarose beads and the GST-UHRF1. We observed that full length UHRF1 interacted with TIP60WT in the presence of 150 mM NaCl (Fig. 4b-c) until 500 mM NaCl (data not shown) supporting a strong interaction between both proteins. Deletion of the TIP60 zinc finger domain or the whole MYST domain significantly reduced its association with GST-UHRF1 in the pull-down assay (Fig. 4b-c). In contrast, deletion of the chromodomain and HAT domains did not significantly affect their interaction with UHRF1. Recombinant TIP60 MYST domain also had a strong association with UHRF1 like the wild type TIP60 protein (Fig. 4b-c) and this interaction was stable up to 1 M NaCl salt concentration (data not shown) predicting the TIP60 MYST domain is playing a key role in this interaction.

The FLIM-FRET technique employing different mutants of TIP60 tagged with eGFP (Fig. 5a) was further used to identify the interacting domain of TIP60 with UHRF1-mCherry inside the nucleus of HeLa cells. TIP60-eGFP wild type and mutants were co-transfected with UHRF1-mCherry and the lifetime of eGFP was measured to assess the interaction. We found that the interaction of TIP60 and UHRF1 was marginally affected by removal of TIP60 chromodomain as the average FRET of TIP60ΔCRD-eGFP co-transfected with UHRF1-mCherry was of 12.2 ± 1.3% as compared to 14.3 ± 0.6% for TIP60WT-eGFP (Fig. 5b). All other mutations affecting the MYST domain of TIP60 strongly perturbed the interaction of these mutants with UHRF1. Indeed, the lifetime of TIP60ΔZnFr-eGFP, TIP60ΔHAT-eGFP and TIP60ΔMYST-eGFP co-transfected with UHRF1-mCherry was 2.49 ± 0.01 ns, 2.46 ± 0.01 ns and 2.49 ± 0.01 ns, respectively which is quite similar to that in control sample with 2.52 ± 0.01 ns (Fig. 5b). To check whether this loss of interaction is not a result of an alteration of subcellular localization, we performed a confocal microscopy analysis of co-transfected HeLa cells. We observed that TIP60WT-eGFP and its mutants including TIP60ΔCRD-eGFP, TIP60ΔZnFr-eGFP, TIP60ΔHAT-eGFP and TIP60ΔMYST-eGFP are localized in the nucleus of HeLa cells (Fig. 6). It is also important to note that TIP60WT and mutants co-localized with UHRF1-mCherry as shown in merge panels and were closely associated to DNA labeled by DAPI. This indicates that the loss of interaction between TIP60ΔZnFr, TIP60ΔHAT and TIP60ΔMYST with UHRF1 is not due to protein delocalization.

In order to check the heterogeneity of lifetime populations in TIP60-eGFP wild type or TIP60ΔCRD-eGFP co-transfected cells showing FRET, the FLIM images were also analyzed by a two-component model: $F(t) = \alpha_1 e_1^{-t/\tau} + \alpha_2 e_2^{-t/\tau}$ [37]. This analysis provides the distribution and population of TIP60-eGFP molecules interacting with UHRF1-mCherry (having FRET) and the TIP60-eGFP molecules which are free in nucleus without having interaction with UHRF1-mCherry (having no FRET). The lifetime for the long lifetime component (τ_2) (having no FRET) was fixed according to the lifetime of eGFP in only TIP60-eGFP transfected samples, while the lifetime (τ_1) of the short

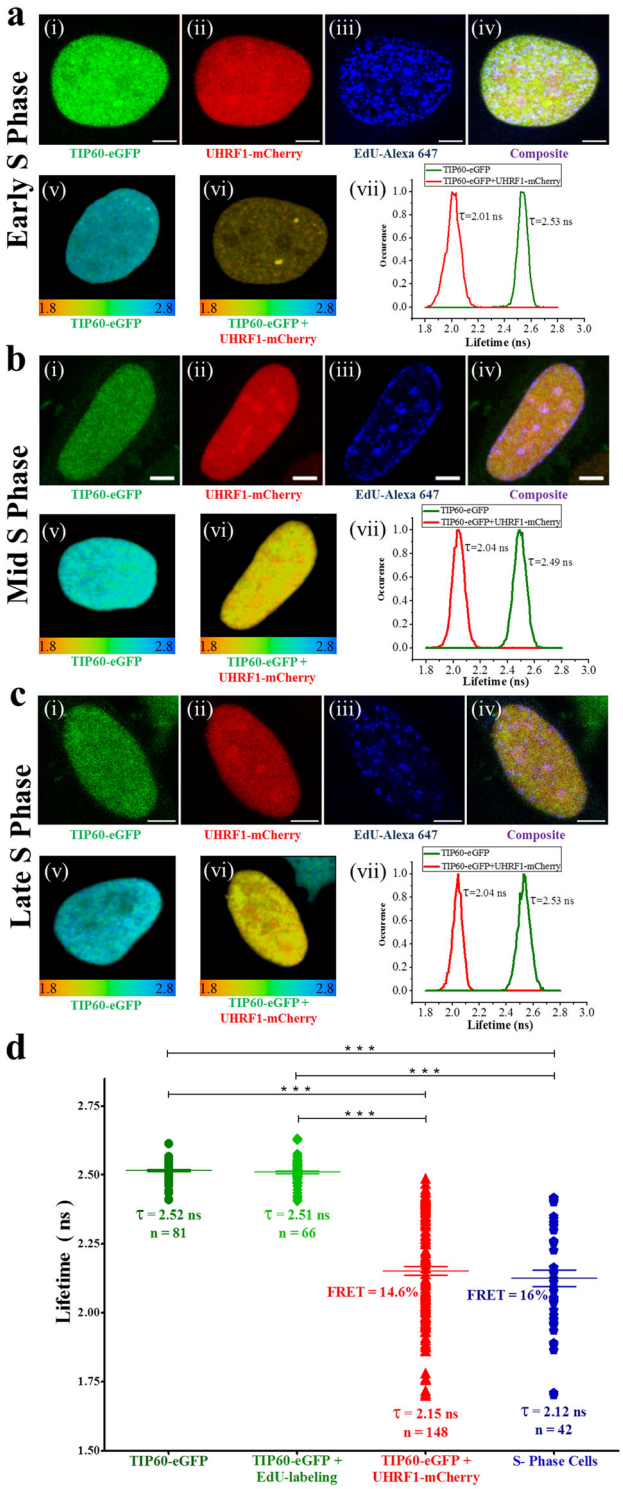

Fig. 3 Interaction between TIP60-eGFP and UHRF1-mCherry in S phase of cell cycle. **a-c** TIP60-eGFP interaction with UHRF1-mCherry in early, mid and late S phases of cell cycle, respectively. Confocal images of cells labeled with TIP60-eGFP, UHRF1-mCherry, EdU-Alexa 647 and merge, respectively (i - iv). The white bar indicates size of 5 μm. 25 μm × 25 μm FLIM images of HeLa cells transfected with TIP60-eGFP (v) or co-transfected with TIP60-eGFP and UHRF1-mCherry (vi) and lifetime distribution curves of the respected cells (vii). Color scale codes for lifetimes ranging from 1.8 ns (red) to 2.8 ns (blue). **d** Fluorescence lifetime distributions of TIP60-eGFP (●), TIP60-eGFP EdU labeled cells (◆), total TIP60-eGFP + UHRF1-mCherry co-transfected cells (▲) and co-transfected cells in S-phase of cell cycle (⬟). Values are means ± SEM from five independent experiments. For statistical analysis, a Student's *t*-test was performed (*** $P < 0.001$)

component (having FRET) and the populations of both component (α_1 and α_2) were obtained from the fits. The short lifetime component (τ_1) in TIP60WT-eGFP and TIP60ΔCRD-eGFP samples having FRET because of interaction with UHRF1-mCherry are shown in green or warmer color in FLIM images (Fig. 7a-b). The lifetime distribution curves of these FRET components for TIP60WT-eGFP and TIP60ΔCRD-eGFP are depicted in Fig. 7c. The mean value of the short lifetime component in TIP60WT-eGFP samples was 1.33 ± 0.01 ns and the average FRET calculated for this component was 45 ± 0.6% indicating close association of TIP60-eGFP with UHRF1-mCherry in HeLa cells. The mean value of the short component in TIP60ΔCRD-eGFP was 1.4 ± 0.03 ns and the average FRET calculated for this component was 43 ± 1.1% (Fig. 7c). Though the short lifetime component had almost similar values in TIP60WT-eGFP and TIP60ΔCRD-eGFP samples, the values of its corresponding population were different in the two samples as shown in Fig. 7d-e. TIP60WT-eGFP had higher population (α_1) of interacting short lifetime component as compared to TIP60ΔCRD-eGFP as its mean value in TIP60WT-eGFP was 37.5 ± 1.2% while it was 19 ± 0.3% in TIP60ΔCRD-eGFP as indicated from their respective distribution curves (Fig. 7f). This shows that TIP60ΔCRD-eGFP can interact with UHRF1-mCherry inside the nucleus but with less efficiency than TIP60WT-eGFP.

TIP60 overexpression down-regulates UHRF1 and DNMT1

Down-regulation of TIP60 has been reported in many cancers [42–45] and TIP60 has a well-established role in regulation of DNMT1. So, we investigated the consequences of TIP60-eGFP overexpression on UHRF1 and DNMT1 in HeLa cells in order to decipher the relationship between these epigenetic partners in the tumorigenesis process. Overexpression of TIP60 led to down-regulation of UHRF1 and DNMT1 in HeLa cells (Fig. 8a). UHRF1 levels were significantly reduced in TIP60-eGFP transfected cells as compared to that in untreated control cells, i.e., without any treatment or cells treated with jetPEI or transfected with eGFP alone (Fig. 8b). Similarly, DNMT1 levels were also significantly reduced in cells overexpressing TIP60-eGFP (Fig. 8c). It is interesting to observe that DNMT1 and UHRF1 levels were not affected by the overexpression of TIP60ΔMYST-eGFP in the nucleus which lacks the acetyltransferase domain of TIP60. Further, we also analyzed the effect of TIP60-eGFP overexpression on global DNA methylation levels. In accordance with the decrease in UHRF1 and DNMT1 levels, global DNA

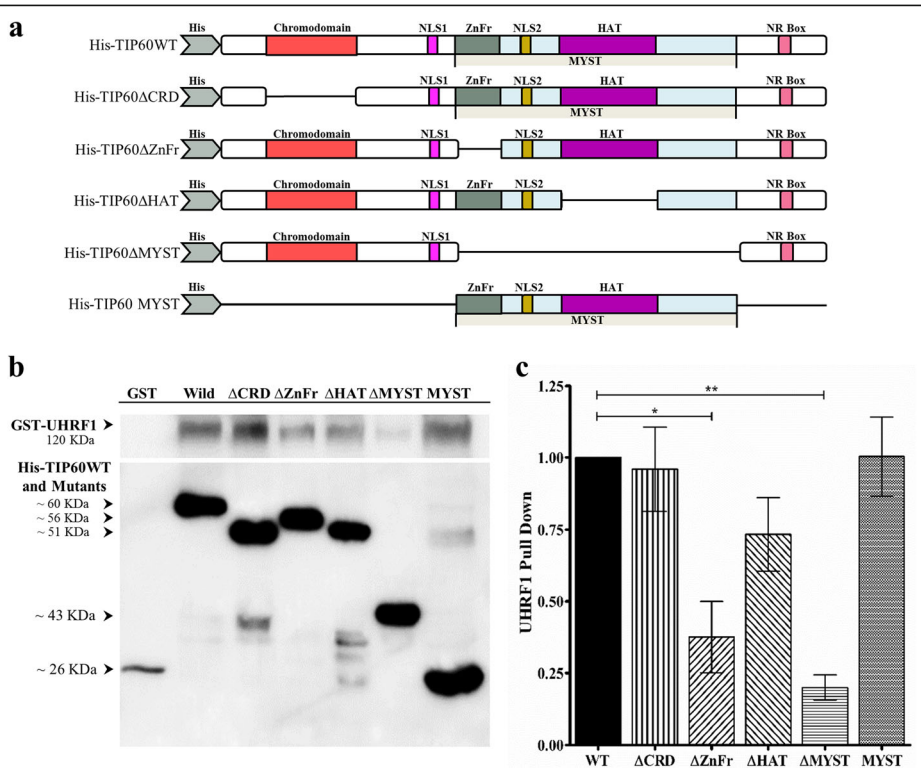

Fig. 4 In vitro pull-down analysis between His-TIP60WT/mutants and GST-UHRF1. **a**, Diagram showing His tag TIP60 wild type and mutants. **b** Western blot of in vitro pull-down assay. His tagged TIP60-WT or mutants were immobilized on Ni-NTA beads and incubated with UHRF1-GST. The complex recovered after washing were subjected to SDS PAGE and analyzed by Western blot. **c**. Western blot images were quantified by Image Studio Lite (Li-Core Biosciences USA) and statistically analyzed by using Student's *t*-test. Values are means ± SEM from three independent experiments (* $P < 0.05$, ** $P < 0.01$)

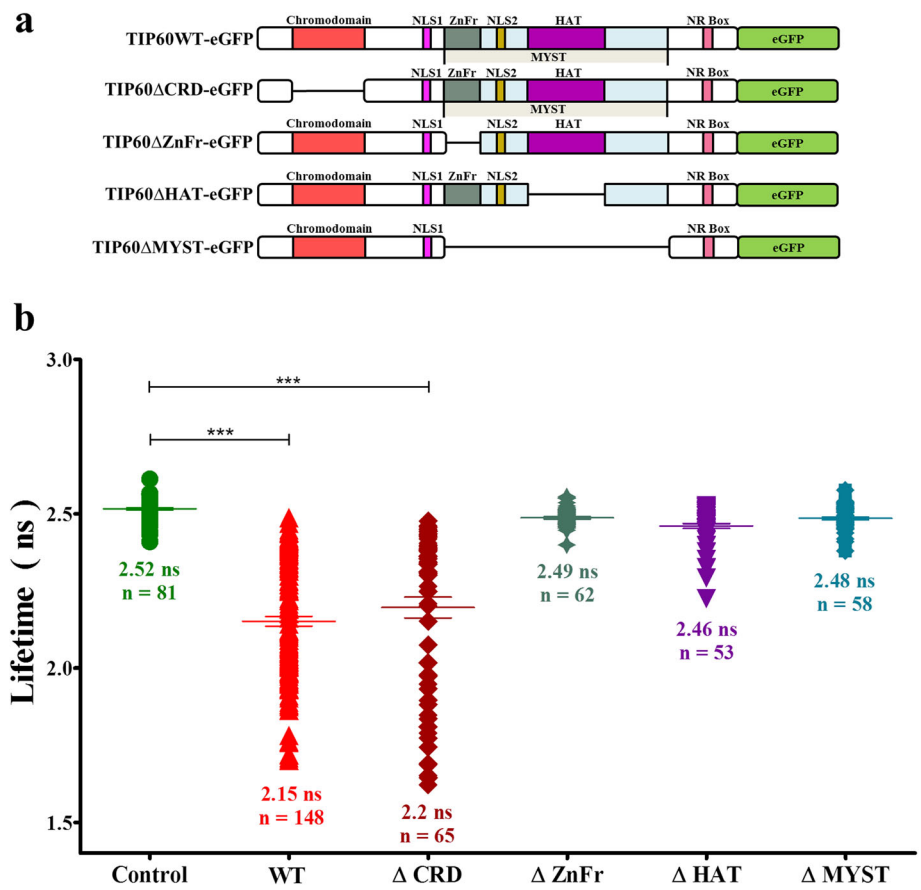

Fig. 5 Interaction between TIP60-eGFP WT/mutants and UHRF1 evidenced by FRET-FLIM. **a** Schematic diagram of TIP60WT/mutants tagged with eGFP at the C-terminus. **b** Lifetime distribution of TIP60-eGFP (●), TIP60 WT-eGFP + UHRF1-mCherry co-transfected cells (▲), TIP60 ΔCRD-eGFP + UHRF1-mCherry co-transfected cells (◆), TIP60 ΔZnFr-eGFP + UHRF1-mCherry co-transfected cells (✦), TIP60 ΔHAT-eGFP + UHRF1-mCherry co-transfected cells (▼), TIP60 ΔMYST-eGFP + UHRF1-mCherry co-transfected cells (✿). Values are means ± SEM from three to five independent experiments. For statistical analysis, a Student's *t*-test was performed (*** $P < 0.001$)

methylation also decreased by 26% after overexpression of TIP60WT-eGFP in 24 h of transfection (Fig. 8d). Overexpression of TIP60ΔCRD-eGFP also decreased the global DNA methylation by 21% (Fig. 8d), however, over expressing TIP60ΔZnFr-eGFP and TIP60ΔMYST-eGFP only lowered the DNA methylation by 9%. Overexpression of TIP60ΔHAT-eGFP had minimal effect on global DNA methylation which decreased only by 5% (Fig. 8d). Altogether these results suggest TIP60 as a regulator of DNMT1, UHRF1 and DNA methylation levels through its enzymatic activity.

Discussion

UHRF1 and TIP60 are part of large protein complexes and their conformation and association with other partners vary with the genomic activity and are regulated during cell cycle [46, 47]. Our results provided evidence for in vivo and in vitro interaction between UHRF1 and TIP60 protein by using the FLIM-FRET technique and pull-down assay. Furthermore, we could also show that MYST domain of TIP60 is playing a major role in its interaction with UHRF1. MYST domain is the conserved part of TIP60 containing a zinc finger involved in protein-protein interaction and a catalytic domain harboring its acetyltransferase activity [47]. In fact, through its MYST domain, TIP60 is able to acetylate both histones and non-histones proteins and regulates the activity of many proteins such as ATM and p53 [25, 36, 48]. Since p53-mediated apoptosis is dependent on its acetylation by TIP60 [35] therefore, interaction of TIP60 through its MYST domain with UHRF1 might impair many cellular functions. This may also explain how overexpressed UHRF1 in cancer negatively regulates the TIP60-p53 interplay in cells by preventing induction of cell cycle arrest and apoptosis. It is interesting to note that although chromodomain is not playing a direct role in its association with UHRF1 as indicated by FLIM and pull-down experiments, its removal can adversely also affect this interaction in vivo. According to two-component model, removal of chromodomain did not

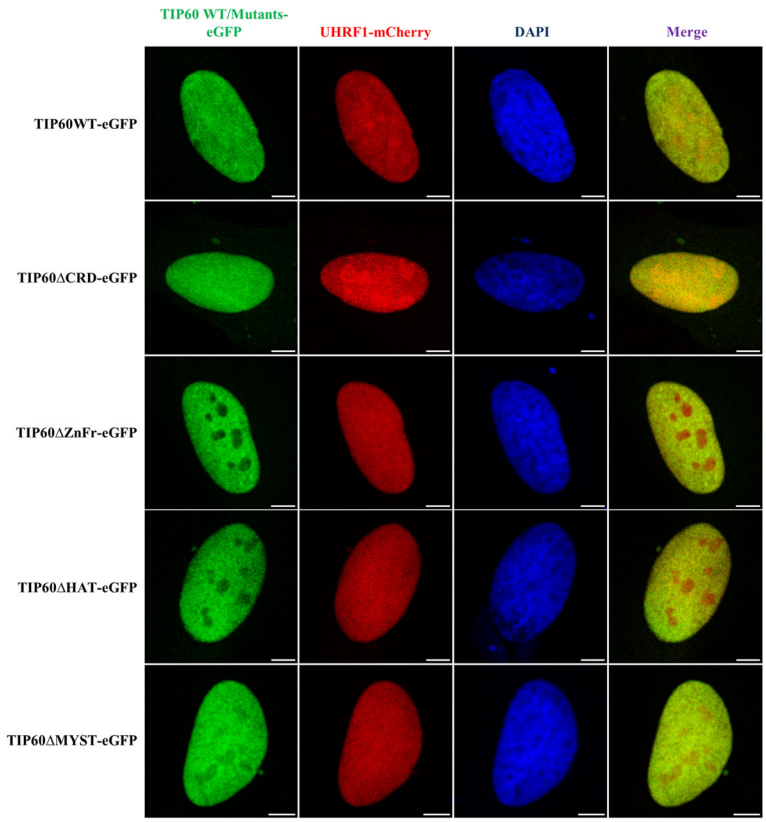

Fig. 6 Expression and localization of TIP60 mutants in HeLa cells. Confocal images show the expression and co-localization of TIP60WT-eGFP and mutants with UHRF1-mCherry in the HeLa cells with DAPI labeling. Green panel indicates TIP60 wild type or mutants tagged with eGFP, red panel shows UHRF1-mCherry, blue panel indicates DAPI and merge panel shows the composite of the TIP60-eGFP and UHRF1-mCherry panels. White bar indicates size of 5 μm

have a big impact on the mean lifetime of short component and FRET efficiencies as compared with wild type. However, the population interacting with UHRF1 was drastically reduced when chromodomain was removed from the structure of TIP60. Chromodomain helps TIP60 in reading out the histone marks and its loading to chromatin which may increase the possibility of TIP60 to interact with UHRF1 present in the same complex [49–51].

UHRF1 is a multi-domain protein which is essential for maintaining the DNA methylation during S phase of cell cycle by recruiting DNMT1 to the replication foci where it forms a multi protein complex with PCNA, DNMT1, TIP60, HDAC1, USP7 and other epigenetic partners [38, 52]. TIP60 is also well known for its role in DNA damage response to interstrand cross linkages or double strand breaks as TIP60-mediated H4K16 acetylation promotes DNA damage repair by homologous recombination (HR) pathway which dominates during the S phase of cell cycle [53, 54]. Recently the role of UHRF1 in DNA damage response has also been reported as it identifies interstrand cross linkages and double strand breaks and facilitates DNA damage repair by the same homologous recombination (HR) pathway through interaction with common partners such as FANCD2 and BRCA1 [55–57]. This predicts that UHRF1 and TIP60 may also work together in coherence to facilitate the DNA damage repair during S phase of cell cycle.

TIP60 along with UHRF1 is known to regulate levels of DNMT1 during cell cycle by inducing proteasomal degradation of DNMT1 through TIP60-mediated acetylation and subsequent ubiquitination by UHRF1 [19, 58, 59]. Accordingly, we have observed increased association of DNMT1 with UHRF1 in TIP60-eGFP transfected samples through co-immunoprecipitation experiments confirming the previous findings. DNMT1 is stabilized in cells by its direct association with USP7, a deubiquitinating enzyme which is present in the same complex. It has been recently reported that TIP60 impairs this protective association of USP7 with DNMT1 by acetylation [60]. Besides DNMT1, UHRF1 is also prevented from proteasomal degradation through its association with USP7 [16, 61, 62] and interruption of this association through cell cycle dependent kinase leads to proteasomal degradation of UHRF1 in M phase [16]. Zang and collaborators have recently suggested an identical role of

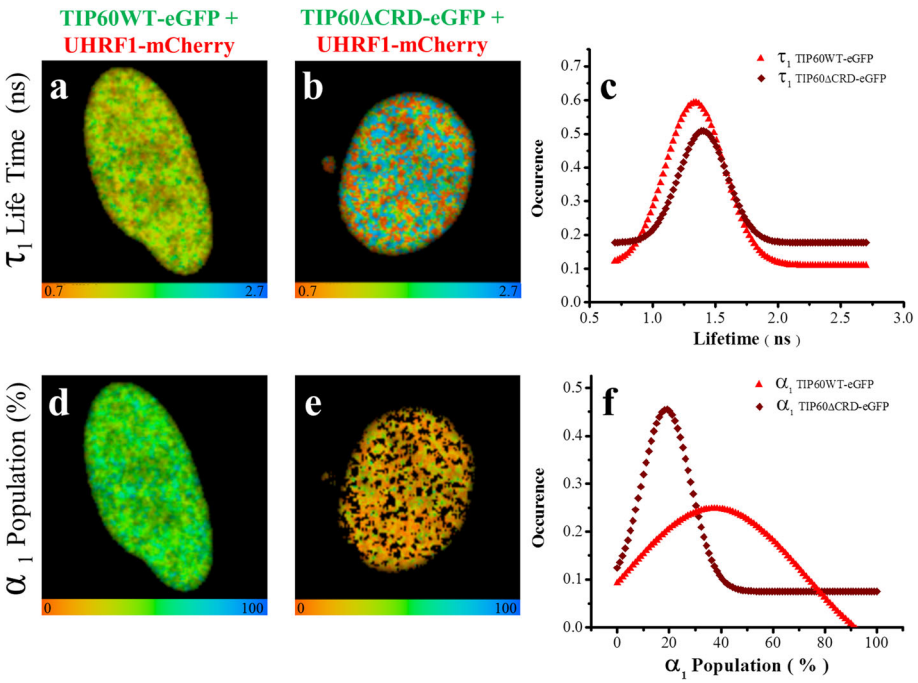

Fig. 7 Two component analyses of the fluorescence decays of TIP60WT-eGFP and TIP60ΔCRD-eGFP lifetime in presence of UHRF1-mCherry. Fluorescence decays were measured at each pixel for the respective cells by using bi-exponential model. In this model, the long-lived lifetime component (τ_2) was fixed to the lifetime of Tip6WT-eGFP when it is transfected alone in HeLa cells (2.52 ns). **a** 25 μm × 25 μm FLIM image of the distribution of τ_1 lifetimes of TIP60WT-eGFP in the presence of UHRF1-mCherry (corresponding to the component undergoing FRET). **b** 25 μm × 25 μm FLIM image of the distribution of τ_1 lifetimes of TIP60ΔCRD-eGFP in the presence of UHRF1-mCherry (corresponding to the component undergoing FRET). Color scale codes for lifetimes ranging from 0.7 ns (red) to 2.7 ns (blue). **c** Distribution of τ_1 lifetimes of TIP60WT-eGFP and TIP60ΔCRD-eGFP transfected cells in presence of UHRF1-mCherry. **d** 25 μm × 25 μm FLIM image of the population α_1 of TIP60WT-eGFP undergoing FRET in the presence of UHRF1-mCherry. **e** 25 μm × 25 μm FLIM image of the population α_1 of TIP60ΔCRD-eGFP undergoing FRET in the presence of UHRF1-mCherry. Color scale codes for population ranging from 0% (red) to 100% (blue). **f** Distribution of population α_1 for TIP60WT-eGFP and TIP60ΔCRD-eGFP transfected cells in presence of UHRF1-mCherry. Values indicated are from 148 TIP60WT-eGFP and UHRF1-mCherry co-transfected cells from five independent experiments and 65 TIP60ΔCRD-eGFP and UHRF1-mCherry co-transfected cells from three independent experiments

TIP60 in regulating the stability of UHRF1 as it regulates the stability of DNMT1. They demonstrated that UHRF1 can be acetylated by TIP60 at the K659 which lies in preferential binding area of USP7 and this acetylation greatly hampered the association of USP7 with UHRF1 [63]. Our results showed that TIP60 interacts with UHRF1 through its enzymatic MYST domain and overexpression of TIP60 in HeLa cells led to downregulation of UHRF1 suggesting another mechanism for the regulation of UHRF1 in cells.

TIP60 is found downregulated in different types of cancers and is believed to have tumor suppressor properties as oncovirus like HPV induces proliferation and tumorigenesis by destabilizing TIP60 in cervical cancer cells [42–45, 64–66]. Downregulation of TIP60 is associated with increased metastasis, decreased DNA damage response to oncogenes and poor survival of patients while enhanced TIP60 levels counters DNMT1-SNAIL2 driven epithelial to mesenchymal transition and inhibits metastasis [67]. UHRF1 on the other hand, is known to play an oncogenic role in cancer as its high expression in cancer is often related to downregulation of tumor suppressor genes through promoter hypermethylation [52, 68]. We observed that overexpression of UHRF1-mCherry decreases the protein level of TIP60-eGFP (Fig. 1d) which might be attributed to promoter hypermethylation or the E3 ligase activity of UHRF1 through which it can ubiquitinate TIP60 and may possibly reduce the level of TIP60-eGFP inside the cells [18]. This is in agreement with our previous findings where knock down of UHRF1 through siRNA upregulated the TIP60 levels in Jurkat cells [21]. It is also reported that targeting UHRF1 and DNMT1 can affect the global methylation [69, 70] and re-expression of tumor suppressor genes [2]. Our results showed that TIP60 overexpression in HeLa cells induced downregulation of UHRF1 and DNMT1, resulting in global DNA hypomethylation.

Conclusion

Epigenetic code replication machinery is a multi-protein complex which is actively involved in maintaining the epigenetic marks after the DNA replication. TIP60 and

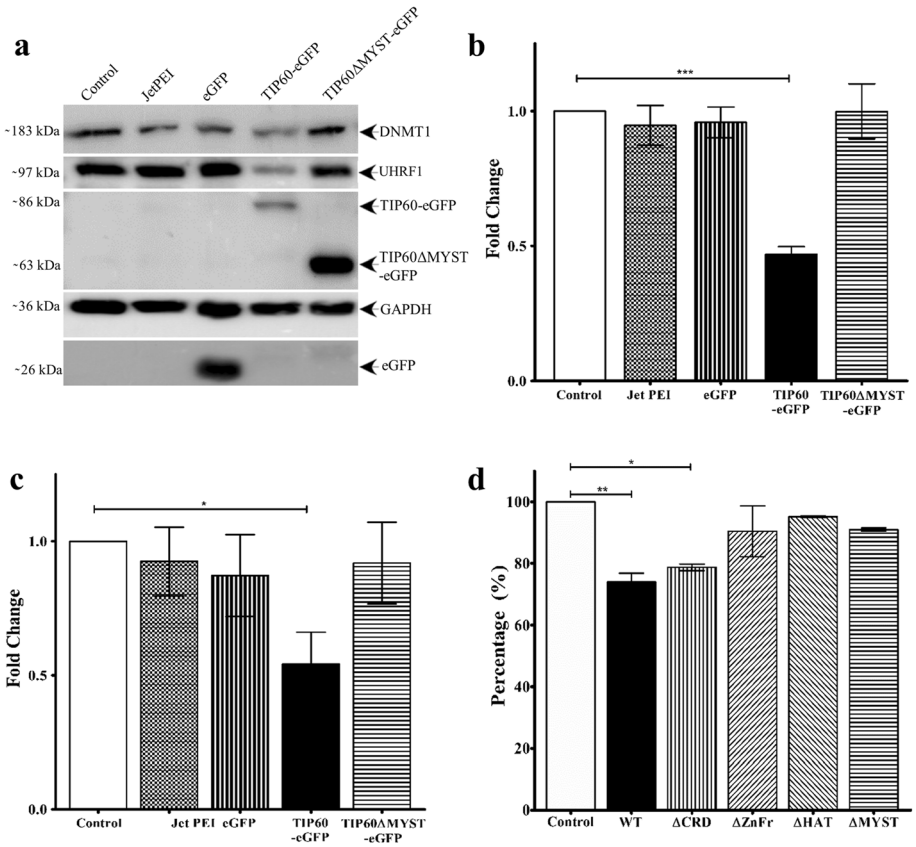

Fig. 8 TIP60 overexpression down-regulates its epigenetic partners UHRF1 and DNMT1. TIP60-eGFP was overexpressed in HeLa cells and the effect of this transient overexpression was compared to that of the control HeLa cells, HeLa cells with transfecting agent (JetPEI), HeLa cells with transfection of eGFP alone or TIP60**Δ**MYST-eGFP. **a** Western blot results showing down-regulation of UHRF1 and DNMT1 in TIP60-eGFP transfected cells. **b** Analysis of effect of TIP60-eGFP overexpression on UHRF1. **c**, Analysis of effect of TIP60-eGFP overexpression on DNMT1. Results indicated are from five independent experiments which are analyzed statistically by Student's *t*-test (* $P < 0.05$, ** $P < 0.01$, *** $P < 0.001$). **d** Effect of TIP60-eGFP overexpression on global DNA methylation. DNA was extracted from HeLa cells transfected with TIP60WT-eGFP and mutants and the methylation levels were compared to control HeLa cells. Results are indicated from three independent experiments and were analyzed by one-way ANOVA with post-hoc Tukey test. (* $P < 0.05$, ** $P < 0.01$, *** $P < 0.001$)

URHF1 are important members of this complex along with DNMT1. Here we conclude that TIP60 directly interacts with UHRF1 during the DNA replication phase of cell cycle and this interaction is dependent on the MYST domain of TIP60. Since UHRF1 interaction with TIP60 is known to perturb TIP60 mediated p53 activation, this study provides us with information to overcome this perturbation and counter the malicious transformations by utilizing the tumor suppressive role of TIP60. Finally, further investigations are required to fully decipher the dialogue within this three-way partnership involving UHRF1, DNMT1 and TIP60.

Abbreviations

ΔCRD: Chromodomain mutant; ΔHAT: Histone acetyltransferase domain mutant; ΔMYST: MYST domain mutant; ΔZnFr: Zinc Finger mutant; DNMT1: DNA methyl transferase 1; eGFP: Enhanced Green Fluorescent Protein; FLIM: Fluorescence Lifetime Imaging Microscopy; FRET: Fluorescence Resonance Energy Transfer; IP: Immunoprecipitation; TIP60: Tat interacting protein 60 kDa; UHRF1: Ubiquitin-like with PHD and RING Finger Domains 1; USP7: Ubiquitin specific protease 7; WB: Western Blotting; WT: Wild type

Acknowledgements

We thank Hugues de Rocquigny and Romain Vauchelles (Plate-forme d'Imagerie Quantitative - PIQ) for their technical support. WA and TA would also like to acknowledge funding support by the Higher Education Commission Pakistan for this work.

Funding

Our work was supported by the Agence Nationale de la Recherche (ANR-12-BS08–0003-02), the Fondation pour la Recherche Médicale (FRM DCM20111223038), Ligue contre le Cancer and by the grant ANR-10-LABX-0030-INRT, a French State fund managed by the Agence Nationale de la Recherche under the frame program Investissements d'Avenir ANR-10-IDEX-0002-02. WA and TA would also like to acknowledge funding support by the Higher Education Commission Pakistan for this work.

Availability of data and materials

Please contact corresponding author for data requests.

Authors' contributions
WA conducted most of the biochemical and cellular experiments with the help of LZ, AI and TA under the supervision of MM and CB. LR helped in the FLIM FRET experiments. WA, MA, CB and MM wrote most of the manuscript with the guidance and help of AH and YM. All authors read and approved the final manuscript.

Ethics approval and consent to participate
Not applicable

Consent for publication
Not applicable

Competing interests
The authors declare that they have no competing interests.

Publisher's Note
Springer Nature remains neutral with regard to jurisdictional claims in published maps and institutional affiliations.

Author details
[1]Laboratoire de Biophotonique et Pharmacologie, UMR 7213 CNRS, Faculté de Pharmacie, Université de Strasbourg, 74, Route du Rhin, 67401 Illkirch Cedex, France. [2]Institut de Génétique et de Biologie Moléculaire et Cellulaire, INSERM U964 CNRS UMR 7104, Université de Strasbourg, Illkirch, France. [3]Department of Biochemistry, Faculty of Science, King Abdulaziz University, Jeddah, Saudi Arabia. [4]Cancer Metabolism and Epigenetic Unit, Faculty of Science, King Abdulaziz University, Jeddah, Saudi Arabia. [5]BioTechnology Research Center (BTRC), Tripoli, Libya.

Received: 9 August 2017 Accepted: 4 December 2017
Published online: 21 December 2017

References
1. Hopfner R, Mousli M, Jeltsch JM, Voulgaris A, Lutz Y, Marin C, et al. ICBP90, a novel human CCAAT binding protein, involved in the regulation of topoisomerase IIalpha expression. Cancer Res. 2000;60(1):121–8.
2. Krifa M, Alhosin M, Muller CD, Gies JP, Chekir-Ghedira L, Ghedira K, et al. Limoniastrum guyonianum aqueous gall extract induces apoptosis in human cervical cancer cells involving p16 INK4A re-expression related to UHRF1 and DNMT1 down-regulation. J Exp Clin Cancer Res. 2013;32:30.
3. Arita K, Ariyoshi M, Tochio H, Nakamura Y, Shirakawa M. Recognition of hemi-methylated DNA by the SRA protein UHRF1 by a base-flipping mechanism. Nature. 2008;455(7214):818–21.
4. Avvakumov GV, Walker JR, Xue S, Li Y, Duan S, Bronner C, et al. Structural basis for recognition of hemi-methylated DNA by the SRA domain of human UHRF1. Nature. 2008;455(7214):822–5.
5. Hashimoto H, Horton JR, Zhang X, Bostick M, Jacobsen SE, Cheng X. The SRA domain of UHRF1 flips 5-methylcytosine out of the DNA helix. Nature. 2008;455(7214):826–9.
6. Liu X, Gao Q, Li P, Zhao Q, Zhang J, Li J, et al. UHRF1 targets DNMT1 for DNA methylation through cooperative binding of hemi-methylated DNA and methylated H3K9. Nat Commun. 2013;4:1563.
7. Nady N, Lemak A, Walker JR, Avvakumov GV, Kareta MS, Achour M, et al. Recognition of multivalent histone states associated with heterochromatin by UHRF1 protein. J Biol Chem. 2011;286(27):24300–11.
8. Nishiyama A, Yamaguchi L, Sharif J, Johmura Y, Kawamura T, Nakanishi K, et al. Uhrf1-dependent H3K23 ubiquitylation couples maintenance DNA methylation and replication. Nature. 2013;502(7470):249–53.
9. Qin W, Wolf P, Liu N, Link S, Smets M, La Mastra F, et al. DNA methylation requires a DNMT1 ubiquitin interacting motif (UIM) and histone ubiquitination. Cell Res. 2015;25(8):911–29.
10. Mousli M, Hopfner R, Abbady AQ, Monte D, Jeanblanc M, Oudet P, et al. ICBP90 belongs to a new family of proteins with an expression that is deregulated in cancer cells. Br J Cancer. 2003;89(1):120–7.
11. Ashraf W, Ibrahim A, Alhosin M, Zaayter L, Ouararhni K, Papin C, et al. The epigenetic integrator UHRF1: on the road to become a universal biomarker for cancer. Oncotarget. 2017;8:51946.
12. Boukhari A, Alhosin M, Bronner C, Sagini K, Truchot C, Sick E, et al. CD47 activation-induced UHRF1 over-expression is associated with silencing of tumor suppressor gene p16INK4A in glioblastoma cells. Anticancer Res. 2015;35(1):149–57.
13. Jeanblanc M, Mousli M, Hopfner R, Bathami K, Martinet N, Abbady AQ, et al. The retinoblastoma gene and its product are targeted by ICBP90: a key mechanism in the G1/S transition during the cell cycle. Oncogene. 2005; 24(49):7337–45.
14. Unoki M, Brunet J, Mousli M. Drug discovery targeting epigenetic codes: the great potential of UHRF1, which links DNA methylation and histone modifications, as a drug target in cancers and toxoplasmosis. Biochem Pharmacol. 2009;78(10):1279–88.
15. Wang F, Yang YZ, Shi CZ, Zhang P, Moyer MP, Zhang HZ, et al. UHRF1 promotes cell growth and metastasis through repression of p16(ink(4)a) in colorectal cancer. Ann Surg Oncol. 2012;19(8):2753–62.
16. Ma H, Chen H, Guo X, Wang Z, Sowa ME, Zheng L, et al. M phase phosphorylation of the epigenetic regulator UHRF1 regulates its physical association with the deubiquitylase USP7 and stability. Proc Natl Acad Sci U S A. 2012;109(13):4828–33.
17. Bronner C. Control of DNMT1 abundance in epigenetic inheritance by acetylation, ubiquitylation, and the histone code. Sci Signal. 2011;4(157):pe3.
18. Dai C, Shi D, Gu W. Negative regulation of the acetyltransferase TIP60-p53 interplay by UHRF1 (ubiquitin-like with PHD and RING finger domains 1). J Biol Chem. 2013;288(27):19581–92.
19. Du Z, Song J, Wang Y, Zhao Y, Guda K, Yang S, et al. DNMT1 stability is regulated by proteins coordinating deubiquitination and acetylation-driven ubiquitination. Sci Signal. 2010;3(146):ra80.
20. Guan D, Factor D, Liu Y, Wang Z, Kao HY. The epigenetic regulator UHRF1 promotes ubiquitination-mediated degradation of the tumor-suppressor protein promyelocytic leukemia protein. Oncogene. 2013;32(33):3819–28.
21. Achour M, Fuhrmann G, Alhosin M, Ronde P, Chataigneau T, Mousli M, et al. UHRF1 recruits the histone acetyltransferase Tip60 and controls its expression and activity. Biochem Biophys Res Commun. 2009;390(3):523–8.
22. Doyon Y, Selleck W, Lane WS, Tan S, Cote J. Structural and functional conservation of the NuA4 histone acetyltransferase complex from yeast to humans. Mol Cell Biol. 2004;24(5):1884–96.
23. Kamine J, Elangovan B, Subramanian T, Coleman D, Chinnadurai G. Identification of a cellular protein that specifically interacts with the essential cysteine region of the HIV-1 tat transactivator. Virology. 1996;216(2):357–66.
24. Lee KK, Workman JL. Histone acetyltransferase complexes: one size doesn't fit all. Nat Rev Mol Cell Biol. 2007;8(4):284–95.
25. Yamamoto T, Horikoshi M. Novel substrate specificity of the histone acetyltransferase activity of HIV-1-tat interactive protein Tip60. J Biol Chem. 1997;272(49):30595–8.
26. Gaughan L, Logan IR, Cook S, Neal DE, Robson CN. Tip60 and histone deacetylase 1 regulate androgen receptor activity through changes to the acetylation status of the receptor. J Biol Chem. 2002;277(29):25904–13.
27. Ikura T, Ogryzko VV, Grigoriev M, Groisman R, Wang J, Horikoshi M, et al. Involvement of the TIP60 histone acetylase complex in DNA repair and apoptosis. Cell. 2000;102(4):463–73.
28. Murr R, Loizou JI, Yang YG, Cuenin C, Li H, Wang ZQ, et al. Histone acetylation by Trrap-Tip60 modulates loading of repair proteins and repair of DNA double-strand breaks. Nat Cell Biol. 2006;8(1):91–9.
29. Squatrito M, Gorrini C, Amati B. Tip60 in DNA damage response and growth control: many tricks in one HAT. Trends Cell Biol. 2006;16(9): 433–42.
30. DeRan M, Pulvino M, Greene E, Su C, Zhao J. Transcriptional activation of histone genes requires NPAT-dependent recruitment of TRRAP-Tip60 complex to histone promoters during the G1/S phase transition. Mol Cell Biol. 2008;28(1):435–47.
31. Mo F, Zhuang X, Liu X, Yao PY, Qin B, Su Z, et al. Acetylation of aurora B by TIP60 ensures accurate chromosomal segregation. Nat Chem Biol. 2016; 12(4):226–32.
32. Niida H, Katsuno Y, Sengoku M, Shimada M, Yukawa M, Ikura M, et al. Essential role of Tip60-dependent recruitment of ribonucleotide reductase at DNA damage sites in DNA repair during G1 phase. Genes Dev. 2010; 24(4):333–8.
33. Taubert S, Gorrini C, Frank SR, Parisi T, Fuchs M, Chan HM, et al. E2F-dependent histone acetylation and recruitment of the Tip60 acetyltransferase complex to chromatin in late G1. Mol Cell Biol. 2004;24(10):4546–56.
34. Berns K, Hijmans EM, Mullenders J, Brummelkamp TR, Velds A, Heimerikx M, et al. A large-scale RNAi screen in human cells identifies new components of the p53 pathway. Nature. 2004;428(6981):431–7.

35. Sykes SM, Mellert HS, Holbert MA, Li K, Marmorstein R, Lane WS, et al. Acetylation of the p53 DNA-binding domain regulates apoptosis induction. Mol Cell. 2006;24(6):841–51.
36. Tang Y, Luo J, Zhang W, Gu W. Tip60-dependent acetylation of p53 modulates the decision between cell-cycle arrest and apoptosis. Mol Cell. 2006;24(6):827–39.
37. El Meshri SE, Dujardin D, Godet J, Richert L, Boudier C, Darlix JL, et al. Role of the nucleocapsid domain in HIV-1 Gag oligomerization and trafficking to the plasma membrane: a fluorescence lifetime imaging microscopy investigation. J Mol Biol. 2015;427(6 Pt B):1480–94.
38. Bostick M, Kim JK, Esteve PO, Clark A, Pradhan S, Jacobsen SE. UHRF1 plays a role in maintaining DNA methylation in mammalian cells. Science. 2007; 317(5845):1760–4.
39. Miura M, Watanabe H, Sasaki T, Tatsumi K, Muto M. Dynamic changes in subnuclear NP95 location during the cell cycle and its spatial relationship with DNA replication foci. Exp Cell Res. 2001;263(2):202–8.
40. Zhang J, Gao Q, Li P, Liu X, Jia Y, Wu W, et al. S phase-dependent interaction with DNMT1 dictates the role of UHRF1 but not UHRF2 in DNA methylation maintenance. Cell Res. 2011;21(12):1723–39.
41. Chakalova L, Debrand E, Mitchell JA, Osborne CS, Fraser P. Replication and transcription: shaping the landscape of the genome. Nat Rev Genet. 2005;6(9):669–77.
42. Bassi C, Li YT, Khu K, Mateo F, Baniasadi PS, Elia A, et al. The acetyltransferase Tip60 contributes to mammary tumorigenesis by modulating DNA repair. Cell Death Differ. 2016;23(7):1198–208.
43. Chen G, Cheng Y, Tang Y, Martinka M, Li G. Role of Tip60 in human melanoma cell migration, metastasis, and patient survival. J Invest Dermatol. 2012;132(11):2632–41.
44. Sakuraba K, Yasuda T, Sakata M, Kitamura YH, Shirahata A, Goto T, et al. Down-regulation of Tip60 gene as a potential marker for the malignancy of colorectal cancer. Anticancer Res. 2009;29(10):3953–5.
45. Sakuraba K, Yokomizo K, Shirahata A, Goto T, Saito M, Ishibashi K, et al. TIP60 as a potential marker for the malignancy of gastric cancer. Anticancer Res. 2011;31(1):77–9.
46. Gelato KA, Tauber M, Ong MS, Winter S, Hiragami-Hamada K, Sindlinger J, et al. Accessibility of different histone H3-binding domains of UHRF1 is allosterically regulated by phosphatidylinositol 5-phosphate. Mol Cell. 2014; 54(6):905–19.
47. Sapountzi V, Logan IR, Robson CN. Cellular functions of TIP60. Int J Biochem Cell Biol. 2006;38(9):1496–509.
48. Sun Y, Jiang X, Chen S, Fernandes N, Price BD. A role for the Tip60 histone acetyltransferase in the acetylation and activation of ATM. Proc Natl Acad Sci U S A. 2005;102(37):13182–7.
49. Kim CH, Kim JW, Jang SM, An JH, Seo SB, Choi KH. The chromodomain-containing histone acetyltransferase TIP60 acts as a code reader, recognizing the epigenetic codes for initiating transcription. Biosci Biotechnol Biochem. 2015;79(4):532–8.
50. Kim MY, Ann EJ, Kim JY, Mo JS, Park JH, Kim SY, et al. Tip60 histone acetyltransferase acts as a negative regulator of Notch1 signaling by means of acetylation. Mol Cell Biol. 2007;27(18):6506–19.
51. Sun Y, Jiang X, Xu Y, Ayrapetov MK, Moreau LA, Whetstine JR, et al. Histone H3 methylation links DNA damage detection to activation of the tumour suppressor Tip60. Nat Cell Biol. 2009;11(11):1376–82.
52. Alhosin M, Sharif T, Mousli M, Etienne-Selloum N, Fuhrmann G, Schini-Kerth VB, et al. Down-regulation of UHRF1, associated with re-expression of tumor suppressor genes, is a common feature of natural compounds exhibiting anti-cancer properties. J Exp Clin Cancer Res. 2011;30:41.
53. Renaud E, Barascu A, Rosselli F. Impaired TIP60-mediated H4K16 acetylation accounts for the aberrant chromatin accumulation of 53BP1 and RAP80 in Fanconi anemia pathway-deficient cells. Nucleic Acids Res. 2016;44(2):648–56.
54. Tang J, Cho NW, Cui G, Manion EM, Shanbhag NM, Botuyan MV, et al. Acetylation limits 53BP1 association with damaged chromatin to promote homologous recombination. Nat Struct Mol Biol. 2013;20(3):317–25.
55. Liang CC, Zhan B, Yoshikawa Y, Haas W, Gygi SP, Cohn MA. UHRF1 is a sensor for DNA interstrand crosslinks and recruits FANCD2 to initiate the Fanconi anemia pathway. Cell Rep. 2015;10(12):1947–56.
56. Tian Y, Paramasivam M, Ghosal G, Chen D, Shen X, Huang Y, et al. UHRF1 contributes to DNA damage repair as a lesion recognition factor and nuclease scaffold. Cell Rep. 2015;10(12):1957–66.
57. Zhang H, Liu H, Chen Y, Yang X, Wang P, Liu T, et al. A cell cycle-dependent BRCA1-UHRF1 cascade regulates DNA double-strand break repair pathway choice. Nat Commun. 2016;7:10201.
58. Qin W, Leonhardt H, Spada F. Usp7 and Uhrf1 control ubiquitination and stability of the maintenance DNA methyltransferase Dnmt1. J Cell Biochem. 2011;112(2):439–44.
59. Shamma A, Suzuki M, Hayashi N, Kobayashi M, Sasaki N, Nishiuchi T, et al. ATM mediates pRB function to control DNMT1 protein stability and DNA methylation. Mol Cell Biol. 2013;33(16):3113–24.
60. Cheng J, Yang H, Fang J, Ma L, Gong R, Wang P, et al. Molecular mechanism for USP7-mediated DNMT1 stabilization by acetylation. Nat Commun. 2015;6:7023.
61. Chen H, Ma H, Inuzuka H, Diao J, Lan F, Shi YG, et al. DNA damage regulates UHRF1 stability via the SCF(beta-TrCP) E3 ligase. Mol Cell Biol. 2013;33(6):1139–48.
62. Felle M, Joppien S, Nemeth A, Diermeier S, Thalhammer V, Dobner T, et al. The USP7/Dnmt1 complex stimulates the DNA methylation activity of Dnmt1 and regulates the stability of UHRF1. Nucleic Acids Res. 2011;39(19): 8355–65.
63. Zhang ZM, Rothbart SB, Allison DF, Cai Q, Harrison JS, Li L, et al. An Allosteric interaction links USP7 to Deubiquitination and chromatin targeting of UHRF1. Cell Rep. 2015;12(9):1400–6.
64. Gorrini C, Squatrito M, Luise C, Syed N, Perna D, Wark L, et al. Tip60 is a haplo-insufficient tumour suppressor required for an oncogene-induced DNA damage response. Nature. 2007;448(7157):1063–7.
65. Jha S, Vande Pol S, Banerjee NS, Dutta AB, Chow LT, Dutta A. Destabilization of TIP60 by human papillomavirus E6 results in attenuation of TIP60-dependent transcriptional regulation and apoptotic pathway. Mol Cell. 2010; 38(5):700–11.
66. Subbaiah VK, Zhang Y, Rajagopalan D, Abdullah LN, Yeo-Teh NS, Tomaic V, et al. E3 ligase EDD1/UBR5 is utilized by the HPV E6 oncogene to destabilize tumor suppressor TIP60. Oncogene. 2016;35(16):2062–74.
67. Zhang Y, Subbaiah VK, Rajagopalan D, Tham CY, Abdullah LN, Toh TB, et al. TIP60 inhibits metastasis by ablating DNMT1-SNAIL2-driven epithelial-mesenchymal transition program. J Mol Cell Biol. 2016;
68. Alhosin M, Omran Z, Zamzami MA, Al-Malki AL, Choudhry H, Mousli M, et al. Signalling pathways in UHRF1-dependent regulation of tumor suppressor genes in cancer. J Exp Clin Cancer Res. 2016;35(1):174.
69. Rothbart SB, Dickson BM, Ong MS, Krajewski K, Houliston S, Kireev DB, et al. Multivalent histone engagement by the linked tandem Tudor and PHD domains of UHRF1 is required for the epigenetic inheritance of DNA methylation. Genes Dev. 2013;27(11):1288–98.
70. Seo JS, Choi YH, Moon JW, Kim HS, Park SH. Hinokitiol induces DNA demethylation via DNMT1 and UHRF1 inhibition in colon cancer cells. BMC Cell Biol. 2017;18(1):14.

Submit your next manuscript to BioMed Central and we will help you at every step:

- We accept pre-submission inquiries
- Our selector tool helps you to find the most relevant journal
- We provide round the clock customer support
- Convenient online submission
- Thorough peer review
- Inclusion in PubMed and all major indexing services
- Maximum visibility for your research

Submit your manuscript at
www.biomedcentral.com/submit

Résumé en Français

L’épigénétique a permis des avancées majeures dans les cancers humains ces dernières années. En effet, la compréhension de l'épigénome du cancer a permis de mieux comprendre les mécanismes moléculaires impliqués dans la cancérogenèse et les moyens possibles de les cibler. Les modifications épigénétiques sont connues pour leur réversibilité, une caractéristique centrale qui fait de la thérapie épigénétique une stratégie prometteuse pour lutter contre les modifications épigénétiques anormales qui se produisent dans les cancers.

La méthylation de l'ADN est la première marque épigénétique identifiée et étroitement associée au cancer. La méthylation abondante de l'ADN dans les régions promotrices des gènes suppresseurs de tumeurs joue un rôle clé dans la répression de leur transcription (1, 2). Afin de parvenir à une transmission fidèle du code épigénétique, la machinerie de méthylation de l'ADN est coordonnée par la protéine UHRF1 (Ubiquitin-like, containing PHD and RING fingers domains), un régulateur épigénétique essentiel.

UHRF1 est une protéine multifonctionnelle caractérisée par ses domaines multiples. Elle assure la reconnaissance du statut de méthylation de l'ADN et du statut de modification des histones. Le domaine SRA de UHRF1 joue un rôle pivot dans la transmission des profils de méthylation en coordonnant la reconnaissance de l'ADN hémiméthylé, le recrutement de l'ADN méthyltransférase 1 (DNMT1) et l'interaction avec différentes protéines impliquées dans la régulation épigénétique telles que HDAC1 et l'histone méthyltransférase G9a. UHRF1 grâce à son domaine SRA se lie spécifiquement à l'ADN hémi-méthylé et fait basculer la cytosine méthylée (5-mC) vers l’extérieur de l'hélice d'ADN. Ce basculement guide DNMT1, l'enzyme responsable de la méthylation, pour méthyler le nouveau brin opposé de l’ADN. UHRF1 joue également un rôle essentiel en tant que promoteur tumoral, car son niveau d’expression est fortement augmenté dans la majorité des cancers tels que le carcinome hépatocellulaire, le cancer du sein, le cancer gastrique, le cancer de la vésicule biliaire et son abondance semble être corrélée avec l'agressivité tumorale.

La régulation de l'expression d’UHRF1 dépend du cycle cellulaire dans les cellules normales, mais cette expression reste élevée tout au long du cycle cellulaire dans de multiples tumeurs. La propriété oncogénique d’UHRF1 est également favorisée par la régulation de la fonction de certains gènes suppresseurs de tumeurs (TSGs). Elle inhibe un certain nombre d'entre eux, y compris p16INK4A,

HlC1, RB1, après le recrutement DNMT1 et HDAC1 conduisant à l'hyperméthylation de leur promoteur. Ainsi, à travers ce mécanisme répressif, UHRF1 affecte le rôle de ces gènes dans la prévention de la tumorigénèse. De nombreuses études ont également souligné l'implication d'UHRF1 dans la promotion de la prolifération des cellules cancéreuses en facilitant leur passage à travers les points de contrôle du cycle cellulaire ainsi que la régulation de plusieurs activités biologiques telles que l'apoptose et la migration cellulaire. Ceci fait de la protéine UHRF1 une cible de choix pour le traitement du cancer.

Récemment, de nombreuses drogues tels que les inhibiteurs d'HDAC, les inhibiteurs de DNMT, HMTi, SIRTi, HATi et divers types de kinases ont été découverts. Ces médicaments sont capables de cibler la machinerie épigénétique et de rétablir l'état normal de méthylation de l'ADN et des modifications des histones dans l'oncogenèse. Cependant, les traitements épigénétiques disponibles sont confrontés à divers problèmes :

- Premièrement, la protéine cible n'est pas limitée aux cellules cancéreuses et est également exprimée dans des cellules saines. C'est le cas de la DNMT1, ciblée par des analogues de la cytidine, qui est exprimée dans les deux types de cellules.
- Le deuxième facteur est que la molécule n'inhibe pas spécifiquement la protéine cible, comme dans le cas des inhibiteurs d'HDAC qui agissent en ciblant tous ou plusieurs HDACs en même temps.

Par conséquent, il est impératif de travailler sur de nouvelles molécules plus spécifiques ciblant de nouvelles cibles afin de réduire les dommages sur les tissus normaux. UHRF1 apparaît comme une cible thérapeutique de choix par sa relation avec l'oncogenèse, mais aussi par le fait qu'en comparaison avec DNMT1 et HDAC1, le niveau d'expression d'UHRF1 est faible dans les tissus normaux, ce qui devrait induire moins d'effets secondaires en thérapie anti-cancéreuse.

Dans ce contexte, notre objectif principal est d'identifier et caractériser de nouveaux inhibiteurs d'UHRF1 à activité anti-tumorale capables de prévenir la méthylation aberrante de l'ADN en ciblant le domaine SRA d'UHRF1. L'originalité du projet repose sur le fait qu'à ce jour, aucun inhibiteur d'UHRF1 n'a atteint la phase clinique. Le projet est basé sur un cadre méthodologique bien établi et repose sur une approche multi-disciplinaire combinant du criblage virtuel et de la

chimie avec des techniques biophysiques et des tests pharmacologiques cellulaires afin de découvrir de nouveaux inhibiteurs de la protéine UHRF1.

Notre approche est basée en premier lieu sur un criblage virtuel in silico. A cette fin, une banque de composés disponibles dans le commerce (Zinc database) a été criblée sur la base de plusieurs critères (liaison au domaine SRA d'UHRF1, affinité théorique, caractéristiques pharmacophoriques). Suite au criblage virtuel, nous avons sélectionné 71 molécules représentant différentes structures chimiques et familles.

Pour tester ces molécules, nous avons mis au point un « **test de basculement de la cytosine »** en fluorescence, qui nous a permis d'avoir une image dynamique du complexe SRA / ADN en présence des molécules étudiées. Pendant la division cellulaire, la liaison du domaine SRA à l'ADN hémiméthylé avec le retournement de la méthylcytosine est considérée comme une étape critique pour le recrutement de la DNMT1, responsable du maintien de la méthylation de l'ADN. Pour cela, un analogue fluorescent de nucléobase, la thiénoguanine thG qui substitue parfaitement la guanine de l'ADN a été utilisé. Incorporant la thG à une position donnée d'un ADN double brin hémiméthylé, on a pu suivre de manière sensible le basculement de la cytosine méthylée, induit par le domaine SRA de UHRF1. En se basant sur l'augmentation du rendement quantique d'un facteur ~ 4 lors de ce basculement par rapport au rendement initial quand l'ADN est tout seul, l'addition de l'inhibiteur doit empêcher le basculement de la cytosine ce qui résultera une diminution du rendement quantique. L'activité est évaluée en présence et en absence de celui-ci.

Ce criblage secondaire des molécules sélectionnées *in vitro,* nous a permis d'identifier un composé issu de la deuxième série de molécules qui appartient à la famille des anthraquinones, l'UM63, qui s'est révélé avoir une activité inhibitrice d'UHRF1, en altérant la liaison du domaine SRA à l'ADN hémiméthylé et en inhibant le basculement de 5mC avec une valeur d'IC50 de l'ordre de micromolaire. La troisième série composée de 6 molécules analogues au composé UM63 a révélé deux molécules (UM63B, UM63D) qui ont montré un effet inhibiteur sur le basculement de la cytosine. Chacun des composés actifs a été testé à différentes concentrations (1 µM, 3 µM, 10 µM, 30 µM, 100 µM). Le composé UM63B étant cancérogène, seuls les composés UM63 et UM63D étaient étudiés afin d'élucider leur mécanisme d'action.

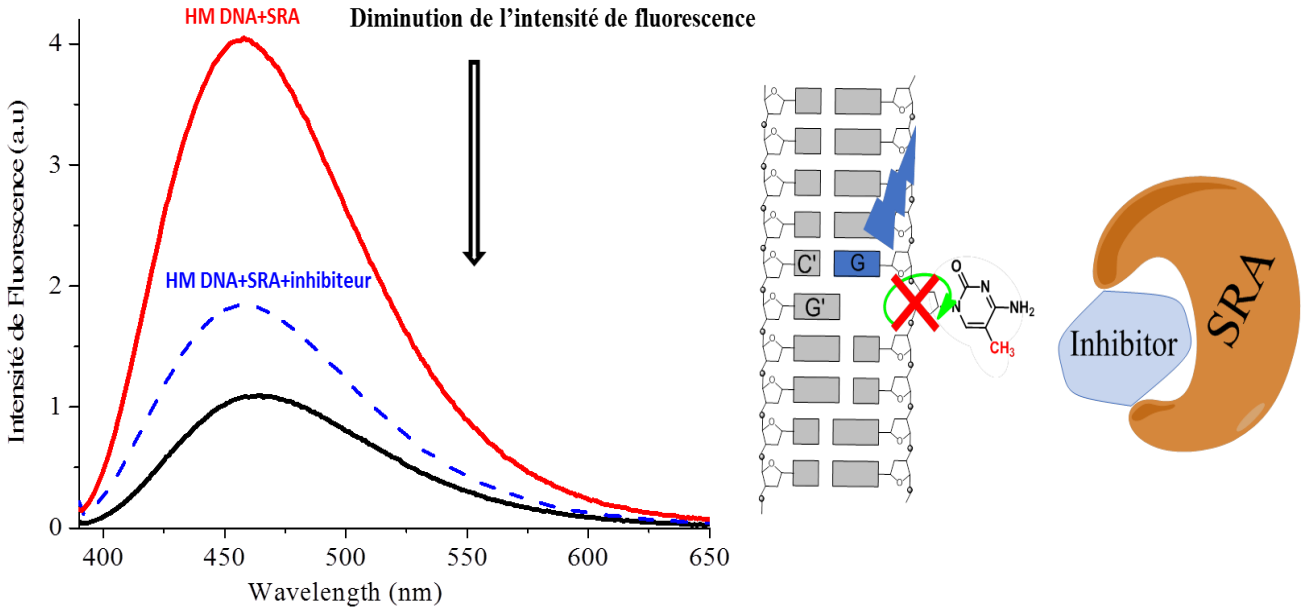

Figure 1. Principe du test de suivi du basculement de la cytosine par le domaine SRA d'UHRF1. L'ADN hémiméthylé est marqué avec la base fluorescente thG, qui substitue la guanine voisine de la cytosine méthylée. La liaison de SRA qui induit le basculement de la cytosine méthylée conduit à une forte augmentation de la fluorescence de la thG. La perturbation de la liaison entre le domaine SRA et l'ADN hémiméthylé par les molécules actives doit empêcher le basculement de la cytosine méthylée et induire ainsi une diminution de l'intensité de la fluorescence.

Afin de suivre la liaison de ces composés avec le domaine SRA, nous avons réalisé des expériences de titration par calorimétrie isotherme (ITC). Cette technique nous a permis de déterminer les paramètres de liaison en mesurant la chaleur libérée ou absorbée au cours de l'interaction. Nous avons déterminé que l'affinité (K_d) du composé UM63 pour le domaine SRA est de 0.73± 0.03 µM. Le composé UM63D ne démontrait aucun changement de chaleur lors sa titration avec le domaine SRA d'UHRF1. Cependant, les deux composés ont montré une liaison à l'ADN hémiméthylé avec des constantes d'affinité k_d de 0.13 ± 0.01 µM, 0.15 ± 0.08 µM respectivement por UM63 et UM63D.

Pour démontrer la spécificité de la liaison de l'UM63 à la poche du domaine SRA d'UHRF1, on a utilisé le mutant G488D. Nous avons montré que l'UM63 n'était pas capable de se lier à ce mutant où la glycine 448 est remplacée par un acide aspartique plus volumineux qui empêche le

basculement de la cytosine méthylée dans la poche de liaison. Donc UM63 se lierait à cette poche. Il est à noter que ce test a été utilisé pour la première fois et que les résultats obtenus mettent en évidence son potentiel comme méthode de criblage de petites molécules inhibitrices d'UHRF1.

En plus, nous avons suivi par anisotropie de fluorescence, une technique qui mesure la dépolarisation de fluorescence, la liaison de la protéine SRA à l'ADN en absence et en présence des inhibiteurs. Nous avons observé une diminution de l'affinité du domaine SRA à l'ADN indiquant que ces molécules empêchent la liaison entre le domaine SRA et l'ADN. Pour étudier davantage l'inhibition de basculement de base par UM63, nous avons étudié par la technique de stopped flow comment UM63 modifie la cinétique de basculement de 5mC induite par SRA dans l'ADN marqué par thG. L'addition d'UM63 ne fait que réduire légèrement la constante de vitesse cinétique, mais réduit efficacement le niveau de fluorescence final d'une manière dépendante de la concentration correspond à la coexistence d'une population SRA liée à UM63 incapable de retourner la base de 5mC avec une population de SRA libre qui retourne 5mC avec une cinétique non modifiée.

Les expériences d'immunofluorescence ont montré que les effets induits après le traitement des cellules avec UM63 au niveau du complexe UHRF1/DNMT1 ont provoqué une baisse au niveau de la méthylation de l'ADN global.

2. Effet du composé UM63 sur les interactions protéiques impliquant UHRF1

Pour évaluer les effets des composés sélectionnés par le criblage secondaire sur l'interaction *in cellulo* entre UHRF1 et DNMT1 impliqués dans l'hérédité du code épigénétique, la technique d'imagerie par temps de vie de fluorescence sera utilisée pour suivre le transfert résonant d'énergie de Förster entre les partenaires cellulaires (FRET-FLIM). Les cellules HeLa sont transfectées par DNMT1-eGFP et UHRF1-mCherry. L'eGFP joue le rôle de donneur alors que mCherry sert d'accepteur dans le mécanisme de FRET. Le temps de vie du fluorophore donneur est significativement réduit si le fluorophore accepteur est proche (<10 nm) du fluorophore donneur, indiquant ainsi une interaction entre les protéines. Cette étude nous a permis de démontrer qu'UHRF1 interagit avec la DNMT1 dans les cellules HeLa en phase S du cycle cellulaire. De plus, cette interaction primordiale dans le processus de la méthylation est perturbée lorsque les cellules sont traitées avec le composé UM63.

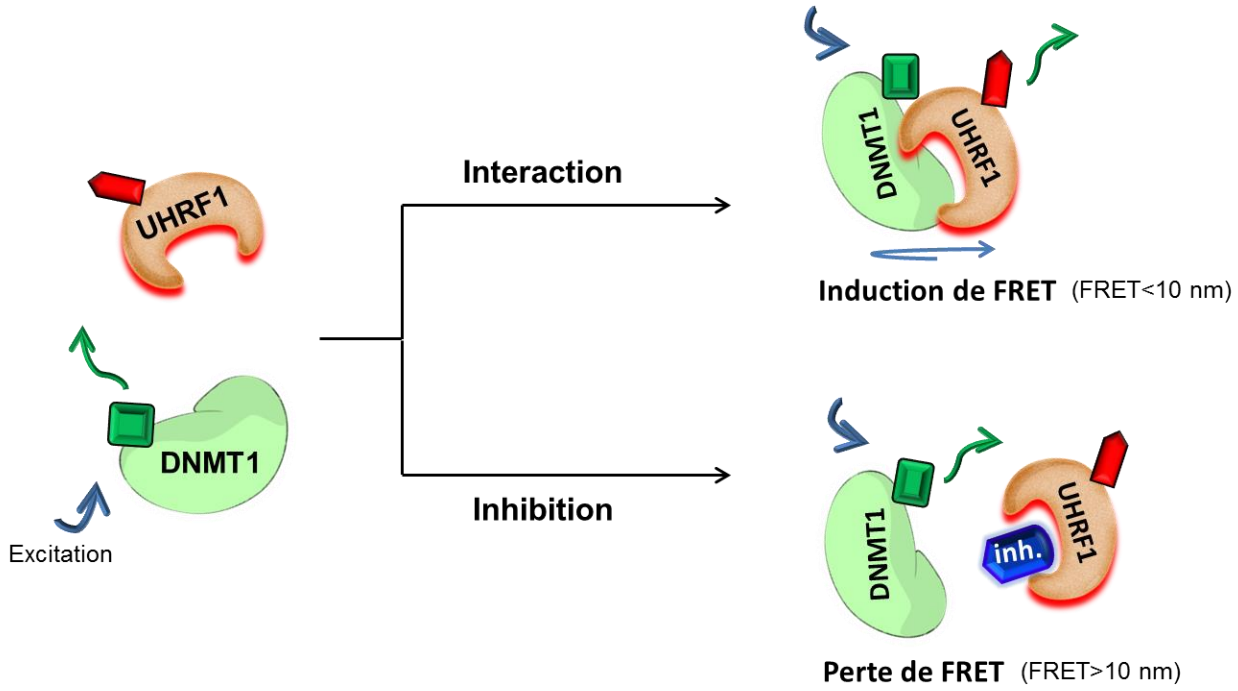

Fig.2. Etude d'interaction entre UHRF1 et DNMT1 par la technique de FLIM. Les cellules HeLa sont transfectées avec DNMT1-eGFP et UHRF1-mCHERRY. L'interaction entre les deux protéines est inhibée par la molécule inhibitrice et entraine la perte du FRET.

3. Propriétés anticancéreuses des molécules actives sur les modèles de cellules cancéreuses

Les caractéristiques anti-tumorales des touches positives ont été évalué par une série de tests sur différentes lignées cellulaires cancéreuses. L'activité antiproliférative était déterminée par le test MTT. UM63 a inhibé la prolifération dans de différentes lignées cancéreuses (HeLa, Huh7 et A375) dans l'ordre du micromolaire. L'effet d'UM63 sur la progression du cycle cellulaire et l'apoptose des cellules cancéreuses a aussi été étudié par cytométrie de flux. Les résultats ont démontré que le traitement avec UM63 a induit l'arrêt du cycle cellulaire dans les cellules Hela à la phase G0/G1 et également induit l'apoptose. Une recherche plus approfondie sur les voies liées à ces processus cellulaires est effectuée en analysant l'expression de protéines impliquées dans ces processus par Western blot. Les cellules non traitées montrent des niveaux indétectables de caspase3 clivée ; ces niveaux commencent à augmenter après traitement avec le composé UM63 d'une manière dépendante de la dose. De plus, le traitement avec UM63 a été suivi par une régulation négative de la PARP avec une augmentation significative de sa forme clivée. Ensuite, nous avons déterminé les niveaux du marqueur pro-survie Bcl2, où les niveaux de la protéine ont diminué significativement.

Au total, nos résultats suggèrent que l'exposition des cellules cancéreuses HeLa à l'UM63 induit une apoptose dépendante de la caspase3.

Afin d'évaluer l'effet sur l'expression de UHRF1 et DNMT1 qui sont principalement impliquées dans la modulation épigénétique, une analyse a été réalisée pour étudier ces protéines. L'expression d'UHRF1 et de DNMT1 a été baissée dans les cellules HeLa traitées avec UM63 ceci s'est accompgnée avec une ré-expression de la p53, le gène suppresseur des tumeurs.

Ces résultats suggèrent que l'UM63 agit comme un inhibiteur d'UHRF1 à activité antiprolifération ciblant le domaine SRA et modifiant l'état de méthylation de l'ADN dans les cellules cancéreuses. À partir de son mode d'action, UM63 pourrait constituer une base solide pour les travaux futurs qui peuvent servir à développer et améliorer les caractéristiques de la prochaine génération d'inhibiteurs UHRF1 en effectuant un certain nombre de modifications chimiques à l'UM63. Tel que :

• Augmenter l'affinité pour le domaine SRA

• Améliorer l'effet inhibiteur sur UHRF1

• Diminuer la cytotoxicité, c'est-à-dire en diminuant l'affinité de liaison pour des séquences d' ADN non spécifiques.

• Déterminer les propriétés pharmacocinétiques, par exemple en augmentant la solubilité dans l'eau et en modulant la stabilité métabolique des nouveaux composés.

Enfin, l'identification in vitro de nouveaux inhibiteurs de l'UHRF1 reste un grand défi, car il est difficile de prédire leur effet sur les cellules, surtout si l'inhibition d'un domaine fonctionnel pourrait conduire à des événements indésirables à d'autres niveaux moléculaires. Nos résultats préliminaires démontrent que le composé UM63 est un candidat potentiel qui peut servir comme point de départ pour le criblage d'inhibiteurs plus sélectifs et spécifiques d'UHRF1. Ces résultats nous encouragent à étudier l'application possible de nouveaux inhibiteurs du domaine SRA dans les pathologies liées à UHRF1 telles que le cancer où les niveaux élevés d'UHRF1 favorisent le développement et la progression des tumeurs. Ce travail non seulement révélera de nouveaux éléments pour la thérapie anticancéreuse, mais aidera également à mieux comprendre le rôle d'UHRF1 dans la réplication des codes épigénétiques.

Liliyana ZAAYTER

Recherche d'inhibiteurs d'UHRF1: Effets sur les aspects épigénétiques dans les cellules cancéreuses

Résumé

La méthylation anormale de l'ADN est l'une des principales caractéristiques du cancer. La nature dynamique et réversible de cette modification épigénétique en a fait une cible potentielle pour le traitement du cancer. UHRF1, une protéine essentielle dans la maintenance de la méthylation de l'ADN, est également impliquée dans la tumorogenèse. UHRF1 est surexprimée dans une variété de cancers et est liée à l'inhibition des TSGs et à la prolifération cellulaire. Dans ce contexte, le but de ma thèse est d'identifier de potentiels inhibiteurs d'UHRF1 qui pourront être efficaces en clinique comme thérapie anti-cancéreuse. Pour atteindre cet objectif, une approche diversifiée a été adoptée qui inclue le criblage virtuel, des techniques biophysiques et biologiques qui permettent à caractériser l'activité inhibitrice des molécules actives et à comprendre leur mécanisme d'action. Nous avons identifié un composé positif de la famille des anthraquinones qui inhibe UHRF1 en se liant à son domaine SRA et perturbe son interaction avec DNMT1, l'enzyme responsable du maintien de la méthylation de l'ADN. Ce composé présente une activité antiprolifération dans différentes lignées cancéreuses.

Résumé en anglais

Abnormal DNA methylation is one of the major hallmarks of cancer. The dynamic and reversible nature of this epigenetic modification has made it a potential target for cancer treatment. UHRF1, a pivotal DNA methylation maintenance protein, is also strongly involved in tumorogenesis. It is overexpressed in a wide array of cancers and leads to silencing of TSGs and tumor growth. In this context, the aim of the thesis is to develop potential UHRF1 inhibitors that may be clinically effective for anti-cancer therapy. To reach this objective, a diverse approach was adopted including virtual screening, biophysical and biological techniques that helped to characterize the inhibitory activity of active molecules and understand their mechanism of action. The tests revealed one positive compound from the anthraquinone family that inhibited UHRF1 by binding to its SRA domain and impairing its interaction with DNMT1, the enzyme responsible for DNA methylation maintenance. This compound showed an anti-proliferative activity in various cancer cells.